

**Role of membrane lipids in regulation of  
Alzheimer's disease associated proteins and  
vice-a-versa**

**Thesis**

Submitted for a Doctoral Degree in Natural Sciences

At the Department of Biochemistry

University of Bonn, Bonn, Germany

Submitted by

**Irfan Yunus Tamboli**

(Date of Birth 17<sup>th</sup> Dec 1976)

From, Pune, INDIA

Bonn, 2007

Supervisor: Prof. Dr. Jochen Walter  
First reviewer: Prof. Dr. Konrad Sandhoff  
Second reviewer: Prof. Dr. Joerg Piel  
Third reviewer: Prof. Dr. Michael Gütschow

Date of examination: **19. 10. 2007**

Thesis work completed at:  
Laboratory of Molecular Cell Biology,  
Department of Neurology  
University Hospital Bonn  
Sigmund-Freud str. 25  
53127 Bonn, Germany.

This thesis is available online under Hochschulschriftenserver of ULB Bonn  
[http://hss.ulb.uni.de/diss\\_online](http://hss.ulb.uni.de/diss_online)

**Publication year** : 2008

## **Declaration**

I solemnly declare that the work submitted here is result of my own investigation, except where otherwise stated. This work has not been submitted to any other university or institute towards the partial fulfillment of any degree.

**Irfan Yunus Tamboli**

Dedicated to Abba, Ammi and Badima

Vande Mataram

## Abbreviations

AD	Alzheimer's Disease
FAD	Familial Alzheimer's Disease
A $\beta$	Amyloid $\beta$ peptide
APP	$\beta$ -Amyloid precursor protein
NFTs	Neurofibrillary tangles
PHFs	Paired helical filaments
APPs $\beta$	Soluble APP generated by $\beta$ -secretase cleavage
APPs $\alpha$	Soluble APP generated by $\alpha$ -secretase cleavage
APP-CTFs/CTFs	C-terminal fragments of APP
APP-CTF $\beta$ /CTF $\alpha$	C-terminal fragment of APP generated by $\beta$ -secretase cleavage
APP-CTF $\beta$ /CTF- $\beta$	C-terminal fragment of APP generated by $\alpha$ -secretase cleavage
p3	Product of APP generated by $\alpha$ - and $\gamma$ - secretase cleavage
AICD	APP intracellular domain
KPI	Kunitz protease inhibition
ADAM	A disintegrin and metalloprotease
BACE-1	$\beta$ -site APP-cleaving enzyme; $\beta$ -secretase
RIP	Regulated intramembranous proteolysis
PS-1/2	Presenilin 1/2
PEN-2	Presenilin enhancer – 2
APH-1	Anterior pharynx defective – 1
TMD	Trans-membrane domain
Apo E	Apolipoprotein E
GSLs	Glycosphingolipids
GCS	Glucosylceramide synthase / Glycosylceramide synthase
LCS/GalT1	Lactosylceramide synthase/ galactosyltransferase I
PDMP	D, L-threo-1-Phenyl-2-decanoylamino-3-morpholino -1-propanol. HCl
GM1	Gal- $\beta$ -GalNAc- $\beta$ -4(NeuAc $\alpha$ -3)Gal- $\beta$ -4-Glc
SLSDs	Sphingolipid storage disorders
GlcCer	Glucosyl ceramide
LDL	Low density lipoprotein
LDLR	Low density lipoprotein receptor
LRP	Low density lipoprotein receptor related protein
PM	Plasma membrane
DNA	Deoxy ribonucleic acid
cDNA	Complementary DNA
RNA	Ribonucleic acid
mRNA	messenger ribonucleic acid
DEPC	Diethyl pyrocarbonate
siRNA	small interfering RNA
RNAi	RNA interference
DAPT	N-[N-(3,5-Difluorophenacetyl-L-alanyl)]-S-phenylglycine t-butyl ester
GC-MS	Gas chromatography mass spectrometry
CYP51	Lanosterol 14- $\alpha$ -demethylase

## Amino acid abbreviations and single letter code

<b>Amino acid</b>	<b>Abbreviation</b>	<b>Single letter code</b>
Alanine	Ala	A
Arginine	Arg	R
Asparagine	Asn	N
Aspartic acid	Asp	D
Cysteine	Cys	C
Glutamine	Gln	Q
Glutamic acid	Glu	E
Glycine	Gly	G
Histidine	His	H
Isoleucine	Ile	I
Leucine	Leu	L
Lysine	Lys	K
Methionine	Met	M
Phenylalanine	Phe	F
Proline	Pro	P
Serine	Ser	S
Threonine	Thr	T
Tryptophan	Trp	W
Tyrosine	Tyr	Y
Valine	Val	V
Any amino acid		X

<b>1</b>	<b>SUMMARY/ABSTRACT .....</b>	<b>ERROR! BOOKMARK NOT DEFINED.</b>
<b>2</b>	<b>INTRODUCTION.....</b>	<b>ERROR! BOOKMARK NOT DEFINED.</b>
<b>2.1</b>	<b>Alzheimer’s Disease.....</b>	<b>Error! Bookmark not defined.</b>
2.1.1	Neuropathological lesions of AD.....	<b>Error! Bookmark not defined.</b>
2.1.2	Generation of A $\beta$ .....	<b>6</b>
2.1.3	Presenilins.....	<b>Error! Bookmark not defined.</b>
2.1.4	Genetics of AD .....	<b>Error! Bookmark not defined.</b>
2.1.5	Amyloid Hypothesis.....	<b>Error! Bookmark not defined.</b>
<b>2.2</b>	<b>Membrane lipids – classification, structure, function .....</b>	<b>Error! Bookmark not defined.</b>
2.2.1	Phospholipids .....	<b>Error! Bookmark not defined.</b>
2.2.2	Glycolipids .....	<b>Error! Bookmark not defined.</b>
2.2.3	Cholesterol.....	<b>Error! Bookmark not defined.</b>
<b>2.3</b>	<b>Rationale and Aim of the study .....</b>	<b>Error! Bookmark not defined.</b>
<b>3</b>	<b>MATERIALS AND METHODS .....</b>	<b>ERROR! BOOKMARK NOT DEFINED.</b>
<b>3.1</b>	<b>DNA recombination techniques.....</b>	<b>Error! Bookmark not defined.</b>
3.1.1	Instruments and materials .....	<b>Error! Bookmark not defined.</b>
3.1.2	Quantitation of nucleic acid.....	<b>Error! Bookmark not defined.</b>
3.1.3	Constructs and Cloning .....	<b>Error! Bookmark not defined.1</b>
3.1.4	Polymerase chain reaction (PCR).....	<b>Error! Bookmark not defined.1</b>
3.1.5	Purification, analysis and modification of DNA.....	<b>Error! Bookmark not defined.</b>
<b>3.2</b>	<b>Gene expression analysis by RT- PCR.....</b>	<b>Error! Bookmark not defined.</b>
3.2.1	Extraction of RNA from eukaryotic cells .....	<b>Error! Bookmark not defined.</b>
3.2.2	cDNA synthesis .....	<b>Error! Bookmark not defined.</b>
3.2.3	PCR .....	<b>Error! Bookmark not defined.</b>
<b>3.3</b>	<b>RNA interference (RNAi).....</b>	<b>Error! Bookmark not defined.</b>
3.3.1	Generation of pSupZeo, a vector for stable expression of siRNA into mammalian cells .....	<b>Error! Bookmark not defined.</b>
	<b>Bookmark not defined.</b>	
3.3.2	Selection of target sequence .....	<b>Error! Bookmark not defined.</b>
3.3.3	Designing RNAi oligonucleotides.....	<b>Error! Bookmark not defined.</b>
3.3.4	Cloning oligonucleotides into pSupZeo .....	<b>Error! Bookmark not defined.</b>
<b>3.4</b>	<b>Cell Culture.....</b>	<b>39</b>
3.4.1	Instruments and materials .....	<b>39</b>
3.4.2	Transfection.....	<b>Error! Bookmark not defined.</b>
3.4.3	Generating stable cell lines.....	<b>Error! Bookmark not defined.</b>
<b>3.5</b>	<b>Biochemical and Cell Biological Methods .....</b>	<b>Error! Bookmark not defined.</b>
3.5.1	Instruments and materials .....	<b>Error! Bookmark not defined.</b>
3.5.2	Sample preparation.....	<b>Error! Bookmark not defined.</b>
3.5.3	Protein metabolic labeling with [ <sup>35</sup> S ] – methionine / cysteine.....	<b>Error! Bookmark not defined.</b>
3.5.4	Polyacrylamide-SDS gel electrophoresis.....	<b>Error! Bookmark not defined.</b>
3.5.5	Tricine gel system for low molecular weight protein detection.....	<b>Error! Bookmark not defined.</b>
3.5.6	Western immunoblotting .....	<b>Error! Bookmark not defined.</b>
3.5.7	Immunocytochemistry .....	<b>Error! Bookmark not defined.</b>
3.5.8	Cholesterol Stain.....	<b>Error! Bookmark not defined.</b>
3.5.9	Analysis of protein and lipid transport .....	<b>Error! Bookmark not defined.</b>
3.5.10	Subcellular fractionation using iodixanol gradient.....	<b>Error! Bookmark not defined.0</b>

- 3.5.11 In vitro  $\gamma$ -secretase assay..... **Error! Bookmark not defined.**
- 3.5.12 Cell viability assay..... **Error! Bookmark not defined.**
- 3.5.13 Analysis of cellular sterols..... **Error! Bookmark not defined.**

## 4 RESULTS ..... **ERROR! BOOKMARK NOT DEFINED.**

### 4.1 Role of GSLs in APP processing ..... **Error! Bookmark not defined.**

- 4.1.1 Pharmacological inhibition of GSL biosynthesis..... **Error! Bookmark not defined.**
- 4.1.2 Analysis of APP processing in GSL deficient GM95 cells ..... **Error! Bookmark not defined.**
- 4.1.3 Targeted suppression of lactosylceramide synthase (LCS) by shRNA ..... **Error! Bookmark not defined.**
- 4.1.4 Addition of exogenous GSLs increases levels of cellular and secreted APP as well as APP-CTFs.. **Error! Bookmark not defined.**
- 4.1.5 APP-CTF levels in sphingolipid storage and deficiency genetic cellular models.... **Error! Bookmark not defined.**

### 4.2 Regulation of cholesterol metabolism by presenilins ..... **Error! Bookmark not defined.**

- 4.2.1 Cellular cholesterol content and distribution regulated by presenilin ..... **Error! Bookmark not defined.**
- 4.2.2 Up-regulation of cholesterol biosynthesis in PS deficient cell..... **Error! Bookmark not defined.**
- 4.2.3 Up-regulation of CYP51 leads to increased turnover of lanosterol in PS deficient cells **Error! Bookmark not defined.**
- 4.2.4 Inhibition of CYP51 reverses increased cholesterol levels in PS deficient cells ..... **Error! Bookmark not defined.**
- 4.2.5 Increase in cholesterol levels in PS deficient cells is independent of exogenously added A $\beta$  ..... **Error! Bookmark not defined.**
- 4.2.6 Inhibition of  $\gamma$ -secretase in human neuroglioma cells increased cholesterol levels. **Error! Bookmark not defined.**
- 4.2.7 PS deficiency is associated with inefficient LDL uptake ..... **Error! Bookmark not defined.**
- 4.2.8 Increased levels of LDL receptor (LDLR) in PS deficient cells ..... **Error! Bookmark not defined.**
- 4.2.9 Cell surface expression of LDLR is regulated by presenilin..... **Error! Bookmark not defined.**
- 4.2.10 Impaired endocytosis of LDLR in PS deficient cells..... **Error! Bookmark not defined.**

### 4.3 Regulation of general endocytosis by presenilins ..... **Error! Bookmark not defined.**

- 4.3.1 Impaired endocytosis of APP and BSA in PS dKO cells ..... **Error! Bookmark not defined.**
- 4.3.2 Inefficient endocytosis of GM1 in PS deficient cells..... **Error! Bookmark not defined.**

### 4.4 PS1 FAD mutations affect homeostasis of membrane lipid and proteins ..... **Error! Bookmark not defined.**

## 5 DISCUSSION ..... **ERROR! BOOKMARK NOT DEFINED.**

- 5.1.1 Modulation of APP metabolism by GSLs ..... **Error! Bookmark not defined.**
- 5.1.2 Role of GSLs in APP-CTF metabolism ..... **Error! Bookmark not defined.**
- 5.1.3 Role of GSLs in A $\beta$  generation..... **Error! Bookmark not defined.**

### 5.2 Link between cholesterol metabolism and AD ..... **Error! Bookmark not defined.**

- 5.2.1 Role of RIP in maintenance of membrane lipid – protein homeostasis .... **Error! Bookmark not defined.**
- 5.2.2 Role of presenilins in cellular cholesterol homeostasis ..... **Error! Bookmark not defined.**
- 5.2.3 Presenilin dependent subcellular distribution of cholesterol..... **Error! Bookmark not defined.**
- 5.2.4 Regulation of global endocytosis and protein transport by presenilin ..... **Error! Bookmark not defined.**
- 5.2.5 GSL metabolism is affected by presenilins..... **Error! Bookmark not defined.**

## 6 LITERATURE ..... **ERROR! BOOKMARK NOT DEFINED.**







# 1 Summary/Abstract

Alzheimer's disease (AD) is associated with extracellular deposits of the amyloid  $\beta$ -peptide ( $A\beta$ ) and intraneuronal aggregates of hyperphosphorylated tau protein in the brain.  $A\beta$  is generated by sequential proteolytic processing of the  $\beta$ -amyloid precursor protein (APP) by  $\beta$ - and  $\gamma$ -secretases.  $\gamma$ -secretase is a multimeric protein complex with presenilins as catalytic subunits, which cleave APP C-terminal fragments (APP-CTFs) generated by  $\beta$ -secretase cleavage of APP. Several studies have indicated dysregulation of protein transport and lipid metabolism as an important aspect of AD. The cleavage of APP by secretases which occurs predominantly in post-Golgi secretory and endocytic compartments is influenced by cholesterol, indicating a role of the membrane lipid composition in the processing of APP. Moreover,  $\gamma$ -secretase activity has been shown to be dependent on membrane lipids. In the present study, on one hand the effects of perturbations in membrane lipid composition on APP processing were analyzed in detail. On the other hand, the role of presenilins in maintenance of membrane lipid homeostasis was investigated as well.

By various approaches, it was established that APP transport, stability, maturation and processing is affected by glycosphingolipids (GSLs). Importantly, the inhibition of GSL biosynthesis decreased secretion of  $A\beta$ , whereas addition of exogenous GSLs lead to higher  $A\beta$  levels as well as strong accumulation of APP-CTFs. Thus, the presented studies identified GSL metabolism as a novel target to regulate the levels of  $A\beta$ . Moreover, there is a growing perception that the increased levels of APP-CTFs contribute to AD pathology by exerting toxic effects. Elevated levels of APP-CTFs were also detected in various sphingolipid storage disorders (SLSDs). Interestingly, tau pathology and inflammation caused by microgliosis is observed both in AD as well as some sphingolipid storage disorders (SLSDs). Therefore, an accumulation of APP-CTFs associated with altered sphingolipid metabolism might be an important common aspect of these disorders, which contributes to the observed neurodegeneration.

In the course of these studies, a novel way by which presenilins regulate the cholesterol and sphingolipid metabolism was also revealed. Inhibition of  $\gamma$ -secretase activity results in inefficient endocytosis of LDL, which led to increased cellular *de novo* cholesterol biosynthesis via transcriptional up-regulation of *CYP51*. Evidence is provided for the global role of presenilins in regulation of endocytosis and degradation of membrane lipids and a broad range of proteins. The lack of  $\gamma$ -secretase activity causes an accumulation of membrane sphingolipids as well as membrane proteins. Thus, results validate the previously proposed hypothesis that presenilin are necessary for membrane protein clearance. Moreover, familial Alzheimer's disease (FAD) associated mutations in presenilin disturbed the membrane lipid-protein homeostasis in a similar fashion by blocking endocytosis, indicating loss of function.

The inhibition of  $\gamma$ -secretase activity is a rational strategy to decrease  $A\beta$  generation in AD therapy. However, since  $\gamma$ -secretase is involved in the cleavage of different substrates, a general inhibition of this enzyme could affect different biological processes. The finding that the inhibition of  $\gamma$ -secretase activity also impaired membrane lipid-protein homeostasis underscores the necessity of targeting  $\gamma$ -secretase cleavage of APP, without affecting other cellular pathways.



## 2 Introduction

### 2.1 Alzheimer's Disease

Alzheimer's disease (AD) is a progressive neurodegenerative disorder and is the most common cause of dementia. Age is considered the major risk factor for AD. Millions suffer from AD worldwide and with continuous rise in life expectancy, the number of AD patients is set to increase steeply in coming years (Ferri et al., 2005). Clinically, AD is characterized by progressive loss of memory associated with cognitive deficits extending to language skills, decision-making ability, movement and recognition (Forstl and Kurz, 1999; Arnaiz and Almkvist, 2003). Neuropathologically, presence of extracellular amyloid plaques and intracellular neurofibrillary tangles (NFTs) (Fig. 1A,B) associated with widespread loss of neurons in brain, first described in 1907 by the German neurologist Alois Alzheimer, still remains the most robust and invariable features of AD. A major component of amyloid plaques is the hydrophobic 4kD amyloid  $\beta$  peptide ( $A\beta$ ), while NFTs are formed by hyperphosphorylated tau (Selkoe, 2001; Masters and Beyreuther, 1991).

Gradual deposition of  $A\beta$  into plaques together with loss of communication among certain neurons, leading to eventual neurodegeneration and inflammation could underlie the clinical progression of disease. No medical tests other than brain autopsy are available to diagnose AD conclusively pre-mortem. The clinical diagnosis is primarily made on the basis of family history, clinical observation, and memory tests. In typical cases, initially there is an isolated impairment of learning and short-term memory, without alterations in other areas of cognition or consciousness. This is followed by changes in long-term memory, personality, orientation and executive function. Cognitive losses are followed by behavioral/psychological problems (e.g. hallucinations, delusions). Finally deterioration of language and visuospatial skills together with impaired motor function leads to loss of activities of daily living (Scarmeas et al., 2005). Additionally, evolving contemporary neuroimaging techniques could offer a great promise for early diagnosis (Hintersteiner et al., 2005).

Currently available therapies, for the most part target a deficiency in the cholinergic neurotransmitter system, a neurochemical system largely thought to be involved in short term memory, which is severely affected in AD. These medications, however, offer only palliative symptomatic relief (Birks, 2006). Recent findings suggest that the therapies based on immunological interventions hold a great promise against AD. However, these therapies face a

challenge of overcoming associated immune-related complications such as encephalitis and T-cell response (Weiner and Frenkel, 2006).

### 2.1.1 Neuropathological lesions of AD

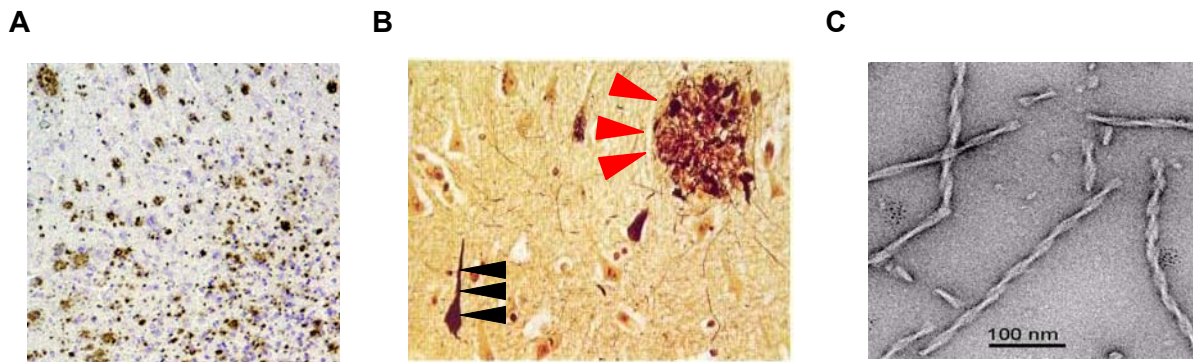


**Fig.1 Neuropathological hallmarks of Alzheimers disease.** A-B, Photomicrograph of a section of brain from AD patient demonstrating the classical neuropathological lesions of this disorder – amyloid plaques and neurofibrillary tangles (NFTs) (A). Higher resolution picture of AD brain section, depicting amyloid plaque and NFTs, red and black arrowheads indicate amyloid plaque and NFT respectively (B), (taken from Selkoe et.al., 1998). C, Ultrastructural visualization of neurofibrillary tangle using electron microscopy showing paired helical filaments twisted around each other that are composed of hyperphosphorylated tau. (Source <http://www.mpasmb-hamburg.mpg.de/>)

NFTs consist of paired helical filaments (PHFs) of the microtubule associated tau protein arranged in a double helix (diameter 20 nm). They are found in the cytoplasm of neurons, particularly of pyramidal cells of the cerebral cortex and hippocampus (Fig. 1). Deposition of NFTs is reported to occur in six stages (Braak and Braak, 1991a). The insidious onset and gradual progression of symptoms in patients with AD are thought to parallel the progression of AD-related brain deterioration from entorhinal cortex to hippocampus to neocortex (Braak and Braak, 1991b). Six isoforms of tau derive by alternative mRNA splicing from a single gene located on chromosome 17. So far more than 20 abnormal phosphorylation sites in tau have been shown to be associated with AD. In AD hyperphosphorylated tau competes with normal tau as well as with microtubule associated protein 1 and 2 inhibiting their microtubule assembly promoting activities. The disruption of the microtubule network probably compromises axonal transport and starts retrograde degeneration of affected neurons. Moreover, the neuronal cytoskeleton is progressively disrupted and is replaced by bundles of PHFs, leading to the formation of NFTs. To date no mutations in tau have been found to be associated with AD. However, mutations in tau are associated with frontotemporal dementia supporting the role of tau in the pathogenesis of neurodegenerative disorders (Lee et al., 2001; Mandelkow et al., 1996).

In contrast to intraneuronal NFTs, amyloid plaques are extracellular, round, spherical structures with diameters of 15 to 20  $\mu\text{M}$ . They consist of a peripheral rim of intimately associated abnormal neuronal processes - dystrophic axons and dendrites (neurites) along with activated microglia, astrocytes as well as blood vessels surrounding a core of densely deposited  $\text{A}\beta$ . Deposits of amyloid peptide that lack altered neurites and glia are known as diffuse plaques and may be found in the brains of normally aged people, as well as in other neurodegenerative diseases (Armstrong, 2006). Plaques are heterogeneous aggregates containing many other components like sulfated glycosaminoglycans, Apo E,  $\alpha$ 1-antichymotrypsin, complement factors, cytoskeletal proteins and lipids such as cholesterol etc. The predominant  $\text{A}\beta$  species found in the plaque is the 40 amino acid long  $\text{A}\beta$ 40. A less abundant, more hydrophobic 42 amino acid long species,  $\text{A}\beta$ 42, is considered more toxic and the initiator of aggregation. An altered  $\text{A}\beta$ 42 to  $\text{A}\beta$ 40 ratio and overall increase of total  $\text{A}\beta$  load is thought to be one of the primary causes for plaque formation.  $\text{A}\beta$  deposition in the entire brain follows a hierarchical sequence in different regions of the brain. A large number of non-demented elderly people also show deposition of  $\text{A}\beta$  plaques in brain, however, plaques are restricted to neocortex, allocortex, basal ganglia and diencephalic nuclei (phase 1 to 3), whereas in AD cases with clinically apparent dementia additional  $\text{A}\beta$  deposits are found in brainstem and cerebellum (phase 4 and 5) (Thal et al., 2002).

Significant correlations have been made between  $\text{A}\beta$  load, plaques deposition and cognition (Beer and Ulrich, 1993), dementia severity (Cummings and Cotman, 1995) as well as between NFT numbers and dementia. However, contradictory reports showing little relation between plaques and tangles with progression of AD have also been published. Studies also suggest a possible role of  $\text{A}\beta$  in the formation of NFTs.  $\text{A}\beta$  appears to promote tau hyperphosphorylation via modulation of glycogen synthase kinase 3 $\beta$  (GSK3 $\beta$ ), mitogen-activated protein kinases (MAPKs) and cyclin-dependent kinase 5 (Cdk5), the other kinases which phosphorylate tau (Hardy, 2003).

## **2.1.2 Generation of A $\beta$**

### **2.1.2.1 Amyloid Precursor Protein – Proteolytic processing and subcellular transport**

A $\beta$  is derived from a larger precursor called  $\beta$ -amyloid precursor protein (APP). APP is a type I transmembrane protein and is co-translationally translocated into ER and subjected to several co- and post-translational modifications such as *N'* and *O'* glycosylation, sulfation and phosphorylation as it is transported through the ER to the cell surface via the *Golgi* compartment. Most of the APP is turned over with relatively short half-life time of 45-60 min in most cell types. APP isoforms exist as immature (APP im; *N*-glycosylated) and mature (APP m; *N*- and *O*-glycosylated) species. Immature APP is localized in the ER and *cis-Golgi*, and mature APP is present within *trans-Golgi*, on the plasma membrane and in the endocytic and lysosomal compartments. Sequential proteolytic processing of APP by secretases in secretory and endocytic pathway could result in generation of A $\beta$  (Fig. 2).  $\beta$ -secretase cleaves APP before Asp 1 of A $\beta$  predominantly in endosomal and lysosomal compartments after its internalization from the cell surface. Cleavage of APP by  $\beta$ -secretase results in the secretion of soluble APP (APPs- $\beta$ ) and generation of a 99 amino acids long APP C-terminal fragment (APP-CTF $\beta$ ) that is tethered within the membrane bilayer and is substrate for a multimeric protein complex called  $\gamma$ -secretase, which cleaves CTF $\beta$  within the transmembrane domain leading to generation of A $\beta$ . Therefore, this pathway of APP processing is termed amyloidogenic pathway. Cleavage of CTF $\beta$  by  $\gamma$ -secretase can occur at variable amino acid positions leading to generation of different A $\beta$  peptides e.g. A $\beta$ 40, A $\beta$ 42 and A $\beta$ 38. Alternatively, APP can also be processed in a non-amyloidogenic fashion, predominantly at cell surface. Initial cleavage by  $\alpha$ -secretase within the A $\beta$  domain between amino acids 16 and 17 precludes the later formation of A $\beta$  peptides. The  $\alpha$ -secretase cleavage produces  $\alpha$ -soluble APP (APPs- $\alpha$ ) and 83 amino acids long CTF $\alpha$ . Subsequently, CTF $\alpha$  could also be cleaved by the  $\gamma$ -secretase complex to generate p3. Unlike A $\beta$ , the p3 fragment does not have the propensity to aggregate. Moreover, APP-CTF can also be cleaved by  $\gamma$ -secretase at  $\epsilon$ - and  $\zeta$ -site which liberates APP intracellular domain (AICD). Because of the differential actions of  $\alpha$ - and  $\beta$ -secretase, the non-amyloidogenic and amyloidogenic processing pathways of APP are mutually exclusive (Walter et al., 2001; Selkoe, 2000).



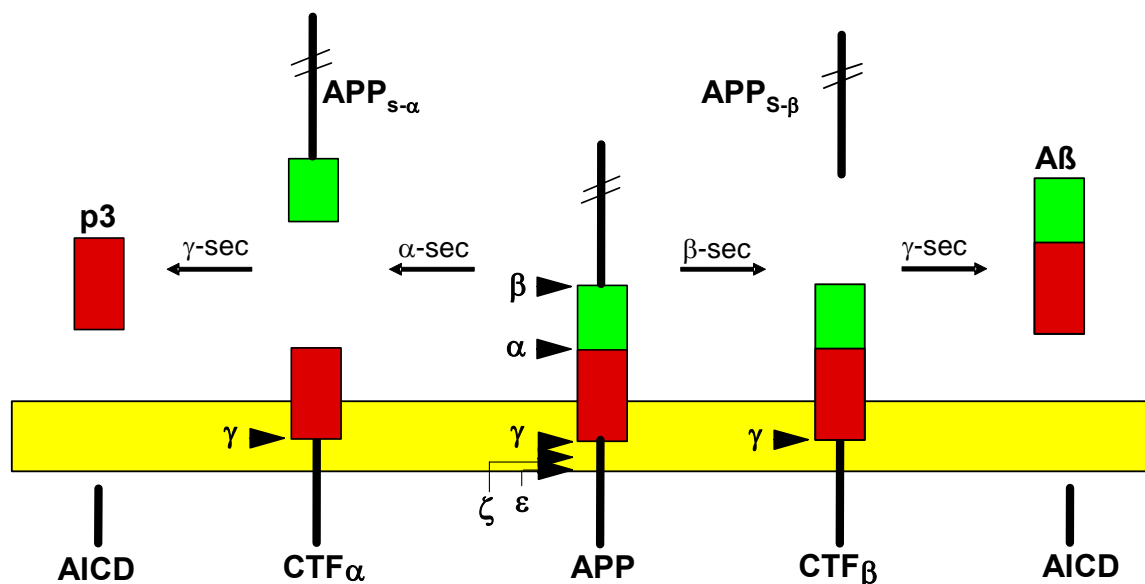


Fig. 2. **Proteolytic processing of APP by secretases.** The respective cleavage sites within APP molecule are indicated by arrowheads. The lipid bilayer is indicated in yellow. In amyloidogenic pathway APP is first cleaved by  $\beta$ -secretase and then by  $\gamma$ -secretase to generate  $A\beta$  (indicated in green). In the non-amyloidogenic pathway APP is first cleaved by  $\alpha$ -secretase within the  $A\beta$  domain and then by  $\gamma$ -secretase to generate non-amyloidogenic p3 (red). Additionally  $\gamma$ -secretase can also cleave APP at  $\epsilon$ - and  $\zeta$ -cleavage site as indicated,  $\epsilon$ -cleavage of  $CTF\alpha/\beta$  generates AICD, (adapted from Walter et al., 2001).

Besides the amyloidogenic and non-amyloidogenic processing pathways, APP is also degraded by lysosomal and proteasomal pathways. Treatment of cells with the lysosomal protease inhibitor leupeptin and proteasomal inhibitors MG132 or lactacystin results in the accumulation of different species of APP-CTFs with molecular weights higher than the expected for  $\alpha$ - or  $\beta$ -secretase cleavage (Haass et al., 1992). Various factors and biological processes that affect APP subcellular transport and metabolism also modulate the processing of APP, eventually affecting  $A\beta$  generation (Haass and de Strooper, 1999).

Levels of  $A\beta$  in the brain are determined by the balance between production and degradation. Neprilysin, insulin degrading enzyme, endothelin converting enzyme-2, angiotensin converting enzyme, plasmin and cathepsin D have been implicated in the degradation of  $A\beta$  (Eckman and Eckman, 2005). Age dependent and brain region specific alterations in the expression of these enzymes have been reported, this may contribute to distinct susceptibilities of particular brain regions in AD as well as the age dependence of this disease. Especially, expression of neprilysin was found to be reduced in AD. Recent *in vivo* and *in vitro* studies demonstrate that the up-regulation of  $A\beta$  degrading enzymes can significantly reduce  $A\beta$  accumulation in brain (Marr et al., 2003).

### 2.1.2.2 Amyloid Precursor Protein – Characteristics and functions

APP and its related family members, the amyloid precursor like proteins-1 and -2 (APLP-1 and APLP-2), are homologous type-I transmembrane proteins with relatively large extracellular domains and short intracellular domains that are similarly posttranslationally modified and processed and have overlapping expression in brain. However, only APP contains the unique amyloidogenic A $\beta$  sequence and therefore receives intense scrutiny. The gene encoding APP is located on human chromosome 21 and contains 19 exons. Several isoforms of APP are generated by alternative splicing of exons 1-13, 13a, and 14-18. The predominant transcripts are APP695 (exons 1-6, 9-18, not 13a), APP751 (exons 1-7, 9-18, not 13a), and APP770 (exons 1-18, not 13a) where respective isoform number indicates the length of amino acid sequence. APP751 and APP770 isoforms contain exon 7, which encodes a kunitz protease inhibitor (KPI) domain. APP770 also contains exon 8, which encodes the proposed domain with homology to the MRC OX-2 antigen. All APP family members are ubiquitously expressed. APP695 is the predominant form in neuronal tissues, whereas APP751 and APP770 are the predominant variants in peripheral tissues (Selkoe, 2001).

APP knockout mice are fertile and viable. Knockout mice of all three genes or of APP and APLP-2 as well as APLP1 and APLP2 are lethal in utero, indicating functional redundancy among APP family members. As shown in Fig. 3, APP harbors multiple domains and sites for interaction with other proteins, metal ions and heparin as well as for posttranslational modifications. It is suggested that the APP holoprotein may be involved in cell-cell interaction, cell adhesion, protease inhibition (via the KPI domain in 751 and 770 APP isoforms), and neurite outgrowth, formation of forebrain commissures, postnatal somatic growth, neurobehavioral development and locomotor activity (Mattson, 1997). There is also biochemical evidence for anti-coagulant properties of APP. The secreted APPs is known to have neuroprotective and neurotrophic properties. Indeed, memory-enhancing effects were observed when soluble APP was administered intracerebroventricularly into mice. Binding of APP to metal ions like Fe<sup>2+</sup>, Cu<sup>2+</sup>, Zn<sup>2+</sup> and Pb<sup>2+</sup> via its cysteine rich domain is known to affect APP processing. Interestingly, the binding of APP with copper is thought to be essential for copper reduction and homeostasis. Moreover, binding of heparin oligosaccharides to APP also modulates APP processing. APP also participates in the regulation of signal transduction via association with a brain G protein, Go protein (Bayer et al., 1999; Bush et al., 2003).

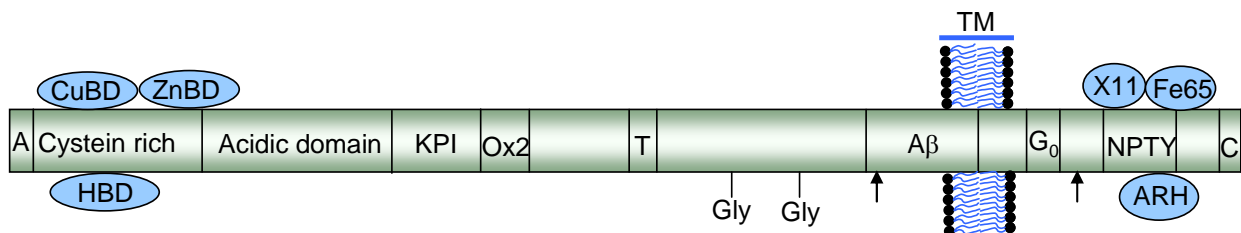


Fig. 3. **Diagrammatic overview of APP domains, based on isoform 770.** Domains involved in major interaction with metal ions, other proteins as well as regions where APP is modified posttranslationally are indicated. Briefly, CuBD/ZnBD/HPD are copper binding, zinc binding and heparin binding domains respectively, KPI - kunitz protease inhibitor domain, Ox2 - Ox2 antigene domain, T - TIMP (tissue inhibitor of metalloproteinases) homology domain are some of the domains present in ectodomain of APP. G<sub>0</sub> - G<sub>0</sub> protein binding site, NPTY - GYENPTY motif present in APP C-terminal is essential for binding of various adaptor proteins like X11, Fe65 and ARH, C - clathrin binding domain. Sulfation and glycosylation sites are marked as SO<sub>4</sub> and Gly respectively. Arrows indicate caspase cleavage sites present in APP. Transmembrane (TM) and amyloid  $\beta$  peptide (A $\beta$ ) domains are indicated.

APP was also shown to function as membrane receptor for kinesin-I, a microtubule motor protein, mediating the axonal transport of vesicles containing  $\beta$ -secretase and presenilin-1. Adaptor proteins with phosphotyrosine-binding (PTB) domains, including those in the Fe65, X11, c-Jun N-terminal kinase (JNK)-interacting protein (JIP) families and ARH (autosomal recessive hypercholesteremia) bind specifically to the highly conserved -GYENPTY- motif in the APP C-terminal (King and Scott, 2004). These interactions play critical roles in tyrosine kinase mediated signal transduction, protein trafficking, phagocytosis, cell fate determination and neuronal development. Especially Fe65 links APP to cytoskeletal dynamics and cellular motility and morphology which could be important for highly dynamic processes such as neurite growth and synapse modification. Binding of adaptor proteins also facilitates the interaction of APP with lipoprotein receptors like the low density lipoprotein related protein (LRP). The GYENPTY and YTSI domains in APP are involved in the regulation of endocytosis of APP. Therefore, binding of adaptor proteins influences processing of APP and regulates generation of A $\beta$  (de Strooper and Annaert, 2000).

AICD, which is released by  $\gamma$ -secretase cleavage, was shown to translocate to nucleus and regulate gene transcription, especially the expression of KAI 1, GSK3 $\beta$ , neprilysin and cellular APP itself was shown to be affected by AICD (Cao and Sudhof, 2004). However, recent findings that AICD could also affect gene transcription by association with Fe65 or X11 independent of  $\gamma$ -secretase and transactivation of wide variety of different promoters by Fe65 alone, casts doubts about translocation of AICD to nucleus and its role in nuclear signaling (Hass and Yankner, 2005). Intriguingly, a number of functions have been attributed to A $\beta$ . It has been

shown that the A $\beta$  peptides compete with insulin for the insulin receptor. Moreover, soluble A $\beta$ 40 was shown to induce NMDA-dependent degradation of postsynaptic scaffolding protein postsynaptic-95 (PSD-95), which plays a critical role in synaptic plasticity and the stabilization of AMPA and NMDA receptors. Furthermore, A $\beta$  can also regulate the trafficking of NMDA receptors and homeostasis of cellular cholesterol and sphingolipids (Pearson and Peers, 2006).

### **2.1.2.3 $\alpha$ -secretase**

In non neuronal cells, APP is mainly cleaved within the A $\beta$  domain between Lys16 and Leu17 by  $\alpha$ -secretase (the first amino acid of amyloid sequence is taken as number 1).  $\alpha$ -secretase is a member of the ADAM (a disintegrin and metalloprotease) family of proteases and is ADAM10, ADAM17/TACE (tumor necrosis factor- $\alpha$  converting enzyme) or ADAM9. Embryonic lethality of ADAM10 deficient as well as ADAM17 deficient mice prevented a reliable analysis of adult mice. Therefore, at present, it is unclear whether only one or all three together constitute the physiologically relevant  $\alpha$ -secretase. By crossing an AD mouse model with ADAM10 transgenic mice, Postina et al. (Postina et al., 2004) recently showed that overexpressed ADAM10 could contribute to  $\alpha$ -secretase cleavage of APP *in vivo* and thus is indeed anti-amyloidogenic. Observed reduction in A $\beta$  peptide generation was sufficient to almost completely prevent amyloid plaque formation in brains of these mice. Overexpression of ADAM10 also alleviated deficits in spatial learning and synaptic plasticity observed in AD mice.

ADAMs are membrane-anchored proteins with several domains, including a metalloprotease domain which requires a zinc co-factor for activity. The cleavage of APP by  $\alpha$ -secretase is either constitutive or regulated through activation of protein kinase C (PKC). Stimulation of phosphorylation by PKC activators increases  $\alpha$ -secretase dependent processing of APP, thereby lowering secretion of A $\beta$  (Etcheberrigaray et al., 2004). It has been suggested that TACE might play a role only in the regulatory component of  $\alpha$ -secretase cleavage, whereas ADAM10 and ADAM9 are implicated in both, constitutive and regulatory processing of APP by  $\alpha$ -secretase. The PKC-dependent  $\alpha$ -secretase is shown to compete with  $\beta$ -secretase for cleavage of APP (Fahrenholz et al., 2000).

ADAM10 and ADAM17 also mediate the ectodomain shedding of Notch, p75, TNF- $\alpha$ -receptor, cell adhesion molecule L-selectin, growth factor co-receptor syndecan and many other type-I transmembrane proteins. Therefore, they are important in many aspects of biology ranging

from cell proliferation, differentiation, remodeling of extracellular matrix and signaling (Primakoff and Myles, 2000).

#### 2.1.2.4 $\beta$ -secretase

$\beta$ -secretase is predominantly expressed in neuronal cells where it cleaves APP at the N-terminus of the A $\beta$  peptide sequence. Four independent approaches led to the identification of the same candidate  $\beta$ -secretase: BACE-1 ( $\beta$ -site APP-cleaving enzyme). BACE-1 can also cleave APP and APP-CTF $_{\beta}$  at Glu-11 site of A $\beta$ , which results in decreased A $\beta$ . BACE-1 shares 55% homology with a second enzyme called BACE-2. Both proteins contain putative prodomains and two characteristic aspartyl protease catalytic motifs D (T/S) G (T/S) in their extracellular domains. They also share a significant homology with other members of the pepsin family of aspartyl proteases. However, in contrast to other proteases of this family, BACE-1 and BACE-2 are type I transmembrane proteins. In addition, BACE-1 is not inhibited by the classical aspartyl protease inhibitor pepstatin and functions optimally at lower pH (4.5-5.5). Heparin sulfate was found to be a negative natural regulator of BACE-1 activity (Vassar, 2004).

Although BACE-1 and BACE-2 are highly homologous, evidence indicates that BACE-1 is the main enzyme involved in neuronal A $\beta$  production. BACE-2 is predominantly expressed in peripheral tissue as well as in glia and is rather implicated in non-amyloidogenic processing of APP. BACE-2 was shown to be able to cleave in the middle of the A $\beta$  domain between phenylalanines 19 and 20 of A $\beta$  sequence. Thus BACE-2 appears to process APP very much like  $\alpha$ -secretase, thereby precluding A $\beta$  formation (Fluhrer et al., 2002).

BACE-1 undergoes complex *N*'-glycosylation and phosphorylation, as it is transported in the secretory and endosomal lysosomal pathway. It is stable for longer time, with a half life of 8 hr. Phosphorylation of BACE-1 cytoplasmic domain within the di-leucine motif modulates its interaction with Golgi-localized,  $\gamma$  ear-containing, ADP ribosylation factor-binding (GGA) proteins, which appear to regulate BACE-1 intracellular trafficking, especially sorting in the endosomal compartments (Wahle et al., 2006).

Initial reports suggested that the BACE-1 deficient mice were healthy, fertile and showed no obvious phenotype and also lacked A $\beta$ , which suggested BACE-1 as a target of choice for AD therapy. However, more recent studies indicated synaptic deficits and behavioral changes in BACE-1 knockout as well as transgenic mice. Increased morbidity, subtle electrophysiological alterations associated with hyperactive behavior has also been reported for

BACE-1 knockout mice. Interestingly, although generation of A $\beta$  was completely blocked in neurons, glial cells from these mice still secreted significant amount of amyloid (Walter, 2006).

BACE-1 does not seem to have stringent substrate specificity for APP. Similar to APP, APLP1 and APLP2 are also cleaved by BACE-1 (Li and Sudhof, 2004). P-selectin glycoprotein ligand-1 (PSGL-1), a protein which mediates leukocyte adhesion to endothelial cells and is critically involved in the inflammation, low density lipoprotein-related protein (LRP),  $\beta$  subunits of voltage-gated sodium channels are some other type I transmembrane proteins shed efficiently by BACE-1. A type II membrane protein,  $\alpha$ 2, 5-sialyltransferase (STGal1), which transfers sialic acid residues from CMP-sialic acid to acceptor glyco chains, was reported to be another physiological substrate of BACE-1. Recently, neuregulin III, a type I protein involved in axonal myelination was identified as physiological substrate of BACE-1 (Willem et al., 2006).

#### **2.1.2.5 $\gamma$ -secretase**

$\gamma$ -secretase is a multimeric membrane bound protein complex that catalyses regulated intramembranous proteolysis (RIP) of APP-CTFs generated by either  $\beta$ -secretase or  $\alpha$ -secretase to liberate A $\beta$  and p3, respectively. Four essential components of  $\gamma$ -secretase, namely Presenilin (1/2), Nicastrin, PEN-2 and APH-1 (Fig. 4) form a series of high molecular weight complexes and cooperatively regulate each others expression and maturation. The  $\gamma$ -secretase complex is sequentially assembled within the ER and *cis-Golgi* compartments. After maturation of its components, the assembled complex may be targeted to its sites of biological activity in late secretory/endocytic compartments and at the PM. Enzymatically active complexes have a mass that is much higher than the predicted mass for a 1:1:1:1 stoichiometric complex, which suggests the presence of other proteins in the complex or alternative stoichiometry. Recently, TMP21, a member of the p24 cargo protein family, was characterized as a protein associated with  $\gamma$ -secretase, which negatively regulates  $\gamma$ -secretase activity. PS1 is also known to interact with  $\beta$ -catenin, an important regulator of cadherin-based cell adhesion and intermediate in the Wnt signaling pathway. Moreover, kinases like GSK3 $\beta$ , PKA and PKC have been shown to associate with presenilin and regulate its phosphorylation and binding with  $\beta$ -catenin as well as caspases. Recent 3D electron microscope structure of  $\gamma$ -secretase complex reported by Lazarov and colleagues revealed a large cylindrical interior chamber which is postulated to provide a hydrophilic milieu necessary to accomplish peptide bond hydrolysis. Contribution of presenilins

trans-membrane domain 6 (TMD6) and TMD7 to such water containing cavity was verified by cysteine scanning. Pores at the top and bottom of the cylinder may release products of RIP into distinct subcellular compartments (Verdile et al., 2007).

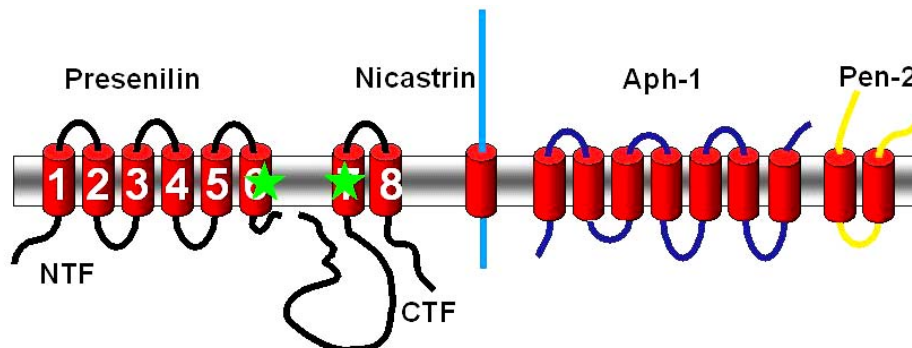


Fig. 4. **Diagrammatic overview of the core components of  $\gamma$ -secretase.** Minimum 18 transmembrane domains provided together by presenilin, nicastrin, APh-1 and PEN-2 form the necessary milieu for RIP. PS belongs to a group of polytopic aspartyl proteases with GXGD motif at the active site. Nicastrin is the largest component of complex, DYIGS domain in its extracellular region is required for its interaction with presenilin whereas a DAP domain is crucial for substrate recognition. Conserved motif GXXXG in APh-1 is essential for assembly and activity of complex. DYLSF domain in the c-terminal region of PEN-2 is required for its interaction with other components. The length of C-terminus of PEN-2 is critical for  $\gamma$ -secretase activity.

Nicastrin is a type I transmembrane glycoprotein, Yu et al. identified it biochemically as a genuine component of  $\gamma$ -secretase complex by co-purification with presenilin. This was further validated by the fact that nicastrin plays a crucial role in notch cleavage in *Drosophila melanogaster*, notch is another important type I protein reported to be cleaved by  $\gamma$ -secretase. Nicastrin plays an important role in stabilization and transport of other  $\gamma$ -secretase components. In turn, transport and stability of nicastrin is dependent on presenilin expression. Nicastrin acts as a gatekeeper of the  $\gamma$ -secretase complex. The extracellular domain of nicastrin binds specifically to the amino terminal residue of membrane bound protein fragments generated by sheddases and is then able to position the bound substrates to facilitate their cleavage by the catalytic presenilin subunit in the  $\gamma$ -secretase complex. Nicastrin knockout mice exhibit a very similar phenotype as that of notch and presenilin knockout mice as described later. Francis et al. identified two presenilin enhancers in *C. elegans* namely APh-1 and PEN-2. Both are multipass polytopic membrane proteins. APh-1a and APh-1b are the human orthologs of APh-1. APh-1a exists in two splice forms APh-1aS and APh-1aL. APh-1 stabilizes the presenilin holoprotein in the complex, whereas PEN-2 is required for endoproteolytic processing of presenilin thus conferring  $\gamma$ -secretase activity to the complex (Kaether et al., 2006).

### 2.1.3 Presenilins

Presenilins constitute the catalytic subunit of the  $\gamma$ -secretase complex and are conserved throughout evolution. Presenilin 1 (PS1) and Presenilin 2 (PS2) are the mammalian prototype members of a steadily growing protein family with a highly conserved GXGD motif at the catalytic site (Haass and Steiner, 2002). Two conserved aspartate residues, each present within the GXGD motifs of TMD6 and TMD7 are essential for  $\gamma$ -secretase activity. Additionally, the GXGD motif is also involved in substrate selection by the  $\gamma$ -secretase complex. This property could be exploited to explore specific means to inhibit cleavage of APP specifically. Lack of A $\beta$ /p3 and accumulation of APP-CTFs in primary neurons from PS1 knockout mice embryos as well as the characterization of  $\gamma$ -secretase as aspartyl protease established presenilins as mediators of  $\gamma$ -secretase activity. These studies also indicated that PS1 is the major presenilin involved in cleavage of APP, while PS2 although has the ability, does not seem to contribute much to APP cleavage by  $\gamma$ -secretase.

Presenilins are polytopic transmembrane proteins that are cleaved endoproteolytically shortly after biosynthesis, in the cytoplasmic loop located between TMD6 and TMD7. The cleavage yields characteristic 30-kD N-terminal fragment (NTF) and 20-kD C-terminal fragment (CTF). The NTF and CTF fragments are stable and incorporated in a 1:1 stoichiometry in a  $\gamma$ -secretase complex. Both PS1 and PS2 undergo phosphorylation *in vivo*. Moreover, PS1-CTF phosphorylation by PKC at Ser 346 is involved in the regulation of apoptosis (Fluhrer et al., 2004).

Prior proteolytic shedding of the large extracellular domain of a type I membrane protein seems to be a major prerequisite for it to be a  $\gamma$ -secretase substrate (Struhl and Adachi, 2000). In line with this, in addition to APP, more than two dozen PS1 substrates with diverse functions have been identified including notch, LRP, cadherin family members, APLP1/2, notch homologs, notch ligands delta and jagged, Erb4, CD44, nectin-1, voltage-gated sodium channel  $\beta$ 2-subunit, MHC class I protein HLA-A2. This has led to the hypothesis that the  $\gamma$ -secretase complex plays an important role in the degradation of membrane proteins (Kopan and Ilagan, 2004).

Knocking out PS1 in mice results in a phenotype that resembles a notch knockout to some extent. Moreover, a double knockout of both PS1 and PS2 shows a phenotype that is almost identical to the phenotype caused by the knockout of notch. Similar phenotypes were



observed in *Caenorhabditis elegans* and *Drosophila melanogaster* which could be functionally rescued by human PS1 or PS2. Notch is a type I transmembrane protein cleaved constitutively in the *Golgi* by furin like convertase, later interaction with ligand at the plasma membrane (PM) induces a subsequent cleavage by a disintegrin/metalloprotease, similar to cleavage of APP by  $\alpha$ -secretase, generating the notch extracellular truncation (NEXT)/notch C-terminal fragment. NEXT is processed by the  $\gamma$ -secretase complex to liberate notch intracellular cytoplasmic domain (NICD). NICD translocates to nucleus where it acts as a regulator of transcription. NICD dependent notch signaling pathway controls embryonic cell-fate decisions in variety of cell lineages. Hence, the lack of NICD generation in presenilin knockout mice results in notch phenotype (Sisodia, 2000).

Conditional inactivation of presenilins restricted to postnatal forebrain in mice results in reduced A $\beta$  generation and impairments in hippocampal memory and synaptic plasticity. With increasing age these mice also show neurodegeneration in the cerebral cortex, associated with worsening memory and deterioration of synaptic function. With its ability to cleave several type I membrane proteins, presenilins are involved in multitude of important biological processes, mainly via the regulation of gene transcription by intracellular domains of various substrates which are released after  $\gamma$ -secretase cleavage. Additionally, presenilins have also been implicated in  $\beta$ -catenin turnover, cellular Ca<sup>2+</sup> homeostasis, apoptosis, protein transport and phagocytic response (Shen and Kelleher, III, 2007).

### **2.1.4 Genetics of AD**

While 95% of all AD cases are sporadic with late age of onset (above 65 years), in a small group of patients, familial Alzheimer's disease (FAD) is inherited with an early age of onset. Mutations in three genes located on the chromosomes 21, 14 and 1, which are essential for A $\beta$  generation and are encoding APP, PS1 and PS2, respectively, have been shown to segregate with the disease. Indeed, presenilins were originally discovered by genetic approaches while searching for mutations causing early onset familial AD. Additionally, a trisomy of chromosome 21 (Down's Syndrome) which results in a triplication of APP-encoding gene and due to increased gene dose causes overproduction A $\beta$  as well as shows AD pathology (Roubertoux and Kerdelhue, 2006; Kahlem, 2006).

The majority of FAD associated mutations affect the generation of A $\beta$ , for example; the "Swedish" APP mutation (i.e. double mutation, K670N/M671L) causes enhanced production of

the two forms of A $\beta$ , A $\beta$ 40 and A $\beta$ 42 due to increased processing of APP by BACE-1. PS mutations seem to elevate A $\beta$ 42 selectively, which is thought to be more amyloidogenic and toxic form of the peptide (Butterfield et al., 1999). The mutations within the APP or PS genes result in a pathological and clinical phenotype that is indistinguishable from the more common late-onset sporadic forms of AD. Overexpressions of mutant human APP in mice produces plaque pathology, co-expression of mutant presenilins further hasten the plaque deposition. These mice also show behavioral and memory deficits and hence are widely used as animal models to study AD (Dewachter et al., 2001).

So far little more than 25 AD related mutations in APP and 10 in PS2 have been reported. More than 150 mutations in PS1 have been found to be linked with AD (a list of FAD mutations in each gene can be found at <http://www.molgen.ua.ac.be/ADMutations/>). Mutations in the APP protein are mainly located in and around the A $\beta$  domain where APP is cleaved by different secretases. The PS1 FAD mutations are more dispersed and are located within or around the all of the highly conserved hydrophobic TMDs (Fig. 5). Most of these are missense mutation with few other types like  $\Delta$ Exon 9 mutation, which is caused by mutations in the splice acceptor site of exon 9. This results in the deletion of residues 291-391 of the protein and change of S290 to cysteine at the splice site. This mutation alters metabolism of presenilin as it deletes the endoproteolytic cleavage site within presenilin. A splice donor site mutation  $\Delta$ 4 has also been reported. This mutation causes many transcripts of the gene leading to truncated forms of proteins. All of these mutations lead to increased plaque deposition and early age of onset AD. Some mutations, for example the polish mutation, P117L, lead to death as early as 28 yrs of age, underscoring the importance of proper PS1 function. Another very aggressive PS1 mutation, L166P, not only induces an exceptionally high increase of A $\beta$ 42 production as mentioned previously but also impairs NICD production and notch signaling, as well as AICD generation. However, no other obvious phenotype is observed in the AD patients carrying these mutations (Menendez, 2004; Tanzi and Bertram, 2005; Perez-Tur et al., 1995).

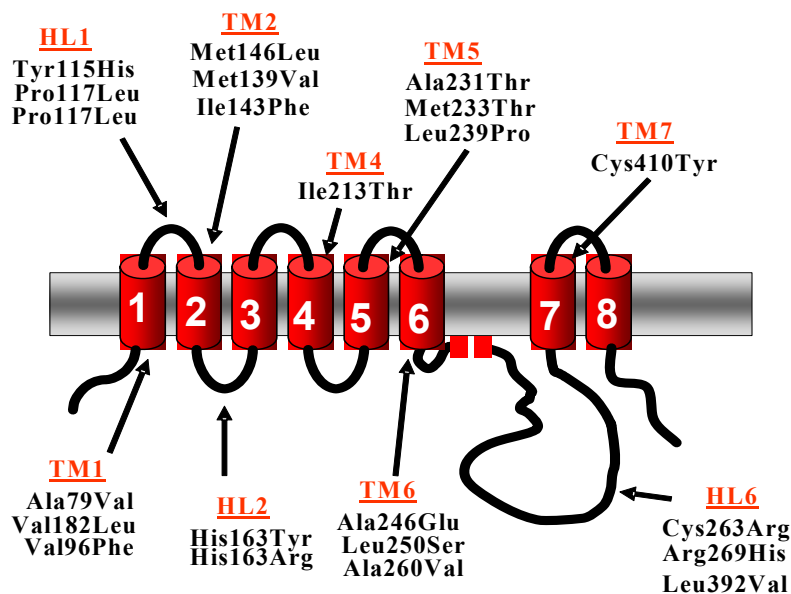


Fig. 5. **PS1 FAD mutations.** Some of the missense FAD mutations in PS1 protein are shown in the diagram. As indicated mutations are not localized in a particular region of the molecule. So far, more than 150 such mutations have been reported in PS1, however only 10 such mutations have been identified in PS2, (adapted from [www.alzforum.org](http://www.alzforum.org)).

In addition, the  $\epsilon 4$  allele of apolipoprotein E (Apo E) is a major risk factor for developing late onset AD. The Apo E gene is present on chromosome 19 and encodes a circulating lipid transport glycoprotein. It is expressed predominantly in liver, but is also expressed in brain primarily by microglia and astrocytes. Neurons in CNS also express Apo E, albeit at a lower level. (St George-Hyslop, 2000; Tanzi and Bertram, 2005).

In humans, there are three common Apo E alleles present:  $\epsilon 2$ ,  $\epsilon 3$  and  $\epsilon 4$ . The three differ only by one or two amino acids ( $\epsilon 2$  - Cys112Cys158;  $\epsilon 3$  - Cys112Arg158;  $\epsilon 4$  - Arg112Arg158) but confer at least twenty fold difference in the risk for developing AD ( $\epsilon 4 > \epsilon 3 > \epsilon 2$ ). Presence of the  $\epsilon 4$  allele also decreases the mean age of onset significantly. Increased frequency of  $\epsilon 4$  allele in AD patients, compared to age-matched healthy controls, has been widely reproduced in numerous epidemiological studies from variety of populations of diverse ethnic origin. By contrast, inheritance of the other alleles appears to reduce the risk of developing AD, even when combined with  $\epsilon 4$  allele or in patients with downs syndrome (Strittmatter and Roses, 1995). It should be emphasized, however, that the  $\epsilon 4$  allele of Apo E does not confer an absolute predisposition to develop AD. Thus, the  $\epsilon 4$  allele is a true genetic risk factor, most likely interacting with other genetic and/or nongenetic factors to facilitate AD. Apo E seems to play a critical role in deposition and fibrilization of A $\beta$  to form amyloid and neuritic plaques in an

isoform dependent manner. However, the detailed cellular mechanism behind this remains to be elucidated. Possible explanation could be the involvement of Apo E in A $\beta$  endocytosis and subsequent clearance as well as differential affinity of Apo E isoforms to A $\beta$  (Carter, 2005).

### **2.1.5 Amyloid Hypothesis**

Over the past two decades understanding of molecular mechanisms involved in AD has increased considerably, which has led to the formation of several hypotheses. Especially the “amyloid hypothesis” and “neuronal cytoskeletal degeneration hypothesis”, emphasizing the role of A $\beta$  in neurodegeneration (Hardy and Selkoe, 2002) and tau in axonal transport respectively, have been widely discussed. Other hypotheses focussed on dysfunction of cholinergic system (Francis et al., 1999), Ca<sup>2+</sup> signaling deficits (Mattson, 2002), NMDA receptor hypofunction, disruption of APP signaling and cell cycle abnormalities, mitochondrial dysfunction forward (Swerdlow and Khan, 2004) have also been put. However, none of the hypotheses is clinically proven and each hypothesis falls short of offering clear molecular basis for AD. Nonetheless the “amyloid hypothesis” has gained widespread acceptance and is the predominant scientific explanation for the cause of AD over the past two decades. An emerging consensus in the field indicates that AD is a complex disorder with involvement of multiple environmental and genetic factors, in other words AD could be considered as a multifactorial syndrome (Shua-Haim and Gross, 1996; George-Hyslop and Petit, 2005).

The "amyloid hypothesis" states that AD is initiated by the enhanced production, aggregation and deposition of the toxic amyloid beta (A $\beta$ ) peptide leading to impaired cell-to-cell communication compromising synaptic function, eventually causing the death of neurons in the brain (Fig. 6). The strongest evidence for the “amyloid hypothesis” comes from studies of the rare familial forms of AD from fact that all the FAD mutations have been shown to affect generation/aggregation of A $\beta$ .

Other multiple factors which affect A $\beta$  generation, clearance and deposition are believed to be involved in the onset of sporadic forms of AD. Various factors like age, ischemia, oxidative stress, higher caloric intake, and head injury, inflammation etc. in concert with Apo E or alone could further modify A $\beta$  metabolism and deposition (Behl, 2005). The “amyloid hypothesis” is further amended and extended to accommodate more recent findings such as the predominant role of A $\beta$  oligomers in the disease than monomers or amyloid plaques (Walsh and Selkoe, 2007) and the presence of toxic intracellular amyloid, as well as modulation of tau phosphorylation by

A $\beta$  through regulation of kinases and phosphatases ( Blurton-Jones and LaFerla, 2006; Billings et al., 2005).

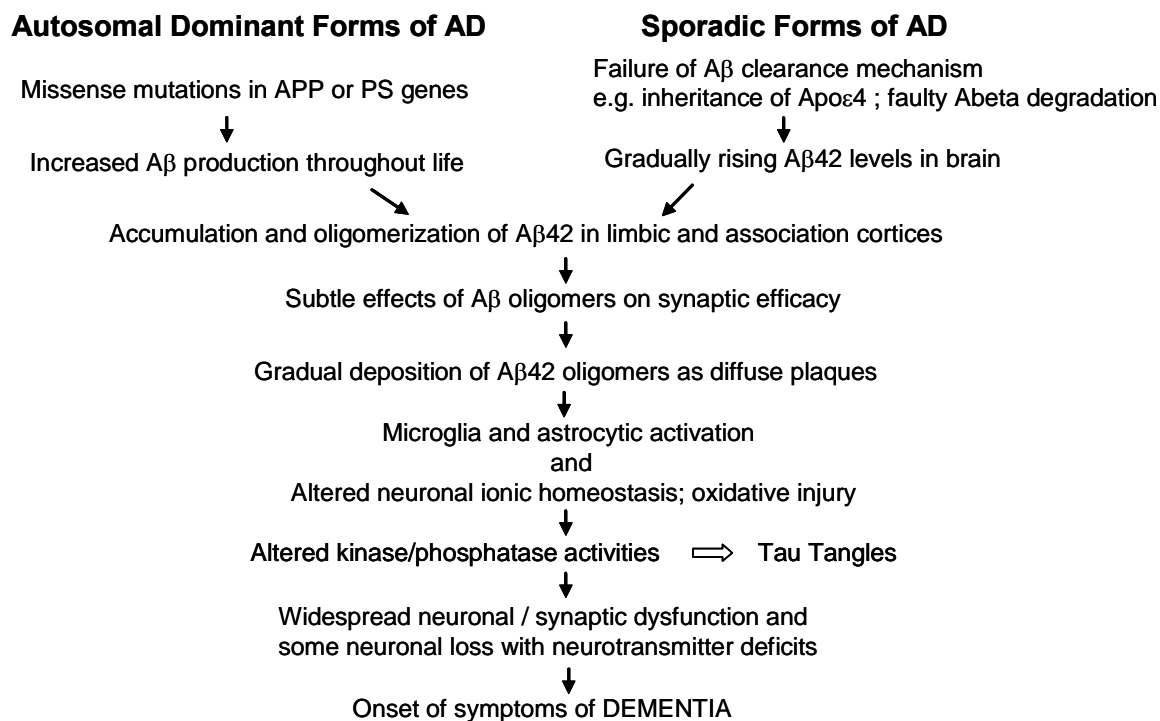


Fig. 6. **The “amyloid cascade”**. The sequence of pathogenic events leading to AD as proposed by the “amyloid hypothesis”. The cascade of events is initiated by altered A $\beta$  metabolism, leading to elevated A $\beta$  levels in limbic and association cortices. A $\beta$  can also directly affect neuronal ionic homeostasis and induce oxidative stress or alter tau phosphorylation.

The toxic nature of the A $\beta$  peptide has been demonstrated by its ability to interfere with many important biological processes such as apoptosis, Ca<sup>2+</sup> storage and release, proteasomal activity, receptor endocytosis as well as synaptic function and long term potentiation (LTP). A $\beta$  also contributes to oxidative stress and binding of A $\beta$  to membrane lipids is proposed to disrupt the metabolism and function of various membrane proteins and lipids (Marchesi, 2005) (Mattson, 1997). Indeed, there is a large body of evidence in support of the “amyloid hypothesis”, but there are also several inconsistencies with the idea that A $\beta$  in one form or the other is unitary cause of AD. Nevertheless, the “amyloid hypothesis” successfully links most genetic findings with pathological and biochemical changes characteristic of AD (Hardy, 2006).

## **2.2 Membrane lipids – classification, structure, function**

Biological membranes are composed of a lipid bilayer with associated proteins and form a semi-permeable barrier, which not only separate the interior of the cell from its environment but also define the internal compartments of eukaryotic cells, including nucleus and vesicular organelles (Singer and Nicolson, 1972; Singer, 2004). Most membrane lipids are amphipathic, with polar/hydrophilic head groups and long non-polar/hydrophobic tails. Lipid molecules spontaneously associate in aqueous surrounding to bury their hydrophobic tails in the interior and expose their hydrophilic heads to water that causes them to form bilayers. Each monolayer of the bilayer shows strikingly different lipid composition, which gives rise to a characteristic asymmetry to bilayer. Depending on the structure, membrane lipids are broadly classified into three groups - phospholipids, glycolipids and sterols as depicted in Fig. 7 (Spector and Yorek, 1985; Fantini et al., 2002).

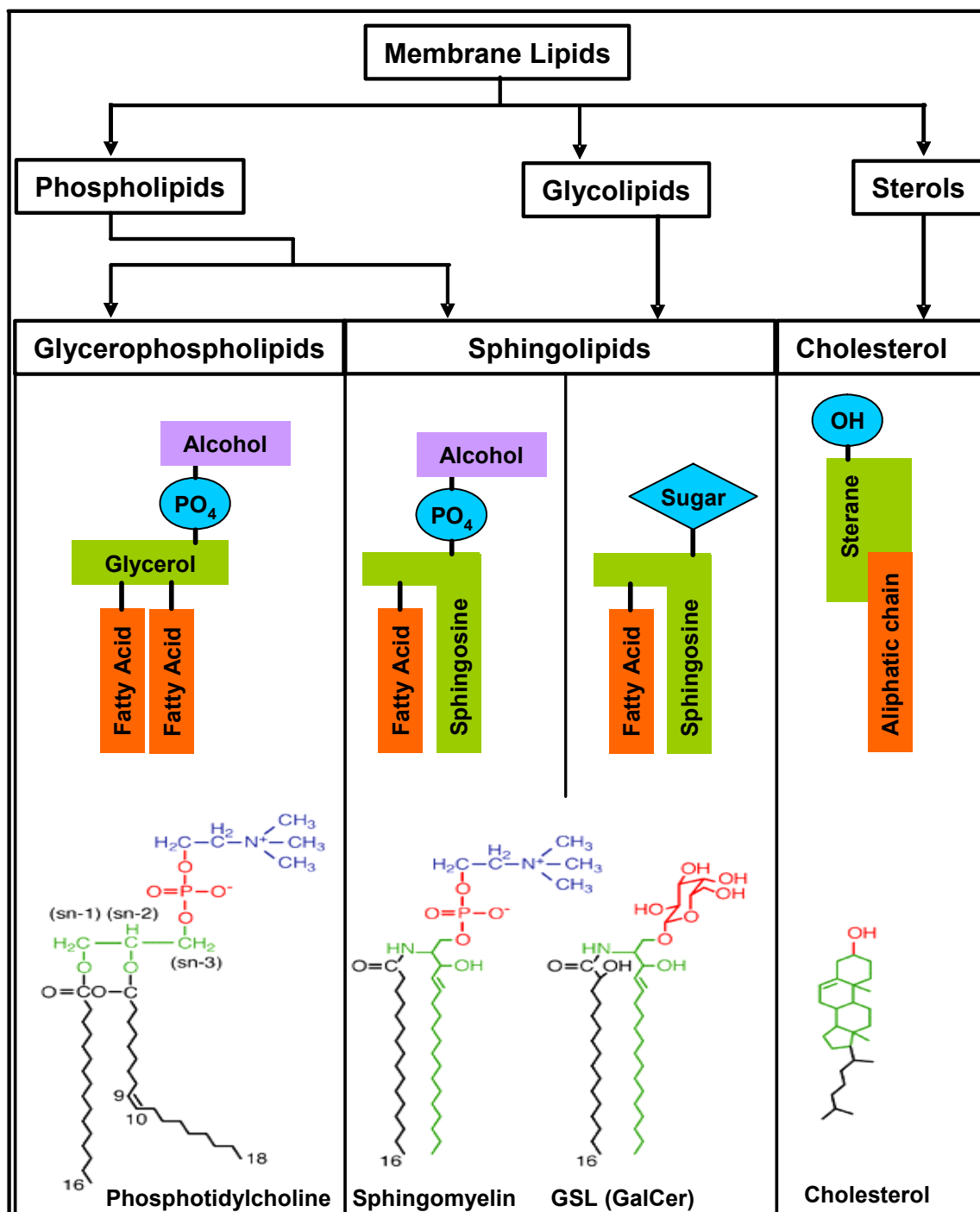


Fig. 7. **Classification of membrane lipids.** Phospholipids are principal types of lipids in almost all cellular membranes, whereas cholesterol amounts vary depending upon the type of membrane, plasma membrane may have one cholesterol molecule per phospholipid. Glycolipids type and amounts changes greatly with cell type. Representative structural depiction along with one example is denoted in the picture. GalCer stands for a glycosphingolipid (GSL) galactosyl ceramide, (adapted) from Fantini et al., 2002). Note that the drawings of the lipids in above figure represent the general structure and do not describe the stereochemical nature of covalent bonds therein.

### **2.2.1 Phospholipids**

The most common phospholipids, phosphatidyl choline consists of a glycerol linked to two fatty acid chains, phosphate and choline (Fig. 7). Besides, the other head groups such as serine, ethanolamine and inositol form the respective glycerophospholipids namely phosphatidylserine, phosphatidylethanolamine and phosphatidylinositol. Since these types of phospholipids contain glycerol, they are called glycerophospholipids. Another type of phospholipids contain a sphingosine backbone instead of glycerol. Sphingosine has a long hydrocarbon chain and a polar amino group. The amino group of sphingosine can form an amide bond with a carboxyl group of fatty acids to yield ceramide. Ceramide is esterified at the terminal hydroxyl group with phosphocholine to form sphingomyelin, which is the most common type of phosphosphingolipid (Bishop and Bell, 1988).

Phosphatidylcholine, phosphatidylethanolamine, phosphatidylserine and sphingomyelin – these four phospholipids constitute more than half of the lipid mass in most membranes. Phosphatidylserine is predominantly present in the cytosolic monolayer and carries a net negative charge at neutral pH, which contributes to the asymmetry of the membrane. Certain cellular kinases like PKC that are activated in response to extracellular signals require negatively charged lipids in the inner membrane leaflet for binding and activity. Phospholipids such as inositol phospholipid, are present in smaller quantities but are essential for the recruitment of kinases and proteins from cytosol that are involved in signaling and protein transport. The cleavage of phosphoinositols and sphingomyelin by lipases generates active lipid molecules involved in cell signaling, apoptosis, ER  $\text{Ca}^{2+}$  release etc (Ikeda et al., 2006).

### **2.2.2 Glycolipids**

Glycolipids, the minor components of cellular membranes mainly present in the non-cytosolic leaflet are named so because of the presence of sugar moiety as a hydrophilic head group. Glycosphingolipids (GSLs) are the most common type of glycolipids. Apart from species dependence, GSLs form cell type specific patterns on the cell surface. These patterns change with cell growth, differentiation, viral transformation, ontogenesis and oncogenesis (Hakomori, 1981; Levery, 2005). Together with glycoproteins and glycosaminoglycans, GSLs contribute to the glycocalyx, which covers the cell surface with a protective carbohydrate layer. In plants and bacteria glycolipids are build on glycerol backbone, therefore termed as glyceroglycolipids. In animals glycolipids predominantly have a sphingosine (ceramide) backbone and hence they are called glycosphingolipids. Cerebrosides are simple GSLs with a monosaccharide moiety such as



glucose or galactose as a polar head group. Sulfate esters of galactosylcerebrosides, called sulfatides, are a special class of GSLs (Thompson and Tillack, 1985).

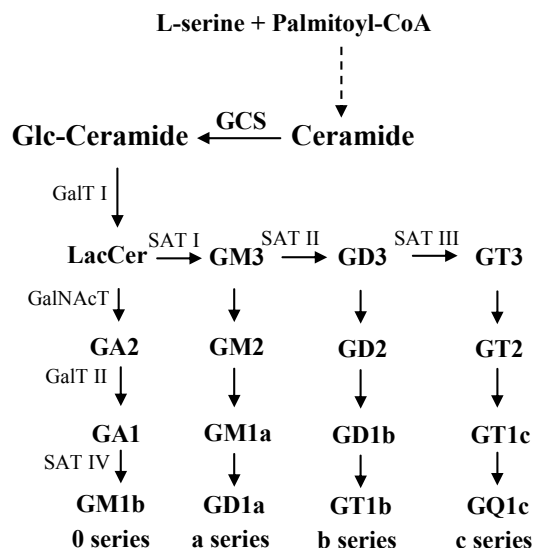


Fig. 8. **Combinatorial biosynthesis of GSLs in humans.** Lactosylceramide and its sialyated derivatives, the hematosides GM3, GD3 and GT3 serve as precursors for complex gangliosides of the 0-, a-, b- and c-series. These different series are characterized by the presence of no (0-series), one (a-series), two (b-series) or three (c-series) sialic acid residues linked to inner galactose moiety. In adult human tissues, gangliosides from 0- and c-series are found only in trace amounts. Presence of sialic acid gives rise to negative charge to ganglioside, respective sialic acid transferase (SAT) at distinct stage adds sialic acid residue.  $\beta$ 1,4-*N*-acetylgalactosaminyltransferase (GalNAcT) transfers *N*-acetylgalactosamine, (modified from Kolter et al., 2002).

Gangliosides are GSLs with complex oligosaccharides as head groups including the acidic sugar derivative sialic acid and are predominantly present in the outer leaflet of bilayer. Variations in type, number, linkage and further modification of sugar- and sialic acid residues within the oligosaccharide chain, but also within the lipid moiety gives rise to a large variety of naturally occurring GSLs. The biosynthesis of GSLs starts with the synthesis of ceramide from serine and palmitoyl-CoA in the ER (Sandhoff and Kolter, 2003; Tettamanti, 2004). Ceramide is later transported to *cis-Golgi* where it acts as a substrate for glucosylceramide synthase (GCS). GCS transfers the glucose residue from UDP-glucose to ceramide, to form glucosylceramide. Glucosylceramide is modified to lactosylceramide with addition of galactose by the action of lactosylceramide synthase (LCS)/galactosyltransferase I (GalT1). In subsequent steps a variety of sugar residues, including negatively charged sialic acid are added to lactosylceramide in the *Golgi* compartment in a combinatorial GSLs biosynthesis (Fig. 8). Ceramide also acts as a substrate for galactocerebrosides and sulfatides.

Gangliosides and sulfatides of the myelin layer are the major constituents of neuronal membranes. Besides being structural components of the membrane, gangliosides are modulators of important biological processes such as cell proliferation and adhesion, inflammation, neuronal differentiation as well as establishment of cellular polarity. Particularly, the ganglioside GM1 has been shown to regulate axonal elongation and synaptogenesis. GSLs also potentiate the effect of neurotrophic factors and act as ligands for various receptors involved in nerve regeneration. One

example of such lipid receptor is the myelin associated glycoprotein (MAG). Recently, GSLs were also shown to induce microglial activation and thereby contribute to inflammation in brain via toll like receptor 4 and the JAK-STAT signaling cascade. Moreover, certain GSLs, for example the GM3, act as a modulator of neuronal cell death. Ganglioside GM3 is also reported as a negative regulator of insulin signaling, making it a potential therapeutic target in type II diabetes. On the cellular level, gangliosides could prevent glutamate and kainate toxicity as well as participate in signal transduction and protein transport. Additionally, gangliosides also serve as functional receptors for various bacterial toxins and are responsible for endocytosis of such toxins. Importantly, sphingolipid biosynthesis has been shown to be necessary for dendritic growth and survival of Purkinje cells (Hoekstra et al., 2003; Smith and Merrill, Jr., 2002).

Sphingolipids are highly enriched on the plasma membrane, but are also internalized and transported to late endosomes and lysosomes where they are degraded in a stepwise fashion, finally resulting in the cleavage of ceramide to sphingosine and fatty acid (Kolter and Sandhoff, 2005). Each of the steps in degradation is carried out by a specific enzyme, water-soluble acid exohydrolase, usually assisted by helper proteins termed sphingolipid activator proteins (SAPs) which present the substrate to hydrolytic enzyme. The SAPs known to date are encoded by only two genes. One gene carries the information for the GM2-activator and other for the Sap-precursor also called prosaposin. Prosaposin is post-translationally processed to four homologous mature proteins, Saps A-D, or saposins A-D. Mutations in either hydrolases or activator proteins lead to defective hydrolysis and accumulation of lipids (Neufeld, 1991; Kolter and Sandhoff, 2006). Fig. 9 depicts the major sphingolipid storage disorders (SLSDs) with the respective deficient enzymes. In Niemann Pick C (NPC) disease and Mucopolipidosis Type IV, lipid accumulation appears to occur as a result of a defect in the transport to or from lysosomes rather than degradation (Abe et al., 2001).

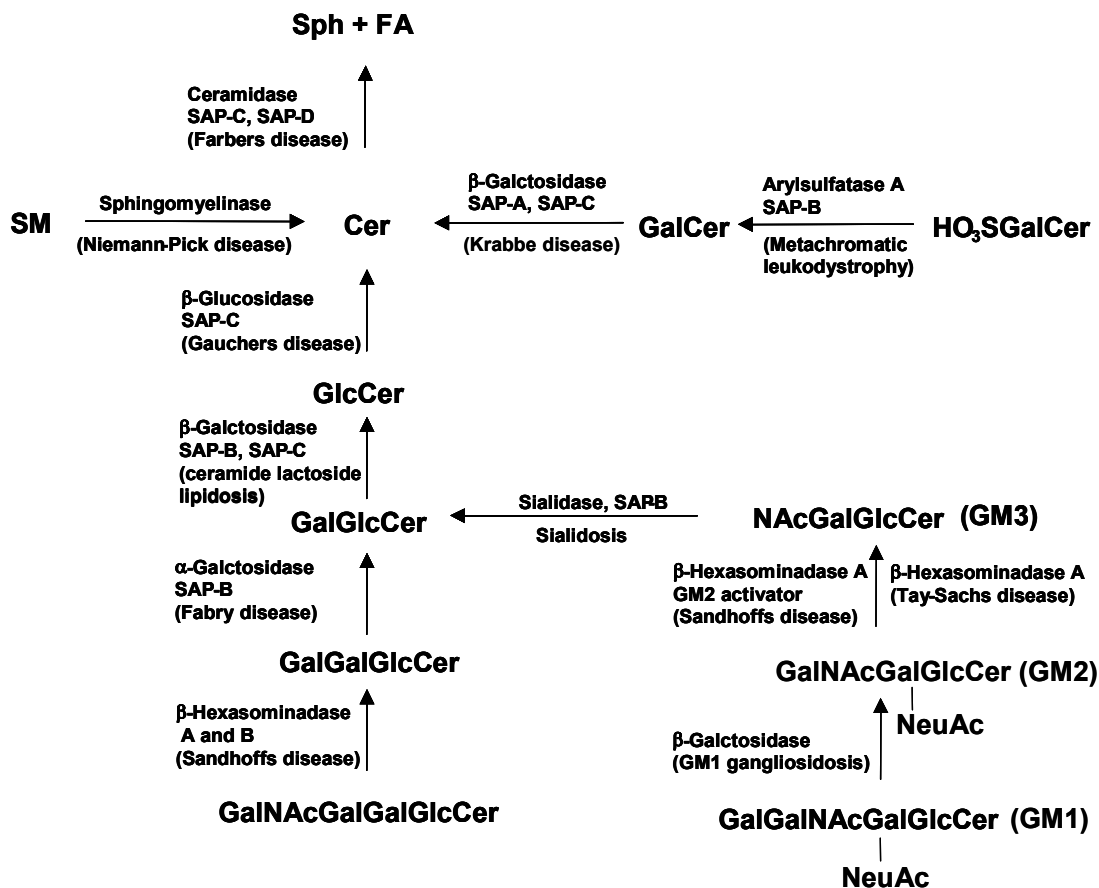


Fig. 9. **GSLs catabolism pathways and disease.** The lysosomal enzyme deficiency diseases are indicated in parentheses. NeuAc, N-acetylneuramic acid; Cer, ceramide; Glc, glucose; Gal, galactose; GalNac, N-acetylgalactosamine; SM, sphingomyelin; HO<sub>3</sub>SGalCer, sulfatide; Sph, sphingosine; FA, fatty acid; SAP, sphingolipid activator protein. Genetic defect in respective enzymes affects the degradation of particular GSLs causing accumulation, (adapted from Abe et al., 2001).

### 2.2.3 Cholesterol

The most abundant member of the sterol family is cholesterol. Cholesterol contains a four-ring steroid structure with a short-branched hydrocarbon chain. Cholesterol is largely hydrophobic, but its polar hydrophilic hydroxy group makes it amphipathic. The interior of a lipid bilayer is normally highly fluid. Presence of *cis* double bonds in the hydrophobic fatty acid chains as well as relatively rigid structure of cholesterol act as important regulators of membrane fluidity. In eukaryotic cells, non-esterified/free cholesterol is found in membranes (primarily in the plasma membrane and to a lesser extent in organelle membranes) whereas, cholesteryl esters are present in cytosolic lipid droplets (Liscum and Underwood, 1995; Soccio and Breslow, 2004; Martin and Parton, 2006). An over accumulation of free cholesterol can be toxic to cells (Tabas, 2002). To regulate the cholesterol content in the membranes, it is converted to cholesterol esters primarily by the enzyme acyl CoA: cholesterol acyltransferase (ACAT). On the other hand, neutral cholesterol ester hydrolase breaks down cholesterol esters liberating free cholesterol.

Cholesterol is needed for the growth and viability of mammalian cells. Besides being an important structural and functional element of cellular membranes, cholesterol also serves as a precursor to other bioactive metabolites, like bile acids, oxysterols and steroid hormones that have important physiologic functions. Cholesterol is derived from the diet as well from endogenous biosynthesis. Both, overall cholesterol content of the cell as well as its distribution in specific organelle membranes is stringently controlled. Cellular cholesterol homeostasis is achieved by a number of molecular mechanisms that regulate its uptake and secretion, as well as biosynthesis and metabolism. The biosynthesis of cholesterol occurs at membranes of the Endoplasmic Reticulum and involves multiple enzyme activities (see 4.2.2). Endogenously synthesized cholesterol is readily transported from its site of synthesis to the plasma membrane (DeGrella and Simoni, 1982; Lange and Matthies, 1984; Kaplan and Simoni, 1985). The plasma membrane of animal cells is thought to contain many small lipid microdomains (~70 nm in diameter), which are rich in sphingolipids and cholesterol (Simons and Ikonen, 1997). Proteins with lipid anchors tend to accumulate in such microdomains. Importantly, caveolin, a protein important for endocytosis, is found to be associated with cholesterol rich microdomains. However, since no current technique can provide the sufficient proof for the presence of such microdomains, their existence remains highly controversial.

Between organs and cells, cholesterol is mainly transported by lipoprotein particles that can be taken up by cells via surface receptor-mediated endocytosis (Fielding and Fielding, 1997; Herz, 2001). The major lipoprotein particle involved in cholesterol transport in the peripheral system is the low density lipoprotein (LDL) that binds to the LDL receptor (LDLR) at the surface of receiving cells. The binding to LDLR results in the clathrin-dependent endocytosis of LDL, containing cholesterol, into early endosomes and subsequent transport to endocytic recycling compartments. Here LDLR dissociates from LDL and is recycled back to the PM. Internalization of LDLR is dependent on a tyrosine-based signal within its cytoplasmic domain that is recognized by the autosomal recessive hypercholesterolemia (ARH) protein, that facilitates internalization of LDLR by connecting the receptor to clathrin in coated pits and vesicles (Mishra et al., 2002; Chang et al., 2006).

The uptake of extracellular cholesterol decreases the de novo-synthesis of cholesterol by feed-back mechanisms that control the expression of genes encoding metabolic enzymes. The major factors in the transcriptional regulation of biosynthetic enzymes are the sterol regulatory element binding proteins (SREBPs) that are activated at low cholesterol levels by proteolytic

cleavage and ensuing translocation in the nucleus. In fact, the first example of RIP was described for the sterol regulated element binding protein (SREBP) that controls cholesterol homeostasis in vertebrate cells. At low cholesterol levels SREBP is transported from the ER to a post ER/*Golgi* compartment, where it undergoes sequential cleavage by site-specific proteases site-1 protease (S1P) and site-2 protease (S2P), thereby allowing translocation of the cytoplasmic domain from the membrane to the nucleus to regulate transcription of target genes involved in cholesterol metabolism, including the low density lipoprotein receptor and the key enzymes in cholesterol biosynthesis. Higher cholesterol levels inhibit transport of SREBP from the ER to the post ER/*Golgi* compartment precluding proteolytic processing by S1P and S2P leading to down-regulation of cholesterol biosynthesis (Goldstein et al., 2006).

Besides SREBPs, liver X receptors (LXRs), members of the nuclear receptor superfamily also play a pivotal role in maintaining cholesterol and lipid homeostasis via transcriptional regulation (Rigamonti et al., 2005). In the excess of cholesterol, certain oxidized derivatives of cholesterol act as natural ligands of LXRs. Binding with ligand leads to their activation and attachment at LXR responsive elements (LXREs) of target genes, as obligate heterodimers with 9-*cis*-retinoic acid receptors (RXRs). LXREs have been identified in the regulatory regions of a number of genes involved in cholesterol metabolism including CYP7A1, which catalyzes the first and rate-limiting step in bile acid synthesis, cholesterol ester transport protein, the transcription factor SREBP-1c, Apo E and some LXR genes itself. LXREs have also been identified in the genes encoding the ATP binding cassette transporters (ABC) A1 and G1, which mediate the efflux of cholesterol as well as phospholipids. Thus, LXRs are important components of the complex regulatory system that senses cholesterol levels and modifies gene expression accordingly (Desvergne et al., 2006; Zelcer and Tontonoz, 2006).

Although brain accounts for only 2% body mass, approximately 25% of the total body cholesterol is found in the brain. It is largely present in two pools comprised of the cholesterol in the plasma membranes of glial cells and neurons, and myelin associated cholesterol. Unlike most other extrahepatic tissues more than 95% of the cholesterol content in the brain can be accounted for by *de novo* synthesis, and there is little if any exchange of plasma and brain cholesterol. Under steady state conditions, synthesis of cholesterol in the brain is balanced by excretion of the cytochrome P-450 generated 24S-hydroxycholesterol, which is capable of traversing the blood-brain barrier (Bjorkhem and Meaney, 2004). It is widely believed that neurons depend on glial cells for their cholesterol needs. However, recent studies have demonstrated the ability of

neurons to synthesize cholesterol under certain conditions (Pfrieger, 2003). Notably, Apo E, a major risk factor for AD, is one of the important lipoproteins involved in cholesterol shuttling between neurons and astrocytes. Apo E is also essential for remodeling and reorganization of neuronal networks after injury, stress and in maintaining neuronal plasticity (Bales et al., 2002).

## **2.3 Rationale and Aim of the study**

A strong etiological association exists between dysfunctional metabolisms of brain lipids, age related changes in cerebral vasculature and neurodegenerative features characteristic of AD brain (Walkley, 1998; Han, 2005). Changes in membrane fluidity in AD were reported in the early 90s. Several independent studies have shown that the ganglioside pattern, distribution, metabolism and amounts are significantly different in the brains of AD patients. However, the exact role and molecular mechanism by which these lipids regulate the APP processing is not well understood. At the cellular level, APP and GSLs follow very similar transport routes and to some extent common metabolic fates. Following synthesis in the ER, APP undergoes extensive posttranslational modifications in the *Golgi*, from where it is routed to the cell surface and endosomal-lysosomal recycling compartments, where it is either sequentially cleaved by secretases or degraded in lysosomes and proteasomes. In a similar fashion GSL biosynthesis starts in the ER with the synthesis of ceramide, which is later transported to the *Golgi*, where a variety of sugar molecules are added to it to give rise to complex GSLs, from here they are transported to the cell surface and endosomal lysosomal recycling compartments. The degradation of GSLs takes place in lysosomes (van Meer, 1989; Schwarzmann and Sandhoff, 1990; Kolter and Sandhoff, 2005). Therefore, in the first part of the present studies, it was planned to investigate the role of GSLs on APP processing. Accordingly, various approaches undertaken to modulate cellular GSL levels would be introduced in this part. First, the use of pharmacological inhibitors to deplete the cells of GSLs and the treatment of cells with purified bovine brain gangliosides to enrich them with GSLs along with effects of these treatments on APP metabolism would be described in detail. Secondly, analysis of genetic models for GSLs deficiency as well as excess would also be discussed. Besides pre-existing genetic models, the use of RNAi technology to suppress the key enzymes involved in GSL biosynthesis would also be presented here. Studies addressing the APP processing and subcellular transport with associated mechanisms in all of the above conditions would be discussed. Towards this end the metabolism of full length APP as well as individual metabolic products of APP, namely, soluble

APP, APP-CTFs and A $\beta$  studied by various biochemical and cell biological techniques after manipulation of cellular GSL levels would be revealed.

Number of studies have focused on the effect of cholesterol metabolism on the regulation of AD associated proteins and A $\beta$  generation (Wolozin et al., 2006). However, few studies addressed the role of AD associated proteins and their processing products on cholesterol metabolism. Importantly, an alteration of cholesterol distribution by U17666A treatment or as it is observed in the NPC disease model mice have been shown to cause redistribution and accumulation of presenilin into endosomal compartments (Burns et al., 2003). These studies indicate a close link of presenilin and cholesterol subcellular localization, which might further be extended to cholesterol metabolism and  $\gamma$ -secretase activity.  $\gamma$ -secretase has also been shown to be associated with lipid microdomains rich in cholesterol. The second part of the studies is an attempt to decipher the link between presenilins and cholesterol. More precisely the role of presenilin mediated RIP in regulation of cholesterol homeostasis would be addressed in this part. Few earlier studies looked at the effect of cholesterol metabolism on presenilin activity and transport. To elucidate the role of presenilins in cholesterol metabolism, a comprehensive analysis of cholesterol metabolites in various genetic models with presenilin deficiency and expression, as well as after pharmacologic inhibition of  $\gamma$ -secretase activity would be presented. Furthermore, the mechanism by which presenilins affect the cholesterol metabolism would also be addressed to some extent.

Together the aim of the study would be to elucidate the co-regulatory mechanisms involved in the metabolism of membrane lipids and AD associated proteins.

### 3 Materials and Methods

All the standard chemicals used for analysis were from Roth. Radiochemicals were obtained from MP Biomedicals. Nucleotides were ordered from Sigma Genosys. Cell culture medium and other biochemicals for cell culture were from Invitrogen. Plastic ware for cell culture was from Corning. For quantitation three independent experiments (n=3) were carried out. Statistical analysis was carried out using Student's T-test. Significance values are as follows: \* (p<0.05); \*\* (p<0.01); \*\*\* (p<0.001).

#### 3.1 DNA recombination techniques

##### 3.1.1 Instruments and materials

PCR-machine (Mastercycler)	Eppendorf
Agarose gel electrophoresis unit	Amersham Pharmacia
Thermomixer	Eppendorf
Agarose gel electrophoresis unit	Eppendorf
UV transilluminator	Syngene
Documentation system (CCD camera, printer)	INTAS
37 °C bacterial incubator	Binder
Bacterial shaker	Edmund Bühler
Block heater	Stuart Scientific
Photometer (Genesis)	Thermo

##### 3.1.2 Quantitation of nucleic acid

Following equation was used to quantitate dsDNA

$$\begin{aligned}\text{DNA concentration } (\mu\text{g}/\mu\text{l}) &= \text{O.D. } 260 \times 10^{-3} \times 50 \times \text{Dilution factor (1 to 20)} \\ &= \text{O.D. } 260 \times 10^{-3} \times 10^3\end{aligned}$$

$$\text{DNA concentration } (\mu\text{g}/\mu\text{l}) = \text{O.D. } 260$$

Following equation was used for RNA quantitation

$$\begin{aligned}\text{RNA concentration } (\mu\text{g}/\mu\text{l}) &= \text{O.D. } 260 \times 10^{-3} \times 40 \times \text{Dilution factor (1 to 40)} \\ &= \text{O.D. } 260 \times 1.6\end{aligned}$$

$$\text{RNA concentration } (\mu\text{g}/\mu\text{l}) = \text{O.D. } 260 \times 1.6$$



### 3.1.3 Constructs and Cloning

#### Vectors

Vector Name	Source	Expression System	Resistance
pcDNA3.0 Neo	Invitrogen	Eukaryote cells	Neomycin
pcDNA3.1 Zeo (+)	Invitrogen	Eukaryote cells	Zeocin
pSUPER	Dr. Agami	Eukaryote cells	-----
pTER	Dr. Agami	Eukaryote cells	Zeocin

Table 1. **Overview of the vectorsystems used.** Mentioned vector systems were used in the study. pcDNA3 and 3.1 has neomycin (Neo) and zeocin (Zeo) resistance gene respectively, for stable expression. pSUPER vector does not have any resistance for expression into eukaryotes whereas pTER has zeocin resistance.

#### DNA constructs

Gene	Vector	Restriction sites
APP695	pcDNA3.0 Neo	HindIII; XbaI; BamH1(internal)
APP695	pcDNA3.1 Zeo (+)	HindIII; XbaI; BamH1(internal)
PS1-WT	pcDNA3.1 Zeo (+)	
PS1-L166P	pcDNA3.1 Zeo (+)	
PS1-M146L	pcDNA3.1 Zeo (+)	
PS1-dEX9	pcDNA3.1 Zeo (+)	

Table 2. **Overview of the DNA constructs.** The APP 695 gene was subcloned from pcDNA3.0 Neo into pcDNA3.1 Zeo. Presenilin DNA constructs were generous gift from Dr. Haass.

### 3.1.4 Polymerase chain reaction (PCR)

#### Reaction volume (1X Mix)

10X PCR Buffer with MgSO <sub>4</sub> (MBI)	5 µl
dNTPs (10mM) (MBI)	1 µl
Forward Primer (100 pmol/µl)	1 µl
Reverse Primer (100 pmol/µl)	1 µl
Template cDNA (conc. 100ng/µl)	1 µl
<i>pfu</i> polymerase (MBI)	0.5 µl ( 1U/µl)
make final volume to 50µl with dH <sub>2</sub> O	X µl
	50 µl

Gene	Oligonucleotides (Sigma)
APP695-fw	CCCAAGCTTGATGCTGCCCGGTTTGGC
APP695-rev	GCTCTAGAGGGTCTAGTTC
APP695-fw	CATGGTGGATCCCAAG

Table 3. **Primers used for cloning.** Primers mentioned in table were used to subclone APP.

## **PCR Programme**

Following program was used to amplify various respective constructs. Amplification time for each construct was variable and was approximately set according to 1 min per 1000 bps.

95°C, 4 min

95°C, 45 sec	} 22 cycles
60°C, 45 sec	
72°C, X min Y sec	

72°C, 20 min

Respective PCR products were visualized in agarose gels. Further purification of PCR was performed by gel extraction (Machery-Nagel gel extraction kit).

## **3.1.5 Purification, analysis and modification of DNA**

### **3.1.5.1 Agarose Gel electrophoresis**

#### **TAE Buffer**

40 mM Tris, 0.05% Acetic acid (v/v), 1mM EDTA in dH<sub>2</sub>O. Adjust pH to 7.5 – 8.0 with HCl

#### **TBE Buffer**

9 mM Tris-borate and 2 mM EDTA in dH<sub>2</sub>O

#### **5X loading dye**

30% Glycerol, 0.25% Bromophenol blue and 0.25% Xylenecynol FF in dH<sub>2</sub>O

Agarose gel electrophoresis was used to resolve DNA constructs. 1-2% agarose gels were casted in TAE Buffer, 0.2 µg/ml ethidiumbromide was added to molten agarose before casting. Samples were diluted in 5X loading dye before loading. 1 kb and 100 bp molecular weight ladder (MBI) were used to analyze the size of DNA. Gels were run at 100 volts in TAE/TBE buffer.

### **3.1.5.2 Purification of DNA from agarose gels**

Desired bands were cut out from the gel using scalpel under UV-light. DNA was extracted from the cut bands using Nucleo Spin Extract Kit (Machery-Nagel).

### **3.1.5.3 Restricting digestion of DNA**

Restriction enzymes Hind III (10 U/µl, MBI), Xba I (10 U/µl, MBI), Bam H I (10 U/µl, MBI), Bgl II (10 U/µl, MBI) were incubated with 20 µg DNA to be digested with appropriate buffer in a final volume of 30 µls for 1- 2 hr at 37°C. Later, the dephosphorylation of DNA was performed

in the same tube if necessary, after heat inactivation of restriction enzymes (65°C/5 min). DNA was purified by agarose gel extraction.

#### **3.1.5.4 Dephosphorylation**

Before ligation 5'-Phosphate group was removed from the linearized vector with Shrimp alkaline Phosphatase (SAP; 1 U/μl, MBI), to avoid self re-ligation of vector. 1 U of enzyme was incubated with DNA for 2 hr at 37°C.

#### **3.1.5.5 Ligation**

200-400 ng of purified linearised vector and PCR product were taken in molar ratio of 1:2 respectively. Ligation was carried out using T4 ligase (5U/μl, MBI) and ligase buffer in 20μl final reaction volume in a PCR machine with alternate 99 cycles of incubation at 30°C followed by incubation at 10°C respectively. 10 μl of ligation reaction volume was used to transform competent *E. coli*.

#### **3.1.5.6 Transformation**

##### **LB medium**

1% Tryptone, 0.5% Yeast Extract and 0.5% NaCl in dH<sub>2</sub>O. Adjust pH to 7.0 with NaOH, autoclave at 120°C / 1.2 bar for 20 min

##### **LB Agar plates**

1% Tryptone, 0.5% Yeast Extract and 0.5% NaCl in dH<sub>2</sub>O. Adjust pH to 7.0 with NaOH, add 15 g/lit agar and autoclave at 120°C/1.2 bar/20min, nearly at 50°C add the desired antibiotic (Ampicillin 100 μg/ml) and pour plates.

##### **Bacteria**

DH5α was the preferred bacterial strain for all transformations

10 μl of ligation product was mixed with 100 μl of competent *E.coli* DH5α and incubated on ice for 30 min. Then the cells were given a heat shock at 42°C for 1 min and were again put back on ice for 2 min. 1 ml warm LB-medium was added and cells were incubated in thermomixer at 37°C with shaking for 1 hr. Tubes were then centrifuged in a tabletop centrifuge for 1 min/ 12000 rpm. The pellet was resuspended in 200 μl of LB medium and cells were streaked on LB-plates containing respective antibiotic. After 14-20 hr incubation at 37°C colonies were picked and 2 ml overnight cultures were grown in LB-liquid medium with respective antibiotic.

#### **3.1.5.7 Crude plasmid preparation from over-night cultures (crude mini – prep)**

##### **STET Buffer**

0.1 M NaCl, 10 mM Tris-HCl pH 8.0, 1 mM EDTA pH 8.0, 5 % Triton-X100

### **Lysozyme**

10 mg/ml in 10 mM Tris-HCl pH 8.0

1.5 ml of overnight cultures were centrifuged at 13,500 rpm for 1 min at room temperature. The pellet was resuspended in 375  $\mu$ l STET buffer and 25  $\mu$ l lysozyme by vortexing, followed by heat shock at 95°C for 40-50 sec. Lysates were centrifuged at 13,500 rpm/10 min and pellets were carefully fished out of the tube using sterile 200  $\mu$ l yellow pipette tip. 35  $\mu$ l 3M Na-acetate pH 5.0 and 420  $\mu$ l isopropanol was added to the cleared lysates. After 5 min of intermittent shaking, samples were centrifuged 5min/13,500 rpm. Pellets were washed with 70% ethanol, air dried and later resuspended in 100  $\mu$ l dH<sub>2</sub>O. 2  $\mu$ l of RNase (10  $\mu$ g/ $\mu$ l) was added to solution and incubated at 37°C for 10 min. 10  $\mu$ l of the crude plasmid was used for further restriction analysis to check if the cloning was successful. New over-night cultures were grown from positive colonies. Plasmid was isolated using plasmid extraction kit (Sigma). Positive cloning was further confirmed by sequencing. A higher amount of DNA was obtained from 200 ml over-night cultures by using maxi-preparation kit (Sigma).

### **3.1.5.8 DNA sequencing**

DNA sequencing was performed at GATC Biotech AG

## **3.2 Gene expression analysis by RT- PCR**

### **Materials**

Trizol Reagent (Invitrogen)

BCP (1-Bromo-3-chloro-propane, Sigma)

DEPC (Dimethylpyrocarbonate, Sigma)

Oligo(dT)<sub>12-18</sub> primer 0.5  $\mu$ g/ml (Invitrogen)

Superscript III<sup>TM</sup> Rnase H- Reverse Transcriptase (Invitrogen)

DNA polymerase (Invitrogen)

### **DEPC treatment of water**

Add 0.1% (v/v) DEPC to dH<sub>2</sub>O and shake vigorously to mix. Let the solution incubate for 12 hr at room temperature. Next day autoclave at 120°C/1.2 bar for 20 min. All the reagents were made in DEPC treated water.

### **Primers**

DNA sequence for the respective gene was obtained from NCBI web site. Primers for PCR were designed loosely based on following rules. Length of the primer should be around 19 bps, melting temperature (T<sub>m</sub>) of the primer should close to 60°C. Nucleotide at 3' end should be either G or

C. Primers to be used in same PCR reaction were checked carefully to avoid formation of primer dimers. Melting temperature ( $T_m$ ) of primer was calculated according to following formula.

$$T_m = 4(G+C) + 2(A+T)$$

Gene	Primer sequence
hLCS	GAACAGACTGGCACACAACC
hLCS	CCTAAGTCTCCCTCTGGTC
hGCS	GCTGCCACCTTAGAGCAGG
hGCS	ACATGGTGGGCTGCCATC
hGCS	GGTGGACTCTGTGCCAGC
hGCS	TTATACATCTAGGATTTCTCTGCTG
hERGIC	GAGGAATTCCAGAAGGGCC
hERGIC	TACTTGTCTCAGAATCTCATGC
hAPP-KPI	GAGGAACCCTACGAAGAAGC
hAPP-KPI	CCTGGGACATTCTCTCTCG
h- $\beta$ -actin	CACGAAACTACCTTCAACTCC
h- $\beta$ -actin	ACATCTGCTGGAAGGTGGAC
hGAPDH	GAAGGTGAAGGTCGGAGTC
hGAPDH	GAAGATGGTGATGGGATTTTC
mAPP	GGTGGACTCTGTGCCAGC
mAPP	TCCGTTCTGCTGCATCTTGG
mCYP51	CTGGACAGCACACATCCTC
mCYP51	CACACACCTGATGTCCTGG
mLanoSyn	AGGAAGCAGAGAGCCGATG
mLanoSyn	TGATCCCTCTCTCCTGAGC
mSeladin1	GAGACACTACTACCACCGAC
mSeladin1	TGTCCACGTAGAGCTCTGC
m- $\beta$ -actin	TGCGTGACATCAAAGAGAAG
m- $\beta$ -actin	GTCATAGCTCTTCTCCAGG
mGAPDH	TGCACCACCAACTGCTTA
mGAPDH	GGATGCAGGGATGATGTTC

Table 4. **Primers used for RT-PCR.** Primers mentioned in the table were used to amplify the fragment of respective gene product. Each primer pair was designed to amplify a gene sequence of ~ 300 bp except primers for house keeping genes which were designed to amplify 150-200 bps. Species from which cDNA sequence was obtained are indicated, human (h) and mouse (m).

### 3.2.1 Extraction of RNA from eukaryotic cells

Cells were washed with cold PBS and lysed with 1.6 ml of Trizol directly in a 3.5 cm diameter culture dish. Cells were further homogenized using syringe by passing through 21-G needle 10 times. Homogenized samples were left at room temperature for 5 min in a 2 ml eppendorf tube to allow complete dissociation of nucleoprotein complexes. 160  $\mu$ l of BCP was added to the tubes.

Tubes were vortexed briefly and centrifuged at 13,500 rpm for 15 min at 4°C. Later aqueous phase was carefully transferred into a fresh tube and 800 µl of isopropanol was added to it. Samples were again vortexed briefly and incubated at room temperature for 10 min. RNA pellets were obtained by centrifugation at 13,500 rpm, which were washed with 1 ml, 75% cold ethanol and resuspended in 100 µl DEPC- H<sub>2</sub>O after drying. RNA concentration was estimated by reading O.D. at 260 nm after appropriate dilution.

### 3.2.2 cDNA synthesis

5 µg of RNA was used for cDNA synthesis and RNA volume was adjusted to 10 µl with DEPC-H<sub>2</sub>O. 1 µl of oligo(dT) was added to RNA and mixture was incubated at 60°C for 5 min. In the meantime, mastermix was made ready in the proportions mentioned below.

1µl DEPC- H<sub>2</sub>O, 1µl 10 mM dNTPs, 4 µl 5X First Strand Buffer, 2 µl 0.1 M DTT and 1 µl reverse transcriptase.

9 µl master mix was added to each tube and tubes were incubated at 42°C for 1 hour followed by 15 min incubation at 70°C in the PCR machine. cDNA was diluted 1 to 10 by adding 180 µl of DEPC treated water for further usage.

### 3.2.3 PCR

#### Reaction volume (1X Mix)

10 X PCR Buffer (without Mg)	5 µl
10 mM dNTPs	1 µl
MgCl <sub>2</sub>	5 µl
Forward Primer (100 pmol/µl)	1 µl
Reverse Primer (100 pmol/µl)	1 µl
Template cDNA	20 µl
Taq polymerase	0.5 µl (1U/µl)
H <sub>2</sub> O	20 µl
	50µls

#### PCR Program

95°C, 3 min

95°C, 45 sec	} 22 cycles
58°C, 45 sec	
72°C, 1 min 30 sec	

72°C, 20 min

### 3.3 RNA interference (RNAi)

#### **3.3.1 Generation of pSupZeo, a vector for stable expression of siRNA into mammalian cells**

Usage of pSUPER vector system, which directs the synthesis of small interfering RNAs (siRNA) in mammalian cells, was described in 2002 by Brummelkamp et al. (Brummelkamp et al., 2002). This vector contains a polymerase-III H1-RNA gene promoter that produces a small RNA transcript lacking a polyadenosine tail and has a well-defined start of transcription and a termination signal consisting of five thymidines in row (T5). The cleavage of transcript at termination site is after the second uridine yielding a transcript resembling the ends of synthetic siRNAs, which also contain an overhang of TT or UU nucleotides at 3' end. Later in 2003 Wetering et al. described a modified pTER vector system that contained doxycycline-regulated form of the H1 promoter with Tet operator upstream of the transcription site (van de et al., 2003). This vector, when transfected together with Tet-repressor expression vector regulates expression of siRNAs in tetracycline dependent manner. It was obtained by cloning the nucleotide sequence containing H1 promoter with the Tet operator into pcDNA3.1-Zeo. Thus, this vector contains zeocin resistance for stable expression in mammalian cells.

Using above two vectors a new vector system, pSupZeo was generated for stable expression of siRNAs into mammalian cells. However, this vector lacked Tet operator and therefore expression of siRNAs was constitutive. To achieve this H1-promoter with Tet operator was cut out from pTER vector and H1-promoter from pSUPER vector was cloned into digested pTER. Thus new vector pSupZeo contained zeocin resistance for stable expression and H1-promoter without inducible system.

Digestion of pTER was performed with Xho I and Xba I to excise H1 promoter with Tet operator and vector backbone was purified from agarose gel. H1 promoter was cut out using EcoR I from pSUPER and purified subsequently. Klenow polymerase reaction was performed on purified pTER vector as well as H1 promoter to generate a product with blunt ends. Briefly, 25  $\mu$ l of cDNA was incubated with 3  $\mu$ l of klenow buffer, 1  $\mu$ l dNTPs (10 mM) and 1  $\mu$ l klenow fragment for 10 min at 37°C. The vector backbone was further dephosphorylated and purified, H1 promoter was purified as well and the ligation of both was performed as described above. Screening of successful ligation product in proper orientation was done by performing sequencing with BGH-reverse primer. The vector with H1-promoter in right orientation was named as pSupZeo, which was used for cloning RNAi oligos.

### 3.3.2 Selection of target sequence

Two different targets were chosen for each gene using Ambion RNAi Target finder ([http://www.ambion.com/techlib/misc/siRNA\\_finder.html](http://www.ambion.com/techlib/misc/siRNA_finder.html)). Target sequence (Tar.Seq.) which fulfilled the necessary criteria for generated siRNAs to be effective in gene suppression was selected. Briefly, nucleotide sequence in the target began with AA, which would offer overhang of UU in siRNA at 3' end. GC content ranged from 30-50 %. Care was taken that chosen sequence did not contain stretch of more than four T's or A's and that the sequence did not have significant homology with other genes.

### 3.3.3 Designing RNAi oligonucleotides

Complementary DNA oligos were designed to direct synthesis of 19 base pair double stranded target sequence, containing a loop of nine nucleotides, seen in small letters in oligo templates indicated below. Oligos contained Bgl II (5') and Hind III (3') restriction sites, indicated in big letters in the template below, for cloning into pSupZeo. Together with the target sequence in sense and anti sense orientation plus loop sequence and restriction sites, each oligo (primer) consisted 64 base pairs in total.

Forward oligo template

GATCCCC-Tar.Seq (sense orientation)-ttcaagaga-Tar.Seq. (anti sense orientation)

Reverse oligo template

AGCTTTTCCAAAA-Tar.Seq. (Sense orientation)-tctctttaa-Tar.Seq. (anti sense orientation)

Name	Target gene	Oligonucleotide Sequence
GCS1-fw	hGCS (D50840)	gatcccGCTCCCAGGTGTCTCTCTTTtcaagagaAAGAGAGACACCTGGG AGCtttttgaaa
GCS1-rev	hGCS (D50840)	AGCTtttccaaaaGCTCCCAGGTGTCTCTCTTTtctctttaaAAGAGAGACAC CTGGGAGCgg
GCS2-fw	hGCS (D50840)	gatcccGCAGGAGGACTTATAGCTTtcaagagaAAGCTATAAGTCCTCCT GCtttttgaaa
GCS2-rev	hGCS (D50840)	AGCTtttccaaaaGCAGGAGGACTTATAGCTTtctctttaaAAGCTATAAGT CCTCCTGCgg
LCS1-fw	hLCS (AF097159)	gatcccGCTCGAGGTATAATGTTGAttcaagagaTCAACATTATACCTCGA GCtttttgaaa
LCS1-rev	hLCS (AF097159)	AGCTtttccaaaaGCTCGAGGTATAATGTTGAtctctttaaTCAACATTATAC CTCGAGCgg
LCS2-fw	hLCS (AF097159)	gatcccCAGACTGGCACACAACCTTtcaagagaAAGGTTGTGTGCCAGT CTGtttttgaaa
LCS2-rev	hLCS (AF097159)	AGCTtttccaaaaCAGACTGGCACACAACCTTtctctttaaAAGGTTGTGTG CCAGTCTGgg

Table 5. **DNA oligo sequence for RNAi knockdown.** Table indicates the sequence of oligos used for knocking down respective genes. Oligos were cloned into pSupZeo vector. When expressed in eukaryotic system, oligos express 19 bp hairpin structures with a loop consisting of 9 base pairs.



### 3.3.4 Cloning oligonucleotides into pSupZeo

#### Annealing of oligonucleotides

##### Annealing Buffer

100 mM Potassium acetate  
30 mM HEPES-KOH pH 7.4  
2 mM Magnesium acetate

Forward and reverse oligos were dissolved in distilled water at 100 pmol/ $\mu$ l concentration. 1  $\mu$ l of each oligo with 5  $\mu$ l of annealing buffer and 43  $\mu$ l dH<sub>2</sub>O were incubated at 95°C for 5 min followed by cooling at 4°C

1  $\mu$ l of the annealed oligo (forward + reverse) were cloned into Bgl II – Hind III digested pSupZeo vector. Screen for positive colonies was done by digestion of isolated plasmid with Hind III - Xba I. Further verification of proper orientation as well as exact sequence was done by sequencing. Finally, pSupZeo containing right oligo in proper orientation was transfected into HEK293 cells and stable clones were selected using zeocin resistance. Obtained clones were further screened by RT PCR for knockdown of respective target genes.

## 3.4 Cell Culture

### 3.4.1 Instruments and materials

-80°C freezer	Thermo
Autoclave	HP
37°C	CO <sub>2</sub> incubator Binder
Cell culture hood	Thermo
Nitrogen tank	Linde
Centrifuge	Eppendorf
Culture dishes, flasks, pipettes	Corning
Vortex	Scientific Industries
Cryo tubes	Nunc

#### Phosphate Buffered Saline (PBS)

140 mM NaCl, 10 mM NaH<sub>2</sub>PO<sub>4</sub> and 1.75 mM KH<sub>2</sub>PO<sub>4</sub> in dH<sub>2</sub>O, adjust to pH 7.4 with HCl, autoclave at 120°C and 120 bar for 20 min.

#### Poly-L-Lysine solution

100  $\mu$ g/ml poly-L-lysine (Sigma) in sterile PBS  
Coverslips or dishes were coated with 100  $\mu$ g/ml

#### Trypsin-EDTA

0.05 % Trypsin, 0.53 mM EDTA.4Na in Hank's B.S.S (Invitrogen)

#### Bovine Fetal Calf serum (FCS)

FCS (Invitrogen) was heat inactivated at 56°C for 30 min.

### **Basic medium for HEK293, HEK293, H4, HeLa and mouse embryonic fibroblast cells**

DMEM (*Dulbecco's modified Eagle's Medium*) High Glucose (Invitrogen) with 2 mM L-Glutamine, supplemented with 10 % heat inactivated fetal calf serum (FCS; Invitrogen), 50 U/ml Penicillin and 50 µg/ml Streptomycin (Invitrogen). FCS was inactivated by heating at 57<sup>0</sup>C for 30 min.

### **Antibiotics**

Neomycin/Gentamycin : (G418) 200 µg/ml , Zeocin : 200 µg/ml, Hygromycin : 150 µg/ml

### **Freezing media**

90 % FCS + 10 % DMSO

### **Cell lines**

Human embryonic kidney (HEK293) cells, HEK293T that stably express the large T-antigen of SV-40 virus were provided by Dr. Mathias Ekhhardt, HeLa cell line, Human neuroglioma (H4) and human neuroblastoma SH-SY5Y were obtained from ATCC. Mouse melanoma B16 and GM95 cells were obtained from RIKEN cell bank, Japan. All cell lines were cultured at 5% CO<sub>2</sub> concentration in incubator maintained at 37<sup>0</sup>C. Wild type and presenilin knock out mouse embryonic fibroblasts were generous gift from Dr. Bart de Strooper

### **3.4.2 Transfection**

Transfection was done using Lipofectamine (Invitrogen), according to manufactures instructions. Briefly 4 µg cDNA and 10µl lipofectamine were suspended in 100 µl optimem separately, Tubes were vortexed and centrifuged briefly. After 10 min cDNA solution was transferred to Lipofectamine solution and was incubated for 10 min at room temperature before adding to cell media.

### **3.4.3 Generating stable cell lines**

Cells were transfected with desired vector in a 6 cm dish as described above. After 48 hr, cells were split in dilutions 1 to 500, 1 to 250, 1 to 100, 1 to 50 and 1 to 10 in 10 cm dishes. Same time respective antibiotic was added to cells and cells were cultured for 2-3 weeks. Also, non-transfected cells were split and cultured in presence of antibiotic in similar way. Antibiotic concentration was adjusted to achieve death of all non-transfected cells within 8 days. During selection period of 2-3 weeks, there was heavy cell death; however, cells left behind were allowed to grow into a cell colony, which was mostly derived from single cell giving rise to single cell clone. When clones were grown up to 5 mm - 10 mm in diameter, they were washed with PBS and cloning cylinders (8 X 8 mm; DUNN Labortechnik) were place around each clone. Clones were trypsinised and transferred to 96 well plates, further each clone was expanded in presence of antibiotic by subsequent subculturing in 48, 24, 12 and 6 well plates and later screened by either western immunoblotting or RT-PCR.

## 3.5 Biochemical and Cell Biological Methods

### 3.5.1 Instruments and materials

Polyacrylamide gel electrophoresis unit	Amersham Pharmacia
Western blotting unit	Amersham Pharmacia
Microwave	LG
Overhead rotor	Scientific Industries
Orbital shaker	Stuart Scientific
pH meter	Mettler Toledo
Weighing balances	Mettler Toledo
Block heater	Stuart Scientific
Water bath	Medigen
Phosphoimager	Fuji Inc.
Phosphoimager plates	Kodak
X-ray films	Kodak
Chemiluminescence imager	Biorad
Ultracentrifuge	Beckman
Ultracentrifuge rotor (SW40Ti)	Beckman
Fluorescence microscope	Nikon

### Biochemicals

D, L-PDMP (Sigma) was dissolved in warm dH<sub>2</sub>O at 50 mM concentration. L-PDMP (Matreya) was dissolved in ethanol at concentration of 50 mM. GM1 (Sigma) was dissolved in dH<sub>2</sub>O at concentration of 5 mg/ml. 3-Sn-Phosphatidylserine (Sigma), 3-Sn-Phosphatidic acid (Sigma), Sphingomyelin (Sigma) were all dissolved at concentration of 5 mg/ml in ethanol. Brefeldin A (Alexis Biochemicals) was dissolved in methanol at concentration of 10 mg/ml. C6-Ceramide (Sigma) was dissolved in ethanol at 10 mM concentration. 10 mg/ml (1000X) Bacitracin A (Sigma) was dissolved in dH<sub>2</sub>O. 50 mM Itraconazole (Jackson lab) solution was made in DMSO, A $\beta$ 40 (EZ Biolab) was dissolved at concentration of 1 mg/ml in dH<sub>2</sub>O. Apo B100 (bovine LDL) was from Calbiochem, DAPI (Roth) was dissolved in dH<sub>2</sub>O at concentration of 1 mg/ml (10,000X).

**Primary Antibodies**

Name	Species	Antigen	IP	WB	IF	Source
5313	rabbit	MBP-hAPP <sub>695</sub> -NT (a.a. 444-592)	1:500	1:1000	1:100	Walter et.al., 2000
6687&5818	rabbit	Peptide-hAPP <sub>695</sub> -CT (a.a. 676-695)	1:500	1:1000	1:100	Walter et.al., 2000
140	rabbit		1:500	1:1000	1:100	Raised in lab
3926	rabbit	A $\beta$ 1-40	1:100			Raised in lab
2964	rabbit	A $\beta$ 1-40	1:100			Raised in lab
6E10	mouse	A $\beta$ 1-17		1:2500		Senetec/Signet Inc
3109	rabbit	MBP-hPS1-CT (a.a. 263-407)	1:500	1:1000	1:100	Raised in lab
LDLR	Chicken	Peptide hLDLR a.a. 29-205		1:1000		abcam
LDL	goat	hLDL		1:1000		Sigma
Anti-CTX	rabbit	<i>Vibrio cholerae</i>		1:5000		Sigma
Giantin	mouse	hGiantin			1:2500	Dr. Hauri, Basel
Calnexin	rabbit	hCalnexin (a.a. 1-17)			1:1000	Santacruz, Inc
Bap-1a	mouse	A $\beta$ 1-40	1:250			Tamboli et.al., 2005
Fas-receptor				1:1000		Upstate biochemicals
Insulin Receptor	rabbit	hInsulin receptor $\beta$ chain - CT		1:1000		Santacruz, Inc
$\beta$ -actin	mouse	h $\beta$ -actin-CT		1:5000		Sigma
TGN46	sheep	hTGN46			1:1000	Serotec
IG7/5A3	mouse	APP ectodomain			1:200	From Dr. Edi. Koo

Table 6. **Primary Antibodies:** Table describes briefly the epitope and source of each antibody, as well as dilutions which were used in various applications are also indicated. Besides above mentioned antibodies peroxidase conjugated streptavidin (calbiochem) and TRITC-conjugated wheat germ agglutinin (WGA, molecular probes) were used to detect biotinylated proteins and glycoproteins respectively. Cholera toxin B subunit conjugated to peroxidase was used to detect GM1 by western blot.

**Secondary Antibodies**

Name	Species	Antigen	Application	Dilution	Source
anti-rabbit-HRP	Rabbit	Rabbit IgG	WB	1:40,000	Sigma
anti-mouse-HRP	Rabbit	Mouse IgG	WB	1:40,000	Sigma
anti-chicken-HRP	Rabbit	Chicken IgG	WB	1:10,000	Sigma
anti-goat-HRP		Goat IgG	WB	1:5000	Sigma
Alexa Fluor 594	Goat	Rabbit IgG	IF	1:1000	Molecular Probes
Alexa Fluor 594	Goat	Mouse IgG	IF	1:1000	Molecular Probes
Alexa Fluor 594	Donkey	Chicken IgG	IF	1:1000	Molecular Probes
Alexa Fluor 488	Goat	Rabbit IgG	IF	1:1000	Molecular Probes
Alexa Fluor 488	Goat	Mouse IgG	IF	1:1000	Molecular Probes

Table 7. **Secondary antibodies:** Peroxidase (HRP) conjugated secondary antibodies were used to detect primary antibodies bound to respective proteins or lipids.

### **3.5.2 Sample preparation**

#### **Total protein extraction**

##### **1X STEN buffer**

50 mM Tris pH 7.6, 150 mM 5M NaCl, 2 mM EDTA, 0.2 % Igepal CA-630 in dH<sub>2</sub>O

##### **1X STEN-lysis buffer (without BSA)**

1% Triton X-100 (v/v), 1% Igepal CA-630 in 1X STEN

Cells were washed with cold PBS and scrapped off the plate in PBS on ice. Cells were pelleted by centrifugation at 1000 rpm/5 min/4°C and lysed with STEN-lysis buffer (200 µls for 6 cm dish and 400 µls for 10 cm dish) on ice for 30 min in the presence of protease inhibitor mix. The lysates were cleared by centrifugation at 16000 rpm. Protein estimation was performed and 20 µg of protein was aliquoted from each sample. Samples were boiled with loading dye.

#### **Extraction of membrane proteins**

##### **Hypotonic Buffer**

10 mM Tris pH 7.6, 1 mM EDTA and 1 mM EGTA in dH<sub>2</sub>O

Cells were washed with cold PBS and scrapped off the plate in PBS on ice. Cells were pelleted by centrifugation at 1000 rpm/5min/4°C. Pellet was resuspended in 750 µls cold hypotonic buffer and incubated on ice for 10 min. Cell suspension was then passed through 2 ml syringe with 0.6 mm diameter needle for 15 times. Cell debris and nuclear fraction was pelleted by centrifugation at 2000 rpm/10 min/ 4°C. Supernatant was transferred to new tubes and centrifuged at 16,000 rpm/ 4°C for one hour to obtain a membrane fraction pellet. Membrane pellet either was resuspended in 100 µl loading dye and boiled or was further lysed with 100 µl STEN-lysis buffer as described in 2.4.5.1 and samples were prepared.

#### **Immunoprecipitation**

##### **1X STEN buffer**

50 mM Tris pH 7.6, 150 mM 5M NaCl, 2 mM EDTA, 0.2 % Igepal CA-630 in dH<sub>2</sub>O

##### **1X STEN-lysis buffer**

1% Triton X-100 (v/v), 1% Igepal CA-630, 2% BSA in 1X STEN

##### **1X STEN-NaCl**

50 mM Tris pH 7.6, 500 mM 5 M NaCl, 2 mM EDTA, 0.2 % Igepal CA-630 in dH<sub>2</sub>O

##### **Protein A/G sepharose suspension (Zymed)**

100 mg/ml protein A/G bound sepharose beads were washed with STEN buffer and resuspended in it. If required beads were blocked with 2 mg/ml BSA to avoid non-specific binding.

Cells were lysed in 700  $\mu$ l STEN-lysis buffer on ice for 10 min in presence of protease inhibitors. Lysates were cleared by centrifugation for 10 min at 14,000 rpm. Appropriate amount of primary antibody and 40  $\mu$ l washed sepharose beads (protein A for rabbit polyclonal and protein G for mouse monoclonal) were added to cleared lysates. Antibody was allowed to bind to respective protein as well as beads by rotation on overhead shaker for 2 hr at 4°C. For A $\beta$  immunoprecipitation rotation time was extended to 12 hr. Antigen-antibody complex bound to beads was separated by centrifugation for 5 min at 5000 rpm and washed twice with STEN-NaCl and once with STEN buffer.

### **Loading Dyes**

#### **2X Loading dye**

100 mM Tris HCl pH 6.8 (100 ml), 4% SDS, 0.2 % bromophenol blue, 20 % (v/v) glycerol, Add 10 %  $\beta$ -mercaptoethanol fresh every time.

#### **5X Loading dye**

2.5 ml upper tris, 1 g SDS, 100 mg DTT, 5 ml glycerol, 8  $\mu$ g bromophenol blue. Make up volume to 10 ml with dH<sub>2</sub>O, freeze aliquots at -20°C.

### **Estimation of protein concentration**

#### **UV-absorption method**

The UV-Absorption of undiluted sample at 280 nm was measured with a photometer. Quartz cuvette was used for measurement. The protein concentration was obtained by following formula.

Protein concentration (mg/ml) = OD<sub>280</sub> X 0.5

#### **BCA method**

Samples were diluted appropriately and BCA kit was used to analyze protein concentration.

### **3.5.3 Protein metabolic labeling with [ <sup>35</sup>S ] – methionine / cysteine**

#### **[ <sup>35</sup>S ] – Methionine/Cysteine label (MPI biomedical)**

L-Methionine, [35S]: L-Cysteine, [35S], ~10 mCi/ml; ~370 MBq/ml

#### **Starvation Medium**

Methionine/Cysteine free medium (MPI biomedical, modified DMEM), 2.45 g/l Dextrose

#### **Labeling Medium**

Methionine free medium with 3.7 MBq/ml Trans [ <sup>35</sup>S ] – Methionine/Cysteine label and 5 % FCS

#### **L-Methionine**

30 mg/ml L-Methionine (100X) in DMEM

#### **Chase medium**

Basic medium with 0.3 mg/ml L-Methionine

80-85 % confluent cells were washed with PBS and incubated with starvation medium for 1 hr. Depending on protein to be analyzed cells were then pulse labeled with labeling medium (1.5 ml for 6 cm dish and 2 ml for 10 cm dish) for desired time. For APP and APP-CTFs analysis cells were labeled for 10 min, for A $\beta$  analysis however, cells were labeled for 1 hr. Subsequently cells were washed with PBS and incubated in chase medium for desired time points. For APP maturation and transport studies cells were chased up to 2 hr, for APP-CTFs chase period was extended up to 12-16 hr and 5 hr chase was done for A $\beta$  analysis. After chase, medium was collected and cells were lysed with 700  $\mu$ l STEN-lysis buffer. Lysates were later cleared by centrifugation at 14,000 rpm/10 min and medium was centrifuged at 1000 rpm/5 min. Immunoprecipitation, followed by blotting was performed and radiolabeled protein intensities were analyzed with a phosphoimager (Fuji, FLA2000) and the Fuji Image Gauge 3.0 software.

### **3.5.4 Polyacrylamide-SDS gel electrophoresis**

#### **Acrylamide : bis**

40% ready to use solution of acrylamide:bisacrylamide (19:1) was used.

#### **4X Upper Tris**

10 ml 20 % SDS, 15.1 g Tris base dissolve in 500 ml dH<sub>2</sub>O and adjust pH to 6.8

#### **4X Upper Tris**

10 ml 20%SDS, 90.8 g Tris base dissolve in 500 ml dH<sub>2</sub>O and adjust pH to 8.8

#### **10X Running Buffer**

100 ml 2 0% SDS, 60.8 g Tris base and 288 g glycine dissolve in 2 liters dH<sub>2</sub>O.

#### **APS**

10% (w/v) Ammonium persulfate in dH<sub>2</sub>O

#### **TEMED**

N,N,N',N'-tetramethylethylenediamine (Merck)

**Gel casting scheme - separating gel**

	For 15% gel		For 12% gel		For 10% gel		For 7% gel	
	4 gels	2 gels	4 gels	2 gels	4 gels	2 gels	4 gels	2 gels
dH <sub>2</sub> O (ml)	5.0	2.5	7.0	3.5	8.3	4.2	10.3	5.5
Acrylamide:Bis (40%) (ml)	10.0	5.0	8.0	4.0	6.7	3.4	4.7	2.3
4X Lower Tris (ml)	5.0	2.5	5.0	2.5	5.0	2.5	5.0	2.5
TEMED (μl)	50	25	50	25	50	25	50	25
APS (μl)	50	25	50	25	50	25	50	25

**Gel casting scheme - stacking gel**

	For 4% stacking gel	
	4 gels (10ml)	2 gels (5ml)
dH <sub>2</sub> O (ml)	6.5	3.25
Acrylamide:Bis (30%) (ml)	1.3	0.65
4X Upper Tris (ml)	2.5	1.25
TEMED (μl)	25	12
APS (μl)	25	12

(Note: 8M (48g/100ml) urea was used instead of dH<sub>2</sub>O for casting urea gels. Samples for presenilins detection were always loaded on urea gels.)

**3.5.5 Tricine gel system for low molecular weight protein detection****Acrylamide: bis (50%)**

48 g acrylamide and 1.5 g bisacrylamide was weighed and dissolved in 100 ml dH<sub>2</sub>O.

**Anode buffer (5X)**

1 M Tris HCl, pH 8.9 (121.1g Tris base/l)

**Cathode buffer (1X)**

0.1 M Tris (12.11 g Tris/l), 0.1 M Tricine (17.92 g/l), 0.1% SDS (5 ml/l from 20% SDS)

**Gel Buffer (store at 4°C)**

3 M Tris HCl (182 g/l), 0.3% SDS (1.5 g/l), pH 8.45

**Glycerol**

32% (v/v) glycerol in dH<sub>2</sub>O

**Gel run**

80 V at the beginning, later run at 100 V



	<b>16.5% Separating gel (10.5 ml)</b>	<b>10% spacer gel (7.5 ml)</b>	<b>4% stacking gel (6.25 ml)</b>
<b>Acrylamide.bis</b>	3.5 ml	1.5 ml	0.5 ml
<b>Gel buffer</b>	3.5 ml	2.5 ml	1.55 ml
<b>dH<sub>2</sub>O</b>	-----	3.5 ml	4.2 ml
<b>32% Glycerol</b>	3.5 ml	-----	-----
<b>10% APS</b>	45.0 $\mu$ l	45.0 $\mu$ l	25.0 $\mu$ l
<b>TEMED</b>	5.0 $\mu$ l	5.0 $\mu$ l	5.0 $\mu$ l
<b>Vol. for 1 gel (1.5mm)</b>	5 ml	2.5 ml	2 ml

Table 10. **Gel casting scheme.** Pour the separating and spacer gels immediately one after other carefully, so that they polymerize at the same time. Schägger gel can be stored at 4°C.

### **Coomassie staining solution**

50% (v/v) Isopropanol, 10% (v/v) Acetic acid, 0.5% (w/v) Coomassie-Blue-R in dH<sub>2</sub>O. Filter and store in glass bottle.

### **Destainer**

5% Isopropanol (v/v), 7% (v/v) acetic acid.

## **3.5.6 Western immunoblotting**

### **Blot Buffer**

25 mM Tris, 0.2 M Glycine and 10 % (v/v) methanol in 1 liter dH<sub>2</sub>O. Adjust pH to 9.0

### **PBS-Tween**

140 mM NaCl, 10 mM NaH<sub>2</sub>PO<sub>4</sub> and 1.75 mM KH<sub>2</sub>PO<sub>4</sub> 0.5 % Tween in dH<sub>2</sub>O, adjust to pH 7.4 with HCl.

### **Transfer conditions**

400 mA constant current for 2 hr

### **Stripping solution**

0.2 M Glycine pH 2.2, 0.1% SDS, 10% v/v Tween

### **Ponceau S**

0.2% ponceau S red in 1% Acetic acid

After electrophoresis, proteins from polyacrylamide gel were transferred to nitrocellulose membrane in a blotting chamber and the transfer was confirmed by ponceau S stain. 5% milk in PBS-T for 1 hr was used as a blocking reagent. Blots were then incubated with appropriately diluted primary antibody solution for 2 hr at room temperature or overnight at 4°C. Blots were then washed 5 times each for 5 minutes, with PBS-T and later incubated with appropriate secondary antibody conjugated to HRP (Horseradish peroxidase) for 1 hr at room temperature. Blots were again washed with PBS-T like earlier and chemiluminescent peroxidase substrate was used to visualize protein bands. Signals were obtained using either chemiluminescence detection film or chemiluminescence imaging. For enhanced chemiluminescence detection, signals were measured and analyzed using an ECL imager (ChemiDoc<sup>TM</sup> XRS, BioRad) and the Quantity One software package (BioRad).

### **3.5.7 Immunocytochemistry**

#### **4% Paraformaldehyde**

Dissolve paraformaldehyde (w/v) in PBS by boiling. Cool down the solution on ice and filter it using filter paper. Adjust the pH to 7.0. Aliquot and store at -20°C

#### **0.1% Triton**

Dissolve the triton X100 (v/v) in appropriate amount of PBS

#### **5% BSA**

Dissolve appropriate amount of BSA in PBS

Cells were cultured on poly-L-lysine-coated glass coverslips to 50-80% confluence. Cells were fixed in 4% paraformaldehyde for 10 min followed by permeabilization with 0.1% triton for 10 min and blocking with 5% BSA. Cells were then incubated with desired primary antibody/antibodies at appropriate concentration, for 2 hr in 1% BSA. Primary antibodies were detected by Alexa 488- or Alexa 594-conjugated secondary antibodies (Molecular Probes Inc.) diluted at 1:1000. Coverslips were mounted on glass slides using 15% mowiol containing 50 mg/ml DABCO. Images were acquired on fluorescence inverted microscope (Nikon Eclipse E800).

### **3.5.8 Cholesterol Stain**

#### **Filipin (Matreya)**

Stock 1 mg/ml in DMSO. Used at 100 µg/ml in PBS for staining

For staining of cholesterol, cells were washed with PBS and fixed with paraformaldehyde. Cells were then incubated with 100 µg/ml filipin in PBS for 30 min at room temperature. After washing with PBS cells were analyzed by fluorescence microscopy ( $\lambda_{\text{ex}} = 360 \text{ nm}$ ;  $\lambda_{\text{em}} = 460 \pm 50 \text{ nm}$ ).

### **3.5.9 Analysis of protein and lipid transport**

#### **3.5.9.1 Treatment with Brefeldin A**

##### **Brefeldin A (BFA)**

10 mg/ml in methanol (1000X stock)

Cells were grown up to to 80% confluence and treated with 10 µg/ml BFA for 10 min at 37°C. Fusion of the *cis-Golgi* compartments with ER was confirmed by immunostaining the *Golgi* compartment and the ER marker proteins, giantin and calnexin respectively.

### 3.5.9.2 Detection of cell surface proteins

#### **EZ-link Sulfo-NHS-Biotin (Pierce)**

50 mg/ml in DMSO (100X stock). Used at 50 µg/ml in PBS.

#### **Glycine**

20 mM Glycine in PBS

#### **Streptavidin Sepharose (Pierce)**

Streptavidin sepharose beads were washed with STEN buffer and were resuspended in the same.

Cells grown on the poly-L-lysine coated dishes up to 70-80% confluency were washed with cold PBS. Cells were then incubated with 50 µg/ml EZ-link Sulfo-NHS-Biotin on ice for 30 min. Excess of biotin was later quenched with 20 mM Glycine washes for 3 times, 10 min each. After one final wash with PBS, cells were lysed in STEN-lysis buffer with BSA and biotinylated cell surface proteins were isolated using streptavidin sepharose beads. Specific protein present at cell surface was detected by western immunoblotting with respective antibody. For detection of cell surface APP-CTFs, total APP-CTFs were first immunoprecipitated from lysates after biotinylation and detection of biotinylated APP-CTFs was performed by probing the blot with streptavidin-HRP.

### 3.5.9.3 Analysis of cell surface protein endocytosis

#### **EZ-link<sup>TM</sup> Sulfo-NHS-SS-Biotin (Pierce)**

50 mg/ml in DMSO (100X stock). Used at 50 µg/ml in PBS. 0.5 mg/ml Glycine

#### **Cleavage buffer**

50 mM Glutathione, 90 mM NaCl, 1.25 mM CaCl<sub>2</sub>, 1.25 mM MgSO<sub>4</sub>, 0.2% BSA in dH<sub>2</sub>O. Adjust to pH 8.6 with NaOH.

Biotinylation of cell surface proteins was performed as above and excess biotin was quenched with glycine. Endocytosis of biotinylated cell surface proteins was allowed by incubation at 37°C and cells were lysed, while other set of cells was lysed directly after biotinylation. At each time point cells were also stripped to cleave biotin. For stripping cells were washed with fresh cleavage buffer three times, 15 min each on ice. Biotinylated proteins were precipitated with streptavidin sepharose.

#### **3.5.9.4 Analysis of extracellular protein endocytosis**

##### **BODIPY-LDL (Molecular probes)**

Stock 1 mg/ml. Used at the concentration 10  $\mu$ g/ml in DMEM.

##### **TRITC-BSA (Molecular probes)**

Stock 25 mg/ml in dH<sub>2</sub>O. Used at the concentration of 50  $\mu$ g/ml in DMEM.

Cells grown on coverslips were washed with DMEM three times and labeled on ice, with BODIPY-LDL/TRITC-BSA for 30 min. Cells were then washed three times with DMEM and incubated for 10 min in culture media at 37°C. After subsequent washes cells were fixed and analyzed by immunofluorescence for LDL uptake.

#### **3.5.9.5 Analysis of GSLs endocytosis**

##### **Cholera toxin (Sigma)**

Stock 1 mg/ml in dH<sub>2</sub>O. Used at 10  $\mu$ g/ml in DMEM.

Cells grown on coverslips were washed with DMEM three times and labeled with cholera toxin on ice for 30 min. Cells were then washed three times with DMEM and incubated for 10 min in culture media at 37°C. After subsequent washes, cells were fixed and stained with anti-cholera toxin antibody, which was visualized using alexa secondary dyes.

#### **3.5.10 Subcellular fractionation using iodixanol gradient**

##### **3.5.10.1 Isolation of cellular membrane vesicles**

Cellular membranes were isolated as described in 2.4.5.2. However, glass hand homogenizer was used instead of needle syringe for homogenization. Membrane pellets were resuspended in 500  $\mu$ l hypotonic buffer (2.4.5.2) and were left overnight at 4°C for formation of vesicles with small magnetic bar rotating inside suspension. Next day vesicle suspension was loaded on the top of iodixanol gradient.

##### **3.5.10.2 Ultracentrifugation**

##### **Iodixanol / Optiprep™ (AXIS-SHIELD)**

60 % (w/v) iodixanol in dH<sub>2</sub>O (Optiprep), density 1.32 g/ml

##### **Diluent**

0.25 mM Sucrose, 6 mM EDTA, 60 mM HEPES-NaOH, pH 7.4

##### **50 % Iodixanol**

5 volume of 60 % iodixanol + 1 volume of diluent.

% layer	50% working soln (ml)	Diluent (ml)	Total volume
50%	10	0	10ml
30%	6	4	10ml
20%	4	6	10ml
17.5%	3.5	6.5	10ml
15%	3	7	10ml
12.5%	2.5	7.5	10ml
7.5%	1,5	8.5	10ml
5%	1	9	10ml
2.5%	0.5	9.5	10ml

Table 11. **Dilution scheme for iodixanol:** Iodixanol with gradually decreasing concentration from 50 % to 2.5 % was obtained from 50 % iodixanol solution by diluting with diluent.

Prepare discontinuous gradient by layering 1.2 ml of each % of iodixanol from bottom to top in a decreasing density starting with 50 % iodixanol. Pre-cool the tubes with gradients at 4°C before loading membrane vesicle suspension on top. Insert gradient tubes with membrane vesicles into cups for SW41Ti swinging-bucket rotor. All the cups with tubes were balanced for equal weight. Centrifuge for 8 hr at 40,000 rpm. Collect the gradient from top to bottom into 1 ml each fraction.

### 3.5.10.3 Protein Precipitation with TCA

#### 2 % Sodium deoxycholate

2 g Sodium deoxycholate in 100 ml dH<sub>2</sub>O

#### 100 % TCA (Trichloroacetic acid)

1 kg TCA in 454 ml dH<sub>2</sub>O. Store at 4°C in a brown bottle

Add 10 µl of 2 % sodium deoxycholate (0.02 % final) to each of the 1 ml gradient fraction. Mix and leave the tubes on ice for 15 min. Add 100 µl of 100 % TCA to the sample, mix and keep at room temperature for 30 min. Spin at 16000 rpm at 4°C for 10 min, discard the supernatant and wash the pellet with ice cold acetone twice. Finally dry the pellet in air and resuspend it in 50 µl of loading dye. Presence of residual TCA might give a yellow colour because of the acidification of loading dye, titrate with 1 N NaOH or 1M Tris HCl pH 8.5 to obtain normal blue colour of loading dye.

### 3.5.11 *In vitro* $\gamma$ -secretase assay

#### Citrate Buffer

150 mM Sodium citrate in dH<sub>2</sub>O, adjust pH to 6.4 with citric acid

#### DAPT - N-[N-(3,5-Difluorophenacetyl-L-alanyl)]-S-phenylglycine t-butyl ester

100 µM DAPT in DMSO (final concentration in assay 1 µM)

Cellular membranes were isolated as described in 2.4.5.2. and membrane pellet was resuspended in citrate buffer containing protease inhibitors. 100 µls resuspended membrane solution aliquoted in various tubes, depending on the treatment. Tubes were later incubated at 37°C for 2 hr in the presence or absence of DAPT as well as in presence of the lipid/substance to be analyzed for its effect on  $\gamma$ -secretase activity. After two hours tubes were centrifuged at 16,000 rpm for 1 hr. Supernatant was analyzed by western immunoblotting for generation of AICD by the action of  $\gamma$ -secretase, whereas APP-CTFs were detected in pellets.

### **3.5.12 Cell viability assay**

#### **MTT (3-(4,5-dimethyl thiazol-2-yl)-2,5-diphenyl tetrazolium bromide)**

5 mg/ml MTT in PBS

Cells were cultured in 96 well microtiter plates with 180 µls medium per well. 20 µl MTT was added directly to the cells (final concentration 0.5 mg/ml). Cells were further incubated at 37°C and 5% CO<sub>2</sub> to allow the MTT to be metabolized. After two hours media was discarded and metabolized product of MTT, formazan, was dissolved in 200 µl DMSO per well. The optical density at 540 nm was determined photometrically, the wells without any cells served as blank. Only living cells can metabolize MTT, optical density at 540 nm is a direct indicator of cell viability. Therefore, lesser the optical density at 540 nm, higher is the toxicity of the tested drug.

### **3.5.13 Analysis of cellular sterols**

For quantitation of sterol concentrations five independent experiments (n=5) were carried out. Statistical analysis was done using Student's T-test. Significance values are indicated by asterisks as follows: \* (p<0.05); \*\* (p<0.01); \*\*\* (p<0.001). Analysis of sterols was performed in collaboration with Institute of pharmacology, University Hospital Bonn. Briefly, lipids were extracted with chloroform/methanol (2:1; v/v) from cultured cells and dried to constant weight in a Speedvac® (Servant Instruments, Inc., Farmingdale, NY, USA). 5 $\alpha$ -cholestane (Serva Electrophoresis Inc., Heidelberg), epicoprostanol (Sigma-Aldrich Chemie Inc), and racemic [23,23,24,25-<sup>2</sup>H<sub>4</sub>] 24(R,S)-OHchol (Medical Isotopes Inc., Pelham, NH, USA) were added as internal standards. After saponification, extraction and derivatization, cholesterol was determined as trimethylsilyl-ethers by using gas-liquid chromatography-flame ionization detection (GC-FID), while, concentrations of lanosterol, desmosterol and cholestanol were estimated by GC- mass spectrometry (GC-MS).



## 4 Results

### 4.1 Role of GSLs in APP processing

#### 4.1.1 Pharmacological inhibition of GSL biosynthesis

In order to analyze the function of glycosphingolipids (GSLs) in the proteolytic processing of APP and generation of A $\beta$ , GSL biosynthesis was inhibited using PDMP (D, L-threo-1-Phenyl-2-decanoylamino-3-morpholino-1-propanol hydrochloride), a specific inhibitor of GSL biosynthesis. PDMP is a selective competitive inhibitor of glucosylceramide synthase (GCS), the very first enzyme involved in complex GSLs biosynthesis (Fig. 1B). Moreover, previously PDMP has also been shown to inhibit synthesis of GSLs efficiently in cell culture as well as in animals (Radin, 1996).

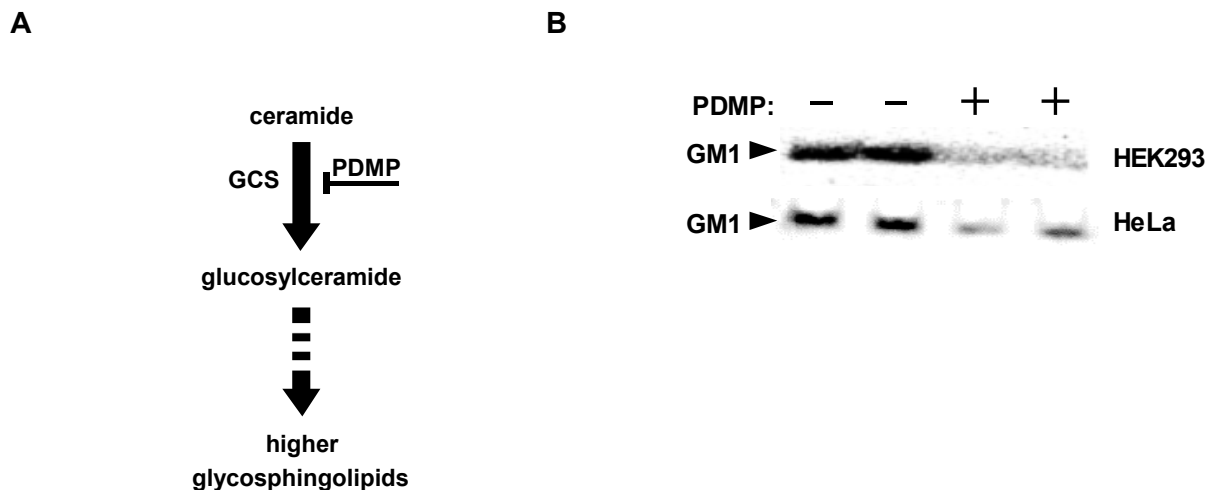


Fig. 1. **Inhibition of GCS by PDMP.** A, Schematic showing of glycosphingolipid biosynthesis pathway and targeted inhibition of glucosylceramide synthase (GCS) by PDMP. B, Detection of GM1 after PDMP treatment - HEK293 (*top panel*) and HeLa (*bottom panel*) cells were cultured in the presence (+) or absence (-) of 10  $\mu$ M PDMP for 48 hr. Cellular membranes were separated by SDS-PAGE and GM1 was detected by western immunoblotting with cholera toxin.

Treatment of HEK293 or HeLa cells with 10  $\mu$ M PDMP for 48 hr led to a significant decrease in GSLs as demonstrated by a strong reduction of GM1 levels in cellular membranes (Fig. 1B), confirming that the treatment with 10  $\mu$ M PDMP is a useful pharmacological tool to reduce cellular GSL levels. As indicated by MTT assays, PDMP did not exert toxic effects up to 25  $\mu$ M (Fig. 2A, 2B).



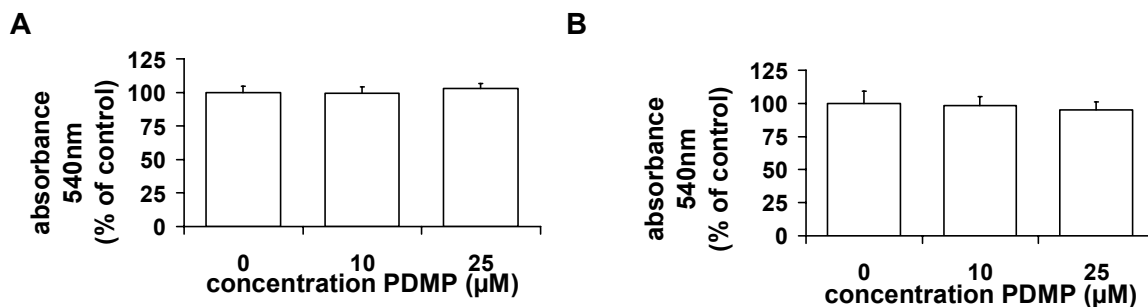
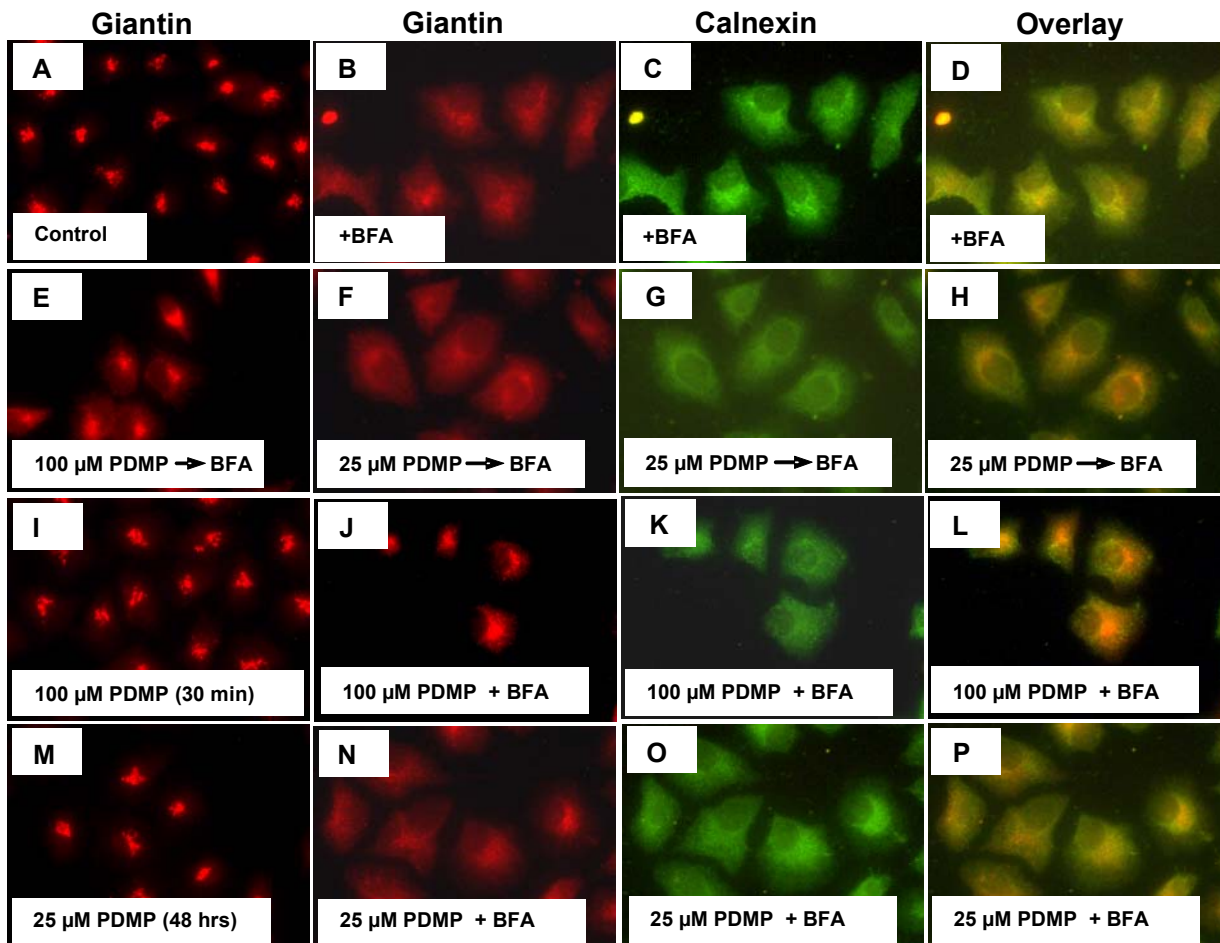


Fig. 2. **Cell viability of HEK293 and HeLa cells upon PDMP treatment.** Cells (A: HEK293; B: HeLa) were split into 96 well microtiter plates and cultured for 24 hr. Cells were then cultured in the absence or presence of PDMP for 48 hr with one medium change after 24 hr. MTT was added directly to the cells. Cells were incubated at 37°C and 5% CO<sub>2</sub> for two hr. Subsequently, the medium was discarded and 100 μl DMSO was added to each well. After solubilization of MTT precipitate, the optical density at 540 nm was determined photometrically.

However, high concentrations of PDMP ( $\leq 100$  μM) are known to inhibit brefeldin A (BFA) induced disintegration of the *Golgi* complex. BFA is a fungal antibiotic widely employed in studies addressing subcellular protein transport and secretion. BFA treatment is known to cause fusion of early secretory compartments e.g. *cis-Golgi* with ER, as well as it also results in fusion of *trans-Golgi network* (TGN) compartments with endosomal vesicles. BFA exerts its effects by targeting ADP ribosylation factor (Arf) (De Matteis et al., 1999). Since PDMP interferes with ADP-ribosylation and cellular calcium homeostasis at higher concentration, it could also abrogate the effects of BFA. To ensure that the PDMP at concentrations used here to inhibit GSL biosynthesis, does not affect important biological functions such as ADP-ribosylation and calcium metabolism, the effect of higher and lower concentrations of PDMP in terms of its ability to inhibit BFA induced redistribution of the *Golgi* compartment was studied.

The effects of PDMP on fusion of *cis-Golgi* vesicles to ER after BFA treatment was studied by immunocytochemical detection of the *Golgi* and ER marker proteins, giantin (red) and calnexin (green) respectively (Fig. 3). Treatment of HeLa cells with 10 μM BFA for 30 min caused the redistribution of giantin into calnexin positive compartments, indicating fusion of ER and *cis-Golgi* (Fig. 3A-D). Pre-treatment of cells with 100 μM PDMP for 30 min inhibited the effect of BFA (Fig. 3E), however, pre-treatment with 25 μM PDMP did not inhibit BFA induced co-localization of giantin and calnexin (Fig. 3F-H). Treatment of 100 μM PDMP alone for 30 min did not affect the distribution of giantin (Fig. 3I). Moreover, when cells were incubated together with PDMP and BFA for 30 min, PDMP was effective in stalling the effect of BFA on giantin localization only at 100 μM concentration (Fig. 3J-L). Pre-treatment of cells with 25 μM PDMP for 48 hr had no effect on giantin and calnexin distribution by itself as well as on BFA induced

redistribution of giantin (Fig. 3M-P). Thus, effect of BFA on giantin redistribution was inhibited by 100  $\mu$ M PDMP, whereas PDMP at 25  $\mu$ M concentration did not have any effect on this process, the latter is not only true for short incubation time but is also valid for longer treatment with PDMP (48 hr) which was used in the study to inhibit the GSLs biosynthesis.



**Fig. 3. Effects of PDMP on BFA induced changes in Golgi and ER morphology.** A-D, Redistribution of giantin by BFA - HeLa cells were incubated in absence (A) and presence (B) of 10  $\mu$ M BFA for 30 min and were stained for giantin, BFA treated cells were also stained for calnexin (C). Overlay of giantin and calnexin in BFA treated cells (D). E-H, Inhibition of giantin redistribution by 100  $\mu$ M but not by 25  $\mu$ M PDMP pre-treatment - HeLa cells were pre-treated with either 100  $\mu$ M (E) or 25  $\mu$ M (F) PDMP for 30 min before incubation with 10  $\mu$ M BFA for 30 min and stained for giantin. 25  $\mu$ M PDMP and BFA treated cells were also stained for calnexin (G). Overlay of giantin and calnexin in 25  $\mu$ M PDMP pre-treated and BFA treated cells (H). I-L, Inhibition of giantin redistribution by co-incubation with 100  $\mu$ M PDMP - Giantin stain after 30 min, 100  $\mu$ M PDMP treatment (I). HeLa cells were treated with 100  $\mu$ M PDMP and 10  $\mu$ M BFA together for 30 min and stained for giantin (J) and calnexin (K), overlay of giantin and calnexin in 100  $\mu$ M PDMP and giantin treated cells (L). M-P, 25  $\mu$ M PDMP treatment for 48 hr does not affect the redistribution of giantin by BFA - HeLa cells were stained for giantin after 25  $\mu$ M, 48 hr PDMP treatment (M). HeLa cells were treated with 25  $\mu$ M PDMP for 48 hr and 10  $\mu$ M BFA was added to the cells for last 30 min. Cells were then stained for giantin (N) and calnexin (O), overlay of giantin and calnexin in these cells (P).

At higher concentrations, PDMP is also known to alter subcellular protein distribution; therefore, the effect of PDMP on APP localization was studied. In control as well as treated cells, APP co-localized predominantly with the *Golgi* marker protein giantin (Fig. 4, right panel) in juxtannuclear compartments and not with ER marker calnexin (Fig. 4, left panel). There was no significant effect on the overall morphology of the ER and *Golgi* after PDMP treatment for 48 hr. However, it should be noted that subtle effects on distribution of APP might not be observed with this staining method.

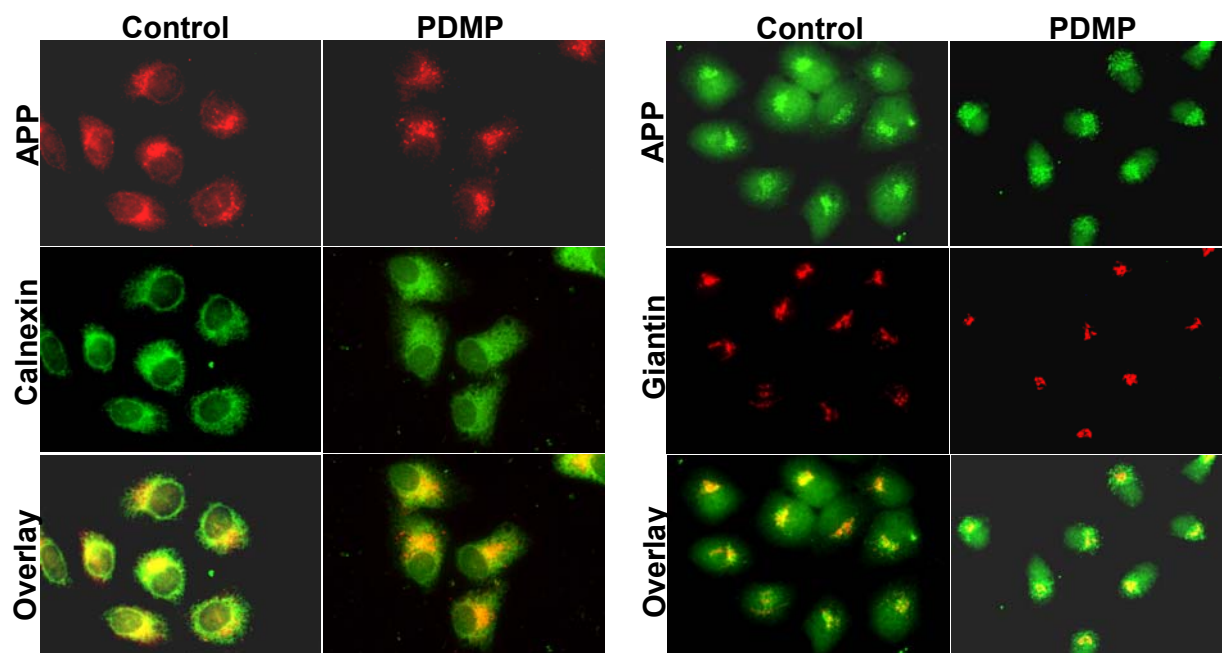


Fig. 4. **Distribution of APP after PDMP treatment** – HeLa cells were cultured without (control) and with (PDMP) 25  $\mu$ M PDMP for 48 hr and were co-stained with anti-APP monoclonal antibody IG7/5A3 and anti-calnexin polyclonal antibody (left panel) or with anti-APP polyclonal antibody 5313 and monoclonal anti-giantin antibody (right panel) as described in materials and methods (2.5.1).

#### 4.1.1.1 Reduction of APP secretion upon PDMP treatment

Thus treatment with 25  $\mu$ M PDMP does not affect cell viability, morphology of the *Golgi* and ER and does not show other non-specific effects reported for higher doses, but it can effectively reduce the cellular GSL content. Therefore treatment with PDMP was used as a first approach to analyze the effects of GSLs modulation on APP processing. HEK293 or HeLa cells were incubated in the presence or absence of PDMP for 48 hr and APP was immunoprecipitated from conditioned media and cell lysates. As shown in Fig. 5, treatment with PDMP of both HEK293 and HeLa cells markedly decreased the secretion of APPs into conditioned media (Fig. 5 A-D). It should be noted that the effects of PDMP on APP secretion were selectively observed in non-transfected cells, but not in cells that stably overexpress APP (data not shown). This might be

due to a tight regulation of the interaction of APP with membrane lipids (see "Discussion"). Therefore, exclusively non-transfected cells were used for further experiments.

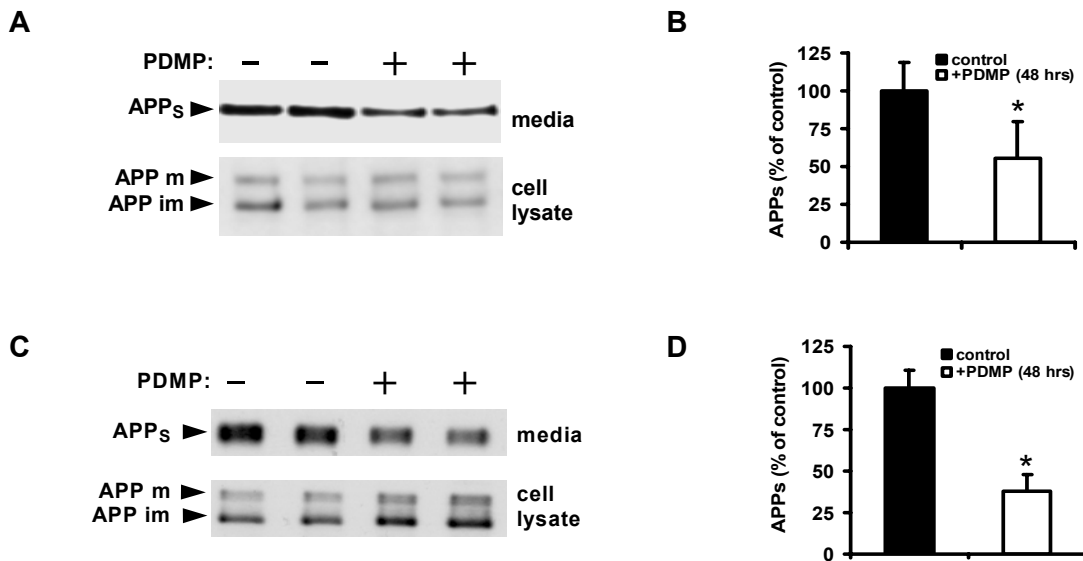


Fig. 5. **Inhibition of GSL biosynthesis decreases the secretion of APPs.** A-D, HEK293 (A,B) and HeLa (C,D) cells were cultured in the absence (-) or presence (+) of 10  $\mu$ M PDMP for 48 hr. APP was immunoprecipitated from conditioned media (A,C; upper panels) and cell lysates (A,C; lower panels) and separated by SDS-PAGE. Secreted APP (APPs) and cellular APP were detected by western immunoblotting. The migration of mature (m) and immature (im) APP is indicated by arrowheads. Secretion of APPs in HEK293 (B) and HeLa (D) cells was quantified by ECL imaging and normalized to cellular APP expression. Values represent means of three independent experiments  $\pm$  s.d. (solid bar, no PDMP; open bar, 10  $\mu$ M PDMP).

Next, it was confirmed that the reduced secretion of APP by PDMP is indeed due to the depletion of GSLs and is not the result of direct interference of PDMP with APP secretion. After 48 hr treatment with PDMP, HeLa cells were washed three times with PBS to remove the residual PDMP which was present in the medium. Control and PDMP treated cells were then cultured in starvation medium for 1 hr followed by [ $^{35}$ S]-methionine metabolic labeling as described in the methods (2.5.3). APPs secretion was investigated in control and treated cells. A strong decrease in APPs levels was observed in cells, which were treated with PDMP (Fig. 6A & 6B). Note that the cells were pre-treated with PDMP for 48 hr and PDMP was not included in medium during the course of experiment. The effect of short-term PDMP treatment was also analyzed. In contrast to long term treatment (48 hr), incubation of cells with PDMP for only 2 hr did not significantly reduce levels of GSLs (data not shown). Under these conditions, the secretion of APP<sub>S</sub> was not significantly changed (Fig. 6C). APP secretion was also studied after treatment of cells with L-PDMP, which is an inactive enantiomer of PDMP. Long-term treatment of cells for 48 hr with L-

PDMP did not reduce APPs secretion (Fig. 6D). Together, these control experiments indicate that the reduced secretion of APPs observed upon PDMP is due to decreased GSL levels in cellular membranes.

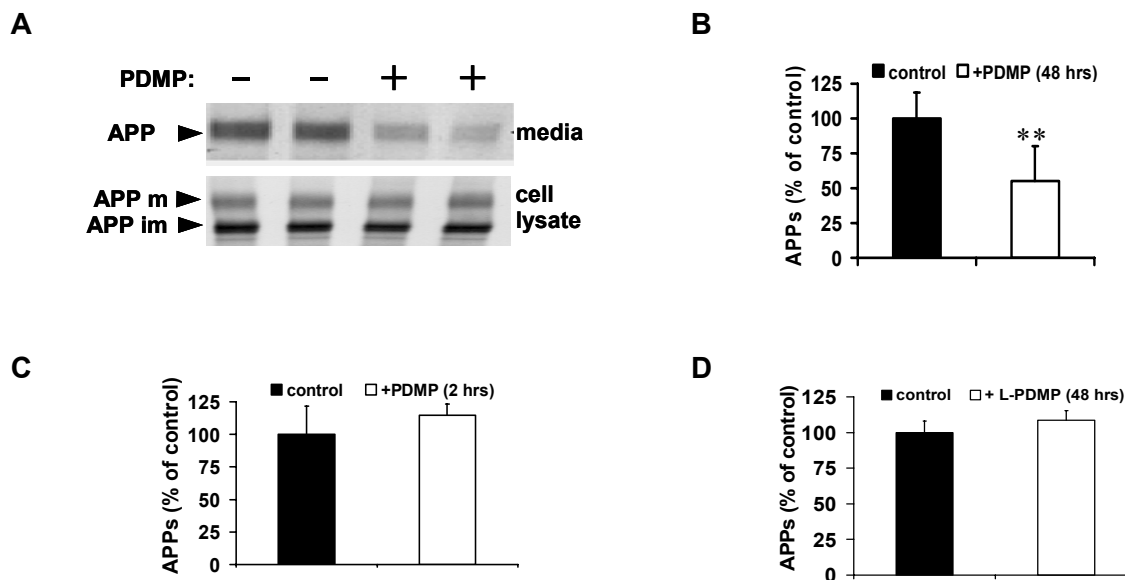
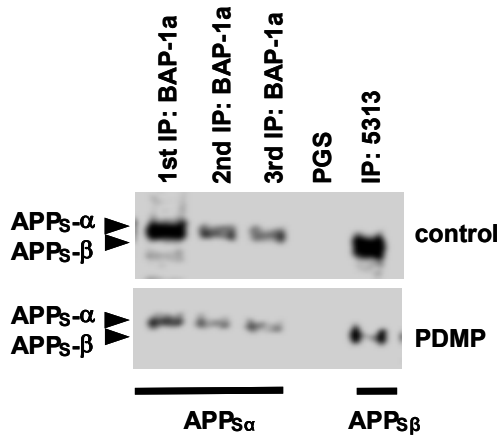


Fig. 6. **Decreased APPs secretion is specific to the depletion of GSLs.** A-B, After culturing in the absence (-) or presence (+) of 10  $\mu$ M PDMP for 48 hr, HeLa cells were washed and starved for 1hr and subsequently labeled with [ $^{35}$ S]-methionine for 1 hr. APP was immunoprecipitated from cell lysates, separated by SDS-PAGE and detected by phosphoimaging (A). Secretion of APPs was quantified (B). C-D, HEK293 cells were cultured without or with 10  $\mu$ M PDMP for 2 hr (C), without or with 10  $\mu$ M L-PDMP for 48 hr (D), APP was immunoprecipitated from conditioned media and cell lysates. Secretion of vehicle treated cells was set as 100% and secretion of APPs was quantified by ECL imaging and normalized to cellular APP expression. Values represent means of three independent experiments  $\pm$  s.d. (solid bar, no PDMP; open bar, 10  $\mu$ M PDMP)

Two distinct cleavage products of APP,  $\alpha$ -soluble APP (APPs- $\alpha$ ) or  $\beta$ -soluble APP (APPs- $\beta$ ) are generated by  $\alpha$ -secretase or  $\beta$ -secretase, respectively. Since any alteration in the ratio of APPs- $\alpha$  to APPs- $\beta$  reflects alterations in amyloidogenic v/s non-amyloidogenic processing of APP, the effect of PDMP treatment on the generation of APPs- $\alpha$  and APPs- $\beta$  was analyzed. The decrease in APP secretion was observed for both variants APPs- $\alpha$  and APPs- $\beta$ , indicating that both APP processing pathways are affected by GSL depletion (Fig. 7).



**Fig. 7. PDMP decreases secretion of both APPs- $\alpha$  and APPs- $\beta$ .** HEK293 cells were cultured in the absence or presence of 25  $\mu$ M PDMP for 48 hr. Cells were then radiolabeled with [ $^{35}$ S]-methionine for 15 min and incubated for a chase period of 2 hr in the presence or absence of PDMP. APPs was immunoprecipitated from conditioned media with monoclonal antibody BAP-1a that recognizes APPs- $\alpha$  (epitope: amino acids 4 - 6 of human A $\beta$ ). Conditioned media was depleted by three sequential immunoprecipitations (IP) with BAP-1a. The medium was subsequently cleared from remaining antibody by incubation with protein G sepharose (PGS). Remaining APPs was immunoprecipitated with antibody 5313 recognizing both APPs- $\alpha$  and APPs- $\beta$ . Immunoprecipitates were separated by SDS-PAGE and radiolabeled proteins were detected by phosphoimaging. As expected, APPs- $\alpha$  migrates slightly slower than APPs- $\beta$  in SDS-gels (arrow heads). PDMP treatment reduced the secretion of both APPs- $\alpha$  and APPs- $\beta$ .

#### 4.1.1.2 Effects of PDMP on APP processing and A $\beta$ generation in neuronal cells

##### Decreased APPs secretion by PDMP treatment in SH-SY5Y cells

Next, human neuroblastoma SH-SY5Y cells were used to prove a role of GSLs in the processing of APP. Two variants of endogenously expressed APP that represent distinct APP splice variants, including the neuron-specific APP<sub>695</sub> form were detected in cell lysates after pulse labeling (Fig. 8A). The presence of distinct splice variants in SH-SY5Y cells was also confirmed by RT-PCR using isoform-specific primers, which amplify different length fragments of APP depending on the isoform. Note the presence of APP<sub>695</sub> isoform only in SH-SY5Y and not in HEK293 cells (Fig. 8C). PDMP treatment did not affect the expression of the distinct APP variants, as demonstrated by the similar levels of cellular APP after pulse labeling (Fig. 8A). As observed in HEK293 and HeLa cells, PDMP treatment also resulted in a significant reduction of APPs in SH-SY5Y cells (Fig. 8A, 8B). The reduction was observed for the APP<sub>751/770</sub> as well as for the neuron-specific APP<sub>695</sub> splice variant.

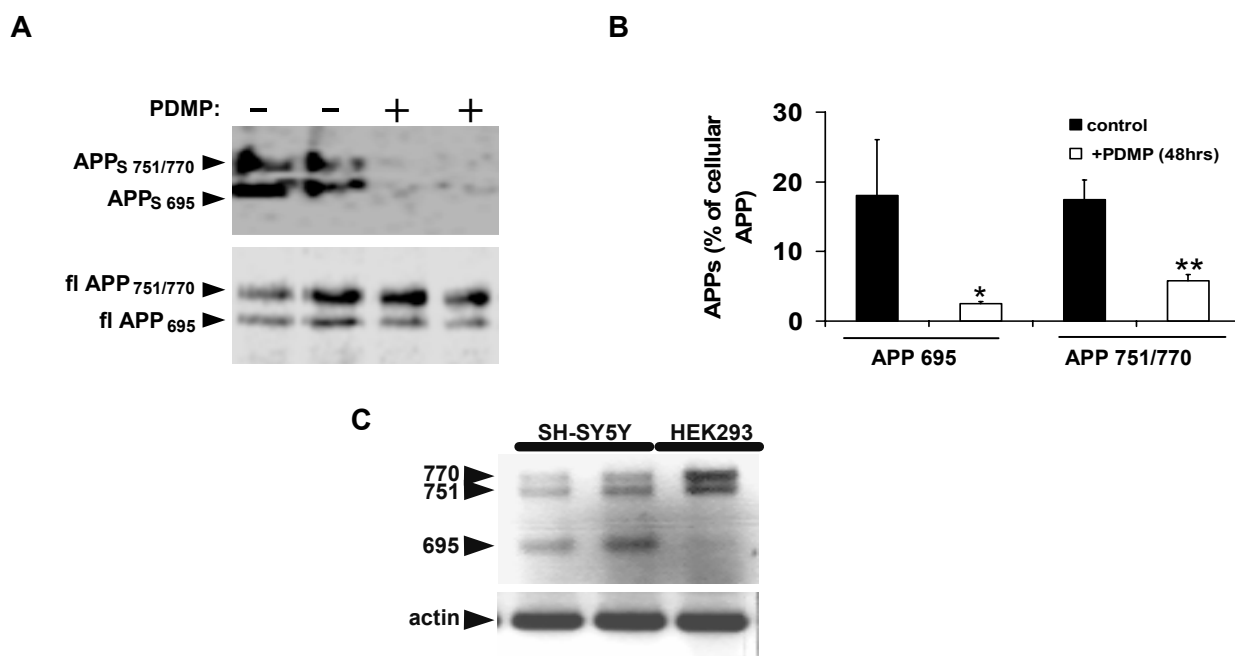


**Fig. 8 GSL depletion inhibits secretion of APP<sub>S</sub> in human SH-SY5Y cells.** *A*, SH-SY5Y cells were cultured in the absence (-) or presence (+) of 25  $\mu$ M PDMP for 48 hr and then pulse labeled with [<sup>35</sup>S]-methionine for 15 min. One set of cells was immediately lysed after the pulse. Another set of cells was incubated for additional 2 hr in the absence or presence of PDMP. APP was immunoprecipitated from the cell lysates (lower panel) and chase media (upper panel) and separated by SDS-PAGE. Radiolabeled APP was detected by phosphoimaging. The migration of APP<sub>S</sub> and full-length APP (fl APP) for the different splice variants APP<sub>751/770</sub> and APP<sub>695</sub> is indicated by arrow heads. *B* Quantification of APP secretion was carried out by phosphoimaging. Values represent means of three independent experiments  $\pm$  s.d. *C*, Total RNA was extracted from SH-SY5Y and HEK293 cells, cDNA synthesis was carried out using oligo(dT) primer and reverse transcriptase. 18 rounds of PCR cycles were performed using synthesized cDNA as a template. Forward and backward PCR primers were designed in the consensus region of the APP, flanking the variable sequences in each isoform.

The ability of PDMP to selectively affect APP secretion in SH-SY5Y cells was further confirmed by quantitative analysis of total protein secretion from control and PDMP treated cells. Cells were pulse labeled with [<sup>35</sup>S]-methionine and chased for 24 hr. Proteins secreted during pulse were precipitated with TCA and pellets were redissolved in 1N NaOH. Secretion of labeled proteins was analyzed by scintillation counting. There was no significant quantitative change in the total protein secretion (Fig. 9A). The inhibition of GCS might lead to the accumulation of its substrate ceramide. Since ceramide was shown to alter the proteolytic processing of APP by stabilizing BACE-1, the effect of C6-ceramide on the secretion of APP<sub>S</sub> was tested. The treatment of cells with ceramide at concentrations of 10  $\mu$ M, which was shown to stabilize BACE1, did not inhibit the secretion of APP<sub>S</sub>, indicating that the inhibition of APP secretion after PDMP was due to decreased levels of GSLs (Fig. 9B).

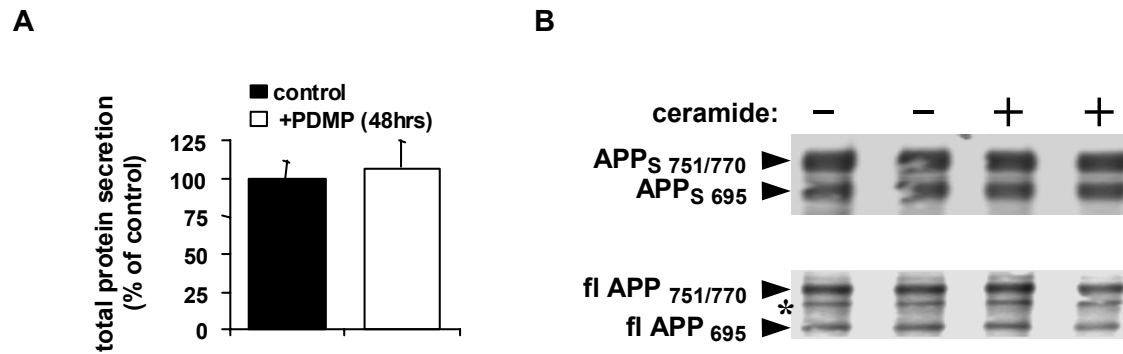


Fig. 9. **GSL depletion selectively inhibits secretion of APP<sub>S</sub> in SH-SY5Y cells.** A, Total protein secretion was analyzed by TCA precipitation of [<sup>35</sup>S]-methionine labeled proteins from the conditioned medium after 24 hr chase period as described in methods (2.5.10.3). Radioactivity was determined by liquid scintillation counting. Values represent means of three independent experiments  $\pm$  s.d. B, Cells were treated with 10  $\mu$ M C6-ceramide for 48 hr and APP was immunoprecipitated from conditioned media and cell lysates and detected by western blotting. The band marked by an asterisk likely represents mature APP<sub>695</sub>.

### GSL depletion decreases levels of secreted A $\beta$

In order to investigate the role of GSLs in the generation of A $\beta$ , SH-SY5Y cells were incubated in the presence or absence of PDMP for 48 hr and A $\beta$  was immunoprecipitated from conditioned media. Secretion of A $\beta$  was significantly reduced upon the inhibition of GSL biosynthesis (Fig. 10A, 10B).

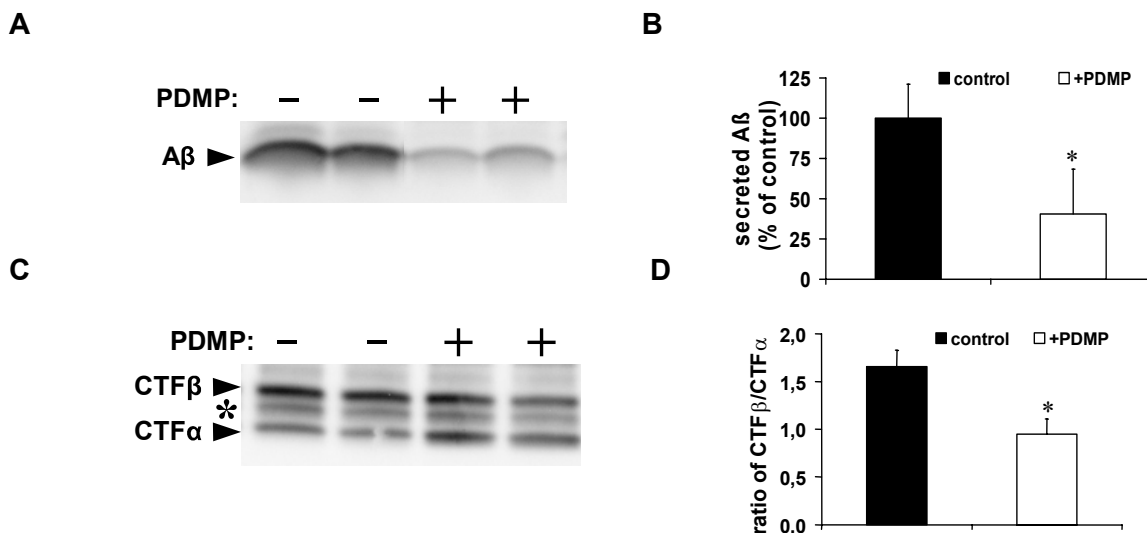


Fig. 10. **GSLs modulate secretion of A $\beta$ .** A, Human SH-SY5Y cells were cultured in the absence (-) or presence (+) of 25  $\mu$ M PDMP for 48 hr and endogenously generated A $\beta$  was immunoprecipitated from conditioned media and detected by western immunoblotting. B, A $\beta$  secretion was quantified by ECL imaging, normalized to cellular APP. C, Membranes were isolated from PDMP-treated (-) and untreated (+) cells. After separation by SDS-PAGE, CTFs were detected by western immunoblotting. CTFs generated by  $\beta$ -secretase cleavage (CTF- $\beta$ ) and  $\alpha$ -secretase cleavage (CTF- $\alpha$ ), are indicated by arrow heads. The CTFs generated by alternative  $\beta$ -secretase cleavage are indicated by an asterisk. D, Quantification of the relative amounts of CTFs was done by ECL imaging. Values represent means of three independent experiments  $\pm$  s.d.



Levels of APP-CTFs that derive from proteolytic processing of APP by  $\beta$ - or  $\alpha$ -secretase were also analyzed. Two major species of APP-CTFs were detected that represent CTF- $\beta$  and CTF- $\alpha$  resulting from  $\beta$ - and  $\alpha$ -secretase cleavage, respectively (Fig. 10 C). In addition, an intermediate band was detected that likely represents CTF- $\beta'$ , a variant generated by an alternative cleavage of APP by  $\beta$ -secretase at Glu-11 within the A $\beta$  domain (Liu et al., 2002). Consistent with predominant secretion of APP<sub>S</sub>- $\beta$  in this cell type, CTF- $\beta$  was the predominant species in control cells (Fig. 10C, 10D). GSLs depletion resulted in almost similar levels of CTF- $\beta$  and CTF- $\alpha$  (Fig. 10C, 10D), probably due to further processing of CTF- $\beta$  by  $\alpha$ -secretase (see "Discussion").

*Thus, above studies establish a role of GSLs in APP processing. Depletion of GSLs using a pharmacological inhibitor PDMP leads to decreased APP secretion. Importantly, secretion of A $\beta$  is strongly reduced upon treatment with PDMP.*

#### **4.1.1.3 Modulation of APP transport by GSLs**

It has been shown that proteolytic processing of APP occurs predominantly in post-*Golgi* secretory and endocytic compartments and at the cell surface. Therefore, expression of APP at the cell surface was assessed by biotinylation with sulfo-*N*-hydroxysuccinimide-biotin. In SH-SY5Y cells, biotinylated APP could not be detected (not shown), probably due to very efficient proteolytic processing and secretion in this cell type that results in low levels of surface APP. In contrast, biotin-labeled APP could be readily detected in HEK293 cells (Fig. 11A). In GSL-depleted cells, the levels of biotin-labeled APP were markedly reduced, demonstrating that suppression of GSL biosynthesis reduces the expression of APP at the cell surface. In contrast, the cell surface expression of the endogenous Fas receptor, also a type I membrane protein, was not decreased upon GSL depletion, indicating a selectivity of PDMP in decreasing the levels of APP at the cell surface (Fig. 11B).

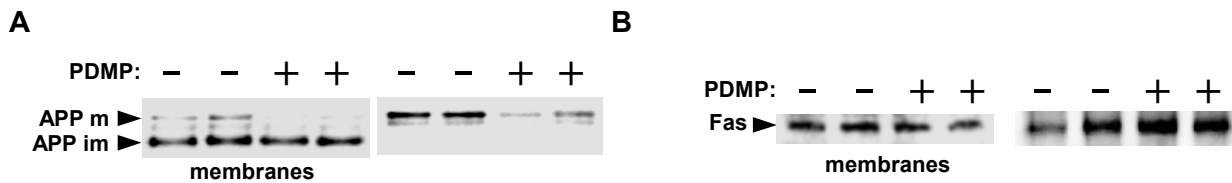


Fig. 11. **GSL depletion decreases the expression of APP at the cell surface.** *A, B*, Cell surface proteins of control (-) and PDMP treated (+) HEK293 cells were labeled with sulfo-NHS-biotin and isolated with streptavidin-conjugated agarose beads as described in the methods section (2.5.9.3). Precipitates were separated by SDS-PAGE and endogenously expressed APP (A) or Fas (B) was detected by western immunoblotting (right panels). As control, cellular levels of APP (A, left panel) and Fas (B, left panel) were also analyzed by western immunoblotting of isolated cell membranes with the respective antibodies. Note the selective biotinylation of mature APP (APP<sub>m</sub>).

Next, the effect of PDMP on the general expression of cell surface proteins was assessed by cell staining with fluorescently labeled wheat germ agglutinin (WGA). WGA is a lectin that binds to glycoproteins with high affinity. In order to label the cell surface glycoproteins control and PDMP treated cells were washed, fixed and incubated with TRITC conjugated WGA without permeabilization. When analyzed by microscopy, no significant difference in the expression of cell surface glycoproteins was observed between treated and non-treated cells (Fig. 12A).

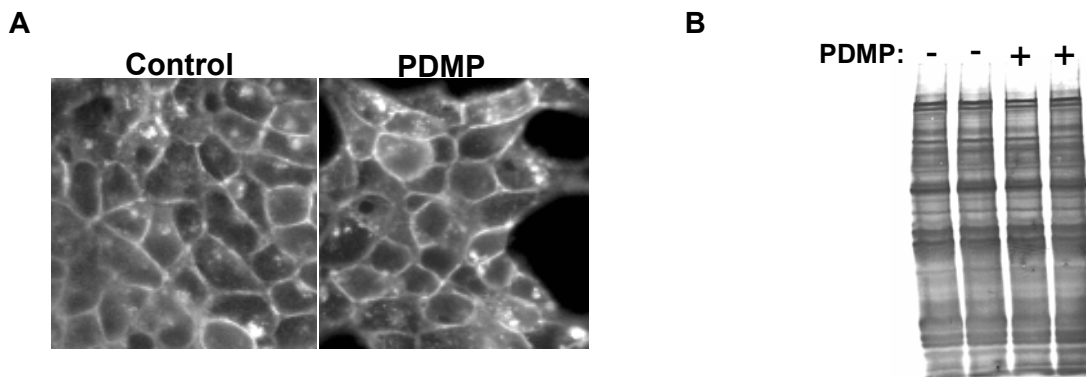


Fig. 12. **GSL depletion does not affect general cell surface protein expression.** *A*, Control (left panel) or PDMP-treated cells (right panel) were stained with TRITC-WGA to detect cell surface glycoproteins and analyzed by fluorescence microscopy. *B*, Cell surface proteins of control (-) and PDMP treated (+) HEK293 cells were labeled with sulfo-NHS-biotin and isolated with streptavidin-conjugated agarose beads. Precipitates were separated by SDS-PAGE and biotin labeled total surface proteins were detected by western immunoblotting using streptavidin

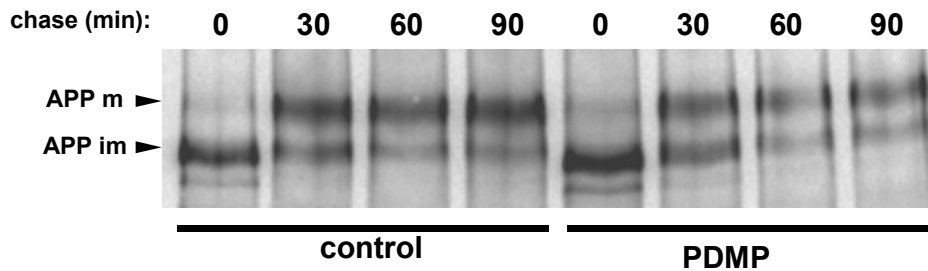
Together, these experiments demonstrate that GSL depletion selectively reduced the cell surface expression of APP without generally affecting the other membrane proteins. In addition, the levels of total surface biotinylated proteins detected by streptavidin-conjugated horseradish peroxidase were very similar in PDMP treated and non-treated cells (Fig. 12B). However, the data do not exclude the possibility that cell surface expression of other selected membrane proteins is also affected by GSL depletion.

#### 4.1.1.4 Decreased APP maturation and stability upon GSLs depletion

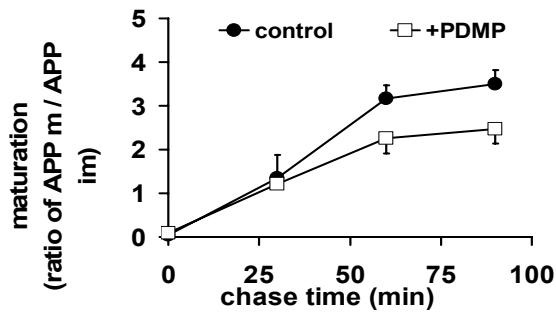
The decreased expression of APP at the cell surface and reduced secretion of APP<sub>S</sub>- $\alpha$  and APP<sub>S</sub>- $\beta$  after GSL depletion suggested that GSLs might be implicated in the forward transport of APP in the secretory pathway. To address this possibility, pulse-chase experiments were performed and the maturation of APP that occurs in the *Golgi* compartment was analyzed. Cells were labeled with [<sup>35</sup>S]-methionine for 10 min and then chased for various time periods.

After pulse labeling, a prominent band was detected representing endogenous immature (*N'*-glycosylated) APP. After 30 min of chase, a slower migrating form appeared that represents mature (*N'*/*O'*-glycosylated) APP. The mature form becomes predominant after 60 to 90 min (Fig. 13A). GSL depletion by PDMP reduced the transport of APP to or within the *Golgi* compartment as indicated by decreased maturation of APP in PDMP-treated cells (Fig. 13A, 13B). In addition, decreased levels of total APP were observed in GSL-depleted cells after chase periods of 60 and 90 min (Fig. 13A, 13C). Since PDMP also reduced the secretion of APP<sub>S</sub> (see Figs. 5 and 6), these data indicate an increased degradation of cellular APP in GSL-deficient cells. Indeed, when cells were cultured in the presence of PDMP for 2 weeks a marked decrease in the levels of mature APP was observed at steady state conditions (Fig. 13D, 13E). In addition, accumulation of immature APP was also evident in these cells. After 2 weeks PDMP treatment GM1 levels were strongly reduced in cellular membranes (Fig. 13D).

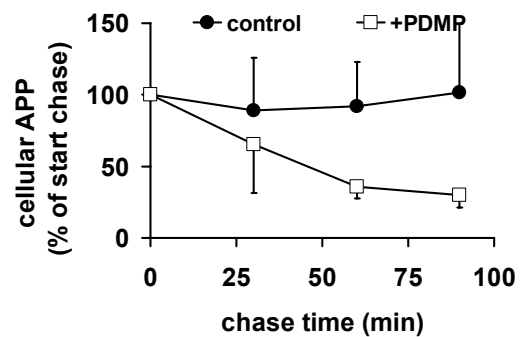
A



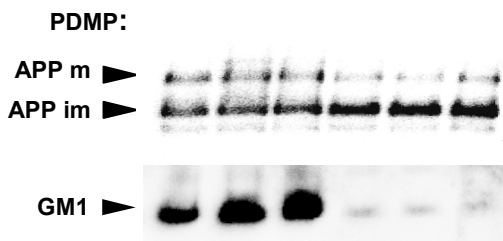
B



C



D



E

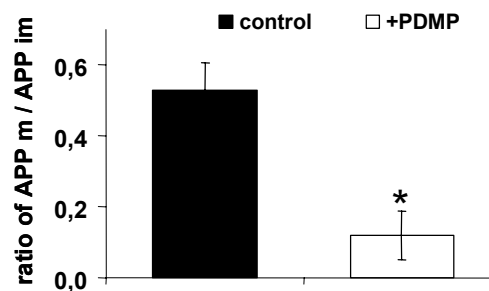


Fig. 13. **Suppression of GSL biosynthesis affects maturation and stability of APP.** A, After culturing in the absence or presence of 10  $\mu$ M PDMP for 48 hr, HeLa cells were labeled with [ $^{35}$ S]-methionine for 10 min and chased for the indicated time periods. APP was immunoprecipitated from cell lysates, separated by SDS-PAGE and detected by phosphoimaging. The migration of mature (m) and immature (im) APP is indicated by arrow heads. B, C, Quantitation of APP maturation (B) and stability (C). In PDMP treated cells (open squares) the maturation of APP is significantly decreased as compared to untreated cells (closed circles) (B). In addition, the stability of cellular APP is reduced in PDMP treated cells (C). Values represent means of three independent experiments  $\pm$  s.d. D-E, HEK293 cells were treated with 10  $\mu$ M PDMP for two weeks. APP (upper panel) and GM1 (lower panel) were detected from isolated cellular membranes. The migration of mature (m) and immature (im) APP is indicated by arrow heads (D). Ratio of mature to immature APP was significantly lower after two weeks PDMP treatment (E).

### 4.1.2 Analysis of APP processing in GSL deficient GM95 cells

GM95, a cell line deficient in GSLs, first described in 1994 was derived from parent B16 mouse melanoma cells by sequential chemical mutagenesis. GM95 cells were characterized for absence of GSLs and the lack of GCS activity. Notably levels of the GCS substrate, ceramide were found to be unchanged in the mutant cell line. Previously, GM95 cells have been used as a model to investigate effects of GSL deficiency in various biological processes. Therefore, to validate the findings in an independent genetic model, B16 and GM95 cells were used to study the effect of GSL depletion on APP processing. As expected, very little if any GM1 could be detected in GM95 cells, whereas B16 cells express robust amounts of GM1 (Fig. 14A) (Ichikawa et al., 1994).

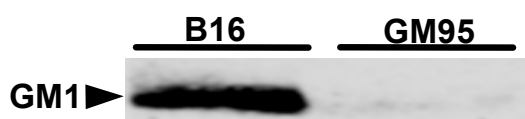


Fig.14. **GSLs deficiency in GM95 cells.** Cellular membranes were isolated from mouse melanoma B16 and GM95 cells and GM1 was detected by western immunoblotting. Cholera toxin-HRP was used for immunodetection of GM1.

To verify the effect of GSLs depletion by PDMP on APP maturation and stability observed in the HeLa, HEK293 and SH-SY5Y cells, pulse-chase experiments in B16 and GM95 cells were performed. In B16 cells, endogenous APP undergoes maturation as indicated by the appearance of a slower migrating band during the chase period (Fig. 15, *left panel*). In contrast, the GSL-deficient GM95 cell line revealed significantly reduced maturation of APP (Fig. 15, *right panel*), which is consistent with the data obtained with pharmacological inhibition of GSL biosynthesis (see Fig. 13A).

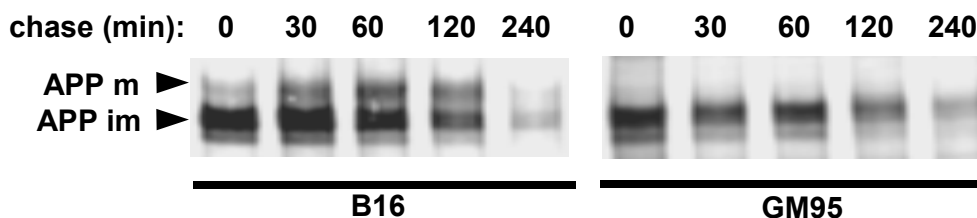


Fig. 15. **Decreased maturation and cellular levels of APP in GSL deficient cells.** Pulse-chase experiment for APP in B16 (left panel) and GM95 (right panel) cells was carried out as described in Fig. 13A. The maturation of APP was strongly inhibited in GSL-deficient GM95 cells as compared to B16 cells.

The steady state levels of cellular APP were strongly decreased in GM95 (Fig. 16A), consistent with decreased stability of cellular APP in absence of GSLs. Expression of APP in both cell lines at the mRNA level was also investigated by RT-PCR. APP mRNA expression was comparable in both cell lines (Fig. 16B), further supporting the finding that APP levels are regulated by GSLs at post-translational steps. Two distinct transcripts of APP were detected by RT-PCR in B16 and GM95 cells. One of which corresponds to 751 amino acids long isoform of APP.

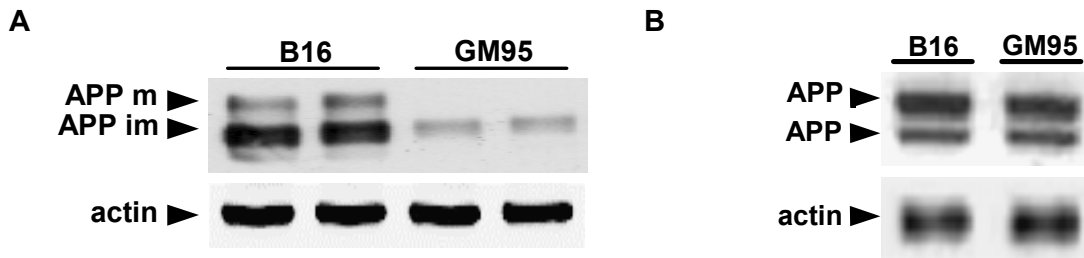


Fig. 16 **Decreased cellular levels of APP in GSL deficient cells.** *A*, Steady state levels of APP in B16 and GM95 cells were compared by western immunoblotting. Actin was used as a loading control. *B*, mRNA expression of APP was analyzed by RT-PCR as described in the methods section (upper panel). Expression of actin mRNA was analyzed as control (lower panel).

#### **4.1.3 Targeted suppression of lactosylceramide synthase (LCS) by shRNA**

Although B16 and GM95 can be used as an independent genetic model for GSL deficiency, it has certain limitations. First, GM95 cells were generated by random mutagenesis and later characterized for the lack of GSLs, second APP processing in mouse is considerably different than in humans. Therefore, to study effects of GSL deficiency in an independent human genetic cellular model, knock down of expression of the key genes involved in GSLs biosynthesis was sought after using RNA interference (RNAi) technology. In recent years RNAi has emerged as a powerful tool to analyze gene function. Targeted suppression of particular gene expression with small interfering RNAs (siRNA) is much quicker compared to classical knockout techniques (see “3.3”).

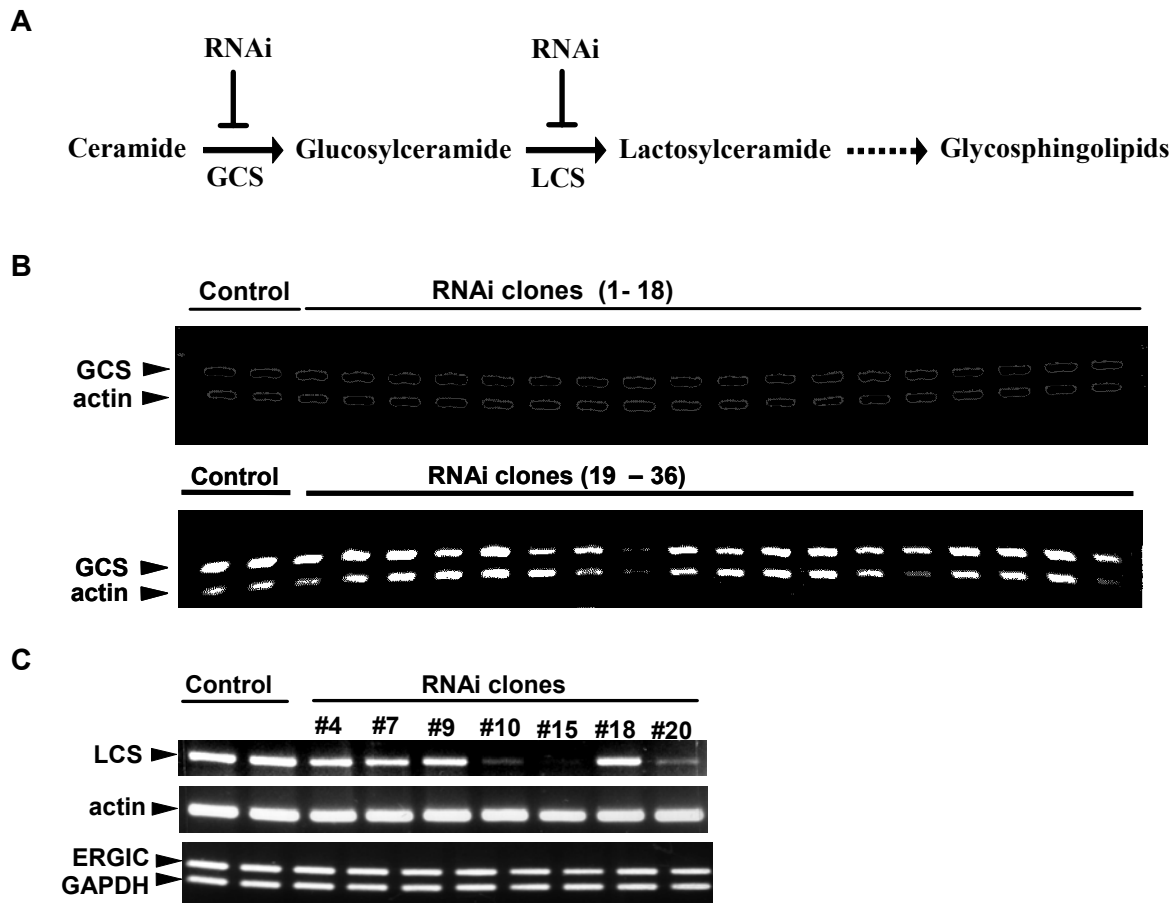


Fig. 17. **Specific knock down of LCS expression.** A, Schematic showing of GCS and LCS knock down by RNA interference. B, HEK293T cells were stably targeted with pSupZeo vector (see methods section 3.3) containing a 19 nucleotide target sequence for GCS. Stable clones were selected and screened for GCS expression by RT-PCR. Actin was amplified as a control. C, HEK293T cells were stably targeted with pSupZeo vector (see methods section 3.3) containing a 19 nucleotide target sequence for LCS. Selected clones were screened for efficient LCS suppression with RT-PCR (*top panel*). Expression of actin (*middle panel*), GAPDH and ERGIC53 (ERGIC) (*bottom panel*) were also analyzed in the same samples.

Two key genes, GCS and lactosylceramide synthase (LCS), involved in GSL biosynthesis were targeted by RNAi technology (Fig. 17A). HEK293T cells were stably transfected with a vector encoding RNA targeting sequence (shRNA) and zeocin resistance. Selected clones were then screened for suppression of expected target gene by RT-PCR. All clones analyzed for GCS knock down still expressed comparable levels of GCS mRNA similar to control HEK293T cells (Fig. 17B). However, successful knock down of LCS was achieved as indicated by efficient down regulation of LCS expression in clones 10, 15 and 20. Expression of other house-keeping genes actin, GAPDH and unrelated gene ERGIC53 was not changed in clones with prominent LCS suppression (Fig. 17C).

#### 4.1.3.1 Altered metabolism of APP in LCS deficient cells

Consistent with GM95 cells and pharmacological suppression of GSL biosynthesis, strongly reduced levels of cellular APP were observed in LCS deficient cells, indicating a decreased stability of APP in these cells. The ratio of mature to immature APP was also altered in RNAi targeted cells. In control cells higher amount of mature APP was present compared to immature APP, whereas in LCS deficient cells immature APP levels were much higher compared to mature APP (Fig. 18). This suggests a slower maturation of APP in LCS suppressed cells. The secretion of APP was also strongly reduced in these cells. Together, these results support earlier findings that the GSLs depletion results in decreased stability, maturation and secretion of APP.

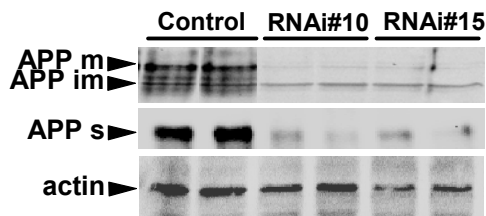


Fig. 18. **Decreased cellular and soluble APP in LCS deficient cells.** A, Cellular (*top panel*) and soluble (*middle panel*) APP levels were analyzed by western immunoblotting in the clones which showed successful knock down of LCS. Actin was detected as control (*lower panel*). Arrow heads indicate migration of the respective APP product.

Next, the subcellular localization of APP in control and LCS suppressed cells was analyzed by co-staining APP with antibodies against calnexin and giantin marker proteins for ER and *Golgi*, respectively (Fig. 19). In control cells, most APP co-localized with giantin. However, in LCS deficient cells, APP stain appeared to be vesicular with more even distribution within the cell body. Some of these vesicles also co-stained with the ER marker calnexin as evidenced by yellow dots in the overlay. Notice the similar distribution of marker proteins in control and LCS suppressed cells, indicating selective effect of knock down of LCS on APP localization. However, further studies need to be performed to characterize the nature of APP positive vesicles in more detail. Since immature APP is the predominant species detected after LCS suppression, vesicles containing APP in LCS suppressed cells should most likely be derived from ER membranes.



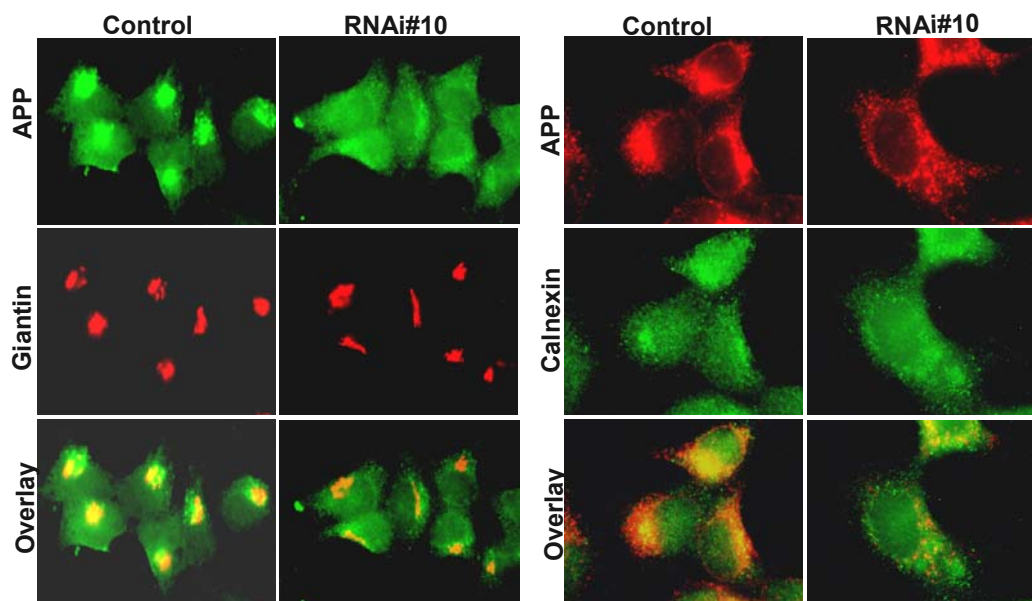


Fig. 19. **Subcellular APP distribution in LCS deficient cells.** HEK293T control and LCS deficient cells were co-stained with anti-APP polyclonal antibody and anti-giantin monoclonal antibody. Samples were analyzed by immunofluorescence microscopy (*left panel*). Similarly, control and LCS deficient cells were co-stained with anti-APP monoclonal antibody and anti-calnexin polyclonal antibody (*right panel*).

To ensure that the observed effects were due to the lack of GSLs in RNAi targeted cells, exogenous bovine brain GSLs were added to these cells for 48 hr and APP secretion as well as APP expression was analyzed. Indeed, incubation with GSLs increased the cellular APP levels as well as restored the secretion of APP (Fig. 20). This result also indicates that the exogenously added GSLs can confer stability to APP in LCS deficient cells and thereby facilitate its transport and secretion.



Fig. 20. **Increased cellular and secreted APP after GSLs repletion in LCS deficient cells.** LCS deficient cells were incubated with indicated concentrations of bovine brain GSLs for 48 hr. Cellular APP (*top panel*) and secreted APP (*bottom panel*) were analyzed by western immunoblotting.

*Thus, independent of cell type, depletion of GSLs decreases APP expression, secretion and stability. GSLs seem to modulate the transport of APP in the secretory pathway. Depletion of GSLs by PDMP decreased the maturation and cell surface expression of APP. Strongly reduced levels of matured APP in GSL deficient GM95 cells as well as in LCS suppressed cells further confirmed the effects observed with PDMP. Moreover, suppression of LCS also caused redistribution of APP, suggesting a role of GSLs in APP subcellular localization. Interestingly, exogenous GSLs treatment could normalize the secretion of APP in LCS targeted cells.*

#### 4.1.4 Addition of exogenous GSLs increases levels of cellular and secreted APP as well as APP-CTFs

Pharmacological treatment and independent genetic models (B16-GM95, LCS RNAi) established the role of GSLs in APP maturation, stability and processing. These studies were based on a GSLs depletion model. Next, the effect of elevated levels of GSLs on APP metabolism was analyzed in detail. Contrary to depletion, addition of GSLs increased cellular APP levels at various GSLs concentrations (Fig. 21A). A dose dependent accumulation of APP-CTFs was also apparent upon incubation with GSLs, which appeared to reach saturation at 50  $\mu\text{g/ml}$  after 48 hr incubation. Since APP-CTFs represent the immediate precursor to  $\text{A}\beta$  by acting as a substrate of the  $\gamma$ -secretase complex, a strong accumulation of APP-CTFs could indicate an impaired  $\gamma$ -secretase activity. Alternatively, APP-CTFs degradation in proteasomes and lysosomal compartments might be affected by GSLs. Thus, any alterations in APP-CTFs metabolism by either of these pathways would probably result in their accumulation, which might affect the generation of  $\text{A}\beta$ . Hence, studies were extended to understand the mechanism by which GSLs cause accumulation of APP-CTFs. Effects of addition of 50  $\mu\text{g/ml}$  GSLs on APP secretion and maturation as well as on APP-CTF levels were validated in HEK293 cells. Increased levels of soluble APP, cellular APP along with strong accumulation of APP-CTFs was obvious in GSLs treated cells (Fig. 21B). Notably, levels of another membrane protein, insulin receptor, were not altered after GSLs treatment.

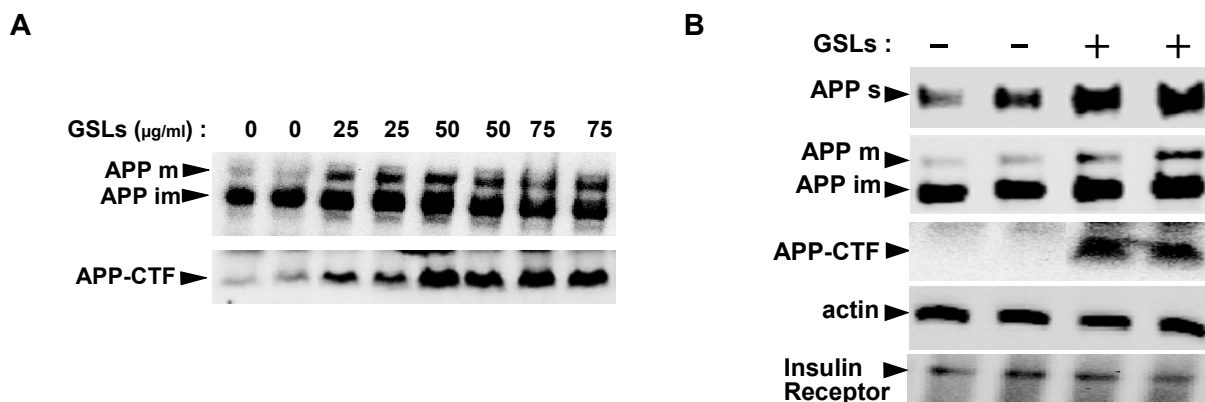


Fig. 21. **Increased expression and secretion of APP and accumulation of APP-CTFs by exogenous gangliosides.** A, HEK293 cells were incubated with indicated concentrations of bovine brain GSLs for 48 hr. Cellular APP (*top panel*) and APP-CTFs were analyzed by western immunoblotting (*bottom panel*). B, HEK293 cells were cultured for 48 hr in the absence (-) or presence (+) of 50  $\mu\text{g/ml}$  purified ganglioside mixture from bovine brain. APP<sub>s</sub> in conditioned media (*top panel*) and cellular APP (*second panel*), APP-CTFs (*third panel*) in isolated cell membranes, were detected by immunoblotting. Mature (m) and immature (im) APP is indicated by arrow heads. Actin (*fourth panel*) and insulin receptor (*bottom panel*) were detected as a loading and specificity control, respectively.

Previous studies have established the uptake of exogenous GSLs in cultured cells, however, a portion of the GSLs are also merely adsorbed to the cell surface rather than getting inserted into the plasma membrane. Effects described here do not distinguish between these two pools (see “Discussion”) (Schwarzmann et al., 1983). GSLs are catabolized by various lysosomal enzymes and generated products could be re-utilized for biosynthesis of other or the same sphingolipids. Since the effects of GSL treatments on APP processing were analyzed after 48 hr, it is important to demonstrate that the GSL levels were still higher at this time point to attribute observed effects to higher amounts of GSLs. After addition of GSLs to cells, cellular GM1 levels were found to be elevated already at 12 hr. This increase in GSLs persisted at least for 72 hr (Fig. 22A). Accordingly, there was also a slight increase in APP-CTFs at 24 hr and a stronger increase was seen at 48 hr. 72 hr after addition of GSLs, APP-CTF levels dropped slightly, but were still much higher than control (Fig. 22B). The second addition of GSLs after media change during the last 12 hr of incubation further boosted the APP-CTFs levels, probably indicating a partial degradation of GSLs during the incubation period that could lead to destabilization of APP-CTFs.

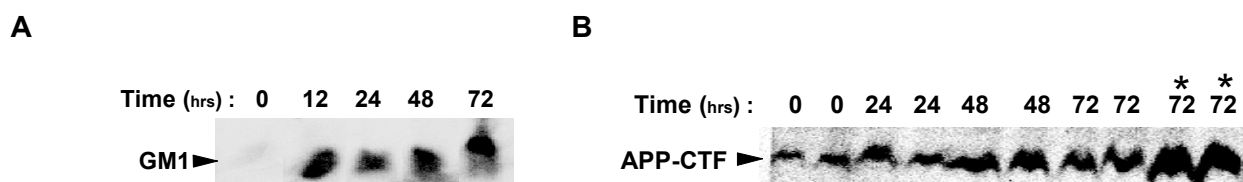


Fig. 22. **Time and dose dependent accumulation of APP-CTFs upon incubation with GSLs.** A, HEK293 cells were incubated with 50 µg/ml GSLs for indicated times and GM1 was detected in cellular membranes by western immunoblotting. B, HEK293 cells were incubated with 50 µg/ml GSLs for indicated time, in the last two lanes (indicated with asterisk) fresh GSLs were added to cells after media change during the last 12 hours. APP-CTFs were detected in cellular membranes.

Cells, stably overexpressing APP<sub>695</sub> (Fig. 23A, 23B) or APP<sub>695</sub> and BACE-1 (Fig. 23C, 23D) did not show comparable increase in APP and APP-CTF levels when treated with GSLs. Thus, consistent increase in APP and APP-CTF levels after GSLs treatment were observed selectively for endogenous APP. This also indicates a saturation effect of higher amounts of APP, with very little or no scope for further up-regulation of APP expression after GSLs treatment.

Furthermore, the effect of increased GSLs on APP subcellular localization was analyzed by immunofluorescence microscopy. Simultaneously, cells were stained for ER and *Golgi* marker proteins, calnexin and giantin, respectively (Fig. 24). Treatment of cells with GSLs did not cause any gross changes in ER and the *Golgi* morphology, however, the giantin stain appeared to be more condensed in treated cells. Most of the APP co-localized with giantin in control as well as

GSLs treated cells. Since more subtle alterations in protein distribution might not be detected by immunofluorescence, subcellular fractionation of control and GSL enriched cells was also performed (see “Results, Fig. 30”).

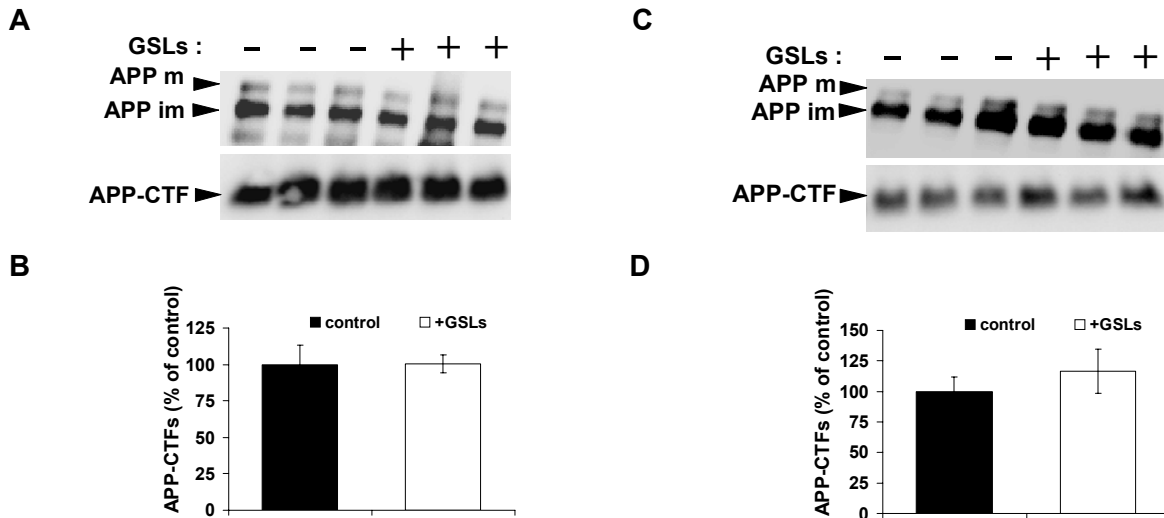


Fig. 23 **No prominent accumulation of APP-CTFs after GSL enrichment in HEK293 cells overexpressing APP<sub>695</sub>.** A-D, HEK293 cells stably expressing APP<sub>695</sub> (A, B) and APP<sub>695</sub> together with BACE-1 (C,D) were incubated with 50 µg/ml GSLs for 48 hr and cellular APP (*top panels*-A, C) and APP-CTFs (*bottom panels*-C, D) were detected in isolated cellular membranes by western immunoblotting. The migration of mature (m) and immature (im) APP is indicated by arrow heads. B and D represent the quantitation of APP-CTF levels after GSLs treatment in cells expressing APP<sub>695</sub> and APP<sub>695</sub> together with BACE-1 respectively.

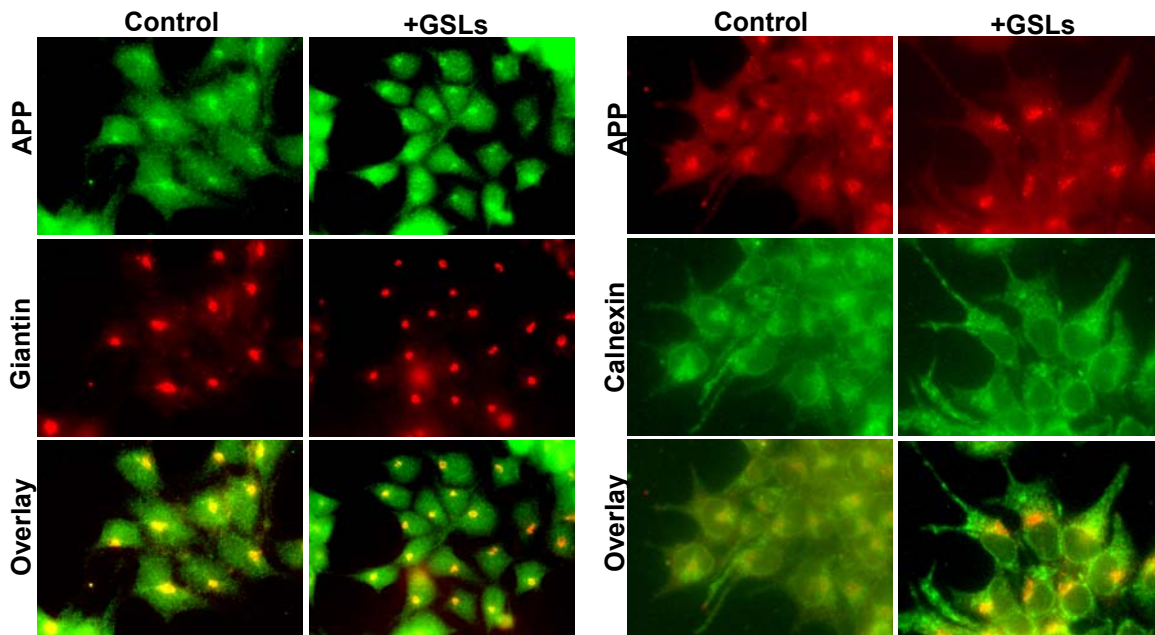


Fig. 24. **Distribution of APP in GSLs enriched cells** – HEK293 cells were incubated with 50 µg/ml GSLs for 48 hr and co-stained with anti-APP monoclonal antibody and anti-calnexin antibody (*right panel*), anti-APP 5313 antibody and anti-giantin antibody (*left panel*) as described in materials and methods. Samples were analyzed by microscopy.

Incubation of human neuroglioma H4 cells with GSLs resulted in a very similar increase in APP levels as well as strong accumulation of APP-CTFs (Fig. 25A). The major constituents of the bovine brain GSL preparation are GM1 (21%), GD1a (40%), GD1b (16%) and GT1b (19%). The ability of these individual GSLs to accumulate APP-CTFs was tested. All four GSLs led to similar accumulation of APP-CTFs after 48 hr of treatment (Fig. 25B). Next, the effect of other type of lipids on APP-CTF levels was analyzed in H4 cells. As demonstrated in Fig. 25C, accumulation of APP-CTFs was also observed with sphingomyelin apart from GM1. Interestingly, phospholipids such as phosphatidyl serine and phosphatidic acid which have diacylglycerol backbone did not cause accumulation of APP-CTFs. These results demonstrate that the metabolism of APP-CTFs is selectively affected by sphingolipids, whereas, other lipids like phospholipids, do not have this effect.

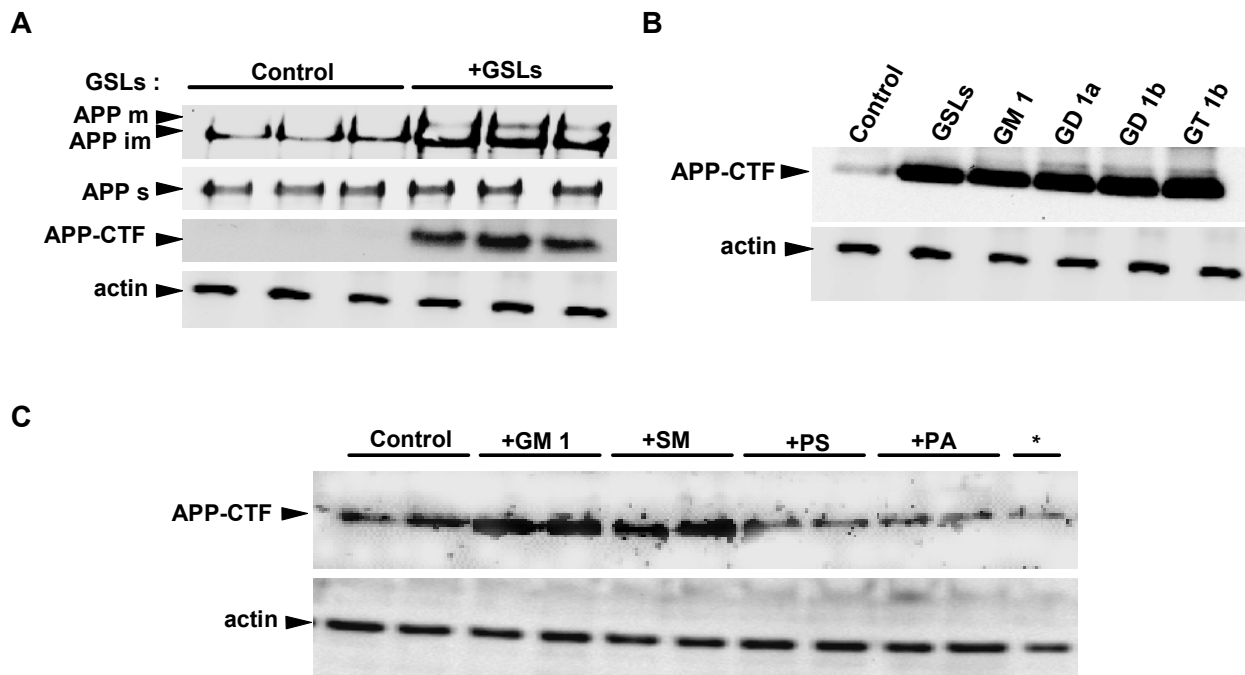


Fig. 25. **Accumulation of APP-CTFs is specific to sphingolipid** A, H4 cells were incubated with 50  $\mu\text{g/ml}$  GSLs, cellular APP (*top panel*) and APP-CTFs (*third panel*) were detected from isolated membranes as well as soluble APP (*second panel*) was detected from conditioned media. B, H4 cells were incubated with 50  $\mu\text{g/ml}$  of individual GSL as indicated for 48 hr. As control, cells were also incubated with GSLs mix. APP-CTFs were analyzed in control and treated cellular membranes by western immunoblotting. C, H4 cells were treated individually with GM1, sphingomyelin (SM), phosphatidylserine (PS), phosphatidic acid (PA) at the concentration of 50  $\mu\text{g/ml}$  or solvent alone (\*) for 24 hr. Cellular APP-CTFs generation was analyzed by western immunoblotting. Actin was detected as loading control.

#### 4.1.4.1 Effect of GSL enrichment in human neuronal cells

To analyze the effect of increased GSLs on A $\beta$  production, SH-SY5Y cells that secrete high amounts of A $\beta$  were used. Earlier observed effects of GSL enrichment, namely, increased cellular and soluble APP as well as accumulation of APP-CTFs were confirmed in these cells (Fig. 26A, 26B). Since sphingolipids can be catabolized into ceramide and respective fatty acids, it could be possible that the accumulation of APP-CTFs is mediated by increased levels of ceramide, rather than sphingolipids themselves. Treatment of SH-SY5Y cells with C6-ceramide caused only mild increase in APP-CTFs as compared to the strong increase observed after GSLs treatment (Fig. 26C, 26D) (“See Discussion”). The generation of A $\beta$  after GSLs treatment was investigated in SH-SY5Y cells by pulse labeling the cells with [<sup>35</sup>S]-methionine for 2 hr and a subsequent chase for 5 hr, followed by immunoprecipitation and detection of A $\beta$ . Secretion of A $\beta$  was found to be significantly enhanced in GSLs treated cells (Fig. 26E, 26F).

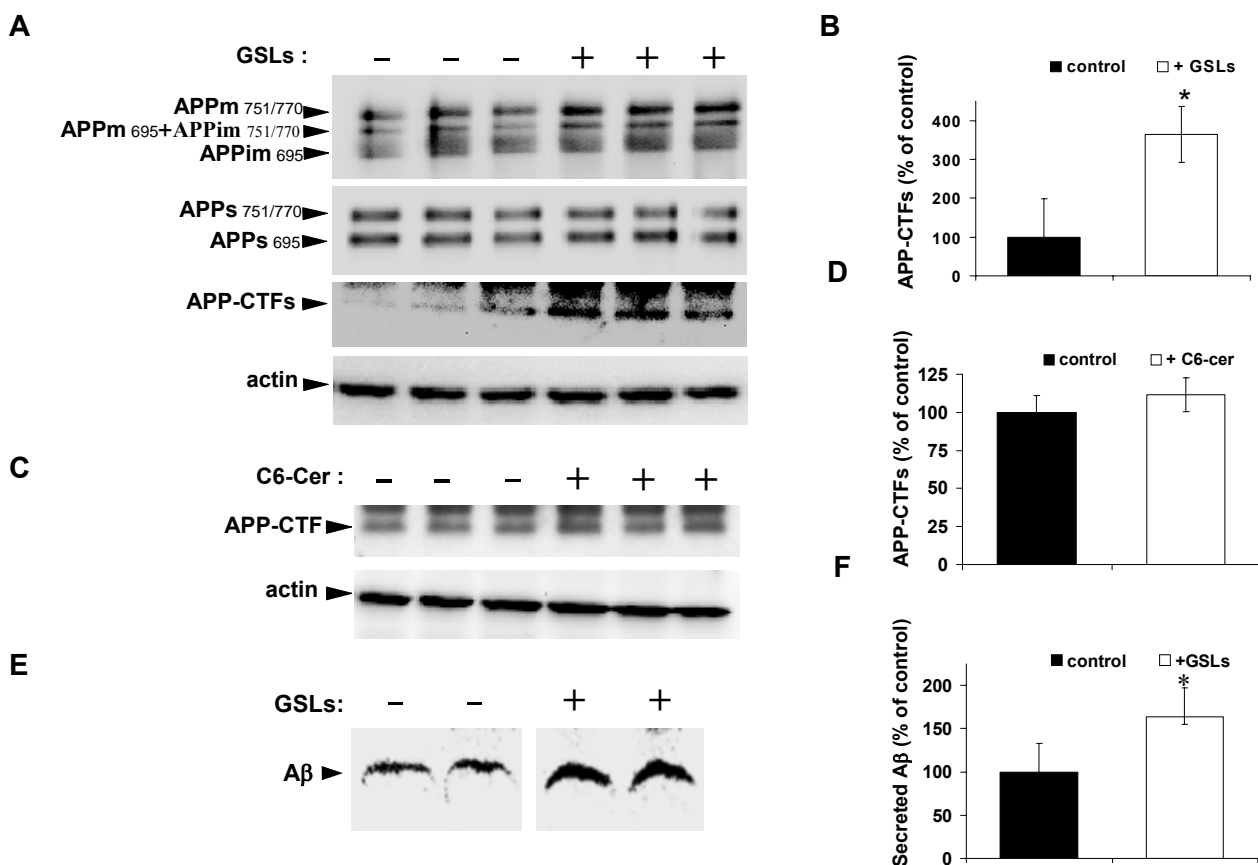


Fig. 26. **Increased A $\beta$  secretion upon GSL enrichment.** A-B, APP processing after GSL enrichment was analyzed in SH-SY5Y cells. Cellular APP (*top panel*), secreted APP (*second panel*), APP-CTFs (*third panel*; B) and actin (*bottom panel*) were analyzed without (-) and with (+) GSLs as described earlier. C-D, SH-SY5Y cells were incubated with 10  $\mu$ M C6-ceramide for 48 hr and APP-CTFs were detected by western immunoblotting. Actin was detected as loading control. E-F, SH-SY5Y cells were cultured in the absence (-) or presence (+) of exogenous GSLs and secretion of A $\beta$  was analyzed.

Simultaneous accumulation of APP-CTFs with increased A $\beta$  levels upon GSL treatment, suggest that  $\gamma$ -secretase dependent effects contribute to the observed effects of GSLs on APP processing. Therefore, the effect of exogenously added GSLs on  $\gamma$ -secretase activity was analyzed by performing an *in vitro*  $\gamma$ -secretase assay. Cellular membranes from control and GSLs enriched cells were resuspended in citrate buffer and incubated at 37°C. Bacitracin A, an inhibitor of insulin degrading enzyme, was added to the assay to stabilize the reaction product, AICD. Incorporation of GSLs into cellular membranes for 48 hr did not affect the generation of AICD. In contrast, the specific  $\gamma$ -secretase inhibitor N-[N-(3, 5-Difluorophenacetyl-L-alanyl)]-S-phenylglycine t-butyl ester (DAPT) hampered the generation of AICD effectively (Fig. 27A). Note the increased levels of APP-CTFs in membranes from GSLs treated cells. Also, unlike DAPT GSLs did not inhibit AICD generation when added directly to isolated membranes during the *in vitro* assay (Fig. 27B).

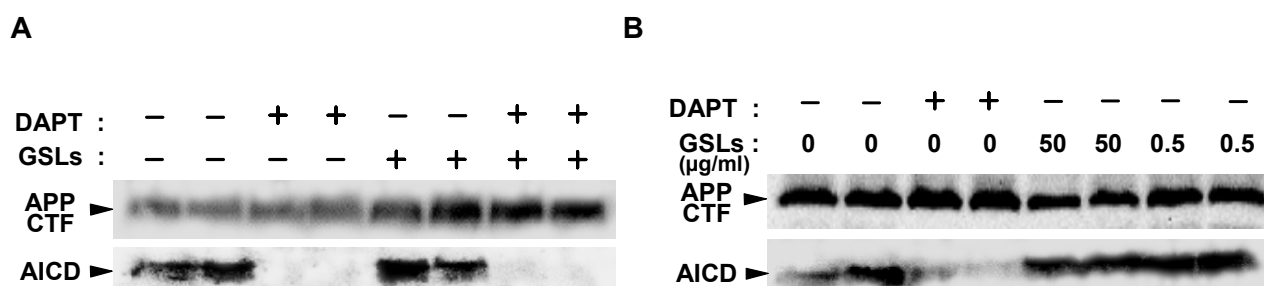


Fig. 27. **GSLs do not affect  $\gamma$ -secretase activity directly.** A, Cellular membranes were isolated from control H4 cells (-) and from the cells incubated with 50  $\mu$ g/ml GSLs (+) for 48 hr. *In vitro*  $\gamma$ -secretase assay was performed using membranes in presence (+) and absence (-) of 1  $\mu$ M DAPT. Later membranes were centrifuged at 13,000 rpm for 1 hr to separate pellet and supernatant. APP-CTFs were detected in the pellet and AICD was detected in the supernatant by western immunoblotting with APP CT antibody. B, Cellular membranes were isolated from H4 cells and *in vitro*  $\gamma$ -secretase assay was performed in the presence (+) and absence (-) of GSLs at indicated concentrations as well as in presence (+) of 1  $\mu$ M DAPT. Similarly, APP-CTFs and AICD were detected in pellet and supernatant after centrifugation.

*Thus, in various cell types, including human neuronal SH-SY5Y cells, enrichment of GSLs led to enhanced cellular and soluble APP levels. Moreover, addition of exogenous GSLs also up regulated secretion of A $\beta$  and increased cellular APP-CTF levels. The observed accumulation of APP-CTFs after GSLs enrichment was not due to  $\gamma$ -secretase inhibition.*

#### 4.1.4.2 Distribution of APP-CTFs in GSLs enriched cells

The above described results indicate that GSLs do not appear to cause accumulation of APP-CTFs by direct inhibition of  $\gamma$ -secretase. An alternative explanation could be an inefficient degradation of APP-CTFs by the proteasome and/or by lysosomal compartments. This could occur either because of improper trafficking of APP-CTFs to these compartments or there could be proper transport of APP-CTFs to these compartments but lack of degradation, due to burden of degradation of excess lipids in these compartments. To address these issues the subcellular distribution of added GSLs as well as accumulated APP-CTFs was analyzed.

The distribution of GSLs, GM1 in particular, was analyzed by staining cells with cholera toxin. GM1 was found to be accumulated at the cell surface as well as within intracellular vesicular compartments (Fig. 28). There was a strong over all accumulation of GM1, indicating incorporation and accumulation of exogenously fed GSLs in varied cellular membranes.

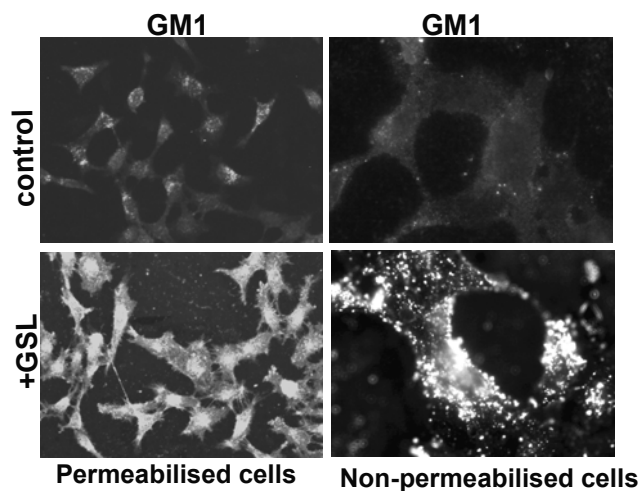


Fig. 28. **Exogenously added GSLs accumulate at cell surface and in intracellular compartments.** H4 cells were incubated in absence (control) or presence (+GSLs) of GSLs 50  $\mu$ g/ml of exogenous bovine brain GSLs for 48 hr. One set of cells was fixed, permeabilized with triton and stained for GM1 using cholera toxin and polyclonal anti-cholera toxin antibody, followed by fluorescent Alexa dye. Other set was fixed and stained for GM1 without permeabilization with triton.

Studies with GCS inhibition revealed that the GSLs facilitate the forward transport of APP and thereby increase cell surface localization of APP. Therefore, the expression of APP-CTFs at the cell surface was analyzed in order to address the effect of GSLs on transport of APP-CTFs in the secretory pathway. Surprisingly, cell surface expression of APP-CTFs was markedly reduced in GSLs enriched cells (Fig. 29). Note, the increase in APP-CTFs in total cellular lysates and the reduction in biotinylated APP-CTF levels in the same lysates upon GSLs treatment. The decreased expression of APP-CTFs at the cell surface can be either due to enhanced endocytosis or slower forward transport of CTFs in presence of excess GSLs.



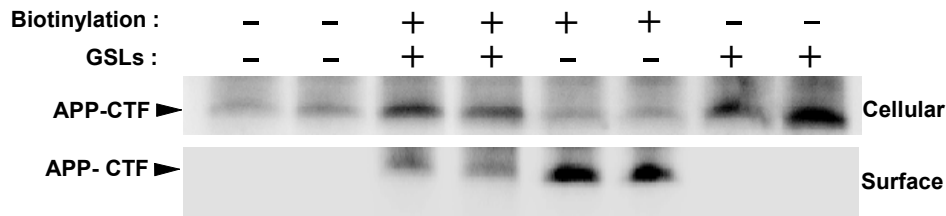


Fig. 29. **APP-CTFs accumulate in intracellular compartments in GSLs treated cells.** H4 cells were cultured in absence (-) or presence (+) of 50  $\mu\text{g/ml}$  exogenous bovine brain GSLs for 48 hr in two sets. One set with control and GSLs enriched cells was further used for biotinylation of cell surface proteins with sulfo-NHS-biotin. Both sets were lysed with STEN-lysis buffer and APP C-terminal fragments were immunoprecipitated with APP CT antibody. Each immunoprecipitated material was split in two parts and loaded on two separate gels. Proteins were transferred to nitrocellulose membrane. Total cellular APP-CTFs (*top panel*) and cell surface APP-CTFs (*bottom panel*) were detected by western immunoblotting using APP-CTFs antibody and streptavidin-HRP respectively.

Reduced expression of APP-CTFs at the cell surface in GSL treated cells indicated an accumulation of CTFs in intracellular compartments. Subcellular fractionation was performed to determine the compartments where APP-CTFs accumulate upon GSLs treatment. Fractionation of ER, *cis-/medial -Golgi*, TGN as well as early endosomal and lysosomal compartments was performed by density centrifugation using iodixanol gradients. Distribution pattern of the ER marker calnexin and the *Golgi* marker TGN46 in gradient fractions was not significantly changed upon GSLs treatment. Distribution of full-length APP and APP-CTFs was studied by comparison with distribution of the corresponding marker proteins (Fig. 30A). In control H4 cells, immature APP was predominantly found in calnexin positive compartments whereas mature APP was predominantly detected in the TGN46 positive fractions as expected. In control cells, APP-CTFs were present in calnexin positive fractions in higher amounts compared to the TGN46 positive fractions. Noticeably, a protein migrating lower than APP-CTFs, which was characterized as AICD, was found to be present mainly in the fractions containing TGN46. On the other hand in GSLs treated cells, full-length APP and APP-CTFs were predominantly found in the TGN46 fraction. Interestingly, a significant amount of immature APP was localized into the TGN46 positive fractions. In addition, strong accumulation of APP-CTFs with efficient generation of AICD was evident in these vesicles, further proving that  $\gamma$ -secretase is not inhibited by excess of GSLs. This shift in distribution of full-length APP as well as APP-CTFs from ER marker positive vesicles to the *Golgi* marker positive compartment indicates that the forward transport in initial secretory compartments of both could be facilitated by GSLs. However egress of APP-CTFs from *Golgi* to cell surface is probably inhibited by excess of GSLs which might lead to their accumulation at the TGN.

AICD is degraded very fast after its generation (Edbauer et al., 2002). Accordingly, only modest levels of AICD could be detected in the vesicles from control cells (Fig. 30A). Inhibition of AICD degradation by Bacitracin A during gradient run further increased its levels (Fig. 30B). This indicates that AICD was most likely produced during fractionation. The generation of AICD was  $\gamma$ -secretase dependent. As indicated, treatment with DAPT completely abolished generation of AICD, note that cells were treated with DAPT for 48 hr as well as DAPT was added during fractionation (Fig. 30B). Absence upon inhibition of  $\gamma$ -secretase, stabilization by insulin degrading enzyme (IDE) inhibition with Bacitracin A, expected molecular weight and detection with specific antibody (140) against APP-CTF validates the identity of the detected protein as AICD. Although significant amounts of APP-CTFs were detected in calnexin positive fractions, both in control as well as GSLs enriched cells, AICD was found to be present only in TGN46 positive fraction. This could be due to presence of an inactive  $\gamma$ -secretase complex in very early compartments like ER.

Inhibition of  $\gamma$ -secretase by DAPT led to an accumulation of APP-CTFs in similar compartments, as that of GSLs treated cells. However, accumulation after DAPT treatment is mostly caused by inhibition of APP-CTFs processing in the *Golgi* compartment, whereas accumulation upon GSLs treatment appears to be the consequence of deficient exit of APP-CTFs from the *Golgi* to subsequent compartments. Importantly, localization of AICD in similar fractions in control and GSLs enriched cells also suggest that there is no effect of GSLs on the distribution of  $\gamma$ -secretase. Higher AICD levels after GSLs enrichment in TGN46 positive fractions are most likely due to higher amounts of APP-CTFs present there.

However, further analysis is necessary to support above findings. Additional methods such as immunoisolation of the APP and APP-CTF containing vesicles and their biochemical characterization as well as visualization of these vesicles using electron microscopy could be carried out.

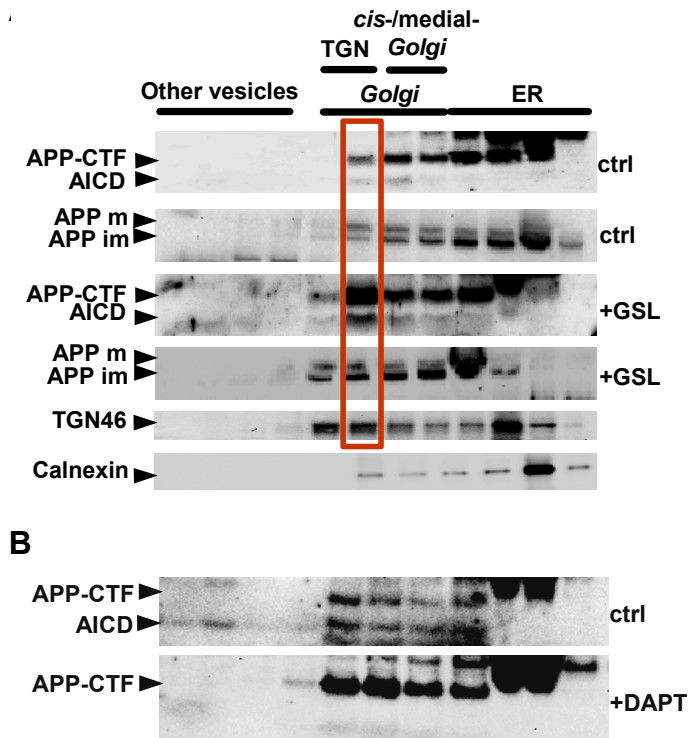


**Fig. 30. Subcellular distribution of APP and APP-CTFs in GSLs enriched cells.** *A*, Isolated membrane vesicles from control and GSLs treated H4 cells were floated on 2.5-30% discontinuous iodixanol gradient as described in methods. Fractions were probed for full length APP and APP-CTFs. In additions fractions were also probed for the *trans-Golgi* marker TGN and ER marker calnexin. GSLs treatment did not alter the markers distribution within fractions. The migration of mature (m) and immature (im) APP is indicated by arrow heads. Notice, the AICD band detected below APP-CTFs. The box indicates TGN46 positive fraction rich in mature APP, APP-CTFs and AICD. Note that the distribution ER and *Golgi* marker protein was analyzed to assign respective compartments. Distribution of other vesicles (such as endosomes and lysosomes) is indicated according to manufacturer's protocol. *B*, Homogenates from control and DAPT (10  $\mu$ M, 48 hr) treated cells were fractionated as described above. DAPT was included at all stages of homogenisation and fractionation in DAPT treated cells. IDE inhibitor bacitracin A (10  $\mu$ g/ml) was also included at homogenisation and fractionation steps of both control and DAPT treated cells. Fractions were probed for APP-CTFs.

#### 4.1.4.3 Increased stability of APP-CTFs upon GSLs treatment

The decreased expression at the cell surface and accumulation in *Golgi* compartment suggested altered metabolism of APP-CTFs by GSLs. APP is known to be degraded by various pathways (see "Introduction/Discussion"), therefore one possible explanation for increased amounts of APP-CTFs can also be the result of altered APP processing to generate higher amounts of APP-CTFs. Therefore generation and degradation of APP-CTFs in control and GSLs treated cells was monitored by pulse chase experiments, with simultaneous analysis of the fate of APP. As shown in Fig. 31A, generation of APP-CTFs was detected 1 hr after labeling which coincided with maturation of significant amounts of APP at this time point. The generated APP-CTFs were stable for four hours of chase.

Notably, the generation of APP-CTFs, with respect to initial amounts of APP appeared to be slower in GSLs treated cells (Fig. 31B). Much lower amounts of APP-CTFs were generated in GSLs enriched cells than control cells after 1 hr, 2 hr and 4 hr of chase period. As indicated in

Fig. 31B, CTF $\alpha$  was the predominant species present in H4 cells, CTF $\beta$  and CTF $\beta'$  (CTFs generated by alternative  $\beta$ -secretase cleavage at Glu-11 site) were also detected. All three different CTFs followed the similar pattern. Overall accumulation of APP-CTFs by treatment with GSLs for 48 hr was confirmed by western immunoblotting. Thus, although there was an overall accumulation of APP-CTFs in GSLs enriched cells during 48 hr of incubation with GSLs, the generation of APP-CTFs, when analyzed by pulse-chase experiment appeared to be relatively decreased. APP maturation followed the expected pattern as described earlier; however, full-length APP appeared to be much more stable in GSL treated cells. Notice after 1 hr of chase relatively higher amount of full-length APP is present in GSLs treated cells compared to control (indicated by box). This indicates stabilization of full-length APP at early stages after its biosynthesis.

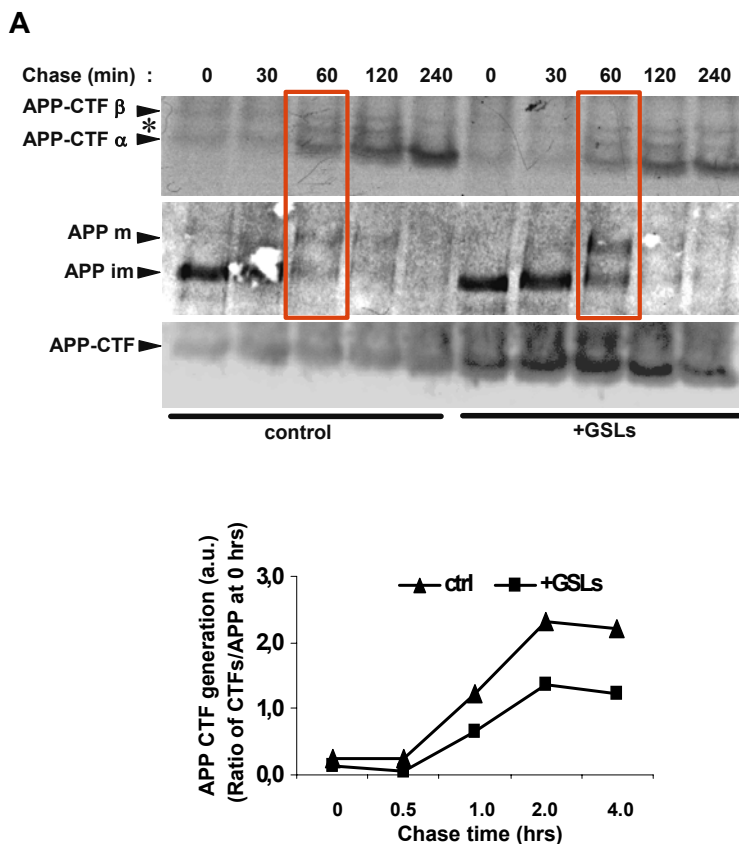


**Fig. 31. Generation of APP-CTFs upon GSLs enrichment studied by pulse-chase.** After culturing in the absence or presence of 50  $\mu$ g/ml GSLs for 48 hr, H4 cells were labeled with [ $^{35}$ S]-methionine for 10 min and chased for the indicated time periods. GSLs were excluded from both pulse and chase media of cells. APP was immunoprecipitated from cell lysates using APP ectodomain antibody, followed by immunoprecipitation with APP-CT antibody to precipitate APP-CTFs. Full length APP was separated by SDS-PAGE (*middle panel*) whereas APP-CTFs were separated by tricine gel (*top panel*), and detected by phosphoimaging. The migration of mature (m) and immature (im) APP is indicated by arrow heads. CTFs generated by  $\beta$ -secretase cleavage (CTF- $\beta$ ) and  $\alpha$ -secretase cleavage (CTF- $\alpha$ ), respectively, are indicated by arrow heads. The CTFs generated by alternative  $\beta$ -secretase cleavage are indicated by an asterisk. In addition, APP-CTFs from the above experiment were also detected using western immunoblotting (*bottom panel*). *B*, Generation of APP-CTFs with respect to initial amounts of cellular APP was reduced in presence of GSLs. (See Quantitation in Fig. 33)

Next, turnover of APP-CTFs upon GSLs enrichment was analyzed in HEK293 and H4 cells by pulse-chase experiments. As indicated in Fig. 32A, APP-CTFs degradation was readily detected only after 10-12 hours after generation in H4 cells, indicating relatively higher stability of APP-CTFs in these cells. Whereas in HEK293 cells a significant degradation of APP-CTFs was already seen at 6 hr of chase, suggesting relatively lower stability of APP-CTFs in these cells compared to H4 cells (Fig. 32B). Nonetheless, GSLs treatment increased the half life of APP-CTFs in both cell types. (Fig. 32A, B). Cellular APP fate was also analyzed in the same experiment at different time points. Most of the APP underwent maturation and was degraded within 2 hr, however some amount of immature APP was stable through out the chase period. Also, stabilization of full-length APP in GSLs treated cells was evident by increased levels of APP in these cells at all time points.

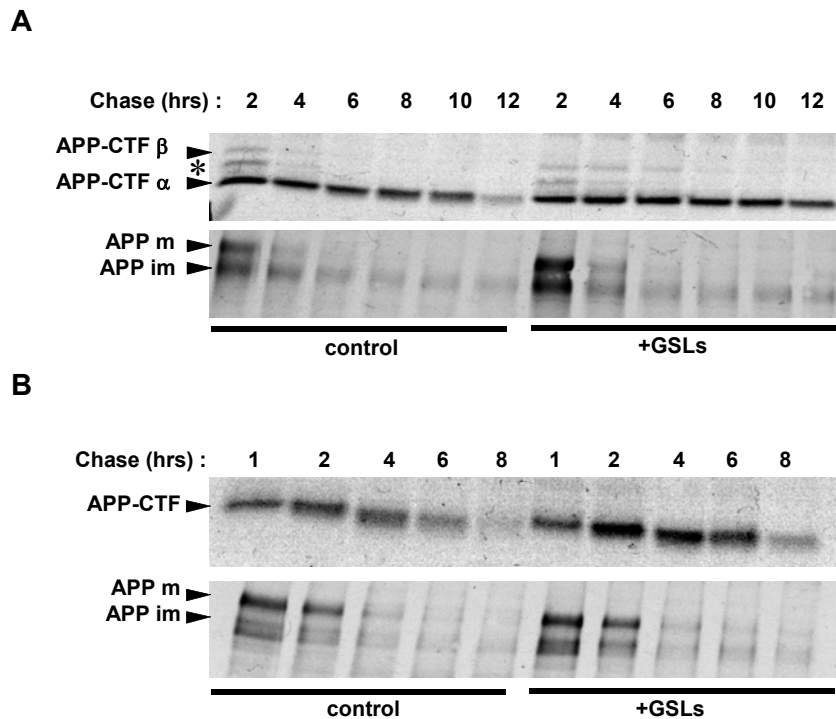
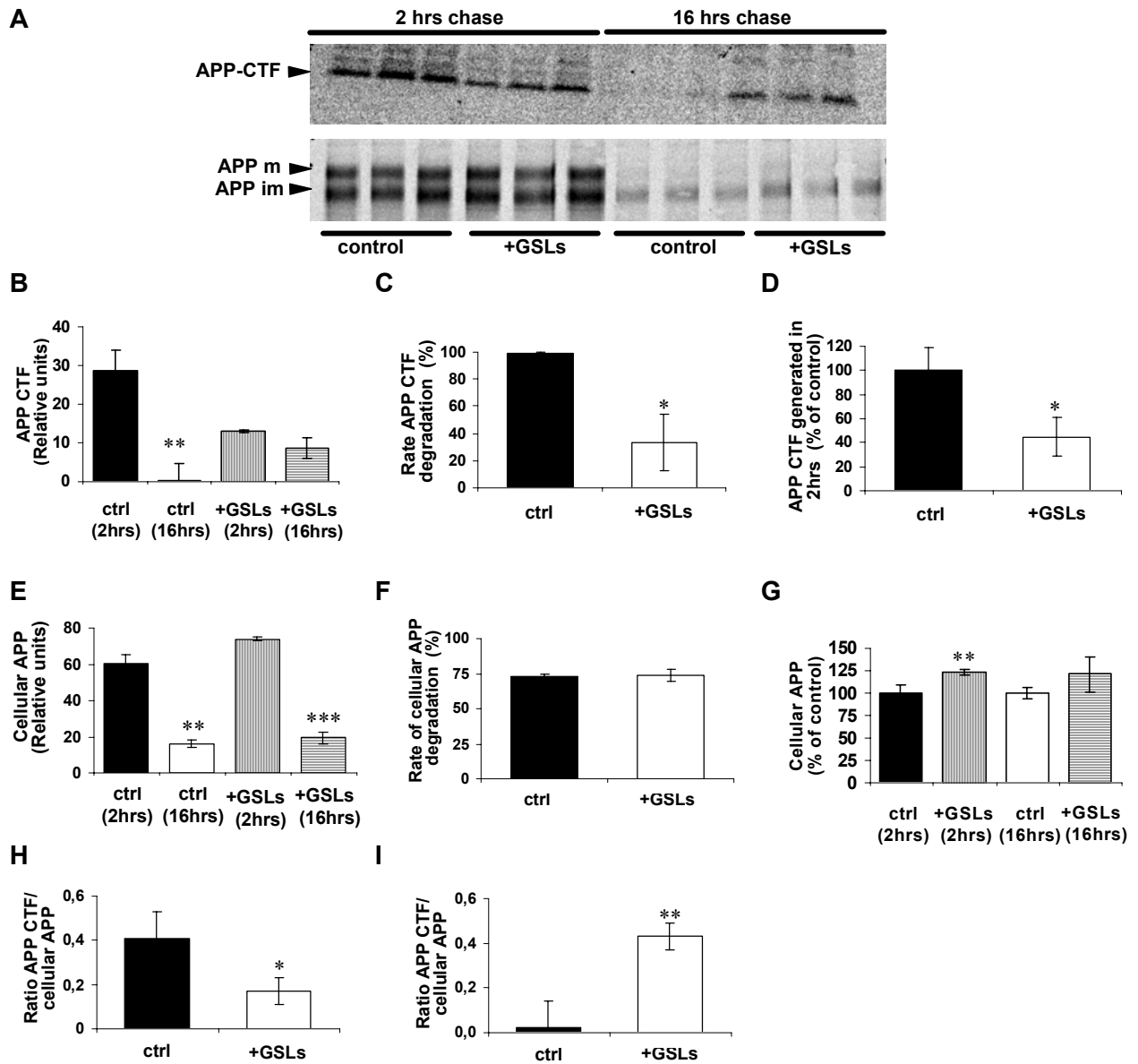


Fig. 32. **Stability of APP-CTFs.** A, B, H4 cells (A) and HEK293 (B) cells were cultured with and without of 50 $\mu$ g/ml GSLs for 48 hr, cells were labeled with [ $^{35}$ S]-methionine for 10 min and chased for the indicated time periods. A pulse-chase was performed in absence of GSLs for control as well as treated cells. APP was immunoprecipitated from cell lysates using 5313 antibody against the APP-ectodomain, followed by immunoprecipitation with APP-CT antibody to precipitate APP-CTFs. Full length APP was separated by SDS-PAGE (*bottom panels*) whereas APP-CTFs were separated by tricine gel system (*top panels*), and detected by phosphoimaging. The migration of mature (m) and immature (im) APP is indicated by arrow heads. CTFs generated by  $\beta$ -secretase cleavage (CTF- $\beta$ ) and  $\alpha$ -secretase cleavage (CTF- $\alpha$ ), respectively, are indicated by arrow heads and CTFs generated by alternative  $\beta$ -secretase cleavage are indicated by an asterisk in H4 cells. Note the longer stability of APP-CTFs in both cell types after GSL treatment.

The results above suggest enhanced stability of APP-CTFs by increased cellular GSLs. This was further validated and quantified by chasing the radiolabeled APP-CTFs for 16 hr in control and GSLs treated H4 cells. After 16 hr there was almost complete degradation of APP-CTFs in control cells, whereas in GSLs enriched cells, APP-CTFs were still stable, indicating attenuated degradation of APP-CTFs in presence of excess of GSLs (Fig. 33A-C). When compared with initial levels of APP-CTFs generated after 2 hr, 99.03% of APP-CTFs were degraded in control cells whereas only 33.5% of APP-CTFs were degraded in GSLs treated cells after 16 hr. Both mature and immature APP was detected in control and GSLs enriched cells at 2 hr. At 16 hr significantly reduced levels of cellular APP were detected in control as well as GSLs treated cells, indicating efficient turnover and secretion of APP. Low levels of immature APP (~24%) were still stable after 16 hr of chase in control as well as GSLs enriched cells. Increase in full-length APP levels after GSLs addition was obvious after 2 hr and after 16 hr of chase (Fig. 33A, 33G). There was nearly 20% more APP present in GSLs treated cells at 2 hours as well as at 16 hours. However, unlike the rate of APP-CTFs degradation, the rate of degradation of full-length APP during 16 hours chase was similar in control and GSLs enriched cells (Fig. 33F). This suggests that GSLs selectively slow down the degradation of APP-CTFs leading to their accumulation. Therefore, increased levels of cellular APP upon GSLs treatment are most likely because of stabilization of APP by GSLs at earlier time points, as discussed earlier.

*Together these data indicate that the GSLs appear to stabilize full-lengths APP at initial stages after its biosynthesis in early secretory compartments and contribute to stabilization of APP-CTFs at later stages. The ratio of APP-CTFs to full-length APP was higher for control cells at 2 hr, whereas at 16 hr it was higher for GSLs treated cells. This reversal of APP-CTFs to full-length APP ratio from 2 hr to 16 hr further corroborates the above findings (Fig. 33H, 33I). The ratio in GSLs treated cells at two hours is lower compared to control indicating a slower generation of APP-CTFs in GSLs treated cells most likely because of an initial stabilization of APP by GSLs, whereas at 16 hours the ratio is reversed, indicating inefficient degradation of APP-CTFs in GSLs treated cells.*



**Fig. 33. Stabilization of APP-CTFs by GSLs.** A, H4 cells were grown with and without 50  $\mu\text{g}/\text{ml}$  GSLs for 48 hr, cells were then labeled with [ $^{35}\text{S}$ ]-methionine for 10 min and chased for 16 hr. Pulse-chase as well as detection of cellular APP (*bottom panel*) and APP-CTFs (*top panel*) was performed as described in previous figure. Migration of immature APP (APP im) and mature APP (APP m) is indicated by arrow heads. B-D, Analysis of APP-CTF metabolism. Relative amounts of radiolabeled APP-CTFs present at 2 hr and 16 hr in control and GSLs treated cells (B). The rate of APP-CTFs degradation in control and GSLs treated cells showing almost complete degradation of APP-CTFs in control cells (99.03%) after 16 hr, whereas only 33.5% of CTFs were degraded in GSLs enriched cells when compared to amounts present at 2 hr (C). Initial amounts of APP-CTFs at 2 hr in control and GSLs treated cells suggesting a slower rate of generation of APP-CTFs in GSLs treated cells (D). E-G, Analysis of cellular APP metabolism. Relative amounts of cellular APP present at 2 hr and 16 hr in control and GSLs treated cells (E). Rate of degradation of APP was not significantly altered in control (73.04%) and GSLs treated (73.50%) cells during 2 hr to 16 hr chase period (F). Nearly 20% more APP was present in GSLs treated cells compared to control H4 cells after 2 hr as well as after 16 hr of chase (G). H-I, Ratio of APP-CTF levels to levels of cellular APP at 2 hr (H) and 16 hr (I) in control and GSLs treated cells. At 2 hr the ratio was higher in control cells compared to GSLs supplemented cells, however after 16 hr of chase a higher ratio was observed for GSLs treated cells.

#### 4.1.5 APP-CTF levels in sphingolipid storage and deficiency genetic cellular models

Next, the effect of GSLs on metabolism of APP-CTFs was verified in primary fibroblasts from patients suffering from sphingolipid storage diseases i.e. NP-A, NP-B, Tay-Sachs and Sandhoff's disease. All tested conditions showed prominent accumulation of APP-CTFs, along with a slight increase in cellular APP levels (Fig. 34). However, in cellular membranes from fibroblasts of Farber disease patient no such accumulation of APP-CTFs was observed. Since in Farber disease there is deficiency of ceramidase resulting in an accumulation of ceramide, these results further prove the selective effect of sphingolipids on APP-CTF metabolism in an independent genetic model.

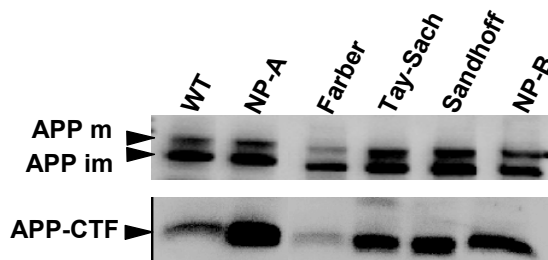


Fig. 34. **Increased APP-CTFs in sphingolipid storage disease.** Primary fibroblasts from indicated sphingolipid storage disease patients and healthy control were obtained and expanded by culturing them further. Cellular APP (*top panel*) and APP-CTFs (*bottom panel*) were detected in isolated membranes of these cells. Note the strong increase in APP-CTFs observed in sphingolipid storage conditions selectively, no accumulation is observed in fibroblast from Farber disease with ceramidase deficiency. The migration of mature (m) and immature (im) APP is indicated by arrow heads.

Next, the expression of APP-CTFs in wild type B16 and GSLs deficient GM95 cells was analyzed. While robust amounts of APP-CTFs were detected in B16 cells, APP-CTFs were almost absent in GM95 cells (Fig. 35). Besides direct effect of GSLs on the metabolism of APP-CTFs, much lower APP levels in GM95 cells (Fig. 16) might contribute to the strong reduction in APP-CTFs in these cells.

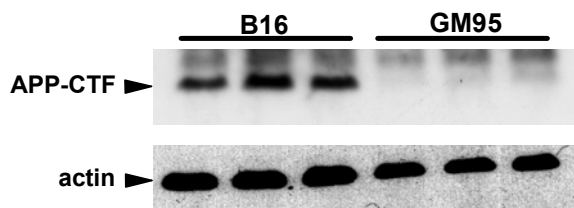


Fig. 35. **Strongly reduced levels of APP-CTFs in GM95 cells.** APP-CTFs were immunoprecipitated from B16 and GM95 cells using an APP-CT antibody and were detected by western immunoblotting. Actin was detected as protein loading control.



## 4.2 Regulation of cholesterol metabolism by presenilins

In order to address the influence of AD associated proteins on lipid metabolism, the role of presenilins in cellular sterol homeostasis was analyzed in detail. More specifically, involvement of presenilin mediated  $\gamma$ -secretase activity in the regulation of membrane lipid and protein metabolism was investigated.

### 4.2.1 Cellular cholesterol content and distribution regulated by presenilin

To analyze the involvement of PS proteins in cholesterol metabolism, cholesterol levels in embryonic fibroblasts of WT and PS1/PS2 double knock-out (PS dKO) mice were analyzed by mass spectrometry. As compared to WT cells, cholesterol levels in the PS dKO cells were significantly increased by approximately 30 % (Fig. 36A). Stable over-expression of human PS1 (hPS1) in PS dKO cell (Fig. 36B) partially normalized cholesterol levels to that of WT cells (Fig. 36A). To test whether cellular cholesterol concentrations are dependent on  $\gamma$ -secretase activity, WT fibroblasts were treated with DAPT, a  $\gamma$ -secretase inhibitor. The inhibition of endogenous  $\gamma$ -secretase activity led to a significant increase in cholesterol (Fig. 36A), demonstrating that PS-dependent  $\gamma$ -secretase activity is implicated in the regulation of cellular cholesterol levels.

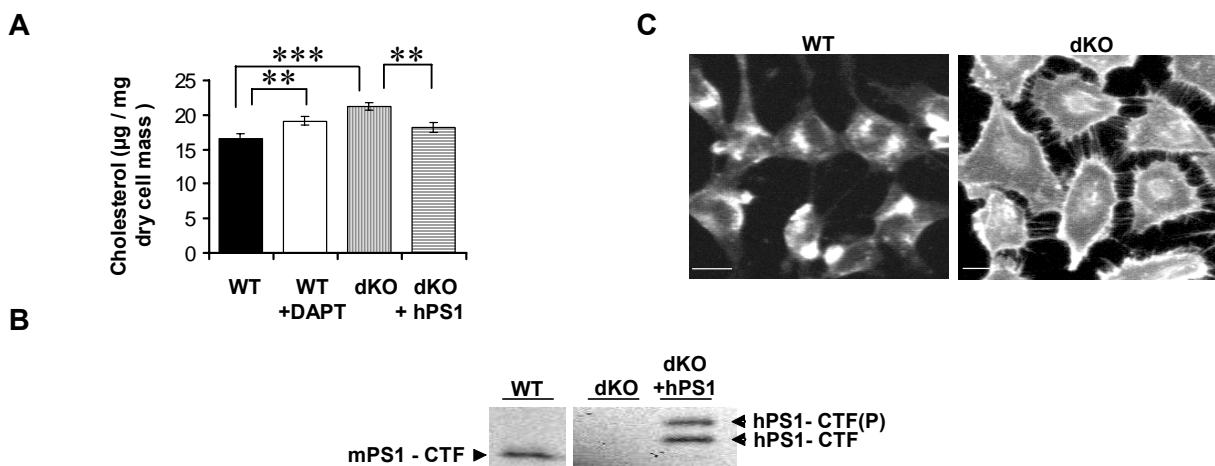


Fig. 36. **Increased cholesterol levels in PS deficient cells.** A, Cholesterol levels in wild type mouse embryonic fibroblasts (WT), fibroblasts treated with  $\gamma$ -secretase inhibitor (10  $\mu$ M DAPT) for 48 hr (WT+DAPT), PS deficient fibroblasts (dKO) and dKO cells stably overexpressing hPS1 (dKO+hPS1) were determined by GC-FID. Values represent means of five independent experiments  $\pm$  s.d. (p values are indicated by asterisks \*\*,  $p < 0.01$  \*\*\*,  $p < 0.001$ ). B, stable re-expression of human PS1 in dKO cells. dKO MEFs were transfected with cDNA encoding human PS1 (hPS1) and selected in zeocin (200  $\mu$ g/ml). PS1 was immunoprecipitated from the indicated cell lines and detected by western immunoblotting. Migration of endogenous mouse PS1 C-terminal fragment (mPS1-CTF) and transgenic hPS1-CTF is indicated by arrow heads. CTF and CTF(P) denote non phosphorylated and phosphorylated forms of hPS1, respectively. C, Visualization of cholesterol in WT and PS dKO cells with filipin by fluorescence microscopy.

Also the distribution of cholesterol in WT and PS dKO cells was analyzed by fluorescence microscopy using the cholesterol-binding antibiotic filipin. WT cells showed cholesterol localization in the plasma membrane as well as in juxtannuclear compartments, while PS deficient cells showed prominent staining of cholesterol in the plasma membrane (Fig. 36C). Overall, the staining intensity appeared increased in PS deficient cells, also indicating elevated levels of cholesterol and enrichment in the plasma membrane. Interestingly, PS deficiency also results in morphological changes. PS dKO cells appeared to be much more flat, spreadout and bigger compared to WT cells.

#### **4.2.2 Up-regulation of cholesterol biosynthesis in PS deficient cell**

Cellular cholesterol homeostasis is achieved by a number of molecular mechanisms that regulate its uptake and secretion, as well as biosynthesis and metabolism. The biosynthesis of cholesterol occurs at the membranes of ER and involves multiple enzyme activities (Fig. 37A). To address whether the increased cholesterol levels in PS-deficient cells were associated with increased *de novo* synthesis, the levels of cholesterol precursors as well as its degradation products in WT and PS dKO cells were analyzed by GC-MS.

The concentration of desmosterol, an immediate precursor of cholesterol, was significantly increased in PS dKO (~ 40%) compared to WT cells (Fig. 37B). As observed for cholesterol, desmosterol levels were decreased upon re-expression of hPS1 in PS dKO cells, while treatment of WT cells with DAPT led to increased levels of desmosterol (Fig. 37B). Several downstream metabolites of cholesterol, including cholestanol, a reduction product of cholesterol, and the hydroxylated derivative 27-OH-cholesterol were also detected in both cell types. The levels of these metabolites were also increased in PS deficient cells (Fig. 37 C-D), indicating that the elevated levels of cholesterol in PS dKO cells, are not caused by impaired downstream metabolism of cholesterol. These data indicate that PS deficiency or inhibition of  $\gamma$ -secretase activity results in increased biosynthesis of cholesterol.

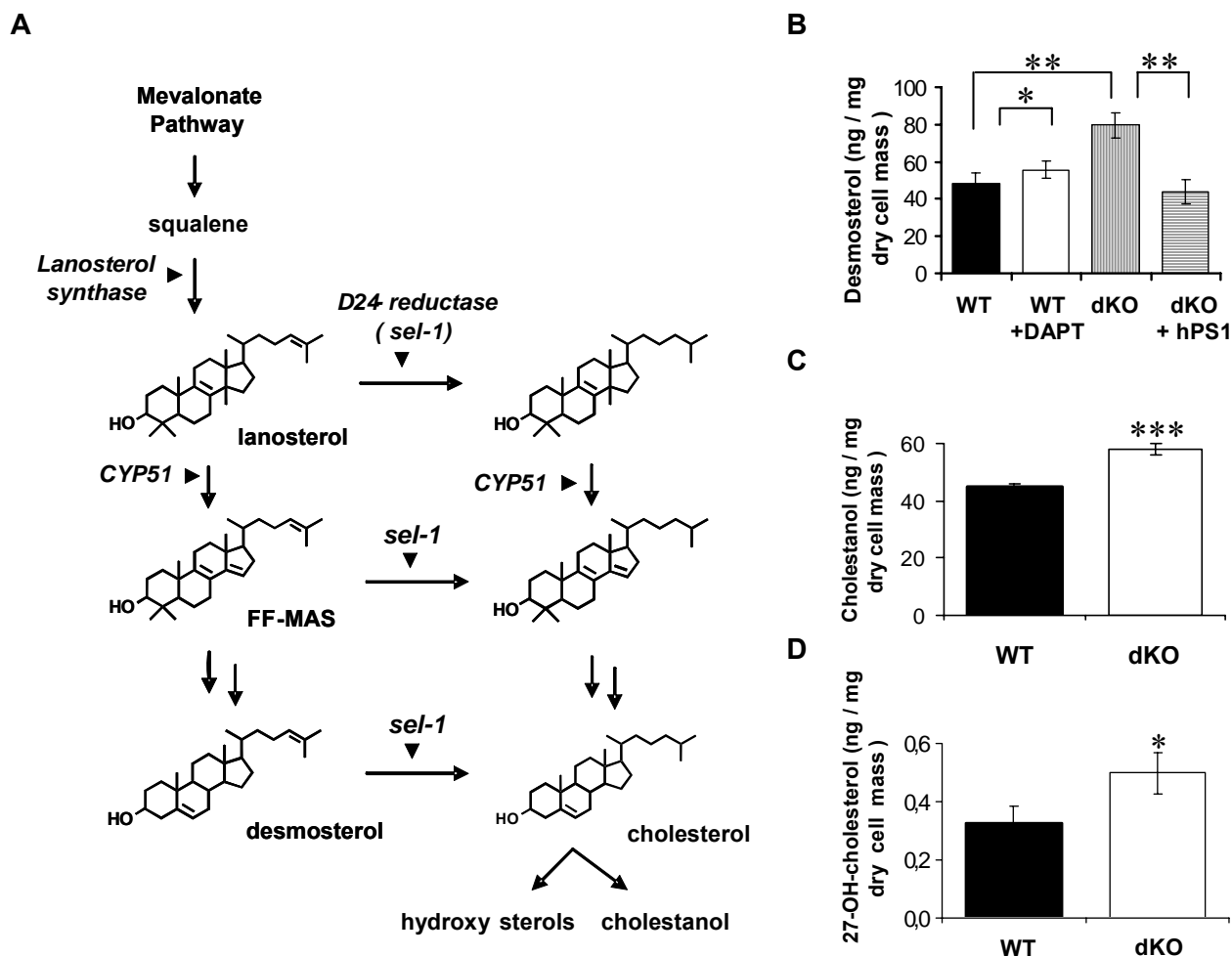


Fig. 37. **Increased cholesterol biosynthesis of cholesterol in PS deficient cells.** A, Schematic showing of the biosynthesis pathway of cholesterol. Lanosterol is the first cyclic metabolite in cholesterol biosynthesis. Metabolites and enzymes involved in lanosterol metabolism are indicated. Cholestanol and hydroxy-sterols are down-stream metabolites of cholesterol. B, Desmosterol levels from indicated cells were measured with GC-MS. C- D, Cellular levels of cholesterol downstream metabolites cholestanol (C), 27-hydroxycholesterol (D) were determined by GC-MS. Values represent means of five independent experiments  $\pm$  s.d. p values are indicated by asterisks \*\*, p < 0.01 \*\*\*, p < 0.001).

#### 4.2.3 Up-regulation of CYP51 leads to increased turnover of lanosterol in PS deficient cells

The first cyclic metabolite in cholesterol biosynthesis is lanosterol that is generated by cyclization of squalene; a reaction catalyzed by lanosterol synthase (Fig. 37A). The analysis of lanosterol revealed decreased levels of this precursor in PS dKO cells as compared to WT cells (Fig. 38A). DAPT treatment of WT cells resulted in decreased lanosterol levels (Fig. 38A). These data indicate that PS proteins affect cholesterol metabolism already at the earlier steps in the biosynthesis pathway. The decreased lanosterol levels in PS deficient cells suggested either decreased synthesis or increased metabolism of lanosterol.

The regulation of cholesterol biosynthesis involves transcriptional control of metabolic enzymes (Horton et al., 2002; Rodriguez et al., 2001). Since there was a significant difference in lanosterol levels in PS deficient cells, mRNA levels of the enzymes involved in lanosterol metabolism, namely, lanosterol synthase, lanosterol-14 $\alpha$ -demethylase (CYP51), and  $\Delta$ 24-reductase/seladin-1 were analyzed. While lanosterol synthase catalyzes the synthesis of lanosterol by cyclization of squalene, CYP51 and seladin-1 metabolize lanosterol to  $\Delta$ 8,14,24-dimethylsterol (FF-MAS) and dihydrolanosterol, respectively (Fig. 37A). As revealed by RT-PCR, mRNA levels of lanosterol synthase and seladin-1 were not significantly altered in PS dKO cells as compared to WT cells (Fig. 38B). In contrast, mRNA expression of CYP51 was markedly increased in PS dKO cells, indicating that PS deficiency led to increased cholesterol biosynthesis by up-regulation of CYP51 expression, and increased metabolism of lanosterol.

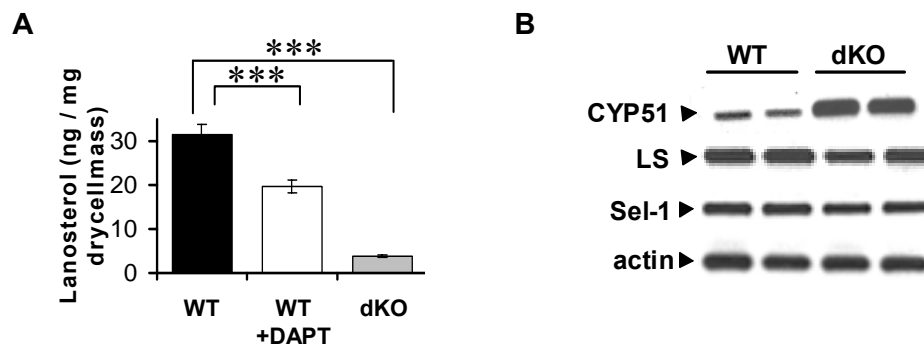


Fig. 38. **Increased metabolism of lanosterol in PS deficient cells.** A, Decreased levels of lanosterol in PS deficient cells. Lanosterol levels were measured in indicated MEFs using GC-MS. WT cells were treated with 10  $\mu$ M DAPT for 48 hr. B, Transcriptional up-regulation of CYP51 in PS dKO MEFs. mRNA of CYP51, LS, and Sel-1 were analyzed by RT-PCR. mRNA analysis of  $\beta$ -actin served as control.

#### 4.2.4 Inhibition of CYP51 reverses increased cholesterol levels in PS deficient cells

To test whether the increased cholesterol biosynthesis in PS deficient cells could be reversed by inhibition of CYP51 activity, the effect of itraconazole, a selective inhibitor of CYP51, was investigated (Fig. 39A). The treatment with itraconazole strongly increased levels of lanosterol in PS dKO cells (Fig. 39B), proving the inhibition of CYP51. A subtle, but highly significant, decrease in cholesterol and desmosterol levels was also confirmed upon itraconazole treatment, demonstrating that increased cholesterol biosynthesis in PS deficient cells could be reduced by selective pharmacological inhibition of CYP51 (Fig. 39C, 39D).

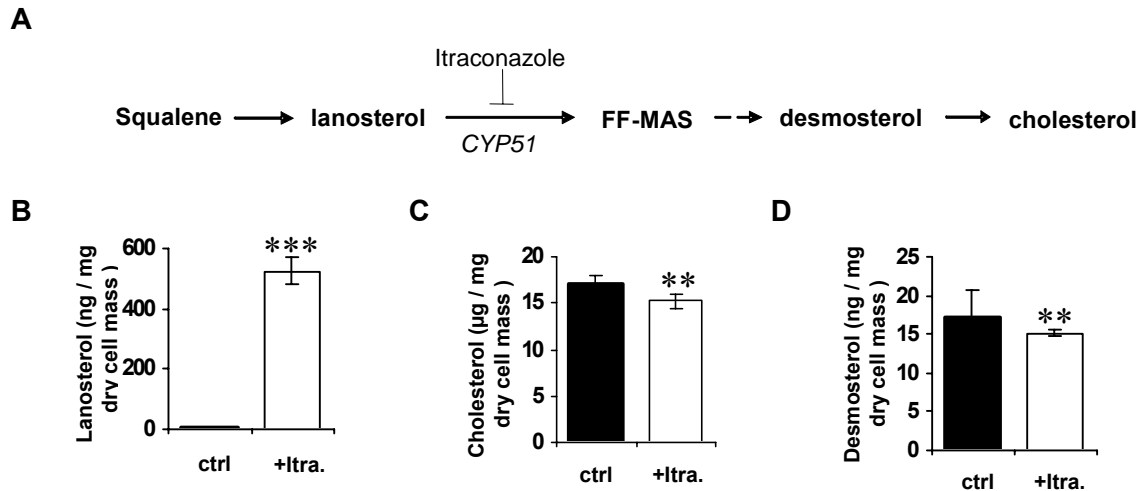


Fig. 39. **Inhibition of CYP51 in PS dKO cells.** A, Inhibition of cholesterol biosynthesis by itraconazole. Itraconazole is a selective inhibitor of CYP51 (lanosterol 14- $\alpha$ -demethylase). C-D, Normalization of increased cholesterol and desmosterol levels in PS dKO cells by CYP51 inhibition. PS dKO cells were treated with 50  $\mu$ M itraconazole (+itra) for 48 hr and cellular levels of lanosterol (B), cholesterol (C) and desmosterol (D) were determined.

#### 4.2.5 Increase in cholesterol levels in PS deficient cells is independent of exogenously added A $\beta$

Earlier studies by Grimm et al. (Grimm et al., 2005) suggested that A $\beta$  40 peptide decreases cholesterol levels by inhibition of HMG-CoA reductase and that the lack of A $\beta$ , either by deficiency of  $\gamma$ -secretase activity or absence of APP, leads to increased levels of cholesterol. Therefore, to check, if increased levels of cholesterol in PS deficient cells observed in this experimental set are caused by lack of A $\beta$ , the PS dKO cells were treated with A $\beta$  40 for 48 hr. Addition of exogenous A $\beta$  to PS dKO cells did not normalize the levels of lanosterol, cholesterol or desmosterol (Fig. 40A-C), indicating that the lack of A $\beta$  in PS deficient cells may not be responsible for increased levels of cholesterol.

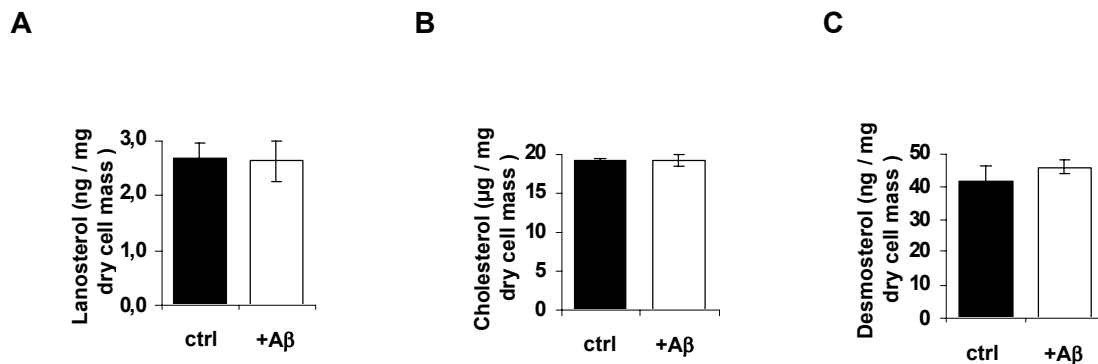


Fig. 40. **Treatment of PS dKO cells with A $\beta$ 40.** A-C, PS dKO cells were treated with 40 ng/ml A $\beta$  40 for 48 hr and cellular levels of lanosterol (A), cholesterol (B) and desmosterol (C) were determined as described earlier.

#### 4.2.6 Inhibition of $\gamma$ -secretase in human neuroglioma cells increased cholesterol levels

To prove above findings in an independent cellular model, human neuroglioma H4 cells were chosen, because of their neuronal origin. Cholesterol levels were significantly increased after DAPT treatment (Fig. 41A), whereas lanosterol levels were decreased (Fig. 41B). These results suggest that the metabolism of lanosterol was increased upon inhibition of  $\gamma$ -secretase activity in H4 cells. Thus, similar to MEF cells, inhibition of  $\gamma$ -secretase in H4 cells could lead to an enhanced cholesterol biosynthesis.

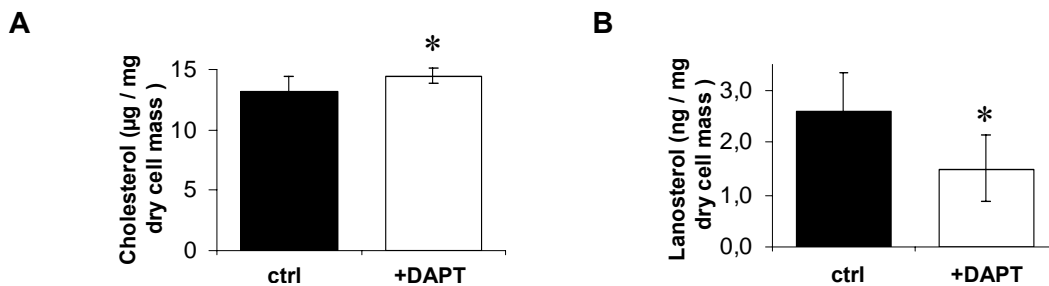


Fig. 41. **Inhibition of  $\gamma$ -secretase in human neuroglioma, H4 cells.** A-B, H4 cells were cultured in the presence or absence of 10  $\mu$ M DAPT for 48 hr. Concentrations of cholesterol (A) and lanosterol (B) were determined by GC-MS as described under methods. Values represent means of five independent experiments  $\pm$  s.d.; \* ( $p < 0.05$ ).

#### 4.2.7 PS deficiency is associated with inefficient LDL uptake

Together, these data suggest that the increased levels of cholesterol in PS deficient cells are caused by increased biosynthesis, as a result of transcriptional up-regulation of CYP51. The expression of CYP51 has been shown to be suppressed by the uptake of extracellular LDL. LDL present in bovine serum acts as a source of cholesterol in cultured cells. Therefore, it was speculated that the increased expression of CYP51 in PS dKO cells might be due to impaired uptake of LDL. To address this, the endocytosis of LDL in WT and PS deficient cells was analyzed by immunocytochemical experiments using fluorescently-labeled BODIPY-LDL. WT cells efficiently internalized BODIPY-labeled LDL into cytoplasmic vesicular structures, demonstrating endocytosis of LDL (Fig. 42A). In contrast, very little internalization of BODIPY-labeled LDL was observed in PS dKO cells, indicating impaired endocytosis of LDL. To prove this, total cellular levels of LDL in PS WT and dKO cells were analyzed by western-immunoblotting with an antibody against apolipoprotein B100 (Apo B100), a major component of

LDL. Cellular levels of Apo B100 were significantly higher in WT cells as compared to PS dKO cells, also indicating decreased internalization of LDL in PS-deficient cells (Fig. 42B).

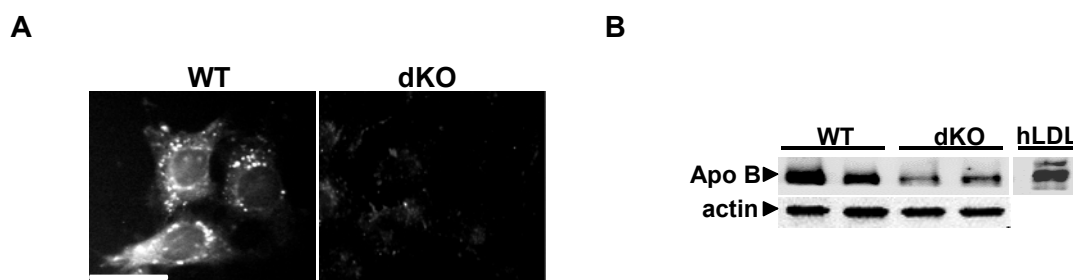


Fig. 42. **Inhibition of LDL uptake in PS dKO cells.** A, Inhibition of LDL endocytosis in PS dKO cells. WT and PS dKO MEFs were incubated in the presence of BODIPY-labeled LDL and analyzed by fluorescence microscopy. WT cells internalized LDL into peripheral vesicular structures, while PS dKO cells showed very little internalization. Scale bar 25  $\mu$ m. B, Decreased levels of LDL in PS dKO cells. Cellular levels of LDL in WT and PS dKO cells were analyzed by immunoblotting with an antibody against apolipoprotein B100 (Apo B). Purified LDL was used as

#### 4.2.8 Increased levels of LDL receptor (LDLR) in PS deficient cells

Lipid rich LDL binds to LDLR at the cell surface and is endocytosed into endosomal and lysosomal compartments where it dissociates from LDLR because of acidic pH. Most of the LDLR is recycled back to cell surface while LDL is degraded and cholesterol is utilised according to cellular requirements. In order to understand more about the regulation of LDL uptake by presenilins, the expression of LDL receptor in WT and PS deficient cells was analyzed. Western-immunoblot analysis revealed that the level of LDL receptor was increased in PS dKO cells (Fig. 43A). The increased expression of the LDL receptor in these cells was attenuated by re-expression of hPS1 (Fig. 43B). In addition, treatment of WT cells with DAPT also increased LDL receptor levels (Fig. 43C). Together these data indicate that PS dependent  $\gamma$ -secretase activity affects cellular levels of the LDL receptor.

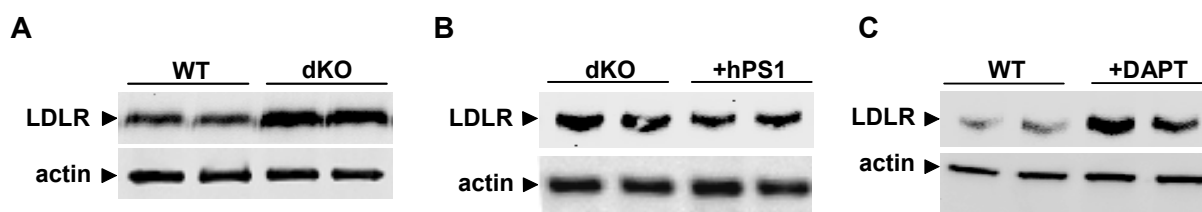


Fig. 43. **PS dependent expression of LDL receptor (LDLR).** The expression of the LDLR in WT and PS dKO (A), PS dKO and PS dKO re-expressing hPS1 (B), WT MEFs and MEFs treated with 10  $\mu$ M DAPT for 48 hr (C) was analyzed by western immunoblotting. Lack of  $\gamma$ -secretase activity increased the levels of LDLR while re-transfection of PS dKO cells with hPS1 reversed increased levels of LDLR.

### 4.2.9 Cell surface expression of LDLR is regulated by presenilin

Next, the subcellular distribution of the LDL receptor was studied by fluorescence microscopy. While LDL receptor was localized predominantly in juxtannuclear structures in WT cells, PS deficient cells showed also a prominent localization of the receptor at the cell surface (Fig. 44A). Re-expression of hPS1 in PS dKO cells decreased the localization of LDL receptor at the cell surface and led to predominant localization in juxtannuclear compartments, very similar to WT cells (Fig. 44A). Notice the presenilin dependent alteration in shape and size of fibroblasts, as mentioned earlier. Importantly, to some extent the re-expression of hPS1 in PS dKO cells restored the normal morphology of cells to that of WT fibroblasts. To specifically analyze the expression of the LDL receptor at the cell surface, biotinylation experiments were carried out. The specific labeling of cell surface proteins with biotin revealed increased levels of LDL receptor at the cell surface of PS deficient cells as compared to WT cells (Fig. 44B). Thus PS deficiency resulted in increased expression of LDL receptor and altered subcellular distribution.

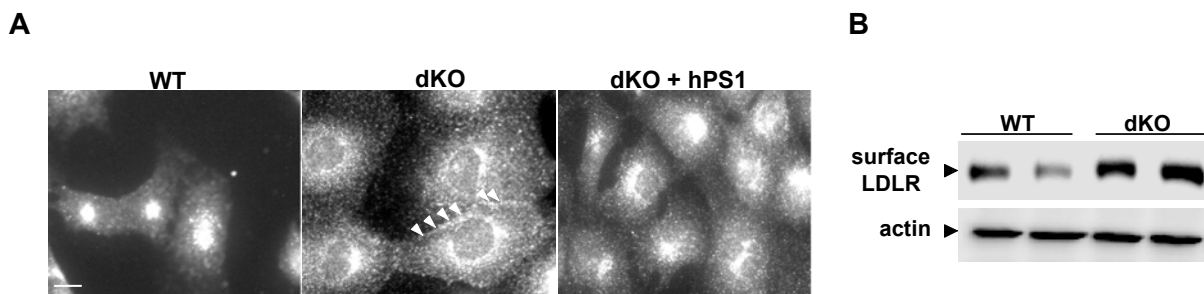


Fig. 44. **PS dependent subcellular localization of LDL receptor.** *A*, The subcellular localization of endogenous LDLR in WT, PS dKO and PS dKO cells stably over-expressing hPS1 was analyzed by fluorescence microscopy. Prominent localization of LDLR at the cell surface in PS dKO cells is indicated by arrow heads. PS dKO cells stably over-expressing hPS1 showed predominant localization of LDLR in juxtannuclear structures, similar to WT cells. *B*, Expression of LDLR at the cell surface. After cell surface biotinylation, biotin labeled-proteins were precipitated with streptavidin-conjugated agarose beads and LDLR was detected by western blotting.

### 4.2.10 Impaired endocytosis of LDLR in PS deficient cells

The increased expression of LDL receptor at the cell surface together with the decreased uptake of LDL strongly suggested impaired endocytosis of the LDL receptor in PS deficient cells. Therefore, next endocytosis of LDLR was analyzed. Reversible labeling of cell surface proteins with cleavable biotin and subsequent incubations to allow endocytosis as well as stripping with reducing buffer to cleave off the biotin was performed as depicted in Fig. 45A. Most of the biotin from labeled LDLR was cleaved off efficiently in both, WT and PS dKO cells



when cells were not allowed to endocytose labeled surface proteins at permissible temperature i.e, 0 min time point as indicated in Fig. 45B. However, when cells were incubated at permissible temperature (37°C) for 15 min to allow endocytosis of biotin labeled proteins, a significant amount of biotin labeled LDLR in WT cells was protected from stripping, indicating efficient internalization. On the other hand, most of the biotin was cleaved off from LDLR in PS dKO cells even after incubation at 37°C for 15 min, indicating inefficient internalization of LDLR in PS deficient cells (Fig. 45B). Thus, inefficient endocytosis of LDLR results in abrogation of LDL uptake in PS deficient cells, which ultimately leads to up-regulation of cellular cholesterol biosynthesis.

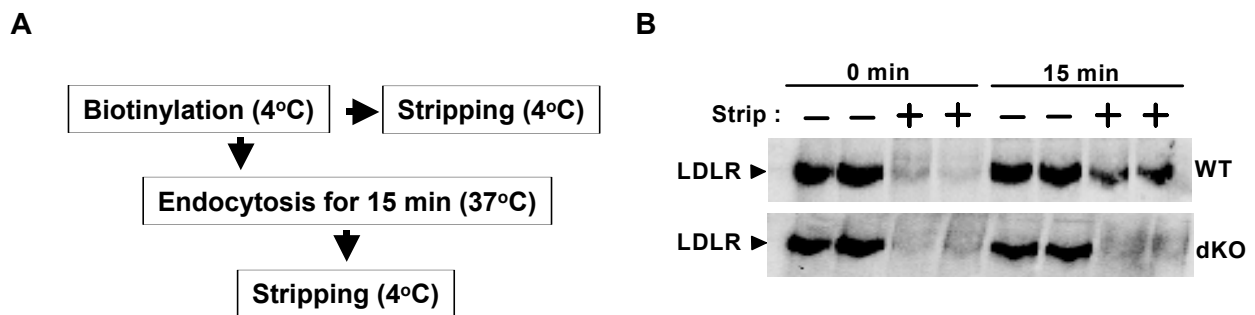


Fig. 45. **PS dependent subcellular localization of LDL receptor (LDLR).** *A*, Schematic representation of the experimental set up to study LDLR endocytosis. *B*, Surface proteins of WT and PS dKO cells were labeled with sulfo-NHS-SS-biotin. Cells were incubated for the indicated time periods at 37°C to allow endocytosis and biotin from residual cell surface proteins was removed by treatment with cleavage/stripping buffer containing glutathione. Internalized biotin-labeled proteins were precipitated and LDLR was detected by western immunoblotting.

## 4.3 Regulation of general endocytosis by presenilins

### 4.3.1 Impaired endocytosis of APP and BSA in PS dKO cells

Previous studies have shown that the endocytosis of APP and BSA is also reduced in PS deficient cells. Accordingly, it could be predicted that the levels of full-length APP should also increase in absence of  $\gamma$ -secretase activity, as observed for LDLR. Indeed, WT cells when treated with DAPT, showed the increased cellular APP levels, as well as cellular APP expression was higher in PS dKO cells compared to WT cells. Re-expression of hPS1 in PS dKO partially reduced the increased APP levels (Fig. 46A). It should be noted that PS proteins are not only involved in endocytosis of APP but they also regulate the forward transport of APP in the

secretory pathway. Thus, the accumulation of full-length APP in PS dKO cells would be the result of an overall impaired subcellular transport of APP in the absence of presenilins.

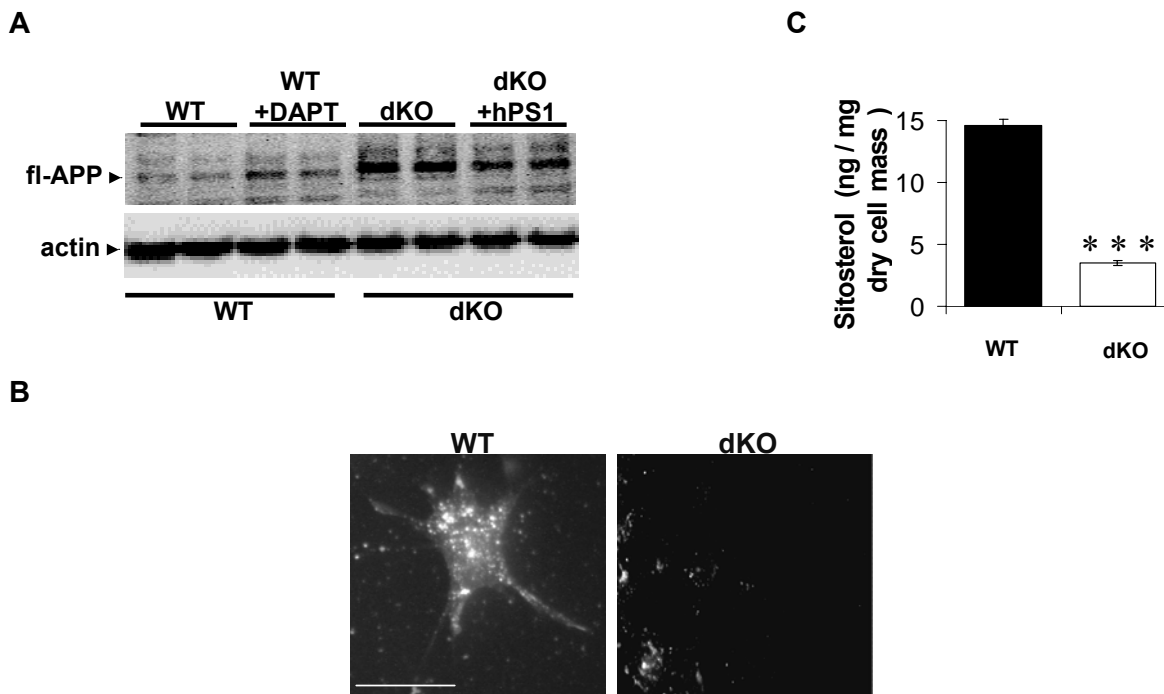


Fig. 46. **PS dependent endocytosis of APP and BSA.** *A*, WT MEFs were cultured in the absence or presence of 10  $\mu$ M DAPT. After 48 hr, the expression of APP was analyzed by western blotting of isolated cellular membranes. In addition, APP was also detected in PS dKO and PS dKO cells re-expressing hPS1 (dKO+hPS1). *B*, WT and PS dKO MEFs were grown on coverslips and incubated with 10  $\mu$ g/ml TRITC labeled BSA in DMEM for 15 min at 37°C. Cells were washed, fixed and processed for fluorescence microscopy. Scale bar 25  $\mu$ m. *C*, Sitosterol levels in WT and PS dKO cells were determined by GC-MS. Values represent means of five independent experiments  $\pm$  s.d.; \*\*\* ( $p < 0.001$ ).

Inhibition of BSA endocytosis in PS dKO cells was confirmed by analyzing the uptake of TRITC-BSA conjugate (Fig. 46B). In WT cells TRITC-BSA was endocytosed in vesicular compartments in 15 min incubation at 37°C, whereas no such TRITC-BSA positive structures were detected in PS dKO cells at this time point. Sitosterol is a plant sterol found to be bound to albumin in bovine serum and is taken up by cells along with BSA but can not be metabolized by cells. Sitosterol levels in PS dKO cells were significantly reduced, also indicating decreased endocytosis (Fig. 46C).

### 4.3.2 Inefficient endocytosis of GM1 in PS deficient cells

The altered endocytosis of distinct extracellular (LDL, BSA) and membrane proteins (LDLR, LRP), indicated a general impairment of endocytosis in PS deficient cells. To prove a more general defect in membrane uptake, the internalization of cholera toxin (CTX), which specifically binds to the ganglioside GM1, was analyzed. CTX was readily internalized in WT cells and found at peripheral and juxtannuclear vesicular structures. Under the similar conditions, significant amounts of CTX were still detected at the plasma membrane of PS dKO cells, indicating impaired internalization of GM1 (Figure 47A). Moreover, levels of GM1 were markedly increased in PS dKO cells as compared to WT cells. Inhibition of  $\gamma$ -secretase with DAPT also led to increased GM1 levels (Figure 47B). These data further demonstrate an intimate relation between  $\gamma$ -secretase activity and endocytic membrane transport of proteins and lipids.

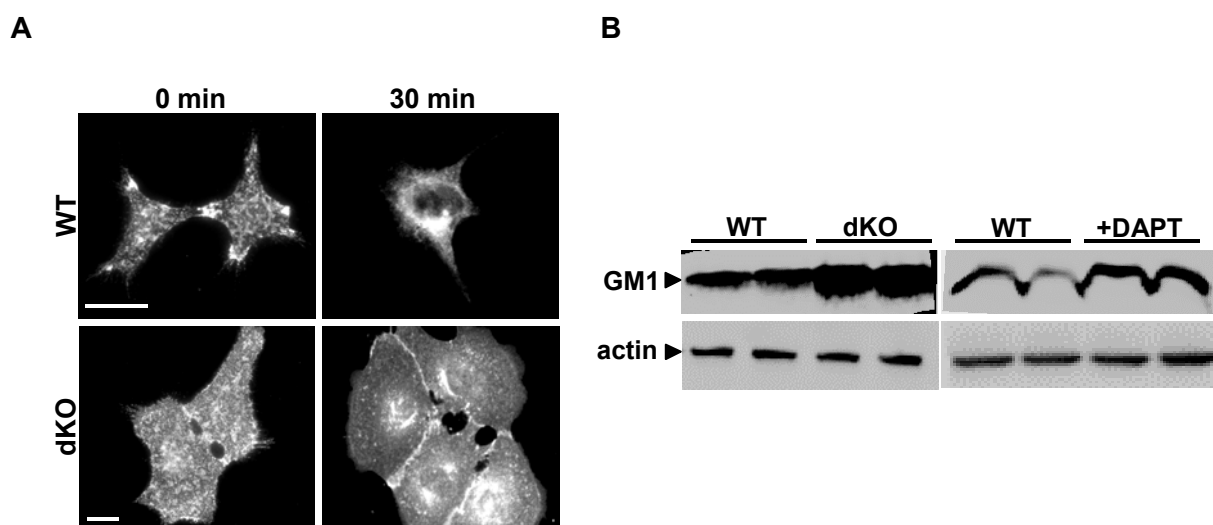


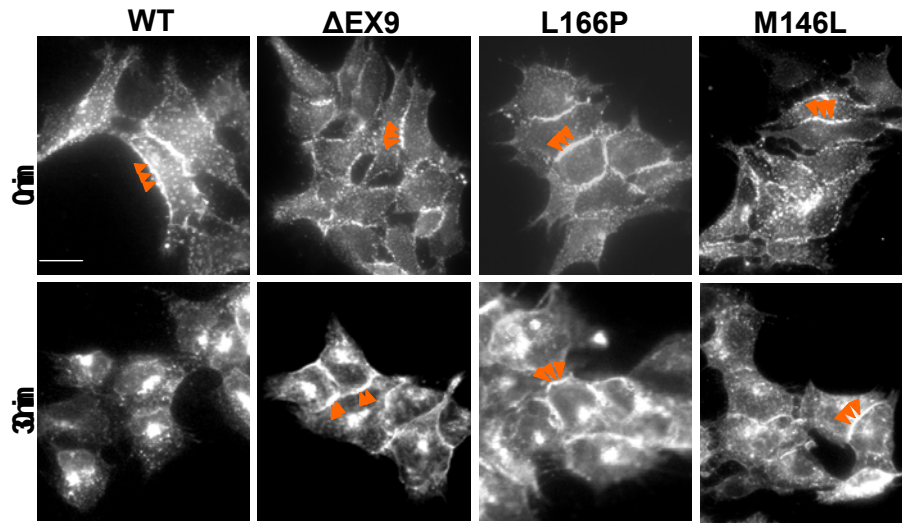
Fig. 47. **Accumulation of GM1 in PS deficient cells.** *A*, Decreased endocytosis of cell surface GM1. Cells were incubated with cholera toxin for 30 min on ice, followed by incubation at 37°C for 30 min. Cholera toxin was then detected with specific primary and Alexa-594 conjugated secondary antibodies. *B*, Detection of GM1 by western immunoblotting. Cellular levels of GM1 were increased in PS deficient cells (*left panel*) or upon pharmacological inhibition of  $\gamma$ -secretase with DAPT (*right panel*).

## 4.4 PS1 FAD mutations affect homeostasis of membrane lipid and proteins

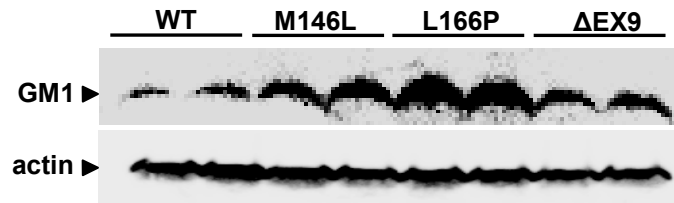
The above described studies established an important role of presenilins in endocytosis as well as membrane homeostasis. Mutations in PS1 are a major cause of early onset FAD. It has been shown that several FAD mutations also led to decreased cleavage of other  $\gamma$ -secretase substrates, including APP, notch and cadherins, indicating a partial loss of function. Thus, PS FAD mutants not only impair specificity, but also total activity of  $\gamma$ -secretase; therefore it was investigated if PS1 FAD mutants also show loss of function with respect to maintenance of membrane homeostasis. To address this, HEK293 cell lines stably expressing PS1 FAD variants were generated. Cells expressing WT PS1 and mutant PS1 were incubated with cholera toxin on ice to allow the binding of toxin with cell surface GM1. Cells were later shifted to 37°C and endocytosis of GM1 was studied as described above (See Fig. 47). Interestingly, the expression of FAD associated mutants of PS1 caused impaired internalization of GM1 (Fig. 48A). Since GSLs are degraded in lysosomal compartments after endocytosis, deficient endocytosis would also lead to impaired degradation of GM1. Accordingly, the accumulation of GM1 was observed in cells expressing PS1 mutants compared to cells expressing WT PS1 (Fig. 48B). Together, these data indicate that a partial loss of  $\gamma$ -secretase function, induced by FAD associated mutations of PS1, led to global impairment of membrane trafficking.

As observed in PS deficient cells, impaired membrane flow in cells which express PS1 with FAD associated mutations should also show an accumulation of membrane proteins because of improper endocytosis. Therefore, the levels of LDLR and APP in cells expressing PS1 FAD mutants as well as WT PS1 were analyzed by western immunoblotting. Expression of these proteins was found to be increased in cells expressing mutant PS1 compared to cells expressing WT PS1 (Fig. 48C). However, the expression of cytosolic actin was not affected in these cells. Thus, PS1 FAD mutations not only affect metabolism of membrane proteins, but also alter the lipid metabolism as indicated by the accumulation of GM1.

A



B



C

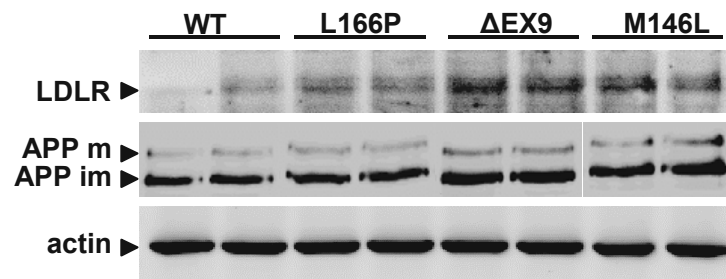


Fig. 48. **PS1-FAD mutations impair endocytic membrane flow.** *A*, PS1 FAD mutations affect endocytosis of GM1. Endocytosis of GM1 in cells expressing PS1 WT or the indicated FAD mutants was analyzed by the uptake of cholera toxin. Localization of GM1 at cell surface is indicated by red arrow heads. *B*, PS1 FAD mutants also led to increased levels of GM1 as detected by western immunoblotting of isolated cellular membranes with cholera toxin. *C*, Endogenous LDLR and APP in cellular membranes of HEK293 cells stably expressing PS1 WT or the indicated PS1 FAD were detected by western immunoblotting.  $\beta$ -Actin was detected as a loading control.



## 5 Discussion

The aim of the work presented here was to characterize the role of membrane lipids in the regulation of AD associated proteins and also to address if there is some influence of AD associated proteins on lipid metabolism. Accordingly, it was demonstrated that membrane lipids, especially GSLs, are implicated in the regulation of proteolytic processing and subcellular transport of APP. On the other hand, the results indicate that  $\gamma$ -secretase also affects cellular cholesterol metabolism and homeostasis of membrane lipids and proteins. Notably, different approaches undertaken to modulate cellular lipids or  $\gamma$ -secretase activity in various cell types led to overlapping findings, which established a close relationship between membrane lipids and AD associated proteins.

As mentioned in the introduction, the cellular distribution, metabolism and amounts of gangliosides are significantly different in the brains of AD patients as compared to brains of non-affected people. Especially, the loss of GSLs along with other lipids leading to loss of nerve endings was described as primary event in AD pathophysiology. AD patients also show the presence of anti-ganglioside antibodies. Moreover, anti-ganglioside antibodies label intracellular neurofibrillary tangles and extracellular senile plaques specifically. A complex of the glycosphingolipid GM1 and A $\beta$  could act as a seed for A $\beta$  aggregation by inducing a conformational transition from  $\alpha$ -helix to  $\beta$ -sheet rich structure. This might facilitate the fibrillization of A $\beta$  and deposition in amyloid plaques (Hayashi et al., 2004). On the other hand, the high affinity of A $\beta$  for GM1 has been exploited in the therapeutic application against AD. Peripheral administration of GM1 in AD patients as well as in AD mice has been shown to reduce brain amyloid load, possibly by sequestration effect of GM1 on A $\beta$  (Svennerholm, 1994). Furthermore, A $\beta$  induced cytokine release in cell culture can be blocked by simultaneous treatment of GM1 (Ariga and Yu, 1998). Significantly reduced levels of sulfatides, sulphate esters of galactosylcerebrosides have also been reported to be a characteristic of AD subjects even with very mild dementia. The role of sphingomyelin and ceramide in AD is often discussed with respect to oxidative stress induced by A $\beta$ . One of the mechanisms by which A $\beta$  induces cell death could be by increasing sphingomyelinase activity and ceramide levels (Lee et al., 2004). On the other hand, alterations in lipid metabolism and catabolism are known to affect APP processing and A $\beta$  generation. For example, irregular trafficking and accumulation of cholesterol and sphingolipids in endosomal lysosomal compartments observed in lipid storage diseases like

NP-C lead to an abnormal processing of APP and increased amyloid production (Jin et al., 2004; Runz et al., 2002).

Thus, physiologically there is already plenty of evidence to implicate GSLs in AD. The studies presented here provide molecular mechanisms by which these lipids could affect APP processing and A $\beta$  generation.

### **5.1.1 Modulation of APP metabolism by GSLs**

The present results indicate that irrespective of APP isoform APP metabolism is modulated by GSLs in neuronal and non-neuronal cell types. Changes in cellular GSLs content affected APP stability, transport, maturation, secretion, subcellular distribution and eventually its proteolytic processing. The depletion of GSLs either by pharmacological inhibition or by genetic deletion affected the APP metabolism in a similar way. The effects observed upon GSLs enrichment further convincingly established the role of GSLs in these processes.

Pulse-chase experiments in these cellular models revealed that GSLs affected the stability of APP after its biosynthesis in early secretory compartments. Moreover, results obtained by RT-PCR indicate that GSLs do not modulate the expression of APP at the mRNA level. In addition to the metabolism of APP by amyloidogenic and non-amyloidogenic pathway, APP is also degraded in a  $\alpha$ - and  $\beta$ -secretase independent fashion. When analyzed by metabolic pulse-chase experiment, a pool of initially synthesized APP is processed by secretases whereas another pool is apparently degraded by alternative pathways. The  $\alpha$ - and  $\beta$ -secretase independent pathways of APP degradation have not been characterized in detail. Several groups have shown the presence of APP in lysosomes. Moreover, the degradation of full length APP in lysosomes and in autophagic vacuoles was also reported. Inhibition of lysosomal proteases results in accumulation of APP proteolytic fragments that are potentially amyloidogenic. An array of these fragments consists of proteolytic products that are higher in molecular weight than that of CTFs generated by either  $\alpha$ - or  $\beta$ -secretase. Besides, calpains and caspases have also been implicated in APP metabolism. Especially, the inhibition of calpains causes partial redistribution of APP to the cell surface leading to increased APPs- $\alpha$  and APPs- $\beta$  secretion as well as elevated APP-CTFs. Therefore, initial stabilization of APP by GSLs, appears to be the result of protection of APP from degradation via alternative less understood pathways, directing more of it into the secretases mediated processing (Galvan et al., 2002; Mathews et al., 2002; Battaglia et al., 2003; Pasternak et al., 2004; Mizushima and Hara, 2006).



Incidentally, sphingolipids have been shown to affect the membrane flow along the endosomal and lysosomal pathway. Especially, proteins which are important for endocytic trafficking, namely, annexin 2 and 6 show distorted distribution upon GSLs accumulation. This could have an impact on sorting of lysosomal enzymes. Prosaposins, the cofactors essential for GSLs degradation were shown to be transported to lysosomes in a GSL dependent manner (Lefrancois et al., 1999; Sillence and Platt, 2004; Pagano et al., 2000). GSLs also mediate apoptosis by changing mitochondrial membrane potential and release of reactive oxygen species from mitochondria. Specifically, ganglioside GD3 seems to be crucial for TNF- $\alpha$  as well as FAS induced apoptosis. These studies also suggest modulatory interaction between GD3 and caspases. In particular, caspase-3 was shown to co-localize with GD3 in tissue sections from Farber's disease patients. Moreover, GD3 also caused the release of caspase-9 from mitochondria. Thus, GSLs might affect APP stability indirectly by modulating lysosomal function or by affecting caspases (Garcia-Ruiz et al., 2002; Farina et al., 2000; Sohn et al., 2006). In addition, GSLs metabolism has been linked to the generation of autophagic vacuoles, which could in turn affect APP processing in these compartments. Interestingly, macroautophagy was shown to be critically involved in AD progression. Moreover, recent studies point to a common role of autophagy in neurodegeneration in different neurological disorders (Komatsu et al., 2006; Yu et al., 2005).

Lower amounts of APP at the cell surface analyzed by biotinylation of cell surface proteins as well as attenuated APP maturation after PDMP treatment, could suggest decreased transport of APP in the secretory pathway after GSLs depletion. The role of GSLs in APP transport was further demonstrated by analyzing the subcellular distribution of APP in control and GSLs enriched cells. Immunofluorescence analysis with RNAi mediated suppression of LCS revealed the accumulation of APP in reticular structures, partially co-staining with the ER marker protein calnexin. Since only immature APP is detected in LCS deficient cells, it is likely that these vesicles are derived from ER membranes. Further studies are necessary to characterize the more defined nature of APP containing vesicles in GSL depleted cells.

The modulation of forward transport of APP affects its secretion. Accordingly, the decreased forward transport and slower maturation of APP in GSLs deficient cells was associated with decreased secretion of APP. Importantly, both APPs- $\alpha$  as well as APPs- $\beta$  levels in conditioned media were reduced after incubation with PDMP, indicating that the overall secretion of APP was regulated by GSLs. Feeding of exogenous GSLs, on the other hand, increased APP secretion due to increased stabilization, maturation and transport.

These data support the hypothesis that GSLs are involved in stability, maturation and transport of APP in early secretory compartments. However, the presence of GSLs in early secretory compartments like ER is a matter of debate, since the post-ceramide stage GSLs biosynthesis occurs in *Golgi*, it is not yet clear if GSLs are transported back to the ER (Funato and Riezman, 2001; van Meer and Lisman, 2002). Therefore, it can not be predicted if the observed effects of GSLs on APP metabolism are direct or there are some intermediate proteins or lipids that indirectly link GSLs with APP metabolism. Apparently elevated glucosylceramide levels were shown to modulate intracellular  $Ca^{2+}$  levels possibly via activation of ryanodine receptor, the major  $Ca^{2+}$  release channel of ER, indicating an ability of GSLs to affect a protein located in ER (Lloyd-Evans et al., 2003). As mentioned in the results section, the effects of addition of exogenous GSLs to cultured cells could be attributed either to the insertion of these lipids in the plasma membrane and subsequent uptake or mere adsorption on the plasma membrane. Accumulation of APP and APP-CTFs in the adsorbed micelles on cell surface could also partly contribute to their strongly increased levels observed after GSLs addition. However, very similar results were obtained in the primary fibroblasts from sphingolipid storage disease patients indicating an emulation of the *in vivo* situation by addition of exogenous GSLs, at least in parts.

GSLs have also been implicated previously in the intracellular membrane transport (Holthuis et al., 2001). Especially caveolar endocytosis is reported to be stimulated by GSLs (Sharma et al., 2004). Studies with yeast cells have shown that the inhibition of GSL biosynthesis affects forward transport and stable membrane association of GPI-anchored proteins. Furthermore, the role of phosphatidylinositols in endocytosis has been well documented (Haucke, 2005). Less is known about the role of GSLs in protein transport in the secretory pathway in mammalian cells. Recently, it has been shown that GSLs are involved in the sorting of tyrosinase, another type I transmembrane protein in mouse melanoma cells. The proper transport of tyrosinase from the *Golgi* to melanosomes (organelles involved in melanin biosynthesis) is essential for melanin biosynthesis. The lack of GSLs in GM95 cells causes inhibition of transport of tyrosinase to melanosomes. This, in turn, affects the melanization in these cells. In agreement with our data, these studies, both yeast and mouse melanocytes, also demonstrated that the inhibition of GSL biosynthesis does not generally impair protein transport or secretion (Sprong et al., 2001). Thus, GSLs appear to regulate the transport of individual proteins, probably at distinct steps in the secretory pathway.

### 5.1.2 Role of GSLs in APP-CTF metabolism

The metabolism of the APP-CTFs is particularly important in the generation of A $\beta$ . The present data demonstrated that the generation as well as degradation of APP-CTFs is strongly affected by sphingolipids. Lipids specifically present in the outer leaflet of PM, the sphingomyelin and GSLs influenced the metabolism of APP-CTFs, whereas glycerophospholipids that are present in both membrane layers did not show similar effects (Daleke, 2003; Hanshaw and Smith, 2005). Increased sphingolipid levels caused a strong accumulation of APP-CTFs. When analyzed by pulse-chase experiments, the generation of APP-CTFs appeared to be retarded in GSLs loaded cells. However, the degradation of APP-CTFs was strongly reduced in GSLs treated cells, which eventually resulted in accumulation of APP-CTFs. Importantly, GSLs did not inhibit  $\gamma$ -secretase activity as shown by *in vitro*  $\gamma$ -secretase assay. In contrast to previous studies, APP-CTFs were found to be relatively stable species. This discrepancy could be due to the over expression of APP in most of the earlier studies. A prolonged stability of endogenous APP-CTFs has several implications regarding the fate of APP-CTFs and A $\beta$  generation. Especially, APP-CTFs have also been shown to interact with presenilin independent of  $\gamma$ -secretase activity (Pitsi and Octave, 2004). Therefore, it would be interesting to investigate if elevated levels of APP-CTFs directly affect the presenilin functions and metabolism.

Exogenously added GSLs were incorporated both in intracellular compartments as well as in the plasma membrane, as indicated by immunofluorescence labeling of GM1 by cholera toxin. However, APP-CTFs selectively enriched in intracellular compartments upon GSLs treatment, while levels of APP-CTFs at cell surface were rather decreased. As compared to control cells the subcellular distribution of APP-CTFs was also considerably changed upon GSLs enrichment. When analyzed by subcellular fractionation in control cells APP-CTFs were present in the ER marker positive and *Golgi* marker positive compartments, albeit in higher amounts in ER positive fractions. Upon addition of GSLs, APP-CTFs accumulated in *Golgi* marker rich fractions, probably also because of enhanced ER to *Golgi* transport of APP-CTFs by GSLs, similar to that of full length APP. However, more biochemical and microscopic evidence is required to strengthen this point. Immunoisolation of the vesicles containing APP-CTFs and then checking for respective compartment markers, as well as detection of structures positive for APP-CTFs with immunoelectron microscopy could help to address this issue. Previous studies have shown the presence of APP-CTFs in pre-*Golgi* compartments including ER. This is mostly because of ability of BACE-1

to cleave APP there, also it is speculated that APP-CTFs can be transported back to ER from endocytic compartments where they are predominantly generated.

Initial studies regarding the subcellular distribution of presenilins with respect to localization of  $\gamma$ -secretase activity were confusing as presenilins were shown to be located predominantly in ER, whereas cleavage of APP-CTFs was reported to take place in *Golgi* and *post-Golgi* compartments. Later, however, many subsequent studies showed the presence of presenilins at *Golgi* and *post-Golgi* compartments as well as at plasma membrane where  $\gamma$ -secretase cleavage occurs (Checler, 2001; Walter et al., 1996). Results here suggest that GSLs might enhance the export of APP-CTFs from ER to *Golgi* where they could be processed by  $\gamma$ -secretase with higher efficiency leading to increased A $\beta$  levels. Accordingly, previous studies have shown that retention of APP/APP-CTFs in the ER by addition of the ER retention motif inhibits the generation of A $\beta$  (Maltese et al., 2001). This is further supported by the presence of immature and inactive  $\gamma$ -secretase complex in ER. Interestingly, familial mutations in presenilins, which cause accumulation of A $\beta$ , also showed increased GSLs levels (Kumar-Singh et al., 2006; Bentahir et al., 2006). Moreover, as observed with GSLs enrichment, expression of presenilins with FAD mutations also caused accumulation of APP-CTFs, further supporting a probable role of GSLs in FAD, caused by mutations in presenilin. Similar accumulation of APP-CTFs was also observed in cells expressing APP with FAD mutation, however it remains to be determined if FAD mutations in APP also cause similar increase in GSLs. Thus, increased GSL levels might probably explain the altered A $\beta$  metabolism in FAD (McPhie et al., 1997).

Degradation of APP-CTFs in proteasomes and lysosomal compartments has been shown to be critical in determining their cellular levels as well as A $\beta$  generation. In a study by Nunan et al. only 30% APP-CTFs were found to be processed by  $\gamma$ -secretase (Nunan et al., 2001). Treatment with proteasome inhibitors increased levels of both, APP-CTFs as well as A $\beta$ . Inhibition of lysosomal proteases either by lysotropic agents such as NH<sub>4</sub>Cl or specific inhibitors such as leupeptin also elevates APP-CTFs. Although, GSLs too seem to decrease degradation of APP-CTFs and increase A $\beta$  secretion, GSLs may not directly inhibit proteases in these compartments. Moreover, reduced expression of APP-CTFs at the cell surface and accumulation in intracellular compartments upon GSLs enrichment together indicates a delayed transport of APP-CTFs to the lysosomal compartments and proteasomes. Thus, the data suggests that degradation of APP-CTFs by  $\gamma$ -secretase independent pathways is inhibited by GSLs, however it might not be

due to direct inhibition degradation of CTFs in these compartments but might rather be due to an inefficient transport of CTFs to these compartments. Proteasomes and lysosomal compartments have been implicated in AD before (Keller et al., 2000; Lam et al., 2000). Immunohistochemical observation of ubiquitin-conjugated tau in NFTs was first insinuation of ubiquitin-proteasomal system in AD. Significant decrease in the proteasomal activity was reported in post-mortem AD brains. In addition, a mutant form of ubiquitin, Ub+1, which potently inhibits degradation of polyubiquitinated substrates, was predominantly detected in AD brains. Moreover, abnormalities in the endosomal-lysosomal systems have also been shown to precede the A $\beta$  deposition in AD (Cataldo et al., 2000). Interestingly, the dysfunction of endocytic-lysosomal system appears to be also a characteristic of certain SLSDs such as NPC (Jin et al., 2004). Thus, regular degradation of proteins by proteasomal and lysosomal system seems to be very important for proper neuronal function and any deficiencies in degradation either directly by lysosomes and proteasomes inadequacies or due to inappropriate protein transport might lead to neurodegeneration (Ding et al., 2007).

The strong influence of sphingolipids on the metabolism of APP-CTFs was substantiated by the observed accumulation of APP-CTFs in primary fibroblasts from SLSD patients. These findings also support the use of exogenous GSLs applied to cells as a valid model to study the storage of GSLs. GSL deficient GM95 cells on the other hand showed a strong reduction in APP-CTFs, but the PDMP treatment did not result in APP-CTFs decrease, rather there was shift from CTFs generated by  $\beta$ -secretase to CTFs generated by  $\alpha$ -secretase, which could be most likely due to further cleavage of  $\beta$ -CTFs by  $\alpha$ -secretase into  $\alpha$ -CTFs as reported previously. Moreover, certain lipid dependent biological functions such as protein transport can be carried out efficiently even at much lower than normal cellular concentrations of these lipids. This might be due to tight regulation of lipid levels in microdomains present in cellular membranes. Therefore, to study the role of lipids with respect to such processes it might be necessary to achieve complete depletion of these lipids (Platt and Butters, 2000). Since there was only a partial reduction in GSL levels after PDMP treatment it might be difficult to achieve similar effects on APP-CTFs as in GM95 cells. Moreover, the strongly reduced levels of APP-CTFs in GM95 cells could also partially be due to reduced levels of APP in these cells.

Besides A $\beta$ , APP-CTF accumulation could also contribute to neurodegeneration in AD (Yankner et al., 1989). An age dependent accumulation of APP-CTFs as well as APP in AD patients was suggested to contribute to AD with advanced age and the accumulation of APP-CTFs

seems to correlate much better with AD progression (Chang and Suh, 2005). Furthermore, CTFs are known to impair calcium homeostasis, learning and memory through blocking LTP and trigger a strong inflammatory reaction through MAPKs- and NF- $\kappa$ B-dependent astrocytosis as well as iNOS induction. CTFs, via their binding with the adaptor protein Fe65, could affect the transcription of genes including glycogen synthase kinase-3, which might result in the induction of neurofibrillary tangles and subsequently cell death. Single intracerebroventricular injection of CTFs to mice caused significant disruption of cued, spatial and working memory performances in a dose dependent manner. Furthermore, spatial memory of transgenic mice overexpressing CTFs was significantly impaired and CTFs were detected in neurons as well as in plaques (Lahiri et al., 2002). As discussed above sphingolipids might play an important role in AD. Especially, the density of GSLs such as GM1 and GM2 within the microdomains was reportedly increased in AD brains. On the other hand, SLSDs are associated with neurodegeneration at early ages (Neufeld, 1991; Tiffit and Proia, 2000). Although the cause for these disorders is the defect in proteins involved in lipid transport and degradation, the potential mechanism as to how accumulation of lipids leads to severe neurodegeneration is not fully understood. Thus, the alteration in sphingolipid metabolism with the associated accumulation of APP-CTFs and/or other membrane proteins might underlie the pathophysiologic events in AD as well as sphingolipid storage disorders along with other reported factors such as impaired membrane trafficking, dysfunctional endosomal-lysosomal and proteasomal system as well as inflammation (Nixon et al., 2000).

### **5.1.3 Role of GSLs in A $\beta$ generation**

Studies presented here clearly demonstrate the importance of membrane GSLs in the generation of A $\beta$ . Depletion of GSLs using PDMP reduced A $\beta$  secretion, whereas addition of exogenous GSLs to cultured cells increased A $\beta$  secretion in neuronal SH-SY5Y cells. The decrease in A $\beta$  secretion could be attributed to the reduced stability, forward transport and cell surface expression of full length APP. The attenuated transport of APP to the cell surface in GSL deficient cells is consistent with decreased secretion of APP by  $\alpha$ -secretase, which is known to occur during transport to or directly at the cell surface. In contrast,  $\beta$ -secretase cleavage occurs predominantly in endocytic compartments after re-internalization of APP from the cell surface (Koo and Squazzo, 1994). Thus, the decreased generation of A $\beta$  upon depletion of cells from GSLs might also be due to decreased access of  $\beta$ -secretase to APP in endocytic compartments. The

decreased levels of CTF- $\beta$  in GSL depleted cells could support this notion. The decrease in A $\beta$  secretion upon PDMP treatment appears to be primarily due to modulation of full-length APP metabolism. However, increased levels of A $\beta$  after GSL enrichment might be due to modulation of both, the metabolism of APP as well as APP-CTFs. Enhanced stability and forward transport of APP by GSLs would lead to increased A $\beta$  production. Similarly, GSLs also inhibit the degradation of APP-CTFs by alternative pathways like lysosomal or proteasomal degradation, making them more available for  $\gamma$ -secretase cleavage. Upon GSL treatment, APP-CTFs probably accumulate in compartments rich in  $\gamma$ -secretase activity, which could further boost the A $\beta$  generation. Incidentally, as discussed earlier, proteasomal and lysosomal inhibitors have been shown to enhance A $\beta$  generation in a similar way.

The inhibition of  $\beta$ -secretase and  $\gamma$ -secretase has been put forward as a promising approach to reduce A $\beta$  secretion. However, recent studies suggest an important role of presenilins in learning, memory, cognition and cell differentiation. Therefore, the search for alternative ways to reduce A $\beta$  levels is becoming increasingly important. Since, the data presented here clearly indicated that increased amounts of cellular (Hamaguchi et al., 2006). GSLs shift APP metabolism towards higher A $\beta$  levels and the reduction in cellular GSL levels might be a reasonable approach to suppress A $\beta$  levels. The pharmacological inhibition of GCS, touted as substrate deprivation therapy, has been identified as an effective approach to lower high sphingolipid levels in SLSDs (Platt and Butters, 2000). Thus, the respective enzymes involved in GSLs biosynthesis could also represent targets to decrease the formation of A $\beta$  in therapeutic strategies for AD.

During the course of the present work, three more related studies addressing the role of sphingolipids in A $\beta$  generation were published. Similar to presented study, these studies also showed that sphingolipids potentiate A $\beta$  generation, however, experimental approaches and interpretation of molecular mechanisms differed to some extent. In the first study, inhibition of ceramide synthesis in chinese hamster ovary cells resulted in an elevated secretion of APP<sub>s</sub>, likely due to an increase in  $\alpha$ -secretase cleavage (Sawamura et al., 2004). In the current study, a significant decrease in the secretion of endogenous APP upon depletion of GSLs was observed. This discrepancy might be explained by strong overexpression of APP in the former study that might mask some effects on transport and/or processing of APP. Moreover, in the present study GSL biosynthesis was targeted selectively, while the inhibition of ceramide synthesis would also lead to a strong decrease in the biosynthesis of sphingomyelin and ceramide itself that might serve

additional functions in APP metabolism. In another study, the direct addition of GM1 to cells led to increased secretion of A $\beta$ , while secretion of APP<sub>S</sub>- $\alpha$  was attenuated specifically without affecting cellular APP levels (Zha et al., 2004). These studies too, were performed in cells overexpressing APP and studies here clearly demonstrated that the cells overexpressing already high levels of cellular APP as well as APP-CTFs do not cause any further increase in APP and APP-CTFs with addition of GSLs. Moreover, they also showed increase in p3 while APP<sub>S</sub>- $\alpha$  levels were decreased upon treatment with GM1. Simultaneous an increase in p3 along with decreased APPs- $\alpha$  levels cannot be explained, as levels of both should be affected in similar ways. Although most of the effects of GSLs on APP processing can be explained by altered trafficking of APP and APP-CTFs, subtle changes in activities of different secretases can not be ruled out completely. Recently, cerebrosides, anionic glycerophospholipids and sterols were shown to stimulate BACE-1 activity. However, only *in vitro* experiments with reconstitution of purified BACE-1 in unilamellar vesicles were performed to analyze the effects of lipids on BACE-1 activity. The role of these lipids in modulating BACE-1 activity in cultured cells or *in vivo* remains to be examined (Kalvodova et al., 2005).

In addition, studies by Puglielli et al. (Puglielli et al., 2003a) showed that stabilization of BACE-1 by ceramide results in higher APP-CTF levels, thereby promoting A $\beta$  generation. With inhibition of GSL biosynthesis as well as GSLs enrichment one might expect increased ceramide levels. First, although both treatments should elevate ceramide levels, opposite effects were observed by GSL depletion and GSL excess suggesting that the effects are indeed caused by two different mechanisms and not because of increased ceramide levels. Moreover, analysis of GM95 cells and PDMP treated cells did not show highly increased levels of ceramide (Komori et al., 1999). Nonetheless, addition of C6-ceramide increased levels of APP-CTFs subtly, however this effect was far weaker compared to the accumulation of CTFs after GSLs addition. Still higher concentrations of ceramide might be toxic to cells. This slight increase in APP-CTFs after ceramide treatment could be attributed to increased levels of sphingolipids caused by increased biosynthesis because of higher substrate availability. Moreover, results here showed an increased stability of APP-CTFs due to an excess of sphingolipids, ruling out their increased generation, as would be expected by stabilization of BACE-1.

Thus, all studies together, including the one presented here establish a clear role of sphingolipids in A $\beta$  generation. Unlike other studies, evidence provided from independent genetic



models here, further strengthens the argument that the effects of GSLs on A $\beta$  generation are mediated by altered subcellular transport and stability of APP as well as of APP-CTFs.

## 5.2 Link between cholesterol metabolism and AD

Several studies in cellular and animal models have shown that the concentration and distribution of cholesterol affects A $\beta$  generation. Moreover, clinical and epidemiological studies have revealed a link between cholesterol and AD pathogenesis. Although initial findings led to the assumption that the reduction in cholesterol is protective in AD, recent developments warn for a more cautious approach. Importantly, the amyloidogenic processing of APP is dependent on lipid microdomains rich in cholesterol and sphingolipids. The  $\gamma$ -secretase complex is also associated with such microdomains (Abad-Rodriguez et al., 2004) (Puglielli et al., 2003b; Simons and Eehalt, 2002).

The levels of total cholesterol and LDL in serum were reported to correlate positively with the amount of A $\beta$  in AD brains. Epidemiological studies showed that the elevated cholesterol levels during mid-life increases the risk of developing AD (Kivipelto and Solomon, 2006). Additionally, elevated dietary cholesterol increased amyloid plaque formation in AD mice. Retrospective and prospective clinical studies indicate that the inhibition of cholesterol biosynthesis by statins cause a significant decrease in the incidence of AD and dementia. In cellular models, the decrease in cholesterol content strongly reduced secreted A $\beta$ . Eehalt et al. (Eehalt et al., 2003) showed that the depletion of cholesterol causes a disruption of lipid microdomains resulting in decreased cleavage of APP by BACE-1, indicating the necessity of intact lipid microdomains for BACE-1 activity. More recently, however, Abad-Rodriguez et al., showed that the moderate reduction in cholesterol causes a disorganization of lipid microdomains, allowing more BACE-1 to cleave APP and resulting in enhanced A $\beta$  generation. On the other hand, a strong reduction in cholesterol inhibits BACE-1/  $\gamma$ -secretase activity and results in a dramatic drop in A $\beta$  generation, even though BACE-1 and  $\gamma$ -secretase can now contact APP directly. There are also *in vivo* findings to support that the depletion of cholesterol can be deleterious. Treatment of female APP transgenic mice with statins enhanced A $\beta$  production and plaque deposition. Recently APP transgenic mice were reported to show an age dependent decrease in cholesterol content (Fassbender et al., 2001).

In addition, the inhibition of acyl-coenzyme A: cholesterol acyltransferase (ACAT) also led to a strong reduction of A $\beta$  generation in cultured cells and transgenic mice, indicating that cholesterol esters could also influence the proteolytic processing of APP. The inactivation of ACAT results in redistribution of intracellular cholesterol. Incidentally, the drugs which inhibit the backward transport of cholesterol from late endocytic compartments to the ER cause a redistribution of cholesterol and increase the A $\beta$  generation (Hutter-Paier et al., 2004). This might mainly be due to decreased  $\beta$ -secretase cleavage of APP. However,  $\gamma$ -secretase activity is strongly increased by treatment with such drug. In NPC disease there is aberrant cholesterol transport resulting in accumulation of cholesterol in endosomes/lysosomes, especially in the brain (Liscum, 2000). In NPC mouse brain  $\alpha$ - and  $\beta$ -secretase activity is not changed but  $\gamma$ -secretase activity is greatly enhanced, which is consistent with increased A $\beta$  levels (Jin et al., 2004).

Thus, there is enough epidemiological, pathological as well as experimental evidence which links cholesterol metabolism to AD. Attempts have also been made to understand the influence of altered cholesterol levels on A $\beta$  generation and metabolism of AD associated proteins. In the present study, however, evidence is provided for the probable role of AD associated presenilins, especially the RIP mediated by them, in maintaining membrane lipid homeostasis, particularly the regulation of cholesterol metabolism.

### ***5.2.1 Role of RIP in maintenance of membrane lipid – protein homeostasis***

$\gamma$ -secretase mediated RIP of type I membrane proteins within or close to their transmembrane domains, results in the generation of soluble intracellular domains and short secreted peptides. The numbers of  $\gamma$ -secretase substrates is steadily increasing and include cell adhesion molecules, surface receptors, and channel proteins (Wolfe and Kopan, 2004). The cleavage of these proteins is predominantly regulated by precedent shedding of their ectodomains. However, a biological function of  $\gamma$ -secretase dependent cleavage has only been demonstrated for some substrates, including notch, N- and E-cadherins, CD44 and receptor tyrosine kinase Erb4. The soluble intracellular domains of these proteins can translocate to the nucleus and modulate transcription of target genes. The function of  $\gamma$ -secretase dependent cleavage of most other substrates is poorly understood. Although AICD could also regulate gene transcription by association with Fe65 and Tip60, release of AICD from cellular membranes by  $\gamma$ -secretase is not absolutely required (Hass and Yankner, 2005). A global function of  $\gamma$ -secretase dependent RIP in

maintaining membrane lipid and protein homeostasis particularly via regulation of endocytosis is indicated by this study.

### **5.2.2 Role of presenilins in cellular cholesterol homeostasis**

PS deficient cells showed a decreased capacity in internalization of extracellular proteins, including LDL. Despite the decreased uptake of LDL, cholesterol levels in PS deficient cells were found to be increased, suggesting an up-regulation of cholesterol *de novo* synthesis. The comprehensive analysis of cholesterol precursors and metabolites together with mRNA expression of cholesterol biosynthetic enzymes indeed demonstrated an enhanced cholesterol biosynthesis in PS deficient cells. Notably, levels of most precursors, including desmosterol, were found to be elevated in PS dKO cells, while levels of lanosterol were strongly decreased. In addition, PS-deficient cells showed transcriptional up-regulation of CYP51 mRNA. mRNA levels of other enzymes involved in lanosterol metabolism, like squalin-1 and lanosterol synthase, were not significantly altered in PS deficient cells. CYP51 is critically involved in cholesterol biosynthesis, since it catalyzes the demethylation of lanosterol, the first cyclic metabolite after squalene biosynthesis. The strong up-regulation of CYP51 mRNA was associated with decreased levels of lanosterol, which indicated increased CYP51 activity in these cells. These data are consistent with a previous study showing that addition of exogenous LDL to porcine vascular endothelial cells led to suppression of CYP51 mRNA expression via SREBP dependent mechanisms (Rodriguez et al., 2001).

Since the levels of cholesterol degradation products were also increased in PS dKO cells, increased cholesterol levels were not caused by impaired degradation of cholesterol. Importantly, pharmacological inhibition of  $\gamma$ -secretase in MEF and human neuroglioma H4 cells altered the cholesterol metabolism similar to genetic deletion of presenilins. Re-expression of PS1 in PS dKO cells partially reversed the observed effects on cholesterol and cholesterol metabolites, further validating the importance of PS1 in the regulation of cellular cholesterol metabolism. Moreover, the treatment of PS dKO cells with itraconazole, a specific inhibitor of CYP51, partially reduced elevated cholesterol and desmosterol levels.

It has been shown recently that A $\beta$  could directly inhibit HMG-CoA reductase activity and it was speculated that the lack of A $\beta$  leads to an up-regulation of HMG-CoA reductase activity (Grimm et al., 2005). However, the addition of A $\beta$  to PS deficient cells did not normalize cholesterol levels, indicating that the lack of A $\beta$  in these cells is not responsible for enhanced

biosynthesis of cholesterol. The present data are consistent with the up-regulation of cholesterol biosynthetic enzymes in response to decreased uptake of LDL.

The present findings might be especially relevant for cholesterol metabolism in the brain. Neuronal cells are dependent on cholesterol uptake from lipoprotein particles that derive from glial cells (Herz and Bock, 2002). Since cholesterol has been shown to modulate dendrite differentiation and synaptogenesis, PS proteins might affect these processes through the regulation of cholesterol uptake. It is noteworthy that PS proteins have been involved in synaptic plasticity and neuronal survival (Vance et al., 2005; Vance et al., 2006). Mice with conditional inactivation of PS in neurons reveal a strong impairment in learning and memory, and show significant synaptic and neuronal loss associated with decreased cAMP responsive element (CRE)-dependent gene expression. Since CYP51 expression is also dependent on CRE/CREB activation, the impaired cholesterol uptake in PS deficient cells might affect synaptogenesis of neurons via these pathways (Harris et al., 2004; Fink et al., 2005; Beglopoulos and Shen, 2006).

### ***5.2.3 Presenilin dependent subcellular distribution of cholesterol***

The levels of cholesterol in membranes of mammalian cells differ strongly between different subcellular compartments. The plasma membrane is reported to contain nearly 85% of cellular cholesterol and only 0.5% of total cholesterol is found in ER (Fielding and Fielding, 1997). In MEF WT cells along with PM staining, significant juxtannuclear cholesterol stain was observed. There might be relatively higher density of cholesterol present in compact perinuclear structures while at the PM cholesterol is distributed with other phospholipids in expanded membrane sheets. In PS dKO cells, the overall stronger cholesterol stain was consistent with increased cholesterol levels. PS deficient cells revealed strong PM stain with relatively reduced juxtannuclear labeling.

Changes in plasma membrane cholesterol near the physiologic set points evoke large responses in ER cholesterol within minutes (Lange and Matthies, 1984; Liscum and Dahl, 1992). This is achieved by the influx of cholesterol from plasma membrane to ER in special transport vesicles likely originating from plasma membrane itself. This backward transport of cholesterol regulates cellular cholesterol homeostasis by controlling cholesterol biosynthesis and esterification in the ER. This is achieved by two cholesterol sensing membrane-embedded proteins – SCAP and HMGCoA reductase, in conjunction with other regulatory proteins like Insigs, SREBPs and site-1/2 proteases (see introduction) (Espenshade, 2006). In PS dKO cells, high cholesterol levels do

not seem to affect ER cholesterol levels, as increased cholesterol biosynthesis in PS dKO cells is not checked/controlled by ER mediated suppression of cholesterol biosynthesis. This could be partly due to improper backward transport of cholesterol from the PM to the ER in PS deficient cells, thus uncoupling cellular cholesterol sensing machinery from increased cholesterol levels. Although the data do not show an inhibition of PM to ER cholesterol transport, the decreased endocytic membrane flow and altered subcellular cholesterol distribution in PS dKO cells supports this idea. Another probable reason could be the altered metabolism of proteins involved in cholesterol regulation, namely Insigs, SCAP, SREBPs, HMGCoA reductase etc. in PS deficient cells. Studying the metabolism of these proteins and analysis of subcellular cholesterol pools in WT and PS KO cells would further improve the understanding of the complex role of presenilins in regulation of cholesterol homeostasis.

#### ***5.2.4 Regulation of global endocytosis and protein transport by presenilin***

Previously, presenilins have been shown to regulate endocytosis of APP and BSA. Increased levels of APP caused by a possible impairment of APP endocytosis alongwith defective BSA uptake were confirmed in PS dKO cells. Endocytic function of PS proteins was further extended to internalization of LDL, LDLR and LRP. Although proteins like LRP and APP are  $\gamma$ -secretase substrates, precedent shedding of ectodomain is essential. Inhibition of  $\gamma$ -secretase activity leads to the accumulation of these proteins, mostly due to inefficient endocytic transport to the compartments where they could be degraded. Thus, presenilins seems to play an important role in general turnover of membrane proteins (Wood et al., 2005; Zhang et al., 2006).

Presenilins together with PS mediated  $\gamma$ -secretase activity have been previously shown to be involved in the regulation of transport of selected proteins. The forward transport of APP in early secretory compartments as well as endocytosis appears to be PS1 dependent. Sorting of tyrosinase is also regulated by  $\gamma$ -secretase activity and deletion of PS in mice results in decreased skin pigmentation. Transport of nicastrin and N-cadherin has also been shown to be influenced by presenilin PS1. Interestingly, the turn over of telencephalin, a neuron specific intercellular adhesion molecule that is involved in dendritic outgrowth and long-term potentiation is also regulated by PS1, but it is not a  $\gamma$ -secretase substrate. In PS deficient cells telencephalin accumulates in autophagic vacuoles because of improper sorting to lysosomes (Annaert and de Strooper, 2002; Wang et al., 2006).

The role of presenilins in the regulation of transport of lipoprotein receptor family proteins was established in this study. Moreover, the data also indicate that the presenilins are involved in general endocytosis. Decreased uptake of GM1 suggests that endocytic membrane flow is globally impaired in the absence of  $\gamma$ -secretase activity. Endocytosis is a vital and indispensable biological process. In addition to initiating or attenuating cell signaling, endocytosis shapes morphogen gradients, activates ligands, and spatially regulates the receptor activation within single the cell. Cells also depend on endocytosis for uptake of nutrients, maintenance of cell polarity and antigen presentation. Thus, presenilin deficiency would affect several important biological processes essential for cell survival (Mukherjee et al., 1997).

The LRP mediated Apo E endocytosis is critically involved in the clearance of extracellular A $\beta$  (Waldron et al., 2006). Extracellular A $\beta$  binds to lipoprotein particles like Apo E and then the complex is internalized via LRP. Subsequently, endocytosed A $\beta$  is degraded via lysosomes. Moreover binding of A $\beta$  to Apo E enhances the fibrillization and deposition of A $\beta$ . Considering these data with the findings that presenilins regulate lipoprotein particles endocytosis, it is conceivable that PS proteins play an important role in clearance and deposition of A $\beta$  as well (Trommsdorff et al., 1998; Rochet and Lansbury, Jr., 2000).

### **5.2.5 *GSL metabolism is affected by presenilins***

A strong accumulation of gangliosides was observed in PS deficient cells. This can be explained by an inefficient uptake of these lipids into lysosomes where they are degraded. However, other mechanisms involving saposins or exohydrolases could also contribute to the observed effects. Nonetheless, the inhibition of general membrane flow should also lead to an accumulation of other membrane lipids like sphingomyelin. Recently an accumulation of sphingomyelin in PS dKO cells was reported, but increased levels were attributed to the lack of A $\beta$ 42 in these cells, as these studies showed that the endogenous A $\beta$ 42 stimulates sphingomyelinase, the key enzyme required for sphingomyelin degradation. Thus, decreased sphingomyelinase activity in the absence of A $\beta$ 42 in PS dKO cells was shown to cause increase in sphingomyelin levels (Lee et al., 2004).

The proper degradation of sphingolipids is essential for the function of the nervous system. Genetic defects in key enzymes involved in the degradation and transport of sphingolipids or sphingolipid activator proteins (SAPs) cause severe neurodegeneration and dementia (Kolter and Sandhoff, 2006). Interestingly, some of these storage disorders like NPC also show prominent

tau pathology as it is observed in AD and other neurodegenerative disorders. Sandhoff's disease, which is characterized by GM2 accumulation in neurons, shows presence of microglial activation and associated inflammation in brain. Incidentally, these processes are also characteristic of AD brains (Griffin, 2006; Terai et al., 2001). Therefore, the finding that presenilins are involved in metabolism of sphingolipids could direct further research to understand the complex relation between AD and SLSDs with respect to common features like tau pathology, glial activation and inflammation observed in both (Distl et al., 2003; Wada et al., 2000).

#### **5.2.5.1 PS1 FAD mutations are loss of function mutations with respect to maintenance of membrane homeostasis and endocytosis**

The egg laying defect observed in *Sel-12*, a presenilin orthologue, deficient *C. elegans* due to inhibition of notch cleavage could only be rescued by WT human PS1 but not by PS1 FAD mutants suggesting that PS associated mutations are loss of function mutations. However, increased levels of the more toxic A $\beta$  species, A $\beta$ 42, by PS1 FAD mutants in mammalian cells is also considered as gain of malfunction of PS1 FAD mutations (Haass and de Strooper, 1999; de Strooper, 2007). Current studies demonstrate that PS1 FAD mutants can not maintain normal membrane lipid and protein homeostasis and hamper endocytosis. Thus, PS1 FAD mutations might be deleterious because of their inability to regulate membrane flow and hence should be termed as loss of function mutations (Sambamurti et al., 2006). In addition, alterations in A $\beta$  levels might further cause more damage by a variety of different routes as described in the introduction. PS1 FAD mutants also led to an accumulation of the ganglioside GM1 because of defective endocytosis. These findings might also predict increased levels of other sphingolipids upon expression of PS1 FAD mutant. However, significant decrease in sphingomyelin levels were reported upon expression of PS1 with FAD mutations compared to WT presenilin (Grimm et al., 2005). These findings were explained by the ability of A $\beta$ 42 to stimulate neutral sphingomyelinase and increased A $\beta$ 42 levels in PS1 FAD mutant expressing cells. However, recent studies indicate that most FAD mutations increased A $\beta$ 42 to A $\beta$ 40 ratio due to decreased production of A $\beta$ 40 rather than increased A $\beta$ 42 levels as was believed earlier. Therefore, it is unlikely that increased sphingolipid levels in PS KO cells are due to absence of A $\beta$  in these cells (Bentahir et al., 2006; Kumar-Singh et al., 2006).

Subtle changes in  $\gamma$ -secretase activity caused by PS1 FAD mutations leading to altered metabolism of transcriptionally active intracellular fragments of various substrates resulting in

transcriptional dysregulation has also been proposed as one of the ways by which these mutations might cause early onset AD (Robakis, 2003). Moreover, PS1 FAD mutations have also been shown to alter PS1 conformation resulting in altered interaction between PS1 CTF and PS1 NTF as well as between PS1 and APP-CTF. Expression of presenilins with FAD mutations are also known to perturb important biological processes like intracellular  $\text{Ca}^{2+}$  metabolism and cell cycle control. PS1 FAD mutations have also been shown to be associated with increased ER and oxidative stress (Tomita and Iwatsubo, 2006; Zatti et al., 2006). One of the PS1 FAD mutations (A260V) affected the vesicle transport from TGN to PM. Expression of PS1 A260V significantly reduced the Rab8 levels which is a GTPase involved in TGN to PM transport. Accumulation of APP-CTFs upon expression of A260V mutant PS1 was also reported in the same study. Interestingly, the present study also indicated an inhibitory effect of excess GSLs on TGN to PM transport which lead to accumulation of APP-CTFs. Elevated GM1 levels were observed in the cells which expressed mutant PS1 and recent reports also indicated an accumulation of APP-CTFs associated with PS1 FAD mutations. Therefore, cellular levels of GSLs and APP-CTFs appear to be regulated co-ordinately, which in turn might regulate TGN to PM transport. Thus, the modulation of GSLs and APP-CTFs metabolism leading to inefficient protein transport could be one of the ways by which FAD associated mutations could cause neurodegeneration (Uemura et al., 2004).



## 6 Literature

Abad-Rodriguez,J., Ledesma,M.D., Craessaerts,K., Perga,S., Medina,M., Delacourte,A., Dingwall,C., de Strooper,B., and Dotti,C.G. (2004). Neuronal membrane cholesterol loss enhances amyloid peptide generation. *J. Cell Biol.* 167, 953-960.

Abe,A., Wild,S.R., Lee,W.L., and Shayman,J.A. (2001). Agents for the treatment of glycosphingolipid storage disorders. *Curr. Drug Metab.* 2001. Sep. ;2(3):331. -8. 2, 331-338.

Annaert,W. and de Strooper,B. (2002). A cell biological perspective on Alzheimer's disease. *Annu. Rev. Cell Dev. Biol.* 18, 25-51.

Ariga,T. and Yu,R.K. (1998). GM1 ganglioside inhibits amyloid beta-protein induced-cytokine release. *Ann. N. Y. Acad. Sci.* 845, 403.

Armstrong,R.A. (2006). Plaques and tangles and the pathogenesis of Alzheimer's disease. *Folia Neuropathol.* 44, 1-11.

Arnaiz,E. and Almkvist,O. (2003). Neuropsychological features of mild cognitive impairment and preclinical Alzheimer's disease. *Acta Neurol. Scand. Suppl* 179, 34-41.

Bales,K.R., Dodart,J.C., DeMattos,R.B., Holtzman,D.M., and Paul,S.M. (2002). Apolipoprotein E, amyloid, and Alzheimer disease. *Mol. Interv.* 2002. Oct. ;2(6. ):363. -75. , 339. 2, 363-75, 339.

Battaglia,F., Trinchese,F., Liu,S., Walter,S., Nixon,R.A., and Arancio,O. (2003). Calpain inhibitors, a treatment for Alzheimer's disease: position paper. *J. Mol. Neurosci.* 2003. ;20. (3):357. -62. 20, 357-362.

Bayer,T.A., Cappai,R., Masters,C.L., Beyreuther,K., and Multhaup,G. (1999). It all sticks together--the APP-related family of proteins and Alzheimer's disease. *Mol. Psychiatry* 4, 524-528.

Beer,R.E. and Ulrich,J. (1993). Alzheimer plaque density and duration of dementia. *Arch. Gerontol. Geriatr.* 16, 1-7.

Beglopoulos,V. and Shen,J. (2006). Regulation of CRE-dependent transcription by presenilins: prospects for therapy of Alzheimer's disease. *Trends Pharmacol. Sci.* 2006. Jan. ;27. (1):33. -40. Epub. 2005. Dec. 7. 27, 33-40.

Behl,C. (2005). Oxidative stress in Alzheimer's disease: implications for prevention and therapy. *Subcell. Biochem.* 2005. ;38. :65. -78. 38, 65-78.

Bentahir,M., Nyabi,O., Verhamme,J., Tolia,A., Horre,K., Wiltfang,J., Esselmann,H., and de Strooper,B. (2006). Presenilin clinical mutations can affect gamma-secretase activity by different mechanisms. *J. Neurochem.* 2006. Feb. ;96. (3):732. -42. Epub. 2006. Jan. 9. 96, 732-742.

Billings,L.M., Oddo,S., Green,K.N., McGaugh,J.L., and LaFerla,F.M. (2005). Intraneuronal Abeta causes the onset of early Alzheimer's disease-related cognitive deficits in transgenic mice. *Neuron.* 2005. Mar. 3;45. (5):675. -88. 45, 675-688.

Birks, J. (2006). Cholinesterase inhibitors for Alzheimer's disease. *Cochrane Database. Syst. Rev.* CD005593.

Bishop, W.R. and Bell, R.M. (1988). Assembly of phospholipids into cellular membranes: biosynthesis, transmembrane movement and intracellular translocation. *Annu. Rev. Cell Biol.* 4, 579-610.

Bjorkhem, I. and Meaney, S. (2004). Brain cholesterol: long secret life behind a barrier. *Arterioscler. Thromb. Vasc. Biol.* 2004. May. ;24. (5):806. -15. Epub. 2004. Feb. 5. 24, 806-815.

Blurton-Jones, M. and LaFerla, F.M. (2006). Pathways by which Aβ facilitates tau pathology. *Curr. Alzheimer Res.* 2006. Dec. ;3(5):437. -48. 3, 437-448.

Braak, H. and Braak, E. (1991b). Demonstration of amyloid deposits and neurofibrillary changes in whole brain sections. *Brain Pathol.* 1, 213-216.

Braak, H. and Braak, E. (1991a). Neuropathological staging of Alzheimer-related changes. *Acta Neuropathol. (Berl)* 82, 239-259.

Brummelkamp, T.R., Bernards, R., and Agami, R. (2002). A system for stable expression of short interfering RNAs in mammalian cells. *Science.* 2002. Apr 29, 550-553.

Burns, M., Gaynor, K., Olm, V., Mercken, M., LaFrancois, J., Wang, L., Mathews, P.M., Noble, W., Matsuoka, Y., and Duff, K. (2003). Presenilin redistribution associated with aberrant cholesterol transport enhances beta-amyloid production in vivo. *J. Neurosci.* 23, 5645-5649.

Bush, A.I., Masters, C.L., and Tanzi, R.E. (2003). Copper, beta-amyloid, and Alzheimer's disease: tapping a sensitive connection. *Proc. Natl. Acad. Sci. U. S. A* 100, 11193-11194.

Butterfield, D.A., Yatin, S.M., Varadarajan, S., and Koppal, T. (1999). Amyloid beta-peptide-associated free radical oxidative stress, neurotoxicity, and Alzheimer's disease. *Methods Enzymol.* 309, 746-768.

Cao, X. and Sudhof, T.C. (2004). Dissection of amyloid-beta precursor protein-dependent transcriptional transactivation. *J. Biol. Chem.* 279, 24601-24611.

Carter, D.B. (2005). The interaction of amyloid-beta with ApoE. *Subcell. Biochem.* 2005. ;38. :255. -72. 38, 255-272.

Cataldo, A.M., Peterhoff, C.M., Troncoso, J.C., Gomez-Isla, T., Hyman, B.T., and Nixon, R.A. (2000). Endocytic pathway abnormalities precede amyloid beta deposition in sporadic Alzheimer's disease and Down syndrome: differential effects of APOE genotype and presenilin mutations. *Am. J. Pathol.* 2000. Jul. ;157. (1):277. -86. 157, 277-286.

Chang, K.A. and Suh, Y.H. (2005). Pathophysiological roles of amyloidogenic carboxy-terminal fragments of the beta-amyloid precursor protein in Alzheimer's disease. *J. Pharmacol. Sci.* 2005. Apr;97. (4):461. -71. Epub. 2005. Apr 9. 97, 461-471.

Chang, T.Y., Chang, C.C., Ohgami, N., and Yamauchi, Y. (2006). Cholesterol Sensing, Trafficking, and Esterification. *Annu. Rev. Cell Dev. Biol.* 2006. Jun. 5; . .

- Checler,F. (2001). The multiple paradoxes of presenilins. *J Neurochem* 76, 1621-7.
- Daleke,D.L. (2003). Regulation of transbilayer plasma membrane phospholipid asymmetry. *J. Lipid Res.* 2003. Feb. ;44. (2):233. -42. Epub. 2002. Dec. 16. 44, 233-242.
- De Matteis,M.A., Luna,A., Di Tullio,G., Corda,D., Kok,J.W., Luini,A., and Egea,G. (1999). PDMP blocks the BFA-induced ADP-ribosylation of BARS-50 in isolated Golgi membranes. *FEBS Lett.* 459, 310-312.
- de Strooper,B. (2007). Loss-of-function presenilin mutations in Alzheimer disease. Talking Point on the role of presenilin mutations in Alzheimer disease. *EMBO Rep.* 8, 141-146
- de Strooper,B. and Annaert,W. (2000). Proteolytic processing and cell biological functions of the amyloid precursor protein. *J Cell Sci* 113, 1857-70.
- DeGrella,R.F. and Simoni,R.D. (1982). Intracellular transport of cholesterol to the plasma membrane. *J. Biol. Chem.* 257, 14256-14262.
- Desvergne,B., Michalik,L., and Wahli,W. (2006). Transcriptional regulation of metabolism. *Physiol Rev.* 2006. Apr;86. (2):465. -514. 86, 465-514.
- Dewachter,I., Moechars,D., Van Dorpe,J., Tesseur,I., Van den,H.C., Spittaels,K., and Van Leuven,F. (2001). Modelling Alzheimer's disease in multiple transgenic mice. *Biochem. Soc. Symp.* 2001. ;(67. ):203. -10. 203-210.
- Ding,Q., Cecarini,V., and Keller,J.N. (2007). Interplay between protein synthesis and degradation in the CNS: physiological and pathological implications. *Trends Neurosci.* 2007. Jan. ;30. (1):31. -6. Epub. 2006. Nov. 28. 30, 31-36.
- Distl,R., Treiber-Held,S., Albert,F., Meske,V., Harzer,K., and Ohm,T.G. (2003). Cholesterol storage and tau pathology in Niemann-Pick type C disease in the brain. *J. Pathol.* 2003. May. ;200. (1):104. -11. 200, 104-111.
- Eckman,E.A. and Eckman,C.B. (2005). Abeta-degrading enzymes: modulators of Alzheimer's disease pathogenesis and targets for therapeutic intervention. *Biochem. Soc. Trans.* 33, 1101-1105.
- Edbauer,D., Willem,M., Lammich,S., Steiner,H., and Haass,C. (2002b). Insulin-degrading enzyme rapidly removes the beta-amyloid precursor protein intracellular domain (AICD). *J. Biol. Chem.* 277, 13389-13393.
- Eehalt,R., Keller,P., Haass,C., Thiele,C., and Simons,K. (2003). Amyloidogenic processing of the Alzheimer beta-amyloid precursor protein depends on lipid rafts. *J. Cell Biol.* 160, 113-123.
- Espenshade,P.J. (2006). SREBPs: sterol-regulated transcription factors. *J. Cell Sci.* 2006. Mar. 15. ;119. (Pt. 6. ):973. -6. 119, 973-976.
- Etcheberrigaray,R., Tan,M., Dewachter,I., Kuiperi,C., Van,d.A., I, Wera,S., Qiao,L., Bank,B., Nelson,T.J., Kozikowski,A.P., Van Leuven,F., and Alkon,D.L. (2004). Therapeutic effects of PKC

activators in Alzheimer's disease transgenic mice. *Proc. Natl. Acad. Sci. U. S. A* 101, 11141-11146.

Fahrenholz,F., Gilbert,S., Kojro,E., Lammich,S., and Postina,R. (2000). Alpha-secretase activity of the disintegrin metalloprotease ADAM 10. Influences of domain structure. *Ann. N. Y. Acad. Sci.* 920, 215-222.

Fantini,J., Garmy,N., Mahfoud,R., and Yahi,N. (2002). Lipid rafts: structure, function and role in HIV, Alzheimers and prion diseases. *Expert. Rev. Mol. Med.* 2002. Dec. 20. ;2002. :1-22. 2002, 1-22.

Farina,F., Cappello,F., Todaro,M., Bucchieri,F., Peri,G., Zummo,G., and Stassi,G. (2000). Involvement of caspase-3 and GD3 ganglioside in ceramide-induced apoptosis in Farber disease. *J. Histochem. Cytochem.* 2000. Jan. ;48. (1):57. -62. 48, 57-62.

Fassbender,K., Simons,M., Bergmann,C., Stroick,M., Lutjohann,D., Keller,P., Runz,H., Kuhl,S., Bertsch,T., von Bergmann,K., Hennerici,M., Beyreuther,K., and Hartmann,T. (2001). Simvastatin strongly reduces levels of Alzheimer's disease beta - amyloid peptides Abeta 42 and Abeta 40 in vitro and in vivo. *Proc. Natl. Acad. Sci. U. S. A* 98, 5856-5861.

Ferri,C.P., Prince,M., Brayne,C., Brodaty,H., Fratiglioni,L., Ganguli,M., Hall,K., Hasegawa,K., Hendrie,H., Huang,Y., Jorm,A., Mathers,C., Menezes,P.R., Rimmer,E., and Scazufca,M. (2005). Global prevalence of dementia: a Delphi consensus study. *Lancet* 366, 2112-2117.

Fielding,C.J. and Fielding,P.E. (1997). Intracellular cholesterol transport. *J. Lipid Res.* 38, 1503-1521.

Fink,M., Acimovic,J., Rezen,T., Tansek,N., and Rozman,D. (2005). CHOLESTEROGENIC LANOSTEROL 14{alpha}-DEMETHYLASE (CYP51) IS AN IMMEDIATE EARLY RESPONSE GENE. *Endocrinology*.

Fluhrer,R., Capell,A., Westmeyer,G., Willem,M., Hartung,B., Condron,M.M., Teplov,D.B., Haass,C., and Walter,J. (2002). A non-amyloidogenic function of BACE-2 in the secretory pathway. *J. Neurochem.* 81, 1011-1020.

Fluhrer,R., Friedlein,A., Haass,C., and Walter,J. (2004). Phosphorylation of presenilin 1 at the recognition site regulates its proteolytic processing and the progression of apoptosis. *J. Biol. Chem.* 279, 1585-1593.

Forstl,H. and Kurz,A. (1999). Clinical features of Alzheimer's disease. *Eur. Arch. Psychiatry Clin. Neurosci.* 249, 288-290.

Francis,P.T., Palmer,A.M., Snape,M., and Wilcock,G.K. (1999). The cholinergic hypothesis of Alzheimer's disease: a review of progress. *J. Neurol. Neurosurg. Psychiatry.* 66, 137-147.

Funato,K. and Riezman,H. (2001). Vesicular and nonvesicular transport of ceramide from ER to the Golgi apparatus in yeast. *J. Cell Biol.* 2001. Dec. 10;155. (6. ):949. -59. Epub. 2001. Dec. 3. 155, 949-959.

- Galvan,V., Chen,S., Lu,D., Logvinova,A., Goldsmith,P., Koo,E.H., and Bredesen,D.E. (2002). Caspase cleavage of members of the amyloid precursor family of proteins. *J. Neurochem.* 2002. Jul. ;82. (2):283. -94. 82, 283-294.
- Garcia-Ruiz,C., Colell,A., Morales,A., Calvo,M., Enrich,C., and Fernandez-Checa,J.C. (2002). Trafficking of ganglioside GD3 to mitochondria by tumor necrosis factor-alpha. *J. Biol. Chem.* 2002. Sep. 27. ;277. (39. ):36443. -8. Epub. 2002. Jul. 12. 277, 36443-36448.
- George-Hyslop,P.H. and Petit,A. (2005). Molecular biology and genetics of Alzheimer's disease. *C. R. Biol.* 2005. Feb. ;328. (2):119. -30. 328, 119-130.
- Goldstein,J.L., DeBose-Boyd,R.A., and Brown,M.S. (2006). Protein sensors for membrane sterols. *Cell.* 2006. Jan. 13;124. (1):35. -46. 124, 35-46.
- Griffin,W.S. (2006). Inflammation and neurodegenerative diseases. *Am. J. Clin. Nutr.* 2006. Feb. ;83. (2):470S. -474S. 83, 470S-474S.
- Grimm,M.O., Grimm,H.S., Patzold,A.J., Zinser,E.G., Halonen,R., Duering,M., Tschape,J.A., Strooper,B.D., Muller,U., Shen,J., and Hartmann,T. (2005). Regulation of cholesterol and sphingomyelin metabolism by amyloid-beta and presenilin. *Nat. Cell Biol.*
- Haass,C. and de Strooper,B. (1999). The presenilins in Alzheimer's disease--proteolysis holds the key. *Science* 286, 916-9.
- Haass,C., Koo,E.H., Mellon,A., Hung,A.Y., and Selkoe,D.J. (1992b). Targeting of cell-surface beta-amyloid precursor protein to lysosomes: alternative processing into amyloid-bearing fragments. *Nature* 357, 500-3.
- Haass,C. and Steiner,H. (2002). Alzheimer disease gamma-secretase: a complex story of GxGD-type presenilin proteases. *Trends Cell Biol.* 12, 556-562.
- Hakomori,S. (1981). Glycosphingolipids in cellular interaction, differentiation, and oncogenesis. *Annu. Rev. Biochem.* 50, 733-764.
- Hamaguchi,T., Ono,K., and Yamada,M. (2006). Anti-amyloidogenic therapies: strategies for prevention and treatment of Alzheimer's disease. *Cell Mol. Life Sci.* 2006. Jul. ;63. (13):1538. -52. 63, 1538-1552.
- Han,X. (2005). Lipid alterations in the earliest clinically recognizable stage of Alzheimer's disease: implication of the role of lipids in the pathogenesis of Alzheimer's disease. *Curr. Alzheimer Res.* 2005. Jan. ;2(1):65. -77. 2, 65-77.
- Hanshaw,R.G. and Smith,B.D. (2005). New reagents for phosphatidylserine recognition and detection of apoptosis. *Bioorg. Med. Chem.* 2005. Sep. 1;13(17):5035. -42. 13, 5035-5042.
- Hardy,J. (2003). The relationship between amyloid and tau. *J. Mol. Neurosci.* 20, 203-206.
- Hardy,J. (2006). Has the amyloid cascade hypothesis for Alzheimer's disease been proved? *Curr. Alzheimer Res.* 2006. Feb. ;3(1):71. -3. 3, 71-73.

Hardy,J. and Selkoe,D.J. (2002). The amyloid hypothesis of Alzheimer's disease: progress and problems on the road to therapeutics. *Science* 297, 353-356.

Harris,F.M., Tesseur,I., Brecht,W.J., Xu,Q., Mullendorff,K., Chang,S., Wyss-Coray,T., Mahley,R.W., and Huang,Y. (2004). Astroglial regulation of apolipoprotein E expression in neuronal cells. Implications for Alzheimer's disease. *J. Biol. Chem.* 2004. Jan. 30. ;279. (5):3862-8. Epub. 2003. Oct. 29. 279, 3862-3868.

Hass,M.R. and Yankner,B.A. (2005). A  $\gamma$ -secretase-independent mechanism of signal transduction by the amyloid precursor protein. *J. Biol. Chem.* 280, 36895-36904.

Haucke,V. (2005). Phosphoinositide regulation of clathrin-mediated endocytosis. *Biochem. Soc. Trans.* 2005. Dec. ;33. (Pt. 6. ):1285. -9. 33, 1285-1289.

Hayashi,H., Kimura,N., Yamaguchi,H., Hasegawa,K., Yokoseki,T., Shibata,M., Yamamoto,N., Michikawa,M., Yoshikawa,Y., Terao,K., Matsuzaki,K., Lemere,C.A., Selkoe,D.J., Naiki,H., and Yanagisawa,K. (2004). A seed for Alzheimer amyloid in the brain. *J. Neurosci.* 24, 4894-4902.

Herz,J. (2001). The LDL receptor gene family: (un)expected signal transducers in the brain. *Neuron.* 2001. Mar. ;29. (3):571. -81. 29, 571-581.

Herz,J. and Bock,H.H. (2002). Lipoprotein receptors in the nervous system. *Annu. Rev. Biochem.* 71, 405-434.

Hintersteiner,M., Enz,A., Frey,P., Jatou,A.L., Kinzy,W., Kneuer,R., Neumann,U., Rudin,M., Staufenberg,M., Stoeckli,M., Wiederhold,K.H., and Gremlich,H.U. (2005). In vivo detection of amyloid-beta deposits by near-infrared imaging using an oxazine-derivative probe. *Nat. Biotechnol.* 23 , 577-583.

Hoekstra,D., Maier,O., van der Wouden,J.M., Slimane,T.A., and van IJzendoorn,S.C. (2003). Membrane dynamics and cell polarity: the role of sphingolipids. *J. Lipid Res.* 2003. May. ;44. (5):869. -77. Epub. 2003. Mar. 16. 44, 869-877.

Holthuis,J.C., Pomorski,T., Raggars,R.J., Sprong,H., and van Meer,G. (2001). The organizing potential of sphingolipids in intracellular membrane transport. *Physiol Rev.* 81, 1689-1723.

Horton,J.D., Goldstein,J.L., and Brown,M.S. (2002). SREBPs: transcriptional mediators of lipid homeostasis. *Cold Spring Harb. Symp. Quant. Biol.* 67, 491-498.

Hutter-Paier,B., Huttunen,H.J., Puglielli,L., Eckman,C.B., Kim,D.Y., Hofmeister,A., Moir,R.D., Domnitz,S.B., Frosch,M.P., Windisch,M., and Kovacs,D.M. (2004). The ACAT inhibitor CP-113,818 markedly reduces amyloid pathology in a mouse model of Alzheimer's disease. *Neuron* 44, 227-238.

Ichikawa,S., Nakajo,N., Sakiyama,H., and Hirabayashi,Y. (1994). A mouse B16 melanoma mutant deficient in glycolipids. *Proc. Natl. Acad. Sci. U. S. A* 91, 2703-2707.

Ikeda,M., Kihara,A., and Igarashi,Y. (2006). Lipid asymmetry of the eukaryotic plasma membrane: functions and related enzymes. *Biol. Pharm. Bull.* 2006. Aug. ;29. (8. ):1542. -6. 29, 1542-1546.

- Jin,L.W., Shie,F.S., Maezawa,I., Vincent,I., and Bird,T. (2004). Intracellular accumulation of amyloidogenic fragments of amyloid-beta precursor protein in neurons with Niemann-Pick type C defects is associated with endosomal abnormalities. *Am. J. Pathol.* 2004. Mar. ;164. (3):975. -85. 164, 975-985.
- Jolly-Tornetta,C. and Wolf,B.A. (2000). Protein kinase C regulation of intracellular and cell surface amyloid
- Kaether,C., Haass,C., and Steiner,H. (2006). Assembly, trafficking and function of gamma-secretase. *Neurodegener. Dis.* 3, 275-283.
- Kahlem,P. (2006). Gene-dosage effect on chromosome 21 transcriptome in trisomy 21: implication in Down syndrome cognitive disorders. *Behav. Genet.* 2006. May. ;36. (3):416. -28. Epub. 2006. Mar. 24. 36, 416-428.
- Kalvodova,L., Kahya,N., Schwille,P., Eehalt,R., Verkade,P., Drechsel,D., and Simons,K. (2005). Lipids as modulators of proteolytic activity of BACE: involvement of cholesterol, glycosphingolipids, and anionic phospholipids in vitro. *J. Biol. Chem.* 2005. Nov. 4;280. (44.):36815. -23. Epub. 2005. Aug. 22. 280, 36815-36823.
- Kametani,F., Usami,M., Tanaka,K., Kume,H., and Mori,H. (2004). Mutant presenilin (A260V) affects Rab8 in PC12D cell. *Neurochem. Int.* 2004. Apr;44. (5):313. -20. 44, 313-320.
- Kaplan,M.R. and Simoni,R.D. (1985). Transport of cholesterol from the endoplasmic reticulum to the plasma membrane. *J. Cell Biol.* 101, 446-453.
- Keller,J.N., Hanni,K.B., and Markesbery,W.R. (2000). Impaired proteasome function in Alzheimer's disease. *J. Neurochem.* 2000. Jul. ;75. (1):436. -9. 75, 436-439.
- King,G.D., Perez,R.G., Steinhilb,M.L., Gaut,J.R., and Turner,R.S. (2003). X11alpha modulates secretory and endocytic trafficking and metabolism of amyloid precursor protein: mutational analysis of the YENPTY sequence. *Neuroscience.* 2003. ;120. (1):143. -54. 120, 143-154.
- King,G.D. and Scott,T.R. (2004). Adaptor protein interactions: modulators of amyloid precursor protein metabolism and Alzheimer's disease risk? *Exp. Neurol.* 185, 208-219.
- Kivipelto,M. and Solomon,A. (2006). Cholesterol as a risk factor for Alzheimer's disease - epidemiological evidence. *Acta Neurol. Scand. Suppl.* 2006. ;185. :50. -7. 185, 50-57.
- Kolter,T., Proia,R.L., and Sandhoff,K. (2002). Combinatorial ganglioside biosynthesis. *J. Biol. Chem.* 277, 25859-25862.
- Kolter,T. and Sandhoff,K. (2005). Principles of lysosomal membrane digestion: stimulation of sphingolipid degradation by sphingolipid activator proteins and anionic lysosomal lipids. *Annu. Rev. Cell Dev. Biol.* 2005. ;21:81. -103. 21, 81-103.
- Kolter,T. and Sandhoff,K. (2006). Sphingolipid metabolism diseases. *Biochim. Biophys. Acta.* 2006. Jun. 14; ..

Komatsu,M., Kominami,E., and Tanaka,K. (2006). Autophagy and neurodegeneration. *Autophagy*. 2006. Oct. -Dec. ;2(4):315. -7. Epub. 2006. Oct. 2. 2, 315-317.

Komori,H., Ichikawa,S., Hirabayashi,Y., and Ito,M. (1999). Regulation of intracellular ceramide content in B16 melanoma cells. Biological implications of ceramide glycosylation. *J. Biol. Chem.* 274, 8981-8987.

Koo,E.H. and Squazzo,S.L. (1994). Evidence that production and release of amyloid beta-protein involves the endocytic pathway. *J Biol Chem* 269, 17386-9.

Kopan,R. and Ilagan,M.X. (2004). Gamma-secretase: proteasome of the membrane? *Nat. Rev. Mol. Cell Biol.* 2004. Jun. ;5(6. ):499. -504. 5, 499-504.

Kumar-Singh,S., Theuns,J., Van Broeck,B., Pirici,D., Vennekens,K., Corsmit,E., Cruts,M., Dermaut,B., Wang,R., and Van Broeckhoven,C. (2006). Mean age-of-onset of familial alzheimer disease caused by presenilin mutations correlates with both increased Abeta42 and decreased Abeta40. *Hum. Mutat.* 2006. Jul. ;27. (7. ):686. -95. 27, 686-695.

Lahiri,D.K., Kotwal,G.J., Farlow,M.R., Sima,A., Kupsky,W., Sarkar,F.H., and Sambamurti,K. (2002). The role of the carboxyl-terminal fragments of amyloid precursor protein in Alzheimer's disease. *Ann. N. Y. Acad. Sci.* 2002. Nov. ;973. :334. -9. 973, 334-339.

Lam,Y.A., Pickart,C.M., Alban,A., Landon,M., Jamieson,C., Ramage,R., Mayer,R.J., and Layfield,R. (2000). Inhibition of the ubiquitin-proteasome system in Alzheimer's disease. *Proc. Natl. Acad. Sci. U. S. A.* 2000. Aug. 29. ;97. (18. ):9902. -6. 97, 9902-9906.

Lange,Y. and Matthies,H.J. (1984). Transfer of cholesterol from its site of synthesis to the plasma membrane. *J. Biol. Chem.* 259, 14624-14630.

Lazarov,V.K., Fraering,P.C., Ye,W., Wolfe,M.S., Selkoe,D.J., and Li,H. (2006). Electron microscopic structure of purified, active gamma-secretase reveals an aqueous intramembrane chamber and two pores. *Proc. Natl. Acad. Sci. U. S. A.* 2006. May. 2;103. (18. ):6889. -94. Epub. 2006. Apr 24. 103, 6889-6894.

Lee,J.T., Xu,J., Lee,J.M., Ku,G., Han,X., Yang,D.I., Chen,S., and Hsu,C.Y. (2004). Amyloid-beta peptide induces oligodendrocyte death by activating the neutral sphingomyelinase-ceramide pathway. *J. Cell Biol.* 2004. Jan. 5;164. (1):123. -31. 164, 123-131.

Lee,S.F., Shah,S., Li,H., Yu,C., Han,W., and Yu,G. (2002). Mammalian APH-1 interacts with presenilin and nicastrin and is required for intramembrane proteolysis of amyloid-beta precursor protein and Notch. *J. Biol. Chem.* 277, 45013-45019.

Lee,V.M., Goedert,M., and Trojanowski,J.Q. (2001). Neurodegenerative tauopathies. *Annu. Rev. Neurosci.* 24, 1121-1159.

Lefrancois,S., Michaud,L., Potier,M., Igdoura,S., and Morales,C.R. (1999). Role of sphingolipids in the transport of prosaposin to the lysosomes. *J. Lipid Res.* 40, 1593-1603.

Leverly,S.B. (2005). Glycosphingolipid structural analysis and glycosphingolipidomics. *Methods Enzymol.* 2005. ;405. :300. -69. 405, 300-369.



- Liscum,L. (2000). Niemann-Pick type C mutations cause lipid traffic jam. *Traffic*. 2000. Mar. ;1(3):218. -25. 1, 218-225.
- Liscum,L. and Dahl,N.K. (1992). Intracellular cholesterol transport. *J. Lipid Res.* 33, 1239-1254.
- Liscum,L. and Underwood,K.W. (1995). Intracellular cholesterol transport and compartmentation. *J. Biol. Chem.* 270, 15443-15446.
- Liu,K., Doms,R.W., and Lee,V.M. (2002). Glu11 Site Cleavage and N-Terminally Truncated Abeta Production upon BACE Overexpression. *Biochemistry* 41, 3128-36.
- Lloyd-Evans,E., Pelled,D., Riebeling,C., Bodennec,J., de Morgan,A., Waller,H., Schiffmann,R., and Futerman,A.H. (2003). Glucosylceramide and glucosylsphingosine modulate calcium mobilization from brain microsomes via different mechanisms. *J. Biol. Chem.* 2003. Jun. 27. ;278. (26. ):23594. -9. Epub. 2003. Apr 22. 278, 23594-23599.
- Lowe,J., Mayer,J., Landon,M., and Layfield,R. (2001). Ubiquitin and the molecular pathology of neurodegenerative diseases. *Adv. Exp. Med. Biol.* 2001. ;487. :169. -86. 487, 169-186.
- Maltese,W.A., Wilson,S., Tan,Y., Suomensaari,S., Sinha,S., Barbour,R., and McConlogue,L. (2001). Retention of the Alzheimer's amyloid precursor fragment C99 in the endoplasmic reticulum prevents formation of amyloid beta-peptide. *J. Biol. Chem.* 2001. Jun. 8. ;276. (23):20267. -79. Epub. 2001. Mar. 7. 276, 20267-20279.
- Mandelkow,E.M., Schweers,O., Drewes,G., Biernat,J., Gustke,N., Trinczek,B., and Mandelkow,E. (1996). Structure, microtubule interactions, and phosphorylation of tau protein. *Ann. N. Y. Acad. Sci.* 777, 96-106.
- Marchesi,V.T. (2005). An alternative interpretation of the amyloid Abeta hypothesis with regard to the pathogenesis of Alzheimer's disease. *Proc. Natl. Acad. Sci. U. S. A.* 2005. Jun. 28. ;102. (26. ):9093. -8. Epub. 2005. Jun. 20. 102, 9093-9098.
- Marr,R.A., Rockenstein,E., Mukherjee,A., Kindy,M.S., Hersh,L.B., Gage,F.H., Verma,I.M., and Masliah,E. (2003). Neprilysin gene transfer reduces human amyloid pathology in transgenic mice. *J. Neurosci.* 23, 1992-1996.
- Martin,S. and Parton,R.G. (2006). Lipid droplets: a unified view of a dynamic organelle. *Nat. Rev. Mol. Cell Biol.* 2006. May. ;7. (5):373. -8. 7, 373-378.
- Masters,C.L. and Beyreuther,K. (1991). Alzheimer's disease: molecular basis of structural lesions. *Brain Pathol.* 1, 226-227.
- Mathews,P.M., Jiang,Y., Schmidt,S.D., Grbovic,O.M., Mercken,M., and Nixon,R.A. (2002). Calpain activity regulates the cell surface distribution of amyloid precursor protein. Inhibition of clathrins enhances endosomal generation of beta-cleaved C-terminal APP fragments. *J. Biol. Chem.* 2002. Sep. 27. ;277. (39. ):36415. -24. Epub. 2002. Jun. 26. 277, 36415-36424.
- Mattson,M.P. (1997). Cellular actions of beta-amyloid precursor protein and its soluble and fibrillogenic derivatives. *Physiol Rev* 77, 1081-132.

Mattson, M.P. (2002). Oxidative stress, perturbed calcium homeostasis, and immune dysfunction in Alzheimer's disease. *J. Neurovirol.* 2002. Dec. ;8. (6. ):539. -50. 8, 539-550.

McPhie, D.L., Lee, R.K., Eckman, C.B., Olstein, D.H., Durham, S.P., Yager, D., Younkin, S.G., Wurtman, R.J., and Neve, R.L. (1997). Neuronal expression of beta-amyloid precursor protein Alzheimer mutations causes intracellular accumulation of a C-terminal fragment containing both the amyloid beta and cytoplasmic domains. *J. Biol. Chem.* 272, 24743-24746.

Menendez, M. (2004). Pathological and clinical heterogeneity of presenilin 1 gene mutations. *J. Alzheimers. Dis.* 2004. Oct. ;6. (5):475. -82. 6, 475-482.

Michailov, G.V., Sereda, M.W., Brinkmann, B.G., Fischer, T.M., Haug, B., Birchmeier, C., Role, L., Lai, C., Schwab, M.H., and Nave, K.A. (2004). Axonal neuregulin-1 regulates myelin sheath thickness. *Science* 304, 700-703.

Mishra, S.K., Watkins, S.C., and Traub, L.M. (2002). The autosomal recessive hypercholesterolemia (ARH) protein interfaces directly with the clathrin-coat machinery. *Proc. Natl. Acad. Sci. U. S. A.* 2002. Dec. 10;99. (25. ):16099. -104. Epub. 2002. Nov. 25. 99, 16099-16104.

Mizushima, N. and Hara, T. (2006). Intracellular quality control by autophagy: how does autophagy prevent neurodegeneration? *Autophagy.* 2006. Oct. -Dec. ;2(4):302. -4. Epub. 2006. Oct. 25. 2, 302-304.

Molander-Melin, M., Blennow, K., Bogdanovic, N., Dellheden, B., Mansson, J.E., and Fredman, P. (2005). Structural membrane alterations in Alzheimer brains found to be associated with regional disease development; increased density of gangliosides GM1 and GM2 and loss of cholesterol in detergent-resistant membrane domains. *J. Neurochem.* 2005. Jan. ;92. (1):171. -82. 92, 171-182.

Mukherjee, S., Ghosh, R.N., and Maxfield, F.R. (1997). Endocytosis. *Physiol Rev.* 77, 759-803.

Nestor, P.J., Scheltens, P., and Hodges, J.R. (2004). Advances in the early detection of Alzheimer's disease. *Nat. Med.* 10 *Suppl*, S34-S41.

Neufeld, E.F. (1991). Lysosomal storage diseases. *Annu. Rev. Biochem.* 60, 257-280.

Nixon, R.A., Cataldo, A.M., and Mathews, P.M. (2000). The endosomal-lysosomal system of neurons in Alzheimer's disease pathogenesis: a review. *Neurochem. Res.* 2000. Oct. ;25. (9. -10):1161. -72. 25, 1161-1172.

Nunan, J., Shearman, M.S., Checler, F., Cappai, R., Evin, G., Beyreuther, K., Masters, C.L., and Small, D.H. (2001). The C-terminal fragment of the Alzheimer's disease amyloid protein precursor is degraded by a proteasome-dependent mechanism distinct from gamma-secretase. *Eur. J. Biochem.* 268, 5329-5336.

Pagano, R.E., Puri, V., Dominguez, M., and Marks, D.L. (2000). Membrane traffic in sphingolipid storage diseases. *Traffic.* 2000. Nov. ;1(11):807. -15. 1, 807-815.

Pasternak, S.H., Bagshaw, R.D., Guiral, M., Zhang, S., Ackerley, C.A., Pak, B.J., Callahan, J.W., and Mahuran, D.J. (2003). Presenilin-1, nicastrin, amyloid precursor protein, and gamma-secretase

- activity are co-localized in the lysosomal membrane. *J. Biol. Chem.* 2003. Jul. 18. ;278. (29. ):26687. -94. Epub. 2003. May. 7. 278, 26687-26694.
- Pearson,H.A. and Peers,C. (2006). Physiological roles for amyloid beta peptides. *J. Physiol* 575, 5-10.
- Perez-Tur,J., Froelich,S., Prihar,G., Crook,R., Baker,M., Duff,K., Wragg,M., Busfield,F., Lendon,C., and Clark,R.F. (1995). A mutation in Alzheimer's disease destroying a splice acceptor site in the presenilin-1 gene. *Neuroreport.* 7, 297-301.
- Peschon,J.J., Slack,J.L., Reddy,P., Stocking,K.L., Sunnarborg,S.W., Lee,D.C., Russell,W.E., Castner,B.J., Johnson,R.S., Fitzner,J.N., Boyce,R.W., Nelson,N., Kozlosky,C.J., Wolfson,M.F., Rauch,C.T., Cerretti,D.P., Paxton,R.J., March,C.J., and Black,R.A. (1998). An essential role for ectodomain shedding in mammalian development. *Science* 282, 1281-1284.
- Pfriegeer,F.W. (2003). Outsourcing in the brain: do neurons depend on cholesterol delivery by astrocytes? *Bioessays* 25, 72-78.
- Pitsi,D. and Octave,J.N. (2004). Presenilin 1 stabilizes the C-terminal fragment of the amyloid precursor protein independently of gamma-secretase activity. *J. Biol. Chem.* 2004. Jun. 11;279. (24. ):25333. -8. Epub. 2004. Apr 15. 279, 25333-25338.
- Platt,F.M. and Butters,T.D. (2000). Substrate deprivation: a new therapeutic approach for the glycosphingolipid lysosomal storage diseases. *Expert. Rev. Mol. Med.* 2000. Feb. 1;2000. :1-17. 2000, 1-17.
- Postina,R., Schroeder,A., Dewachter,I., Bohl,J., Schmitt,U., Kojro,E., Prinzen,C., Endres,K., Hiemke,C., Blessing,M., Flamez,P., Dequenne,A., Godaux,E., Van Leuven,F., and Fahrenholz,F. (2004). A disintegrin-metalloproteinase prevents amyloid plaque formation and hippocampal defects in an Alzheimer disease mouse model. *J. Clin. Invest* 113, 1456-1464.
- Primakoff,P. and Myles,D.G. (2000). The ADAM gene family: surface proteins with adhesion and protease activity. *Trends Genet.* 16, 83-87.
- Puglielli,L., Ellis,B.C., Saunders,A.J., and Kovacs,D.M. (2003). Ceramide stabilizes beta-site amyloid precursor protein-cleaving enzyme 1 and promotes amyloid beta-peptide biogenesis. *J. Biol. Chem.* 278, 19777-19783.
- Quest,A.F., Leyton,L., and Parraga,M. (2004). Caveolins, caveolae, and lipid rafts in cellular transport, signaling, and disease. *Biochem. Cell Biol.* 2004. Feb. ;82. (1):129. -44. 82, 129-144.
- Radin,N.S. (1996). Treatment of Gaucher disease with an enzyme inhibitor. *Glycoconj. J.* 13, 153-157.
- Rigamonti,E., Helin,L., Lestavel,S., Mutka,A.L., Lepore,M., Fontaine,C., Bouhrel,M.A., Bultel,S., Fruchart,J.C., Ikonen,E., Clavey,V., Staels,B., and Chinetti-Gbaguidi,G. (2005). Liver X receptor activation controls intracellular cholesterol trafficking and esterification in human macrophages. *Circ. Res.* 2005. Sep. 30. ;97. (7. ):682. -9. Epub. 2005. Sep. 1. 97, 682-689.

Robakis,N.K. (2003). An Alzheimer's disease hypothesis based on transcriptional dysregulation. *Amyloid*. 2003. Jun. ;10(2):80. -5. 10, 80-85.

Rochet,J.C. and Lansbury,P.T., Jr. (2000). Amyloid fibrillogenesis: themes and variations. *Curr Opin Struct Biol* 10, 60-8.

Rodriguez,C., Martinez-Gonzalez,J., Sanchez-Gomez,S., and Badimon,L. (2001b). LDL downregulates CYP51 in porcine vascular endothelial cells and in the arterial wall through a sterol regulatory element binding protein-2-dependent mechanism. *Circ. Res.* 88, 268-274.

Roubertoux,P.L. and Kerdelhue,B. (2006). Trisomy 21: from chromosomes to mental retardation. *Behav. Genet.* 2006. May. ;36. (3):346. -54. Epub. 2006. Apr 5. 36, 346-354.

Runz,H., Rietdorf,J., Tomic,I., de Bernard,M., Beyreuther,K., Pepperkok,R., and Hartmann,T. (2002). Inhibition of intracellular cholesterol transport alters presenilin localization and amyloid precursor protein processing in neuronal cells. *J. Neurosci.* 22, 1679-1689.

Sabo,S.L., Ikin,A.F., Buxbaum,J.D., and Greengard,P. (2001). The Alzheimer amyloid precursor protein (APP) and FE65, an APP-binding protein, regulate cell movement. *J Cell Biol* 153, 1403-14.

Sambamurti,K., Suram,A., Venugopal,C., Prakasam,A., Zhou,Y., Lahiri,D.K., and Greig,N.H. (2006). A partial failure of membrane protein turnover may cause Alzheimer's disease: a new hypothesis. *Curr. Alzheimer Res.* 3, 81-90.

Sandhoff,K. and Kolter,T. (2003). Biosynthesis and degradation of mammalian glycosphingolipids. *Philos. Trans. R. Soc. Lond B Biol. Sci.* 2003. May. 29. ;358. (1433. ):847. -61. 358, 847-861.

Sastre,M., Steiner,H., Fuchs,K., Capell,A., Multhaup,G., Condron,M.M., Teplow,D.B., and Haass,C. (2001). Presenilin-dependent gamma-secretase processing of beta-amyloid precursor protein at a site corresponding to the S3 cleavage of Notch. *EMBO Rep* 2, 835-41.

Sawamura,N., Ko,M., Yu,W., Zou,K., Hanada,K., Suzuki,T., Gong,J.S., Yanagisawa,K., and Michikawa,M. (2004). Modulation of amyloid precursor protein cleavage by cellular sphingolipids. *J. Biol. Chem.* 279, 11984-11991.

Scarmeas,N., Brandt,J., Albert,M., Hadjigeorgiou,G., Papadimitriou,A., Dubois,B., Sarazin,M., Devanand,D., Honig,L., Marder,K., Bell,K., Wegesin,D., Blacker,D., and Stern,Y. (2005). Delusions and hallucinations are associated with worse outcome in Alzheimer disease. *Arch. Neurol.* 62, 1601-1608.

Schwarzmann,G., Hoffmann-Bleihauer,P., Schubert,J., Sandhoff,K., and Marsh,D. (1983). Incorporation of ganglioside analogues into fibroblast cell membranes. A spin-label study. *Biochemistry.* 22, 5041-5048.

Schwarzmann,G. and Sandhoff,K. (1990). Metabolism and intracellular transport of glycosphingolipids. *Biochemistry.* 29, 10865-10871.

- Selkoe,D.J. (1998). The cell biology of beta-amyloid precursor protein and presenilin in Alzheimer's disease. *Trends Cell Biol.* 8, 447-453.
- Selkoe,D.J. (2001). Alzheimer's disease: genes, proteins, and therapy. *Physiol Rev* 81, 741-66.
- Selkoe,D.J. (2000). The genetics and molecular pathology of Alzheimer's disease: roles of amyloid and the presenilins. *Neurol Clin* 18, 903-22.
- Sharma,D.K., Brown,J.C., Choudhury,A., Peterson,T.E., Holicky,E., Marks,D.L., Simari,R., Parton,R.G., and Pagano,R.E. (2004). Selective stimulation of caveolar endocytosis by glycosphingolipids and cholesterol. *Mol. Biol. Cell.* 2004. Jul. ;15. (7. ):3114. -22. Epub. 2004. Apr 23. 15, 3114-3122.
- Shen,J. and Kelleher,R.J., III (2007). The presenilin hypothesis of Alzheimer's disease: evidence for a loss-of-function pathogenic mechanism. *Proc. Natl. Acad. Sci. U. S. A* 104, 403-409.
- Shua-Haim,J.R. and Gross,J.S. (1996). Alzheimer's syndrome, not Alzheimer's disease. *J. Am. Geriatr. Soc.* 44, 96-97.
- Sillence,D.J. and Platt,F.M. (2004). Glycosphingolipids in endocytic membrane transport. *Semin. Cell Dev. Biol.* 15, 409-416.
- Simons,K. and Ehehalt,R. (2002). Cholesterol, lipid rafts, and disease. *J. Clin. Invest* 110, 597-603.
- Simons,K. and Ikonen,E. (1997). Functional rafts in cell membranes. *Nature.* 387, 569-572.
- Singer,S.J. (2004). Some early history of membrane molecular biology. *Annu. Rev. Physiol.* 2004. ;66. :1-27. 66, 1-27.
- Singer,S.J. and Nicolson,G.L. (1972). The fluid mosaic model of the structure of cell membranes. *Science.* 175, 720-731.
- Sisodia,S.S. (2000). Neuroscience. An accomplice for gamma-secretase brought into focus. *Science.* 2000. Sep. 29. ;289. (5488. ):2296. -7. 289, 2296-2297.
- Smith,W.L. and Merrill,A.H., Jr. (2002). Sphingolipid metabolism and signaling minireview series. *J. Biol. Chem.* 2002. Jul. 277, 25841-25842.
- Soccio,R.E. and Breslow,J.L. (2004). Intracellular cholesterol transport. *Arterioscler. Thromb. Vasc. Biol.* 24, 1150-1160.
- Sohn,H., Kim,Y.S., Kim,H.T., Kim,C.H., Cho,E.W., Kang,H.Y., Kim,N.S., Kim,C.H., Ryu,S.E., Lee,J.H., and Ko,J.H. (2006). Ganglioside GM3 is involved in neuronal cell death. *FASEB J.* 2006. Jun. ;20. (8. ):1248. -50. Epub. 2006. Apr 24. 20, 1248-1250.
- Spector,A.A. and Yorek,M.A. (1985). Membrane lipid composition and cellular function. *J. Lipid Res.* 26, 1015-1035.

Spilsberg,B., van Meer,G, and Sandvig,K. (2003). Role of lipids in the retrograde pathway of ricin intoxication. *Traffic*. 4 , 544-552.

Sprong,H., Degroote,S., Claessens,T., van Drunen,J., Oorschot,V., Westerink,B.H., Hirabayashi,Y., Klumperman,J., van der,S.P., and van Meer,G. (2001). Glycosphingolipids are required for sorting melanosomal proteins in the Golgi complex. *J. Cell Biol.* 155, 369-380.

St George-Hyslop,P.H. (2000). Genetic factors in the genesis of Alzheimer's disease. *Ann N Y Acad Sci* 924, 1-7.

Strittmatter,W.J. and Roses,A.D. (1995). Apolipoprotein E and Alzheimer disease. *Proc. Natl. Acad. Sci. U. S. A.* 92, 4725-4727.

Struhl,G. and Adachi,A. (2000). Requirements for presenilin-dependent cleavage of notch and other transmembrane proteins. *Mol Cell* 6, 625-36.

Swanson,T.L., Knittel,L.M., Coate,T.M., Farley,S.M., Snyder,M.A., and Copenhaver,P.F. (2005). The insect homologue of the amyloid precursor protein interacts with the heterotrimeric G protein Go alpha in an identified population of migratory neurons. *Dev. Biol.* 288, 160-178.

Tabas,I. (2002). Consequences of cellular cholesterol accumulation: basic concepts and physiological implications. *J. Clin. Invest.* 2002. Oct. ;110. (7. ):905. -11. 110, 905-911.

Tanzi,R.E. and Bertram,L. (2001). New frontiers in Alzheimer's disease genetics. *Neuron* 32, 181-184.

Tanzi,R.E. and Bertram,L. (2005). Twenty years of the Alzheimer's disease amyloid hypothesis: a genetic perspective. *Cell* 120, 545-555.

te,V.D., Lloyd-Evans,E., Veldman,R.J., Neville,D.C., Dwek,R.A., Platt,F.M., van Blitterswijk,W.J., and Sillence,D.J. (2004). Accumulation of glycosphingolipids in Niemann-Pick C disease disrupts endosomal transport. *J. Biol. Chem.* 2004. Jun. 18. ;279. (25. ):26167. -75. Epub. 2004. Apr 12. 279, 26167-26175.

Terai,K., Iwai,A., Kawabata,S., Sasamata,M., Miyata,K., and Yamaguchi,T. (2001). Apolipoprotein E deposition and astrogliosis are associated with maturation of beta-amyloid plaques in betaAPPswe transgenic mouse: Implications for the pathogenesis of Alzheimer's disease. *Brain Res.* 2001. May. 4;900. (1):48. -56. 900, 48-56.

Tettamanti,G. (2004). Ganglioside/glycosphingolipid turnover: new concepts. *Glycoconj. J.* 2004. ;20. (5):301. -17. 20, 301-317.

Thal,D.R., Rub,U., Orantes,M., and Braak,H. (2002). Phases of A beta-deposition in the human brain and its relevance for the development of AD. *Neurology* 58, 1791-1800.

Thompson,T.E. and Tillack,T.W. (1985). Organization of glycosphingolipids in bilayers and plasma membranes of mammalian cells. *Annu. Rev. Biophys. Biophys. Chem.* 14, 361-386.

Tift,C.J. and Proia,R.L. (2000). Stemming the tide: glycosphingolipid synthesis inhibitors as therapy for storage diseases. *Glycobiology.* 2000. Dec. ;10(12. ):1249. -58. 10, 1249-1258.

- Tomita,T. and Iwatsubo,T. (2006). gamma-secretase as a therapeutic target for treatment of Alzheimer's disease. *Curr. Pharm. Des.* 2006. ;12. (6. ):661. -70. 12, 661-670.
- Trommsdorff,M., Borg,J.P., Margolis,B., and Herz,J. (1998). Interaction of cytosolic adaptor proteins with neuronal apolipoprotein E receptors and the amyloid precursor protein. *J. Biol. Chem.* 273, 33556-33560.
- Uemura,K., Kuzuya,A., and Shimohama,S. (2004). Protein trafficking and Alzheimer's disease. *Curr. Alzheimer Res.* 2004. Feb. ;1(1):1-10. 1, 1-10.
- van de,W.M., Oving,I., Muncan,V., Pon Fong,M.T., Brantjes,H., van Leenen,D., Holstege,F.C., Brummelkamp,T.R., Agami,R., and Clevers,H. (2003). Specific inhibition of gene expression using a stably integrated, inducible small-interfering-RNA vector. *EMBO Rep.* 2003. Jun. ;4(6. ):609. -15. 4, 609-615.
- van Meer,G (1989). Lipid traffic in animal cells. *Annu. Rev. Cell Biol.* 5, 247-275.
- van Meer,G and Lisman,Q. (2002). Sphingolipid transport: rafts and translocators. *J. Biol. Chem.* 2002. Jul. 277, 25855-25858.
- Vance,J.E., Karten,B., and Hayashi,H. (2006). Lipid dynamics in neurons. *Biochem. Soc. Trans.* 2006. Jun. ;34. (Pt. 3):399. -403. 34, 399-403.
- Vance,J.E., Hayashi,H., and Karten,B. (2005). Cholesterol homeostasis in neurons and glial cells. *Semin. Cell Dev. Biol.* 2005. Apr;16. (2):193. -212. 16, 193-212.
- Vassar,R. (2004). BACE1: the beta-secretase enzyme in Alzheimer's disease. *J. Mol. Neurosci.* 23, 105-114.
- Verdile,G., Gandy,S.E., and Martins,R.N. (2007). The Role of Presenilin and its Interacting Proteins in the Biogenesis of Alzheimer's Beta Amyloid. *Neurochem. Res.* 2007. Apr;32. (4-5):609. -623. Epub. 2006. Aug. 31. 32, 609-623.
- Wada,R., Tiff,C.J., and Proia,R.L. (2000). Microglial activation precedes acute neurodegeneration in Sandhoff disease and is suppressed by bone marrow transplantation. *Proc. Natl. Acad. Sci. U. S. A.* 2000. Sep. 26. ;97. (20. ):10954. -9. 97, 10954-10959.
- Wahle,T., Thal,D.R., Sastre,M., Rentmeister,A., Bogdanovic,N., Famulok,M., Heneka,M.T., and Walter,J. (2006). GGA1 is expressed in the human brain and affects the generation of amyloid beta-peptide. *J. Neurosci.* 26, 12838-12846.
- Waldron,E., Jaeger,S., and Pietrzik,C.U. (2006). Functional role of the low-density lipoprotein receptor-related protein in Alzheimer's disease. *Neurodegener. Dis.* 2006. ;3(4-5):233. -8. 3, 233-238.
- Walkley,S.U. (1998). Cellular pathology of lysosomal storage disorders. *Brain Pathol.* 8, 175-193.
- Walsh,D.M. and Selkoe,D.J. (2007). Abeta Oligomers - a decade of discovery. *J. Neurochem.* 2007. Feb. 5; . . .

Walter,J., Kaether,C., Steiner,H., and Haass,C. (2001a). The cell biology of Alzheimer's disease: uncovering the secrets of secretases. *Curr Opin Neurobiol* *11*, 585-90.

Walter,J. (2006). Control of amyloid-beta-peptide generation by subcellular trafficking of the beta-amyloid precursor protein and beta-secretase. *Neurodegener. Dis.* *3*, 247-254.

Wang,R., Tang,P., Wang,P., Boissy,R.E., and Zheng,H. (2006). Regulation of tyrosinase trafficking and processing by presenilins: partial loss of function by familial Alzheimer's disease mutation. *Proc. Natl. Acad. Sci. U. S. A* *103*, 353-358.

Weiner,H.L. and Frenkel,D. (2006). Immunology and immunotherapy of Alzheimer's disease. *Nat. Rev. Immunol.* *6*, 404-416.

Willem,M., Garratt,A.N., Novak,B., Citron,M., Kaufmann,S., Rittger,A., Destrooper,B., Saftig,P., Birchmeier,C., and Haass,C. (2006). Control of Peripheral Nerve Myelination by the {beta}-Secretase BACE1. *Science.* 2006. Sep. 21;

Wirths,O., Thelen,K., Breyhan,H., Luzon-Toro,B., Hoffmann,K.H., Falkai,P., Lutjohann,D., and Bayer,T.A. (2006). Decreased plasma cholesterol levels during aging in transgenic mouse models of Alzheimer's disease. *Exp. Gerontol.* 2006. Feb. ;41. (2):220. -4. Epub. 2005. Nov. 22. *41*, 220-224.

Wolfe,M.S. and Kopan,R. (2004). Intramembrane proteolysis: theme and variations. *Science.* 2004. Aug. 20. ;305. (5687. ):1119. -23. *305*, 1119-1123.

Wolozin,B., Manger,J., Bryant,R., Cordy,J., Green,R.C., and McKee,A. (2006). Re-assessing the relationship between cholesterol, statins and Alzheimer's disease. *Acta Neurol. Scand. Suppl.* 2006. ;185. :63. -70. *185*, 63-70.

Wood,D.R., Nye,J.S., Lamb,N.J., Fernandez,A., and Kitzmann,M. (2005). Intracellular retention of caveolin 1 in presenilin-deficient cells. *J. Biol. Chem.* *280*, 6663-6668.

Yankner,B.A., Dawes,L.R., Fisher,S., Villa-Komaroff,L., Oster-Granite,M.L., and Neve,R.L. (1989). Neurotoxicity of a fragment of the amyloid precursor associated with Alzheimer's disease. *Science.* *245*, 417-420.

Yu,W.H., Cuervo,A.M., Kumar,A., Peterhoff,C.M., Schmidt,S.D., Lee,J.H., Mohan,P.S., Mercken,M., Farmery,M.R., Tjernberg,L.O., Jiang,Y., Duff,K., Uchiyama,Y., Naslund,J., Mathews,P.M., Cataldo,A.M., and Nixon,R.A. (2005). Macroautophagy--a novel Beta-amyloid peptide-generating pathway activated in Alzheimer's disease. *J. Cell Biol.* *171*, 87-98.

Zatti,G., Burgo,A., Giacomello,M., Barbiero,L., Ghidoni,R., Sinigaglia,G., Florean,C., Bagnoli,S., Binetti,G., Sorbi,S., Pizzo,P., and Fasolato,C. (2006). Presenilin mutations linked to familial Alzheimer's disease reduce endoplasmic reticulum and Golgi apparatus calcium levels. *Cell Calcium.* 2006. Jun. ;39. (6. ):539. -50. Epub. 2006. Apr 18. *39*, 539-550.

Zelcer,N. and Tontonoz,P. (2006). Liver X receptors as integrators of metabolic and inflammatory signaling. *J. Clin. Invest.* 2006. Mar. ;116. (3):607. -14. *116*, 607-614.



Zha,Q., Ruan,Y., Hartmann,T., Beyreuther,K., and Zhang,D. (2004). GM1 ganglioside regulates the proteolysis of amyloid precursor protein. *Mol. Psychiatry*.

Zhang,M., Haapasalo,A., Kim,D.Y., Ingano,L.A., Pettingell,W.H., and Kovacs,D.M. (2006). Presenilin/gamma-secretase activity regulates protein clearance from the endocytic recycling compartment. *FASEB J.* 20, 1176-1178.

---

## Acknowledgements

I express my deep gratitude to Prof. Dr. Jochen Walter whose continued guidance, unwavering support and understanding made this possible. It truly was a wonderful learning experience and a great training. I have always enjoyed all those stimulating discussions with him, which have helped me broaden my scientific aptitude.

I am grateful to Prof. Dr. Sandhoff for his support and critical feedback. I am also thankful to Prof. Dr. Gütschow and Prof. Dr. Piel for their valuable time.

Many people have contributed to my academic development over the years, and, especially I want to thank all my teachers from school till university who encouraged me and had faith in my abilities. I am also grateful to wider scientific community, their intriguing work provoked me and helped me direct my work in a right way.

It has been a privilege and pleasure to get to know my present and past lab colleagues. Each one of them deserves my heartfelt thanks for their friendship and extraordinary hospitality. I am indebted to Ms. Heike Hampel and Ms. Ester Barth for providing me with a highest degree of support throughout. I am thankful to Dr. Kai Prager, Dr. Lihua Wang and Dr. Natasa Kukoc for their timely help and advice. Being first doctoral students in the lab I and Dr. Tina Wahle have sailed through several ups and downs of our scientific quest and I am very grateful to her for constant hearing and sharing during this course.

In no particular order I would like to thank Martin, Satish, Patrick, Jessica, Thorsten, Dr. Magdalena Sastre and other labmates for all the help, laughter and fun filled lab environment. I am also grateful to colleagues from neurobiology and muscle lab, as they have always been very kind and willing to help. My circle of friends has played a part in helping me get here, I thank them all.

I thank Dr. Dieter Lüthjohan, Dr. Karin Thelen and Dr. Dietmer Thal for their co-operation and inputs. Their expertise and knowledge have played a very positive part in completion of my work.

I consider myself very lucky to have parents from whom I have learnt to fight against all odds and to be on right side no matter what. In no words I can express my gratitude and affection towards my brothers, sister and their spouses, all the kids and my wife. They are the best reason that I have to strive for the best.

---

## Curriculum Vitae

**Irfan Yunus Tamboli** (Date of birth: 17<sup>th</sup> Dec 1976, Pune, India)

- Since Oct 2002 - **University of Bonn, University Hospital Bonn, Germany**  
Doctoral student in Molecular Cell biology, Neurology
- Jan 2002 – Sep 2002 - **University of Giessen, Germany**  
Research fellow in university hospital Giessen
- Jun 1999 – Dec 2001 - **Unilever research pvt ltd, Bangalore, India**  
Research officer in the laboratory of Cell biology
- Jun 1997 – Jun 1999 - **University of Pune, Pune, India**  
Masters in bio-chemistry, M.Sc.
- Jun 1994 – Jun 1997 - **University of Pune, Poona College, Pune, India**  
Bachelors in Chemistry, B.Sc.
- Jun 1992 – Jun 1994 - **Pune Board, Poona College, Pune, India**  
Higher secondary school
- Jun 1982 – Jun 1992 - **Pune Board, K.V. Piliv (Solapur), India**  
Secondary school

## Publications

**Tamboli IY**, Prager K, Barth E, Heneka M, Sandhoff K, Walter J.  
Modulation of proteolytic processing by glycosphingolipids generates amyloid beta-peptide.  
Sphingolipid Biology (Y. Hirabayashi, Y. L., A. H., Merrill, Jr., ed.) Springer, 2006.

**Tamboli IY**, Prager K, Barth E, Heneka M, Sandhoff K, Walter J.  
Inhibition of glycosphingolipid biosynthesis reduces secretion of the beta amyloid precursor protein and amyloid beta peptide. **J Biol Chem**. 2005 Jul 29;280(30):28110-7.

Sharma AK, Kumar S, Sharma V, Nagpal A, Singh N, **Tamboli I**, Mani I, Raman G and TP Singh Lactoferrin-Melanin interaction and its possible implications in melanin polymerization: Crystal structure of the complex formed between mare lactoferrin and melanin monomers at 2.7Å resolution.  
**Proteins**.2001, Nov, 15;45(3):229-36.

Mani I, Shurma V, **Tamboli I** and Raman G: Interaction of melanin with proteins – The importance of an acidic intramelanosomal pH. **Pigment Cell Res** 14: 170-179, 2001

**Tamboli IY**, Prager K, Thelen KM, Thal DR, Wahle T, Breiden B, Sandhoff K, and Dewachter I, Bogdanovic N, Frommelt P, George-Hyslop P, and Sisodia SS, van Leuven F, Lütjohann D, and Walter J. Global role of  $\gamma$ -secretase dependent RIP in endocytosis of lipoprotein particles and membrane lipid homeostasis. Submitted.